GEORG A. HEISS

CORAL REEFS IN THE RED SEA:

GROWTH, PRODUCTION, AND STABLE ISOTOPES.

GEOMAR
Forschungszentrum
für marine Geowissenschaften
der Christian-Albrechts-Universität
zu Kiel

Kiel 1994

GEOMAR REPORT 32

GEOMAR
Research Center
for Marine Geosciences
Christian Albrechts University
in Kiel

Dissertation
zur Erlangung des Doktorgrades
der mathematisch-naturwissenschaftlichen Fakultät
der Christian-Albrechts-Universität zu Kiel
Zum Druck genehmigt am 27.1.1994

Redaktion der Serie: Gerhard Haass
Umschlag: Kerstin Kreis, Harald Gross, GEOMAR Technologie GmbH

Managing Editor: Gerhard Haass
Cover: Kerstin Kreis, Harald Gross, GEOMAR Technologie GmbH

GEOMAR REPORT
ISSN 0936 - 5788

GEOMAR REPORT
ISSN 0936 - 5788

GEOMAR
Forschungszentrum
für marine Geowissenschaften
D-24148 Kiel
Wischhofstr. 1-3
Telefon (0431) 7202-0
Telefax (0431) 72 53 91, 7 20 22 93, 72 56 50

GEOMAR
Research Center
for Marine Geosciences
D-24148 Kiel / Germany
Wischhofstr. 1-3
Telephone (49) 431 / 7202-0
Telefax (49) 431 / 72 53 91, 7 20 22 93, 72 56 50

CONTENTS

ABSTRACT

Growth rates

Coral growth and carbonate production of scleractinian corals was studied in the Red Sea. The first long-term sclerochronological record from scleractinians in the Red Sea-Indian Ocean reef province is presented. Length of cores reaches a maximum of 320 cm and was drilled with a simple and handy pneumatic underwater drill. This core represents a time span of more than 200 years of coral growth in the fringing reefs at Aqaba, Jordan. Growth rates of *Porites* are unexpectedly high for reefs at this latitude. They vary between 8.60 to 12.52 mm/yr. Average linear growth rates show strong oscillations and a general increase since 1880 for a large hemispherical colony of *Porites* sp. could be observed. The relationship to environmental variables as light intensity, temperature, and sediment input is discussed.

Studying core samples of the genus *Porites* in the northern Gulf of Aqaba, has revealed large variations in the growth rate of this coral over the last 20 years. Individual growth rates show high variations even in colonies growing close together. These variations are attributed to locally restricted differences of reef environment, like water temperature, outflow from the lagoon, and turbidity. A general increase in linear extension rate in a relatively healthy reef area was observed at a depth range from 1 m to 15 m. A major variation in climate conditions affecting coral growth was not recorded. A reduction in terrestrial sediment influx is the most likely reason for an accelerated growth.

The effect of extreme sediment load on coral growth rates in a stressed environment is demonstrated on one *Porites*-core taken from a colony growing in vicinity of the phosphate loading berth at Aqaba. The drastical decrease in growth rate of this coral in the observed time span is contrary to the general trend at Aqaba´s reefs and is most probably caused by sediment stress.

A comparison was made between annual growth rates of *Porites* in Red Sea fringing reefs. Locations extend from Aqaba, Gulf of Aqaba, in the North over the northern and southern Egyptian coast and islands to the Gulf of Tadjoura in the Gulf of Aden (Djibouti). The upper limit of growth potential decreases with depth with the decrease of light availability. The variation of growth rates is very high in shallow depth, indicating that other environmental factors than light are able to depress coral growth markedly. This zone reaches at Aqaba (29°27´N) to a depth of ca. 10 m. In the reefs off southern Egypt (24°30´N) this zone extends to ca 15 m water depth. This effect is probably a result of the stronger reduction of winter light levels and water temperature to the northern regions. Mean growth rates in the shallow water zone increase with decreasing latitude and are highest at the southernmost studied reefs in the Gulf of Tadjoura. However, the observed latitudinal growth reduction is restricted to the upper ca. 15 m of the water column. Compared to other oceans the decrease of growth with increasing latitude of Red Sea *Porites* corals is far less, and growth rates at Aqaba are the highest observed at these latitudes.

Porites sub-colonies from a 6 m high pinnacle in the middle fore-reef at Aqaba, which are assumed to be genetically identical, show a wide range of skeletal extension rates from ca. 3 to 17 mm·yr^{-1}. The decrease of growth rates of these sub-colonies can be

attributed almost exclusively to decreasing light intensity due to increasing water depth from ca 5 to 10 m and the peripheral position of the colonies at the sides of this pillar. Colonies sampled at the top of the pillar show high growth rates which can be attributed to the ideal conditions for coral growth due to rapid water exchange and optimal light exposure. The absence of resuspension of bottom sediments in the pinnacle-environment may enable the high growth rates of these colonies. Sediment stress through resuspension might depress growth rates of colonies from the reef-bottom at similar depths.

Stable isotopes

Growth rate variations, stable oxygen and carbon isotopic composition were investigated in two cores drilled from a large *Porites* colony at Aqaba. The sclerochronological record of the longest core (320 cm) reaches back to the year 1788. This core was drilled vertically. The horizontal core comprises 107 years and is drilled from the southern side into the colony. Growth rates are high and seem to be enhanced by increase of water temperatures. $\delta^{18}O$ displays a decrease since 1800 by about 0.4 ‰ and indicates a warming of sea water temperature by ca. 2°C. Carbon isotopes composition is mainly controlled by metabolic effects, with a higher portion of kinetic behaviour at the side of the colony. Both oxygen and carbon isotopes display responses to global variations of temperature and atmospheric CO_2. Similarities with coral records from other oceans are observed. Anthropogenic activities since the 1960s affected growth rates and isotopic composition drastically.

The stable isotopic composition of scleractinian corals (*Porites* sp.), two recent and one fossil, from the Egyptian Red Sea coast was studied. The oxygen isotope record proves the assumption that recent sea surface temperatures are comparable to the time of last sea level highstand in Eemian (stage 5e, 125,000 yBP). Deposition of high-density and low-density bands with respect to season shows the same patterns as today with high-density band deposition in winter (low water temperatures) and low-density band deposition in summer (high water temperatures). $\delta^{18}O$ is negatively correlated with $\delta^{13}C$ with a shift in phase of 1 to 2 months. Thus a coupling of carbon isotopes to light intensity and oxygen isotopes to water temperature is suggested. To get an overview on seasonal patterns of stable isotope composition a sampling technique with a resolution of four samples per year is of sufficient precision.

Carbonate production

In the fringing reef at Aqaba at the northern end of the Gulf of Aqaba (29°27′N) growth rates, density and calcification rate of *Porites* was investigated in order to establish calculations of gross carbonate production for the reefs in this area. The density of coral skeletons is, beside the growth rate, the other important factor for the assessment of carbonate production rates by corals. The relation between density of coral skeletons and water depth has been studied by various authors with remarkably different results. Recently computed tomography has been introduced as a new method for the evaluation of skeletal density. An outline of the methodology of density measurements used for production calculations is given.

Colony accretion of *Porites* decreases linearly with depth as a function of decreasing growth rates and increasing skeletal density. Calcification rate of *Porites* is highest in shallow water (0-5 m depth) with 0.94 $g \cdot cm^{-2} \cdot yr^{-1}$ and decreases to 0.49 $g \cdot cm^{-2} \cdot yr^{-1}$ below 30 m. Gross production by scleractinian corals is calculated from potential productivity and coral coverage and is mainly dependent on living coral cover and to a lesser extent on potential productivity. Maximum coral gross production at Aqaba occurs at the reef crest (0.29 $g \cdot cm^{-2} \cdot yr^{-1}$) and in the middle fore reef from 10 to 15 m water depth (0.21 to 0.27 $g \cdot cm^{-2} \cdot yr^{-1}$). Production is low in sandy reef parts. Below 30 m depth values are still at 0.14 $g \cdot cm^{-2} \cdot yr^{-1}$. Mean potential production of colonies and gross carbonate production of the whole coral community at Aqaba is lower than in tropical reefs. However, carbonate production is higher than in reef areas at the same latitude in the Pacific, thus indicating a northward shift of reef productivity in the Red Sea.

ZUSAMMENFASSUNG

Korallenwachstum

Im Roten Meer wurden Wachstumsraten und Karbonatproduktion von Scleractinia (Steinkorallen) untersucht. Es wird zum ersten Mal ein über lange Zeit belegtes kontinuierliches Korallenwachstum aus dem Bereich der Riffprovinz des Indischen Ozeans und des Roten Meeres präsentiert. Die Analysen wurden an Bohrkernen durchgeführt, die mittels eines einfachen, pneumatischen Unterwasserbohrers gewonnen wurden. Die maximale Kernlänge erreichte 320 cm, was ein Korallenwachstum von über 200 Jahren in den Saumriffen von Aqaba repräsentiert. Die Wachstumsraten von *Porites* sind für diese geographische Breite mit durchschnittlich 8,60 bis 12,52 mm/a unerwartet hoch. Das lineare Wachstum zeigt zwar deutliche Schwankungen, aber generell eine Zunahme seit etwa 1880. Der Einfluß der steuernden Umgebungsvariablen wie Temperatur, Lichtintensität und Sedimenteintrag wird diskutiert.

Die Untersuchung von Kernproben aus Kolonien der Gattung *Porites* im nördlichen Golf von Aqaba zeigte große Schwankungen der Wachstumsraten über die letzten 20 Jahre. Individuelle Wachstumsraten zeigten große Variation, selbst in Kolonien, die nahe beieinander wuchsen. Diese Schwankungen werden lokal begrenzten Unterschieden der Umweltfaktoren, wie Wassertemperatur und -trübung sowie Ausfließen von Wasser aus der Lagune zugeschrieben. Es wurde eine generelle Zunahme der linearen Wachstumsrate in Wassertiefen von 1 bis 15 m in einem relativ ungestörten Riffbereich beobachtet. Einschneidende Veränderungen der Klimabedingungen, die Auswirkungen auf das Korallenwachstum haben könnten, sind aus dieser Gegend nicht bekannt. Eine Verminderung des terrestrischen Sedimenteintrags ist die wahrscheinlichste Ursache für das beschleunigte Wachstum.

Die Auswirkungen extremer Sedimentlast auf das Wachstum von Korallen in einer gestörten Umgebung wird an einem *Porites*-Kern gezeigt, der einer Kolonie in der Nähe des Phosphatverlade-Terminals von Aqaba entnommen wurde. Die drastische Abnahme der Wachstumsrate in dieser Koralle im beobachteten Zeitraum ist gegensätzlich zum generellen Trend in den Riffen vor Aqaba und sehr wahrscheinlich durch Sedimentbelastung verursacht.

Weiter wurde ein Vergleich zwischen den jährlichen Wachstumsraten von *Porites* in verschiedenen Bereichen des Roten Meeres durchgeführt. Die Herkunft der untersuchten Proben erstreckt sich von Aqaba im Golf von Aqaba im Norden, über die nördliche und südliche Küste und Inseln vor Ägypten bis zum Golf von Tajoura (Djibouti) im Golf von Aden. Die Obergrenze des Wachstumspotentials verringert sich mit zunehmender Tiefe als Folge verringerter Lichtintensität. Die Variation der Wachstumsraten einzelner Korallen ist in flachen Bereichen sehr hoch, was darauf hindeutet, daß andere Faktoren das Korallenwachstum bedeutend verringern können, sofern Licht nicht die limitierende Größe bildet. Die Zone hoher Variabilität reicht in Aqaba (29°27´N) bis in etwa 10 m Tiefe, während sie sich in den Riffen vor Südägypten (24°30´N) bis in ca. 15 m Tiefe erstreckt. Dieser Effekt ist vermutlich eine Folge der stärkeren Reduzierung der Lichtintensität und Wassertemperaturen im Winter in den nördlichen Bereichen. Die mittleren Wachstumsraten im Flachwasserbereich nehmen mit abnehmender geographischer Breite zu und sind am höchsten in den am südlichsten gelegenen Riffen im Golf von Tajoura. Der beobachtete latitudi-

nale Gradient ist jedoch beschränkt auf die oberen 15 m der Wassersäule. Verglichen mit anderen Ozeanen ist die Abnahme des Wachstums der *Porites*-Koralle mit zunehmender geographischer Breite im Roten Meer weit geringer, und die Wachstumsraten in Aqaba sind die höchsten, die in diesen Breiten bisher gemessen wurden. *Porites*-Teil-Kolonien, die als genetisch identisch betrachtet werden, wurden einem Riffpfeiler von 6 m Höhe im mittleren Vorriff von Aqaba entnommen. Die Wachstumsraten zeigen eine große Spanne von etwa 3 bis 17 mm/a. Die Abnahme der Wachstumsrate an den Seiten dieses Pfeilers kann fast ausschließlich auf die Abnahme der Lichtintensität von 5 auf 10 m Tiefe sowie die randliche Position an den beschatteten Seiten des Pfeilers zurückgeführt werden. Kolonien, die an der Oberseite des Pfeilers wuchsen, zeigen durchweg hohe Wachstumsraten, was auf ideale Wachstumsbedingungen durch schnellen Wasseraustausch und optimale Lichtexposition schließen läßt. Resuspension von Sediment findet in dieser Position nicht statt, was vermutlich die beobachteten hohen Wachstumsraten ermöglicht. Im Gegensatz könnte Sedimentfracht durch Resuspension die Wachstumsraten von Kolonien im Vorriff vermindern, die in vergleichbaren Tiefen wachsen.

Stabile Isotope

Schwankungen der Wachstumsraten und der Verhältnisse stabiler Sauerstoff- und Kohlenstoffisotope wurden an zwei Bohrkernen untersucht, die einer großen *Porites*-Kolonie in Aqaba entnommen wurden. Die sclerochronologische Aufzeichnung im längsten Kern (320 cm) reicht bis ins Jahr 1788 zurück. Dieser Kern wurde vertikal gebohrt. Der horizontale Kern umspannt 107 Jahre Wachstum und wurde von der südlichen Flanke in die Koralle gebohrt. Die Wachstumsraten sind hoch und scheinen vom Anstieg der durchschnittlichen Wassertemperatur positiv beeinflußt worden zu sein. $\delta^{18}O$ zeigt eine Abnahme um etwa 0,4 ‰ seit 1800, was eine Erwärmung des Meerwassers um etwa 2°C anzeigen könnte. Die Zusammensetzung stabiler Kohlenstoffisotope in dieser Kolonie ist hauptsächlich durch metabolische Effekte kontrolliert, wobei der Anteil kinetischer Effekte an der Seite der Kolonie etwas stärkeren Einfluß zu haben scheint. Sowohl Sauerstoff- als auch Kohlenstoffisotope zeigen Reaktionen auf globale Veränderungen der Temperatur und des CO_2-Haushalts der Atmosphäre. Seit den 60er Jahren beeinflussten anthropogene Einflüsse drastisch die Wachstumsraten und Isotopenverhältnisse.
An einer fossilen und zwei rezenten *Porites*-Kolonien von der ägyptischen Küste des Roten Meeres wurden ebenfalls die stabilen Isotopenverhältnisse untersucht. Das Sauerstoff-Isotopenverhältnis unterstützt die Annahme, daß die heutigen Meerwassertemperaturen mit denen während des letzten Meeresspiegelhochstandes im Eem (Isotopenstadium 5e, 125.000 J.v.h.) vergleichbar sind. Die Ablagerung von Dichtebändern im Korallenskelett in Abhängigkeit von den Jahreszeiten zeigt ein vergleichbares Muster wie bei den rezenten Korallen. Bänder hoher Dichte werden im Winter (niedrige Wassertemperaturen), Bänder geringer Dichte im Sommer (hohe Wassertemperaturen) gebildet. $\delta^{18}O$ ist negativ mit $\delta^{13}C$ korreliert, wobei eine Phasenverschiebung um etwa 1 bis 2 Monate beobachtet wird. Es wird eine Abhängigkeit des $\delta^{13}C$ von der Lichtintensität und des $\delta^{18}O$ von der Wassertemperatur angenommen. Um eine Überblick über jahreszeitliche Veränderungen der Isotopenverhältnisse zu gewinnen, erscheint eine Probennahme mit einer Auflösung von vier Proben pro Jahr ausreichend.

Karbonatproduktion

In einem Saumriff vor Aqaba am nördlichen Ende des Golfs von Aqaba (29°27'N) wurden Wachstumsraten, Skelettdichte und Calcificationsraten von *Porites* untersucht, um Berechnungen der Brutto-Karbonatproduktion für Riffe in diesem Gebiet zu erstellen. Die Dichte des Korallenskeletts ist, neben der Wachstumsrate, der zweite wichtige Faktor, der die Bestimmung der Karbonatproduktion durch Korallen beeinflußt. Die Beziehung zwischen Skelettdichte und Wassertiefe wurde von verschiedenen Autoren untersucht, mit bemerkenswert unterschiedlichen Ergebnissen. Vor kurzem wurde Computer-Tomographie als eine neue Methode zur Bestimmung der Skelettdichte eingeführt und in dieser Arbeit benutzt. Die Methodik, die dabei zur Bestimmung der Dichte angewandt wurde, wird beschrieben.
Der jährliche Karbonatzuwachs der *Porites*- Kolonien nimmt mit zunehmender Tiefe als eine Funktion von abnehmender Wachstumsrate und zunehmender Skelettdichte ab. Die Calcifikationsrate von *Porites* ist am höchsten in flachen Wasser (0-5 m Tiefe) mit 0,94 $g \cdot cm^{-2} \cdot a^{-1}$ und geht auf 0,49 $g \cdot cm^{-2} \cdot a^{-1}$ unterhalb von 30 m zurück. Die Bruttoproduktion durch Scleractinia wird aus der potentiellen Produktivität und der Bedeckung des Riffs mit lebenden Korallen ermittelt. Sie ist hauptsächlich bestimmt durch die Bedeckung und in geringerem Maß von der potentiellen Produktivität. In Aqaba findet die maximale Karbonatproduktion durch Korallen an der Riffkante (0,29 $g \cdot cm^{-2} \cdot a^{-1}$) und im mittleren Vorriff in 10 bis 15 m Wassertiefe statt. In sedimentbedeckten Arealen ist die Produktion gering. Unterhalb von 30 m erreichen die Werte immer noch 0,14 $g \cdot cm^{-2} \cdot a^{-1}$. Die mittlere potentielle Karbonatproduktion durch Korallenkolonien sowie die Bruttoproduktion der gesamten Riffgemeinschaft sind im nördlichen Golf von Aqaba geringer als in tropischen Riffen. Die Karbonatproduktion ist jedoch höher als in Riffgebieten auf gleicher geographischer Breite im Pazifik, was eine Verschiebung der Riffproduktivität im Roten Meer nach Norden andeutet.

INTRODUCTION

The extreme oligotrophic conditions in the Red Sea and Gulf of Aqaba (Reiss and Hottinger 1984) and the deep euphotic zone, down to 170 m (Hallock and Schlager 1986) result in a depth distribution of hermatypic corals that is greater than in most other reef areas of the world. The production potential of modern reefs is determined in first order by the growth potential of the coral community. The composition of the coral community, its coverage of the reef bottom, and the individual growth rates are the factors which influence carbonate production. It must be noted that active coral growth is different from active reef-building by corals (Bosscher 1992). The depth for high growth rates is much shallower and, in many cases, close to the zone of light saturation (Bosscher and Schlager 1992). This has implications for the ability of a reef to keep up with rising sea level. The condition of the reef is dependent on numerous environmental variables, e.g. water temperature, light availability, sedimentation and nutrient input.

Coral growth

The temporal variability in coral growth does affect the production of carbonate substantially. Climate is the main cause for changing growth rates. It affects the environment in various ways through wind, precipitation, currents and water chemistry, temperature, turbidity, and sedimentation. Corals react to these influences in various degrees, and at the same time they record these environmental conditions in their skeleton.
Corals are exceptionally well-suited for examining the history of tropical ocean/atmosphere variability, continuously over the past several centuries. No other climate recording systems of similar fidelity, resolution, and distribution exist in tropical oceans. They can provide histories of large-scale climate variability that approach the quality and resolution of those derived from instrumental data.
The skeletons incorporate many independent chemical tracers of key oceanic and atmospheric phenomena. The tracers incorporated yield quantitative reconstructions of parameters that include sea surface temperature (SST), rainfall, salinity, vertical mixing, water mass provenance, anthropogenic influences, and others that depend on site-specific factors.

Coral paleoclimatic studies are underway at sites throughout the tropics. Most regions yield records of at least 100 years in length. From Bermuda a record spanning 1000 years is available (Pätzold and Wefer 1992). The Indian Ocean - Red Sea reef province has been a white spot on this map until today. Our objective was to fill this gap with first studies on long coral cores beginning in the Gulf of Aqaba. Further work is planned in the central and southern Red Sea.

Corals of the genus *Porites* are probably the most important reef builders due to their ubiquitism and their ability to secrete huge massive colonies. In contrast to most corals of branching and foliaceous growth form *Porites* colonies often persist in vivo position over the ages. This fact and the high age of individual colonies make *Porites* ideal recorders of environmental factors which leave their traces in the skeleton.

Stable Oxygen Isotopes

Oxygen isotope records provide an excellent tool for coral paleoclimatic studies, other chemical tracers ($\delta^{13}C$, ^{14}C, Ba, Cd, Mn) figure prominently in coral paleoclimatology in a more site-specific manner. Oxygen isotope data currently provide the "workhorse" tracer for coral paleoceanography; these measurements are readily developed in quantity and are relatively straightforward to interpret in climatic terms (NOAA 1993). Coral skeletal $\delta^{18}O$ reflects a combination of local sea surface temperature and the $\delta^{18}O$ of ambient seawater. The $\delta^{18}O$ of biogenic calcium carbonate decreases by about 0.22‰ for every 1°C rise in water temperature (Epstein et al. 1953). In corals, this effect is biologically mediated in way such that the $\delta^{18}O$ of the coral sketon is offset below seawater $\delta^{18}O$. This offset is constant within a coral genus (Weber and Woodhead 1972) for the rapidly growing central axis of the skeleton (Land et al. 1975; McConnaughey 1989a). Coral $\delta^{18}O$ records taken along the axis of maximum growth thus track ambient temperatures at subseasonal resolution (Fairbanks and Dodge 1979; Dunbar and Wellington 1981; Pätzold 1984; McConnaughey 1989a).

Stable Carbon Isotopes

Controls on skeletal $\delta^{13}C$ include the isotopic signature of seawater (Nozaki et al. 1978), the geometry and growth rate of the coral head (McConnaughey 1989a), and endosymbiontic photosynthesis (Weber and Woodhead 1970; Goreau 1977; Fairbanks and Dodge 1979; Swart 1983; McConnaughey 1989a). Endosymbiontic photosynthesis depends to a large extent on ambient light levels, mediated in the coral's environment by depth and insolation. Insolation varies both seasonally, with changes in the duration, angle, and intensity of solar radiation, and over a range of time scales in response to cloud cover variations (NOAA 1993) and solar changes (IPCC 1992).

The interpretation of the $\delta^{13}C$ signal incorporated in coral skeletons is often difficult because of complicated interactions of environmental influences and physiological processes that involve strong isotopic fractionation. The lack of detailed understanding of the factors that affect carbon isotopic fractionation during skeletogenesis produces divergent interpretations of skeletal $\delta^{13}C$ records. In certain environments coral $\delta^{13}C$ correlates highly to climatic variables. Observed correlations to factors such as insolation and ocean productivity suggest that coral $\delta^{13}C$ may provide environmental information available from no other source, if the processes controlling carbon isotope fractionation in the coral skeleton can be better constrained.

It was not beyond the scope of this study to solve these forementioned problems. We are aware of the fact that the interpretations on $\delta^{13}C$ records in our samples can only contribute another aspect on the $\delta^{13}C$ patterns in corals.

Anthropogenic influences

Corals also can provide information on environmental changes caused by human activities. Examples are radioactive isotopes derived from atmospheric nuclear testing (Knutson et al. 1972; Buddemeier et al. 1974; Druffel and Linick 1978; Druffel 1980, 1981) and industrial heavy metal contamination (Shen and Boyle 1987, 1988; Guzmán and Jiménez 1992). Increase of sediment load, pollution by chronical and catastrophic oil influx (Guzmán et al. 1991; Guzmán and Holst 1993), and eutrophication by increased discharge of sewage (Walker and Ormond 1982; Wittenberg and Hunte 1992;) caused severe damages of coral reefs in all parts of the tropical oceans. In the Gulf of Aqaba oil and phosphate pollution influence possibly the marine environment (e.g. Fishelson 1973; Wahbeh 1993). The anthropogenic influences are either recorded in the coral skeleton as chemical tracers or lead to changes of the deposition patterns and extension rates.

Structure of this thesis

The single chapters of this thesis are written in the form of papers to be published in scientific journals. Therefore some descriptions of study areas and methods occur repeatedly in different parts.
Chapter one provides a general introduction to the study area. Chapters two, three, and four deal mainly with the growth rates of the scleractinian coral *Porites* in the Gulf of Aqaba and the controlling factors over a decadal and centennial time scale. In chapter four and six studies on stable isotopic composition are described and linked to the growth record. The growth rate patterns of the Gulf of Aqaba are then compared to those of other areas in the Red Sea and the Gulf of Aden (Chapter five) and latitudinal variations discussed. Controlling factors of coral growth are the objective of a study described in chapter seven. Finally, in chapter eight a first approach to quantify carbonate production by scleractinians in the reefs of the Gulf of Aqaba, is presented.

CHAPTER ONE

STUDY AREA

Red Sea

As a part of the Syrian-African rift system, the Red Sea extends from 13°N (Bab-el-Mandeb Strait) to 30°N (Gulfs of Aqaba and Suez), over 2300 km length.
Climate of the Red Sea and the surrounding land masses is arid and hot with high evaporation rates. This results in higher water temperatures and salinities than any other oceanic waters with similar depths (Locke and Thunell 1988).
The Red Sea is famous for its classical fringing reefs which extend on both sides from the entrance of the Gulfs of Suez and Aqaba to the central Red Sea at 18-20°N. Coral reefs disappear to the south and are replaced by broad stands of mangrove, reefs constructed by calcareous red algae, and sand shores without any coral growth at the coast of Yemen and Eritrea (Sheppard and Sheppard 1991). The most northerly reefs of the Arabian region and of the entire Indian Ocean are some coral patches in the Gulf of Suez (Sheppard and Sheppard 1991). Coral reefs growing at higher latitudes can only be found in the Atlantic Ocean at Bermuda and in the Pacific Ocean at the Ryuku-Islands.

Along the eastern and western coasts of the Red Sea raised fossil reef terraces occur from the northern Gulf of Aqaba (Al-Rifaiy and Cherif 1988) down to Djibouti. These reefs developed more than 350,000 years ago in four cycles corresponding to global eustatic changes in sea level (Gvirtzman and Friedman 1977; Dullo 1990; Strasser et al. 1992).

Gulf of Aqaba

The Gulf of Aqaba (or Gulf of Eilat in the Israeli nomenclature) is the northernmost sea-flooded part of the rift system. This Gulf is a semi-isolated basin, separated from the proper Red Sea by the Straits of Tiran, a narrow passage about 250 m deep. The Gulf extends over a length of 180 km and a width of 5 to 26 km, and reaches almost 2000 m depth. The isolation and topography results in the formation of a "depth trap" for sedimentation and silt (Fishelson 1980). Thus, sedimented material can not be re-agitated by water motions. Freshwater influx occurs only episodically in winter times through wadis. This keeps planktonic primary production low, because nutrient input is limited. All these factors create an exceptional water transparency that extends the depth limit of hermatypic corals down to ca 130 m (Fricke and Schuhmacher 1983; Reiss and Hottinger 1984).
Fringing reefs, that are usually narrow, occur along eastern and western shores. The different coral habitats appear as "lagoonar reefs" with a back-reef channel, "platform reefs" which form a continuous platform from the beach rock to the fore-reef portion, and "contour reefs" which grow as a narrow band attached to the crystalline substrate on steep slopes. "Sharem reefs" develop around and within bays at the mouth of recent or fossil wadis. In addition, "coral islets" and "mangrove reefs" are described by Fishelson (1980) in the Gulf of Aqaba.

Water temperature

Although no continuous long term measurements are available, data from various sources show a strong seasonal change of water temperatures in the northern Red Sea and in the Gulf of Aqaba (Fig. 1.1, 1.2). Temperature difference between winter and summer reaches up to 10°C.

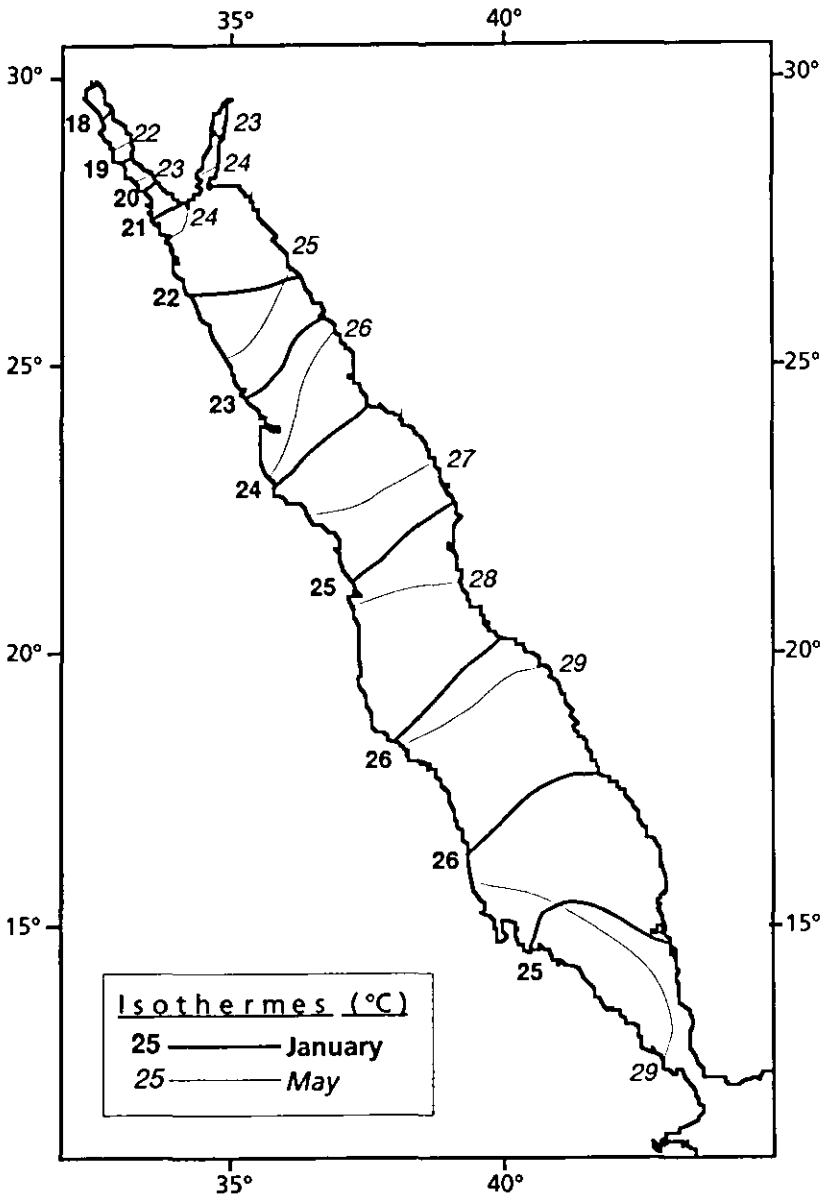

Figure 1.1
Sea surface isothermes in the Red Sea for January and May (modified from Schuhmacher and Mergner 1985).

Figure 1.2 displays temperatures published in the literature. Recently measured data in 1991/92 at the Marine Science Station (unpublished) show a slightly higher range of temperatures (Fig. 1.2). However, the variation throughout the years shows more or less the same fluctuation pattern.

Nutrients and primary production (Gulf of Aqaba)

Land-derived nutrient transport by rivers to the Gulf of Aqaba is very low. Thus, primary production in the Gulf of Aqaba is entirely dependent on nutrient supply from the Red Sea.The shallow sill at the Straits of Tiran at the southern end of the Gulf of Aqaba prevents the influx of nutrient-enriched deep waters from the Red Sea. Thus, most of the waters flowing into the Gulf of Aqaba are nutrient-depleted upper

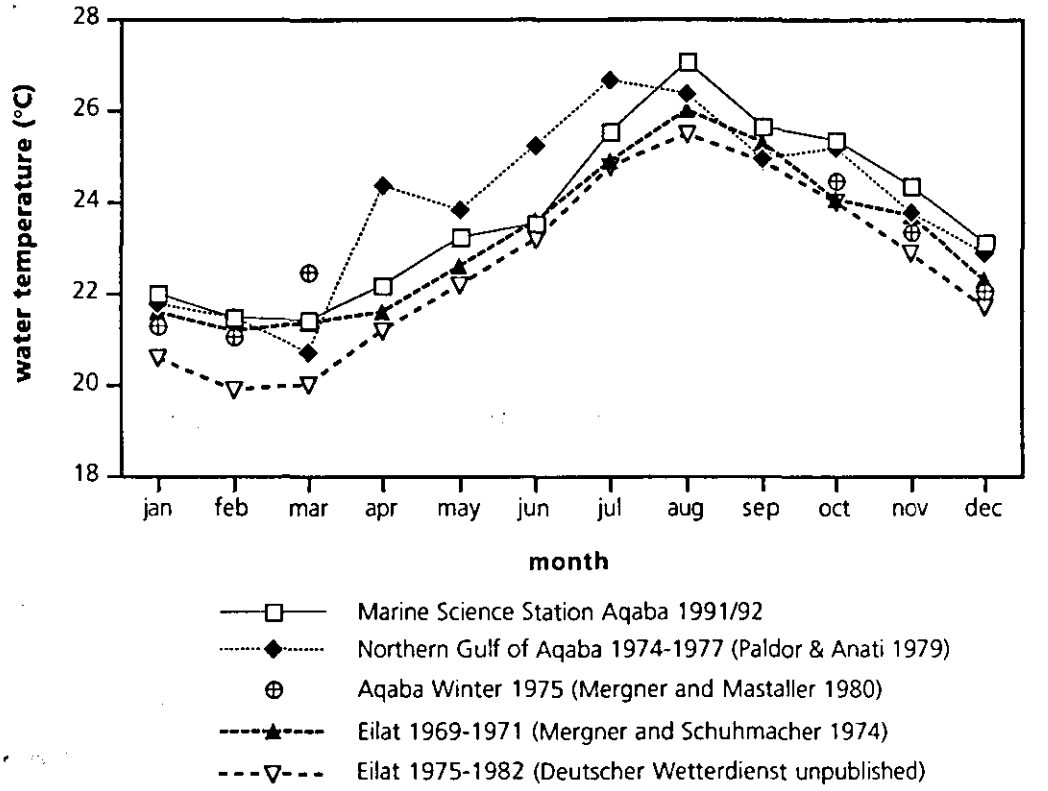

Figure 1.2 Yearly temperature range in the northern Gulf of Aqaba. Data from different sources.

Red Sea waters that give the Gulf of Aqaba an oligotrophic character during most of the year. During a short mixing period in winter, the productivity in the upper 200 m, of the water column is enhanced only in the southern part of the Gulf (Reiss and Hottinger 1984).

Currents

Surface circulation in the northern Gulf is primarily driven by prevailing northerly winds and the inflow from the Red Sea which compensates for the evaporative loss of water masses (Reiss and Hottinger 1984). A generalized pattern of clockwise circulation with deviations presumably caused by irregular coastlines, coastal and bottom topography, and wind direction. The occurrence of upwelling on the eastern side of the Gulf has been suggested but has not yet be fully documented (Hulings 1979; Hulings and Abu-Hilal 1983).

Currents on the fore-reef of the Marine Science Station (MSS) at Aqaba are generally between 3 and 10 $cm \cdot s^{-1}$, with directions either counter-current to the surface (northwards) or southwards (Hulings 1979; Schuhmacher and Mergner 1985). On the middle fore-reef a mainly southern contour-current with intermediate speed, generally up to 5 $cm \cdot s^{-1}$, is reported (Mergner and Schuhmacher 1981).

Tides

Normal tidal amplitudes are 0.4-0.7 m, while spring tides reach 1.2 m (Mergner 1979). Catastrophically low tides seem to occur in the northern part of the Gulf every 20-40 years (Fishelson 1980). These are caused by the coincidence of strong northern monsoon winds with the neap tides in September/October. Huge masses of water can be moved southwards, thereby causing a temporary catastrophic reduction in sea level. If it occurs during the hot part of the day for several hours, many corals die as a result of prolonged exposure to air and high temperatures. It is assumed that this periodic event prevents the development of a climax-situation of the coral communities (Fishelson 1980).

Salinity

Salinity of seawater in the Gulf and at the Marine Science Station at Aqaba has consistent values near 40 ‰ (surface salinity 40.829 ‰, at 10 m depth 40.654 ‰; Mergner 1979). Seasonal changes are low (0.24 ‰) and secular changes are not significant when present data are compared with those reported from the Austrian »*Pola*«-expedition of 1896 (Paldor and Anati 1979).

Morphology and sedimentary facies of fringing reefs of the Jordanian coast

The fringing reefs along the Jordanian coast are discontinuous and separated by the outlets of episodic rivers (wadis) which form sandy embayments (Gabrié and Montaggioni 1982). The lack of a spur and groove system which characterizes many reefs of the Indopacific area is due to the very low hydrodynamic conditions in the Gulf of Aqaba (Bouchon 1980). Where reefs are well developed, a succession of reef zones are present: beach zone, back reef, reef flat (with micro-atolls), and fore-reef, which can be divided into upper, middle and lower fore-reef (Mergner and Schuhmacher 1974; Gabrié and Montaggioni 1982).
Sedimentary facies of the fringing reefs is a result of input of erosion products from the Pan-African basement rocks in the hinterland and carbonate production and erosion by reef organisms. Quartzofeldspatic material is the main sediment in the beach zone. Its proportion decreases seawards, where coral and coralline algae-derived particles and foraminifera characterize the sedimentary facies (Gabrié and Montaggioni 1982).

Human impacts

Pollution of the marine environment in the Gulf of Aqaba is caused by various factors. Discharge of sewage from cities and ships possibly leads to eutrophication and increase of organic suspended matter. Heavy sedimentation generated by filling and constructing activities and the stagnation of seawater in back of solid jetties affects coral reefs and seagrass beds. Increased tourism leads to degradation of the marine environment by collection of corals and shells and coral damage by swimmers and divers. Industrialization is probably the most serious source of pollution at the Gulf of Aqaba. Thermal pollution by cooling waters from power plants and fertilizer production and chemical pollution with heavy metals and biocid anti-fouling agents has increased in the last decades (Wahbeh 1993). Probably the major type of pollution from the port of Aqaba is phosphate. Phosphate rock in the

form of flourapatite is one of the main export products of Jordan. Between 1980 and 1983 14 million tons of phosphate have been exported. The amount of phosphate export increases and is expected to reach 12 million tons per year by the year 2000. The phosphate powder is exported through Aqaba´s ports 4 km north and 7 km south of the Marine Science Station (see Chapter 3). A small proportion of phosphate is lost as dust during transportation and loading. The amount is calculated between 0.05% (Jordan Phosphate Mines Company) and 1% (Freemantle et al. 1978) and blown over the Gulf by the mostly northern winds. Abnormally high values of phosphate content in sediments are, not surprisingly, found in the vicinity of the phosphate loading berth. The level of this pollution has drastically increased in the last decades (Abu Hilal 1985).

Another source of severe stress on the natural environment is the pollution by oil in catastrophic oil spills and chronical discharge to the sea waters at Eilat and Aqaba. It has been increasing since the rapid development of the harbours in the 1960s and the construction of an oil terminal north of the Nature Reserve of Eilat at the western coast of the Gulf (Fishelson 1973; Rinkevich and Loya 1977; Mergner 1981).

CHAPTER TWO

SHORT- AND LONG-TERM GROWTH HISTORY OF MASSIVE *PORITES* SP. FROM AQABA (RED SEA)

Abstract

In this chapter the first long-term sclerochronological record from scleractinians in the Red Sea-Indian Ocean reef province is presented. A simple and handy pneumatic underwater drill was used. Length of cores reaches 130 cm and thus represents a time span of more than 100 years of coral growth in the fringing reefs at Aqaba, Jordan. Growth rates of *Porites* are unexpectedly high for reefs at this latitude. They vary between 8.60 to 12.52 mm/yr. Average linear growth rates show strong oscillations and a general increase since 1880 for a large hemispherical colony. The relationship to environmental variables as light intensity, temperature, and sediment input is discussed.

Introduction

The study of growth rates of some major reef building scleractinia at the reefs of the Marine Science Station in Aqaba, Jordan began in 1990. The coral reefs in the northern Gulf of Aqaba are amongst the northernmost reefs in the world lying at 29°27´N (Fig. 2.1).

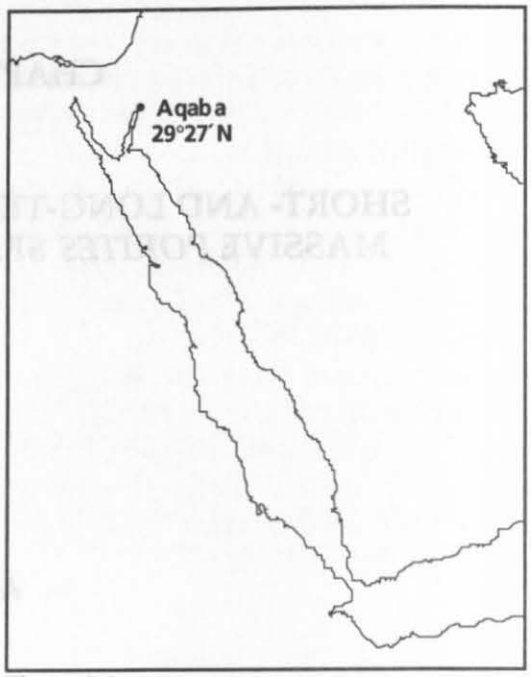

Figure 2.1
Location of the study area.

The data published on coral growth in the Red Sea and the Gulf of Aqaba are very scarce and cover either only the very recent history (Klein and Loya 1991; Klein et al. 1992, 1993) or the growth of Pleistocene corals (Klein et al. 1990).
The annual nature of density banding patterns in scleractinian corals has, since the first description by Knutson et al. (1972), been confirmed by several authors (see Barnes and Lough 1989 for a review). For shallow growing corals in the Gulf of Aqaba (Eilat), the deposition of high-density (HD) in winter and low-density bands (LD) in summer could be correlated to seasonal changes in seawater temperatures (Klein and Loya 1991; Klein et al. 1992).
For the present investigation, a Scuba-diver-operated coring device was built in order to obtain growth records of living corals covering decades of skeletal accretion patterns in different depths in the Gulf of Aqaba.
Several attempts of underwater coring are recorded in the history of coral reef research. The dimension of the operations as well as the means used vary.
After the early crude method of blasting reef sections, hydraulic submersible drills have widely been used with great success (Macintyre 1975; Hudson et al. 1976; Hudson 1977; Druffel and Linick 1978; Hudson 1981; Macintyre et al. 1981; Druffel 1982; Schneider and Smith 1982; Isdale 1984; Barnes and Lough 1989; Winter et al. 1991).
The first drill for underwater coring driven by pressured air is described 1975 at Lizard Island, Great Barrier Reef (Davies and Stewart 1976) but as far as we know, no study on cores obtained with this drill has been published. In contrast to their drill we didn´t use an impact tool and we could work independently from a boat. Further attempts were made by Stearn and Colassin (1983) who gave a description of an underwater pneumatic hand drill. Potts et al. (1985) took short cores (10-15 cm long) of *Porites* with a hole saw welded to a 30 cm pipe and mounted in a pneumatic drill. At Curaçao the growth rates of *Montastrea annularis* were recently studied on cores taken by a pneumatic drill similar to our equipment (Bosscher 1992).

The intention was to build a simple, cheap and small coring tool, which can be operated by one Scuba-diver independent from any supply on the sea-surface. For our fieldwork, we wanted to avoid some disadvantages of the already described

machines (large size, limited mobility, and/or the need of energy support from a boat). A technique for gaining long coral cores with a handy instrument has been developed.

Besides sampling of several smaller individual colonies over the depth range to 45 m see Chapter 3 and 5) we wanted to get records on growth rate and proxy dates over a longer period. Another important objective was the possibility of comparing with other long-term growth records in corals in other localities of the world. In the last 20 years several successful attempts of large scale coring in living corals have been made (Macintyre 1975; Hudson et al. 1976; Druffel and Linick 1978; Macintyre 1978; Hudson 1981; Druffel 1982; Isdale 1984).

Materials and Methods

Field work

Due to the availability of Scuba-tanks and the need for easy handling from small boats we chose compressed air as the best power source for the drill. A commercially available RODCRAFT 4200-pneumatic drill was selected on the basis of its size and technical characteristics. It works at a speed of 2000 rpm with an air consumption of 220 l/min under full power. Although the operating pressure is 0.6 MPa (6 bar, manufacturer´s information), we operated the drill at a pressure of 8-9 bar which is the pressure supplied by an ordinary first stage regulator for Scuba-diving. We used in the first year a SCUBAPRO Mark II first stage. We later improved the system by using a balanced first stage (SCUBAPRO Mark X) in order to have a better air supply in water depths greater than 10 m. The air came from 15 l dive tanks, pressurized to 200 bar, which provides an air capacity of 3000 l. The connection between tank and drill was a standard industrial pressure hose of 2 m length. The core-cutter is a diamond-tipped steel tube of 300 mm length and an outside diameter of 41 mm (36 mm inside) manufactured by DIA-G Diamantwerkzeuge GmbH, Kiel (Fig. 2.2). With this instrument we could easily obtain cores of 30 cm length from different massive growing genera like *Platygyra, Porites, Hydnophora, Favia* and *Favites*.

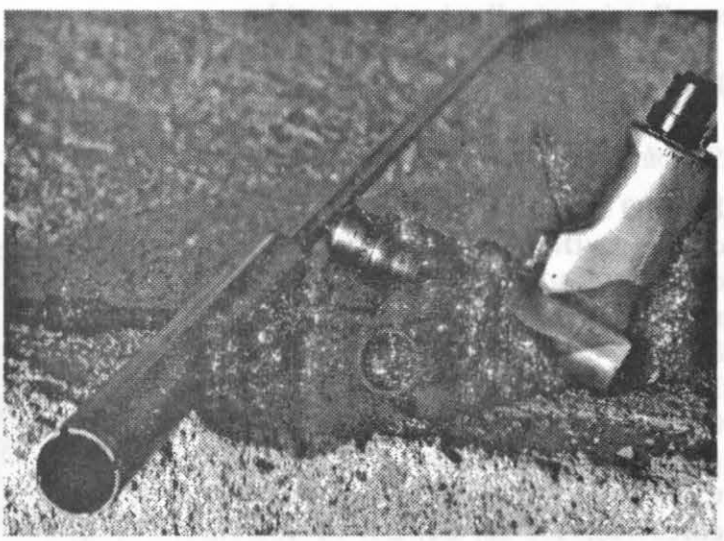

Figure 2.2 Pneumatic drill and core cutter

The initial millimeters were drilled by turning the core barrel by hand several times on the coral surface. No template was necessary for the drilling procedure. Drilling

of one 30 cm core took only a few minutes. Depending on the rigidity of the coral we could obtain up to four cores out of one 15l-tank.

In 1992 an unusual big colony of *Porites* sp. in front of the reef edge of the reef south of the Marine Science Station in Aqaba was found. The colony grows from a depth of ca 5 m to a height of 3.5 m with a maximum diameter of approximately 5.5 m. To get a longer record of coral growth history and regional climate we constructed an extension of 100 cm length to the drill bit. The extension is made from a 17 mm diameter steel rod with a screw thread attached to the core barrel. We could obtain five 130 cm long cores in 30 cm lengths with 100% recovery from different sides of the colony (Fig. 2.3).
Occasionally, the core broke inside the core barrel and caused grinding of two pieces of core before they were removed. However the maximum loss of core material in these cases was only 1-2 mm of length. We released the cores from the coral head by breaking it with a long thin steel rod. The cores were pulled out of the hole after drilling with the core barrel. To reduce the inside diameter of the core barrel we put small strips of adhesive tape inside.
The core holes were filled with cement plugs after drilling to prevent bioerosion (see Hudson 1981; Winter et al. 1991).

Sample collection

Five 30 cm cores of *Porites* sp. were drilled at the reef edge (1-3 m water depth; cores 1, 2, 13, 23) and the fore-reef (14.5 m water depth; core 6) of the fringing reef south of the Marine Science Station in Aqaba, Jordan (29°27´N). The cores were drilled parallel to the growth axis (perpendicular to the coral surface, Fig. 2.3). Five cores (18, 19, 20, 21, 24) of 130 cm length were extracted from the "big" *Porites* at different sides of the colony (Tab. 2.2).

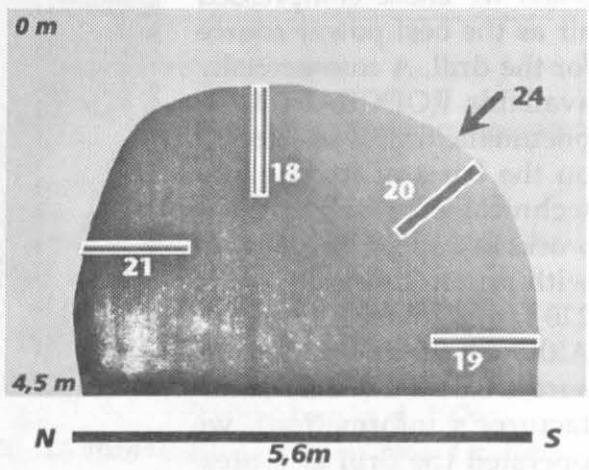

Figure 2.3 Position of cores taken from the "big" Porites-colony. Core 18-21 were drilled along the N-S direction, core 24 on the SW side of the colony.

Processing core samples

All cores were sectioned using a diamond rock saw to a thickness of ca 3mm. Coral slabs were cleaned for several hours in an ultrasonic bath (demineralized water) to remove saw mud.
The slabs were X-rayed using a SEIFERT-industry-X-ray-unit (Type ERESCO 120kV/5mA) at 35kV and 5mA to reveal annual density banding (Knutson et al. 1972; Hudson et al. 1976). Agfa Gevaert Structurix D4 film was used. Growth rates were measured along the major (vertical) growth axis (Buddemeier et al. 1974; Logan and Tomascik 1991) from positive prints as the distance between the top edge of low-density bands (LD) which are the most distinct boundaries in our samples.
Those parts of the cores not drilled parallel to the growth axis were rejected.

Assessment of band width from X-ray images

To find out the effect of subjective measurements, three persons measured the cores of the "big" *Porites*-colony independently. The criteria to define a HD/LD band couplet were standardized before and the top of LD bands was taken as the beginning and as the end of a coral's year, respectively. As expected, the results of the measurements differed in the range from ca 1 to 2 mm. The mean growth rates were then computed for each data series and compared with each other (Tab. 2.1).

Table 2.1 Independent measurements by three persons measured at the same X-radiographs from cores of the *Porites*-colony. Values are mean annual growth rates (mm/yr) computed over periods of 47 to 188 years (cf. Table 2.2).

	person 1	person 2	person 3	max. difference
core 18	12.03	11.96	12.38	0.42
core 19	10.86	9.59	10.76	1.27
core 20	11.07	11.69	11.64	0.62
core 21	10.28	10.46	10.89	0.61

The individual measurements agreed with each other very well. Therefore we conclude that separate measurements by different persons do not improve the quality of resulting data.
The measurement of growth band width is affected by the difficulty to get an exactly parallel cut to the growth axis. If we measure a growth band which is cut in an angle to the growth axis, we will get a seemingly wider band. The resulting magnification is a function of the angle. This effect influences the results notably. A growth band cut at 20° deviation gives an apparent magnification of 6% (Fig. 2.4). We corrected the band width measured on X-radiographs (eq. 1) and used these results in the assessment of growth rates.

Growth rates were computed as:

$$W_{real} = W_{meas} \cdot \cos \alpha \qquad (1)$$

where W_{real} = real band width

W_{meas} = measured band width

α = angle between growth direction and coral slab plane

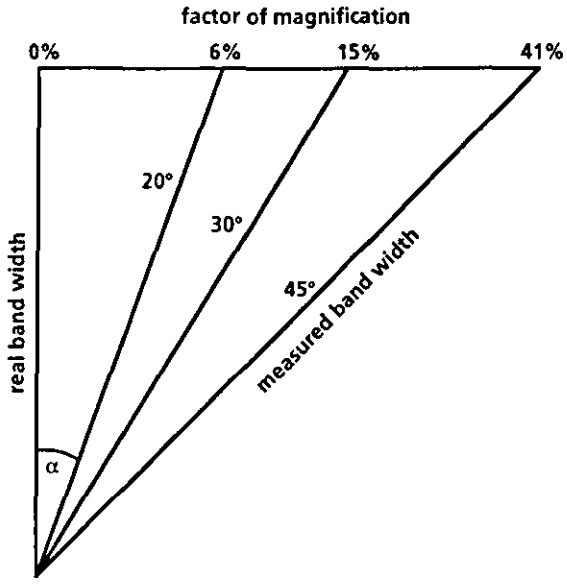

Figure 2.4
Difference between measured and real band width in oblique sections of coral slices.

Results

The first sclerochronological record of coral cores in the Red Sea reported in this paper reaches back to the year 1880 (Tab. 2.2). This means that we have a look at skeletal carbonate deposited at a time when the coral reefs in the Gulf of Aqaba were visited by Johannes Walther. He was one of the first geologists to describe these modern reefs and their uplifted Pleistocene counterparts (Walther 1888).

Mean linear growth rates for colonies growing in shallow water (1-3 m) at or close to the reef edge lie between 8.60 and 12.52 mm·yr^{-1} with maximum values of 16 mm (Tab. 2.2). Thus, growth rates of *Porites* sp. at Aqaba are relatively high for reefs growing at this latitude. At the Midway and Kure Islands in the Pacific growth rates for *Porites lobata* do not exceed 5 mm·yr^{-1} (Grigg 1982).
A marked difference of coral growth rate between cores taken at shallow waters and one core from 14.5 m water depth (core 6) is obvious (Tab. 2.2). The growth rate of this coral is only 4.18 mm·yr^{-1}. Of course one sample cannot provide statistical significance, but from the study of other samples (see Chapter 5) a clear decrease of growth rates with increasing depth is observed.

Table 2.2 Averages of the linear growth rate (± Standard Deviation)

Core sample	Core position	Water depth (m)	Average linear growth rate (mm/yr)		Number of years
1	top	reef edge (1-3)	9.87	(±1.34)	8
2	top	reef edge (1-3)	10.94	(±2.89)	20
13	top	reef edge (1-3)	8.60	(±1.14)	14
23	top	reef edge (1-3)	9.33	(±1.55)	15
6	top	14.5	4.18	(±0.99)	20
18	top	1.5	12.52	(±1.79)	188
19	horizontal (south)		10.72	(±2.20)	108
20	45° (south)		10.94	(±1.94)	77
21	horizontal (north)		10.27	(±1.27)	47
24	45° (SE)		12.13	(±1.73)	87

Average linear growth rates for the five cores taken from the "big" *Porites*-colony show some interesting changes (Fig. 2.5). From 1880 to the first decade of this century we see an increase of mean annual band widths from 10 to 12 mm·yr^{-1}, followed by a decrease to the 1940s, strong oscillations between 10 and 12 mm·yr^{-1} until the end of the 1960s and a final, remarkably steep, rise to a rate of ca 14 mm·yr^{-1},which hasn't stopped yet.

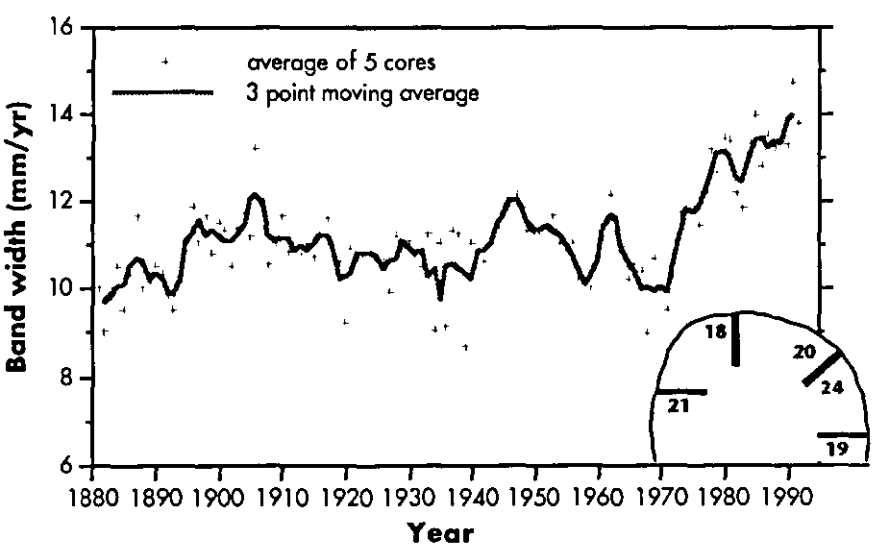

Figure 2.5 Linear growth rates of *Porites* sp. ("big" colony). Data are averages of five cores, smoothed with 3 point moving average.

Discussion

The decrease in linear growth rates of most scleractinian corals with depth is widely accepted (Buddemeier et al. 1974; Baker and Weber 1975; Dustan 1975; Highsmith 1979; Hubbard and Scaturo 1985; Logan and Tomascik 1991; Bosscher 1992) and best explained as an effect of decreasing light intensity (Baker and Weber 1975; Huston 1985). Our data do support this for the first time in the Red Sea.
Light and temperature have been shown to be the most important variables controlling skeletal growth of scleractinian corals (Knutson et al. 1972; Baker and Weber 1975; Dodge and Lang 1983; Wellington and Glynn 1983; Huston 1985; Tomascik and Logan 1990; Klein and Loya 1991; Logan and Tomascik 1991; Bosscher 1992). Other factors influencing coral growth are hydraulic energy (Scoffin et al. 1992), light intensity, sediment resuspension/turbidity (Dodge et al. 1974; Hudson 1981) and nutrients (Dodge and Vaisnys 1975). Endogenic factors (e.g. reproduction) are of varying importance (Wellington and Glynn 1983; Klein and Loya 1991).
Sea-surface temperature and light intensity in the Gulf of Aqaba show strong seasonal patterns with highest temperatures occuring in July and August (26-27°C) and minimum in March (~20°C, Paldor and Anati 1979; Klein and Loya 1991) .
Klein and Loya (1991) suggested that seawater temperature and light intensity are the major factors influencing density patterns in *Porites* corals in the Red Sea. We believe that the same is valid for coral growth rates.
The question arises whether the fluctuation (and/or the overall increase) in coral growth rate during the last 108 years in the Gulf of Aqaba is related to the well-documented warming of the atmosphere in the northern Hemisphere (air-land) by about 0.5°C (see Grigg 1992) and the increase in global sea surface temperature (SST). Routine measurements of SST have been carried out since the middle of the nineteenth century. There is strong evidence that these data represent real global fluctuations, at least in the latitude range 40°N to 40°S. These data are well-correlated with solar irradiance (Reid 1991). For the time period represented by our coral cores a SST decrease of 0.3°C from 1880 to a minimum in 1905 is recorded. At the same time an increase in growth rates occurs. A warming of 0.5°C in the first half of the twentieth century coincides with decreasing growth. The period of cooling during the 1960s (-0.1°C) was followed by a steep upturn since about 1970 (Reid 1991). The variation in growth rates for this time does not follow the temperature variations. This might be due to lag time effects. It seems that the growth rates of the investigated coral are in the long-term trend negatively correlated with the variations in global SST. This relation is not strong and is most probably modulated by other influences.
Friis-Christensen and Lassen (1991) could show a close association between northern Hemisphere temperature anomalies and the variation of sunspot cycle length. Could these changes affect the growth of coral heads in the Gulf of Aqaba? We compared the growth rate curve for our cores 18 to 21 with their data sets and found some similarities which are clearest in the growth record for core 18. Probably this core, in its position at the top of the colony, shows effects of changing light levels more clear than cores at the shaded sides of the colony. Most noteworthy are a minimum in the early decades of this century, another minimum in the 1960s and a steep rise since the early 1970s which is also present in all other cores (Fig. 2.5). But there is a major deficiency in the similarity: the steep rise of temperature anomalies from the 1920s to

the 1950s has no counterpart in the coral's growth record. One of many possible explanations for this could be local climate changes which differ markedly from the global pattern. Unfortunately continuos long-term records of local climate are not available, even though Paldor and Anati (1979) disregarded secular changes of oceanographic data in the Gulf of Aqaba by comparison of April-observations from the »*Pola*«-expedition of 1896 with those during 1974 to 1977. We expect that stable isotope data (Chapter 4) will give a more clear picture of the regional climate in the last 200 years.

The strong decrease in growth rate in the 1960s and the increase since the early 1970s coincides with major building activities along the coastline south of Aqaba. A road and harbour were built and the Marine Science Station was founded. The road to the southern harbour comes quite close to the reef and functions probably as a barrier, although there are large gullys as outlets for the wadis which drain the hinterland during rainfall. Even though the region presently has extremely dry conditions (with episodic precipitation during winter (Hulings 1989) this might have reduced the continuous wind-driven sediment input.

Sedimentation is known to decrease coral growth (Dodge and Vaisnys 1977; Cortés and Risk 1985). Reduced sediment load, therefore, should enhance coral growth. At present, it is difficult to determine if the observed trend in growth rates is natural or related to man's activities.

CHAPTER THREE

VARIATION IN ANNUAL BAND WIDTH OF *PORITES* SP. AT AQABA, GULF OF AQABA, RED SEA

Abstract

Studying core samples of the genus *Porites* in the northern Gulf of Aqaba, has revealed large variations in the growth rate of this coral over the last 20 years. Individual growth rates show high variations even in colonies growing close together. These variations are attributed to locally restricted differences of reef environment, like water temperature, outflow from the lagoon, and turbidity. A general increase in linear extension rate in a relatively healthy reef area was observed at a depth range from 1 m to 15 m. A major variation in climate conditions affecting coral growth was not recorded. A reduction in terrestrial sediment influx is the most likely reason for an accelerated growth. The effect of extreme sediment load on coral growth rates in a stressed environment is demonstrated on one *Porites*-core taken from a colony growing in vicinity of the phosphate loading berth at Aqaba. The drastical decrease in growth rate of this coral in the observed time span is contrary to the general trend at Aqaba's reefs and is most probably caused by sediment stress.

Introduction

Measuring the variation in growth of scleractinian corals at different sites of one reef and comparing it with the growth pattern in a stressed environment were the objectives of this study. Samples were taken at the Jordanian Red Sea coast in the northern Gulf of Aqaba. The fact of changing growth rates in different habitats is well known (e.g. Brown et al. 1986; Scoffin et al. 1992). But do corals show the same response to the variation of regional environmental conditions notwithstanding the influence of their individual habitat? In other words, are the regional signals strong enough to override the conditions determining individual growth patterns? If this is the case, only a few well chosen samples could give us an impression of the history of growth for a greater part of a reef. We chose the well studied reef at Aqaba´s Marine Science Station to sample cores from several colonies of *Porites* sp. This genus is present in reefs over the entire Indo-Pacific. Growth rate patterns were studied in the Pacific Ocean at Hawaii (Grigg 1982), the Philippines (Pätzold 1984), and the Great Barrier Reef (Isdale 1977; Barnes and Lough 1989; Lough and Barnes 1992). In the Indian Ocean *Porites* was studied by Guillaume and Carrio-Schaffhauser (1985) and Guillaume (1988). This genus shows well-defined annual density banding like the intensively studied species *Montastrea annularis* in the Caribbean (Hudson et al. 1976). Growth chronology can thus be established quite easily. Colonies of *Porites* occur frequently in the reefs in the Gulf of Aqaba and the Red Sea and are therefore suitable to compare the different sites. Studies on the influences of environmental variables on growth rates of corals growing in a reef in the Gulf of Mexico were carried out by Dodge and Lang (1983). Common patterns in coral growth variations over a time span of ca 80 years could be related to water temperature and river discharge.

Water depth, turbidity, and temperature appear to be the key elements that affect growth and survival of *Montastrea annularis* at Florida´s coral reefs (Hudson 1981). Depressed growth rates coincide with times of increased dredge and fill activities in the Florida Keys.

An inter-site comparison of skeletal growth patterns in a 10-year period from St. Croix showed significant differences which were related to pollution by sewage and dredging (Dodge and Brass 1984). Negative influence of phosphate and oil pollution on the coral reef community of the Gulf of Aqaba, namely high mortality and eutrophication, was reported in some papers (Fishelson 1973; Freemantle et al. 1978; Walker and Ormond 1982; Abu Hilal 1985). A number of papers are published on the effects of sediment load on coral growth and reef communities. For example, eutrophication and sedimentation causes less abundance and higher mortality of juvenile corals (Te 1992; Wittenberg and Hunte 1992). Coral growth rates are depressed by sedimentation (Dodge et al. 1974; Dodge and Vaisnys 1977; Hudson 1981; Cortés and Risk 1985; Hubbard 1986; Guzmán and Jiménez 1992; Hands et al. 1993). Deleterious effects of oil pollution on reef corals and coral reproduction were reported by Fishelson (1973) and Guzmán and Holst (1993, with a review).

Materials

Sample collection

Cores of *Porites* sp. colonies were drilled at the fringing reef south of the Marine Science Station (MSS) at Aqaba, Jordan (29°27′N) and at a sediment-polluted site at the phosphate loading berth of Aqaba, 4 km north of the MSS (Fig. 3.1). At the MSS from the reef edge we sampled four cores at 1 to 3 m water depth. One sample was obtained from the fore-reef (14.5 m water depth).

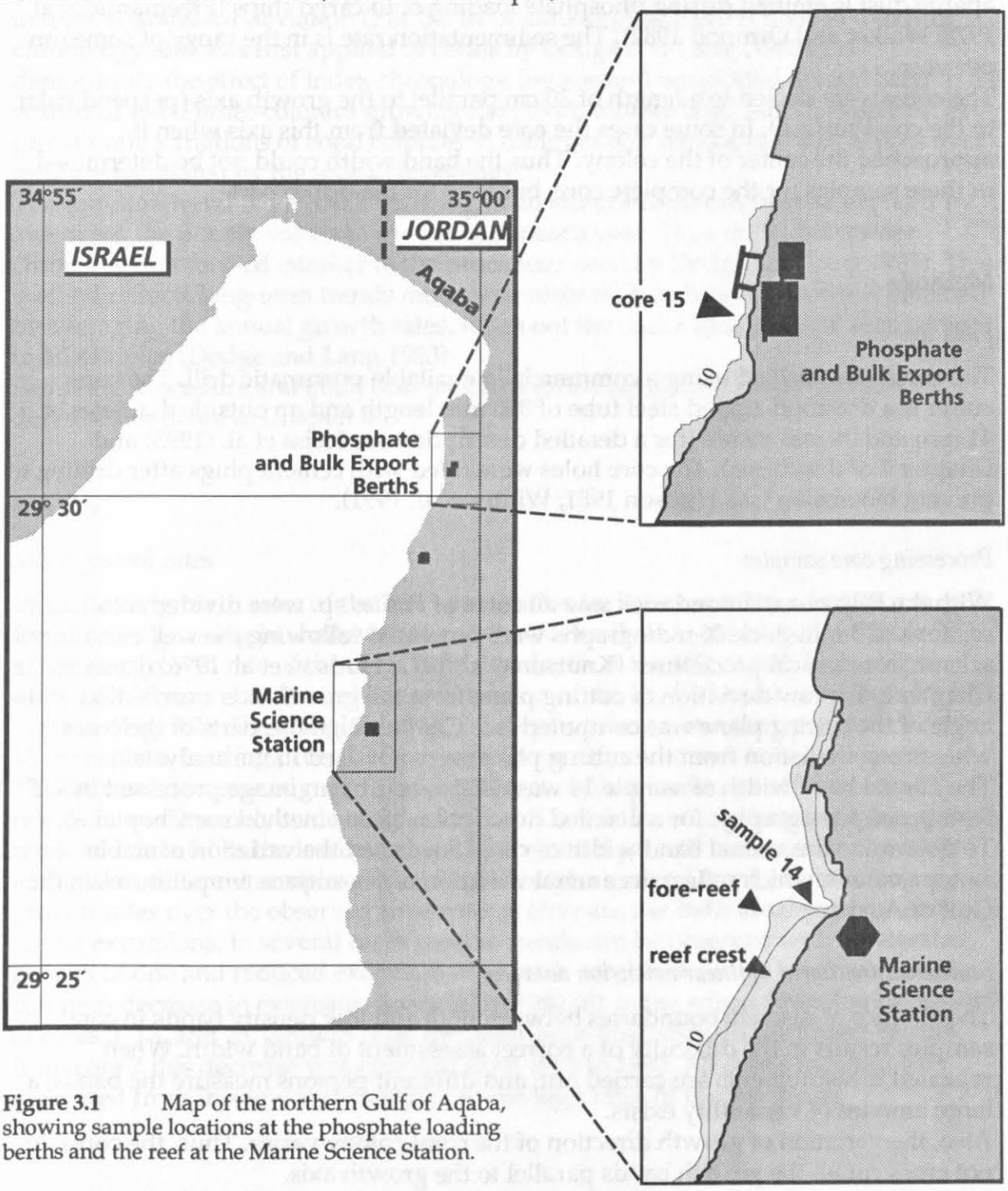

Figure 3.1 Map of the northern Gulf of Aqaba, showing sample locations at the phosphate loading berths and the reef at the Marine Science Station.

The upper part of a longer core from a *Porites* colony in the southern fore-reef was also included in this comparison (core 18, water depth 1.5 m, see Chapter 2; Heiss et al. 1993), as well as one colony growing at a depth of 8 m at the MSS bay (Fig. 3.1). The greatest distance between two sampling sites at this reef is ca 500 m (sample 14 - core 18).
One core of *Porites* sp. (core 15) was taken at a depth of 7 m close to the phosphate loading berth (Fig. 3.1). The colony grows at a reef knob together with other scleractinians ca 1-2 m above the sediment bottom. At this site a huge amount of apatite dust is emitted during phosphate loading onto cargo ships (Freemantle et al. 1978; Walker and Ormond 1982). The sedimentation rate is in the range of some dm per year.
The cores were drilled to a length of 30 cm parallel to the growth axis (perpendicular to the coral surface). In some cases the core deviated from this axis when it approached the center of the colony. Thus the band width could not be determined in these samples for the complete core, but only for the upper part.

Methods

Field work

The cores were drilled using a commercially available pneumatic drill. The core-cutter is a diamond-tipped steel tube of 300 mm length and an outside diameter of 41 mm and 36 mm inside (for a detailed description see Heiss et al. (1993) and Chapter 2 of this thesis). The core holes were filled with cement plugs after drilling to prevent bioerosion (see Hudson 1981; Winter et al. 1991).

Processing core samples

With the help of a diamond rock saw all cores of *Porites* sp. were divided into sections ca 3 mm thick. X-radiographs were processed following the well established sclerochronological procedures (Knutson et al. 1972; Hudson et al. 1976) described in Chapter 2. For low deviation of cutting plane from the growth axis a correction of the angle of the cutting plane was computed (see Chapter 2), those parts of the cores with strong deviation from the cutting plane were not used in the analysis.
The annual band width of sample 14 was determined by an image processed by CT (computed tomography, for a detailed description of this method see Chapter 8).
To determine the annual band width of core 15 we used the variation of stable isotope values, which reflect the annual variation of sea surface temperatures in the Gulf of Aqaba.

Statistical treatment of linear extension data

The absence of discrete boundaries between high and low density bands in coral samples results in the difficulty of a correct assessment of band width. When repeated measurements are carried out, and different persons measure the bands, a large amount of variability exists.
Also, the variation of growth direction of the coral colony varies. Thus, the cores do not cross cut all the growth bands parallel to the growth axis.

Therefore, a sophisticated statistical treatment would give a false feeling of precision, which does not exist in the raw data. We smoothed the annual band widths using a 3-point moving average and fitted the resulting data points with a linear curve fit (least squares method, Fig. 3.5a). This reduces (a) the inaccuracy of band width measurements and (b) annual growth variations.
In addition to analyzing the raw growth data measured in $mm \cdot yr^{-1}$ we computed the z-score for each coral. Values are normalized by this procedure into deviations from the mean for a given coral, where the mean = 0 and annual growth rate is expressed in units of standard deviation (Fig. 3.5 b). A similar procedure is used in tree-ring chronology and was first applied to corals by Dodge and Lang (1983). To demonstrate the effect of index chronology (by z-score) we plotted annual band widths of two *Porites*-colonies growing next to each other (Fig. 3.6). Comparison of growth rate variations of coral colonies in different reef parts and water depths over time are facilitated by the index chronology.
The common trend of all corals growing in an environment can then be exposed by averaging the z-score values of the corals for each year. Thus an "index master chronology" is formed (similar to the procedure used by Dodge and Lang 1983). This method reflects long-term trends more accurately than a chronology that is obtained by averaging the annual growth rates, when not the entire time range is represented in all samples (Dodge and Lang 1983).
Sampling procedure and analytical methods for stable isotope determination is described in detail in Chapter 4.

Results

Mean growth rates

Mean linear growth rates of the last two decades lie between 8.70 and 14.39 $mm \cdot yr^{-1}$ for colonies growing in shallow water (1-3 m) at or close to the reef edge (Table 3.1). The mean growth rate of the coral from 8 m depth at the MSS is still high with a mean of 9.30 $mm \cdot yr^{-1}$. Annual linear extension of the studied coral samples is highly variable (Fig. 3.2). The box plot in Fig. 3.2 displays the outstanding position of core 15 (phosphate loading), core 18 (southern fore-reef), and core 6 (middle fore-reef). The unusual decrease of growth rates at the phosphate-sediment affected coral results in an extremely wide range of values. Core 18 has considerably higher growth rates, and core 6 has the lowest values. Inter-annual growth rate variations are not identical in different samples (Fig. 3.5). Although a general trend to increasing growth rates over the observed time span is obvious, the individual patterns show strong excursions. In several cases reverse trends can be observed with accelerated growth of one and reduced extension of another coral in the same environment. A common decrease in extension occurred in 1980/81 in the sclerochronological record of cores 2, 13, and 23. Growth rates dropped simultaneously. In the longer record from core 2 this decrease was constant from 1974 to 1980. All corals continuously recovered from this low and switched to the high rates of the last years.

Table 3.1 Averages of the linear growth rates of *Porites*-cores from the Jordanian Red Sea coastal fringing reefs (± standard deviation). All cores were drilled from the top of the colonies.

Core sample	Site	Water depth (m)	Average linear growth rate (mm/yr)	Number of years
18	MSS fore reef	-1.5	14.39 (±1.16)	20
23	MSS reef crest	-1.5	9.33 (±1.55)	15
1	MSS reef crest	-2	9.64 (±1.41)	8
2	MSS reef crest	-2	11.94 (±1.47)	20
13	MSS reef crest	-1-3	8.70 (±1.44)	14
14	MSS Univ. Bay	-8	9.30 (±2.20)	11
6	MSS fore reef	-14.5	4.18 (±0.99)	20
15	Phosphate loading berth	-7	10.17 (±4.63)	9

The decrease in growth with increasing depth is demonstrated by core 6 (14.5 m, Table 3.1, Fig. 3.2). The mean growth rate of this coral is only 4.18 mm/yr. Of course, one sample cannot provide statistical significance, but from our other samples (Chapter 5) this relation is supported.

The core from the phosphate loading berth needed special attention, as its density banding is not as well defined as in the samples from the undisturbed reef area. This type of irregular banding could be produced by events that cause the coral to produce stress bands, that are not linked to normal seasonal changes. The production

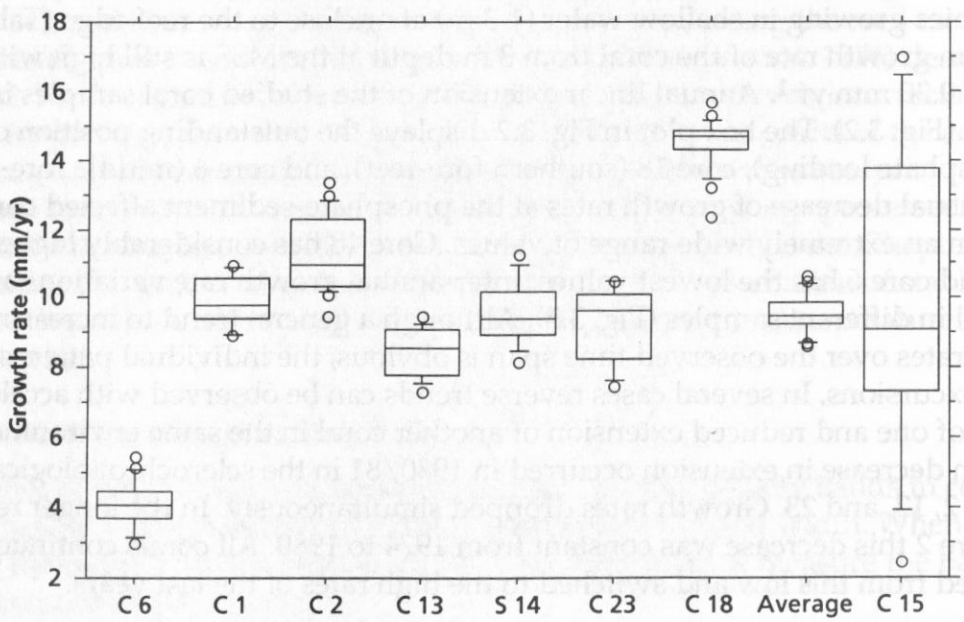

Figure 3.2 Box plot of growth rate for all samples showing the 10th, 25th, 50th, 75th and 90th percentiles. The specific growth rate patterns of the deep colony C6, the "big" colony C18 and the colony at the phosphate loading berths (C15) are conspicious.

of stress bands is a well known phenomenon (Brown et al. 1986) that may camouflage annual growth patterns.
In order to get another chronology which is independent from sclerochronology we used stable oxygen isotopes as an indicator of annual growth. The assessment of annual band width by oxygen isotope analysis provides an independent method to control the results obtained from density banding (e.g. Klein et al. 1992). The results are plotted in Figure 3.3 (Carbon isotopes are shown in Chapter 4 as well as a more detailed discussion of stable isotope composition). The maximum width for one HD/LD band couplet is 17 mm, the minimum 2.5 mm, and the mean is 10.17 mm (± 4.63 mm). The annual band width decreased drastically in the nine years of the growth record revealed by oxygen isotope variation (Fig. 3.4) which is in good accordance with previous results from this colony by sclerochronology (Dullo et al. 1993).

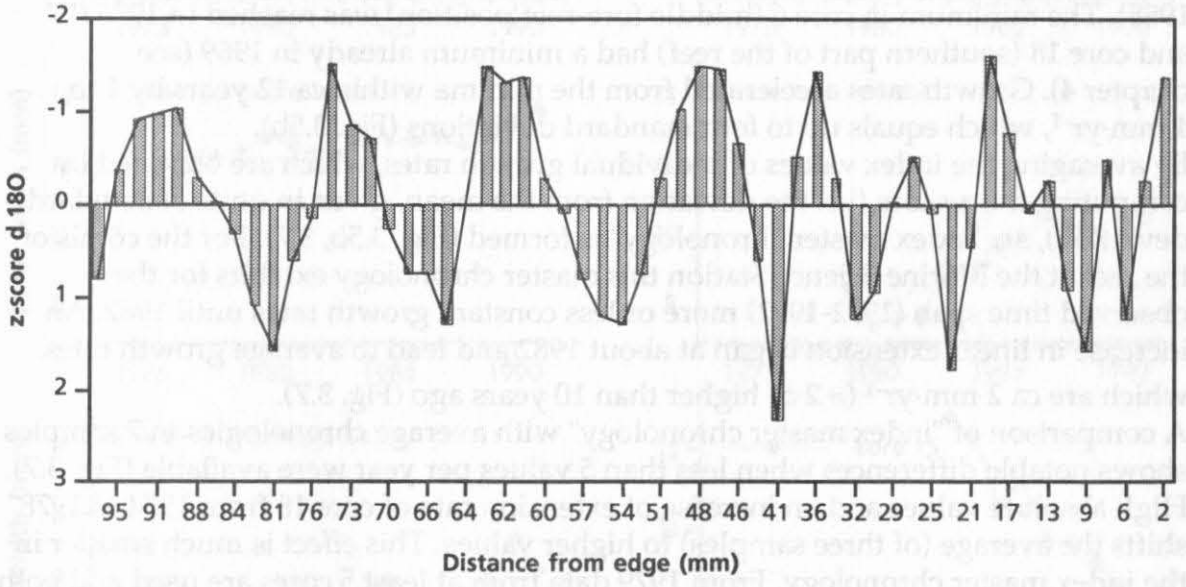

Figure 3.3 Oxygen isotope composition of core 15, drilled at 7 m depth at the phosphate loading berths. Values are plotted in units of standard deviation. Negative values represent light isotope composition (warm season), positive values heavy isotope composition. Growth direction is from left to right, living surface at zero in October 1992.

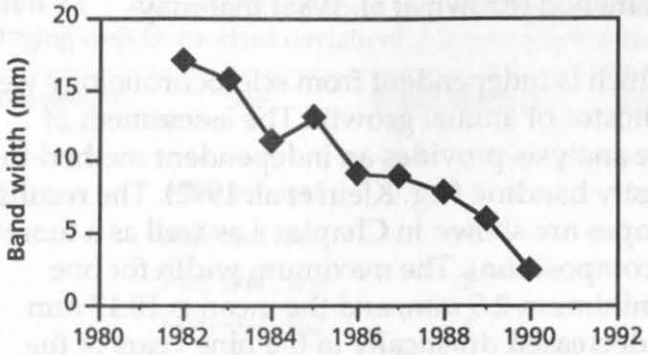

Figure 3.4
Annual band width of core 15 from 1983 to 1991 obtained from the oxygen isotope curve.

Growth rates of MSS corals 1972-1992

All corals growing in the reef of the Marine Science Station show a general trend to an increase in linear extension rate for the last two decades, when a linear curve fit is applied (Fig. 3.5 a). Corals that grew close to the northern reef crest (core 2, 13, 23) had a simultaneous minimum of extension in 1980 (the record of core 1 starts in 1985). The minimum in core 6 (middle fore-reef position) was reached in 1976/77 and core 18 (southern part of the reef) had a minimum already in 1969 (see chapter 4). Growth rates accelerated from the minima within ca 12 years by 1 to 4 mm·yr^{-1}, which equals up to four standard deviations (Fig. 3.5b).
By averaging the index values of individual growth rates, which are obtained by computing the z-score (i.e. the deviation from the mean, given in units of standard deviation), an "index master chronology" is formed (Fig. 3.5b, 3.7). For the corals of the reef at the Marine Science Station this master chronology exhibits for the observed time span (1972-1992) more or less constant growth rates until 1982. An increase in linear extension began at about 1982 and lead to average growth rates, which are ca 2 mm·yr^{-1} ($\approx 2\,\sigma$) higher than 10 years ago (Fig. 3.7).
A comparison of "index master chronology" with average chronologies in 7 samples shows notable differences when less than 5 values per year were available (Fig. 3.7). High absolute values and an increase of extension rate of core 18 from 1974 to 1978 shifts the average (of three samples) to higher values. This effect is much smaller in the index master chronology. From 1979 data from at least 5 cores are used and both chronologies display a similar variation of growth rates.

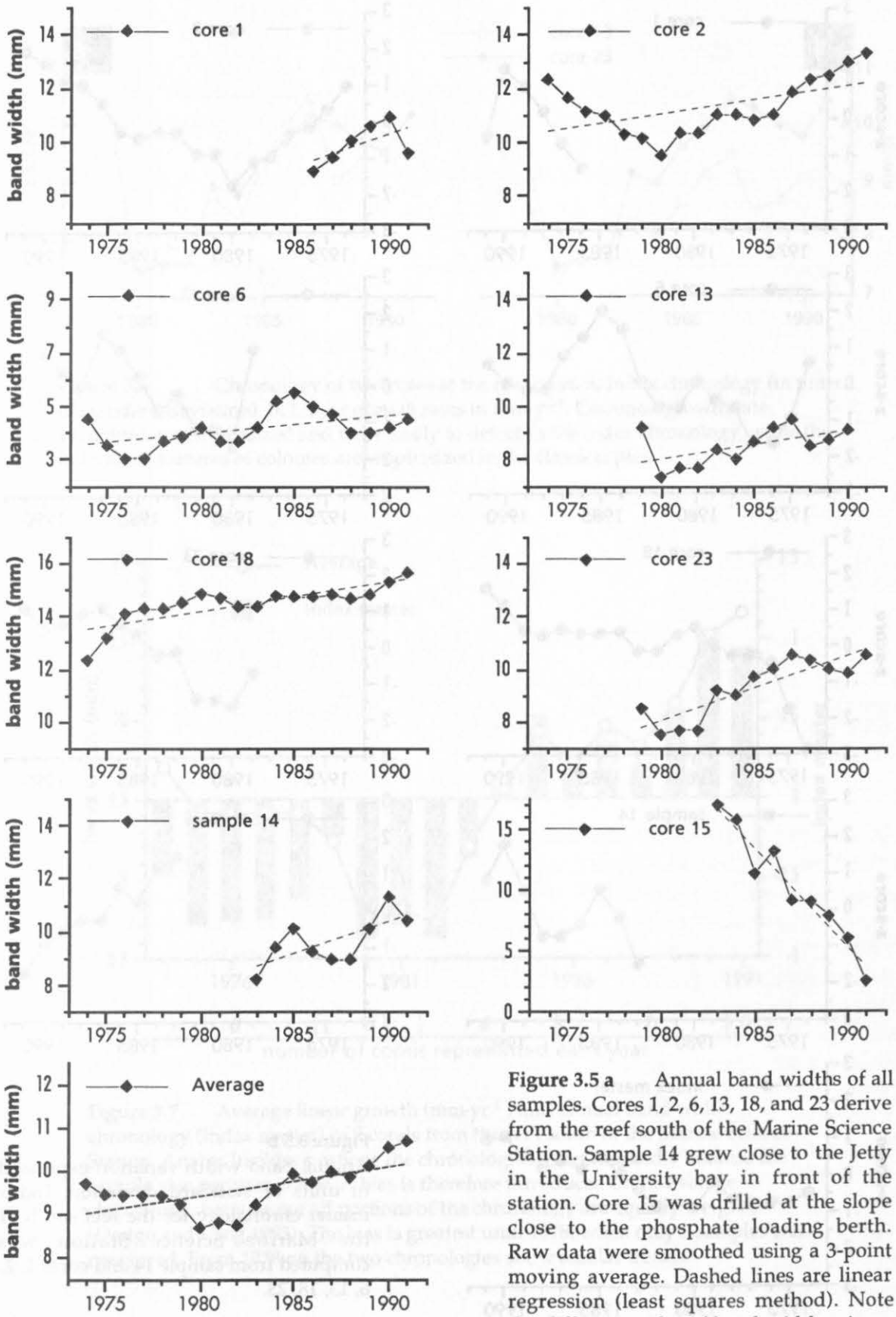

Figure 3.5 a Annual band widths of all samples. Cores 1, 2, 6, 13, 18, and 23 derive from the reef south of the Marine Science Station. Sample 14 grew close to the Jetty in the University bay in front of the station. Core 15 was drilled at the slope close to the phosphate loading berth. Raw data were smoothed using a 3-point moving average. Dashed lines are linear regression (least squares method). Note the different scales of band width axis.

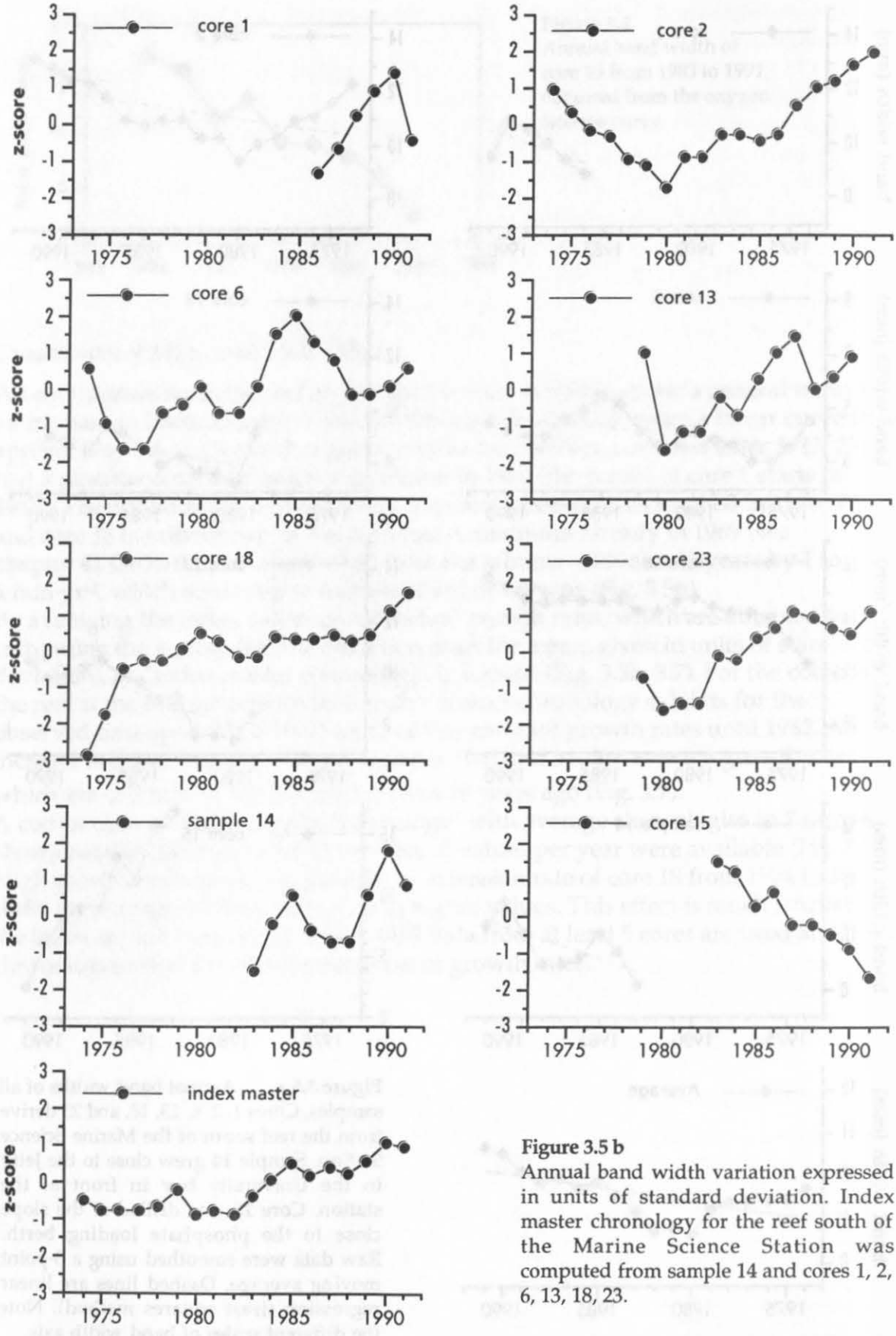

Figure 3.5 b
Annual band width variation expressed in units of standard deviation. Index master chronology for the reef south of the Marine Science Station was computed from sample 14 and cores 1, 2, 6, 13, 18, 23.

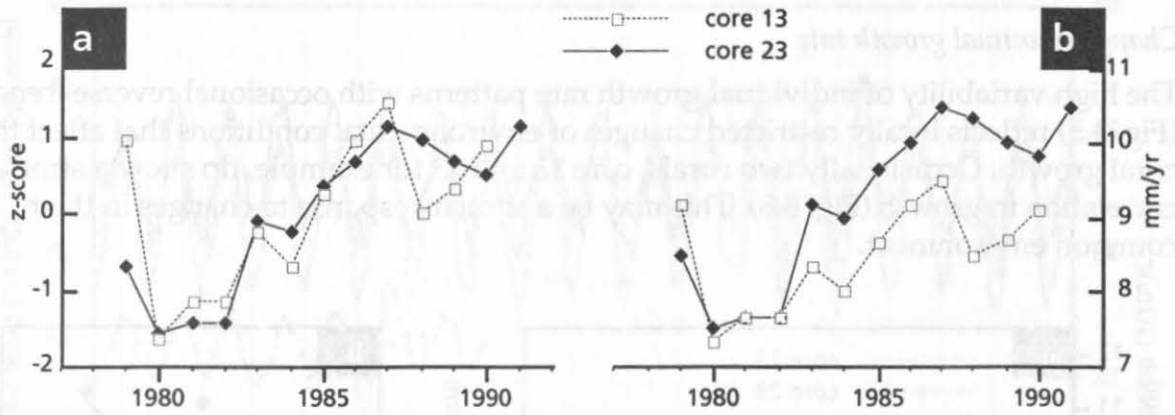

Figure 3.6 Chronology of two cores at the reef crest. **a.** Index chronology (in units of standard deviation) **b.** Linear growth rates in mm·yr^{-1}. Common growth rate variations are emphasized and more easily to detect in the index chronology, while the individual features of colonies are emphasized in the classical plot.

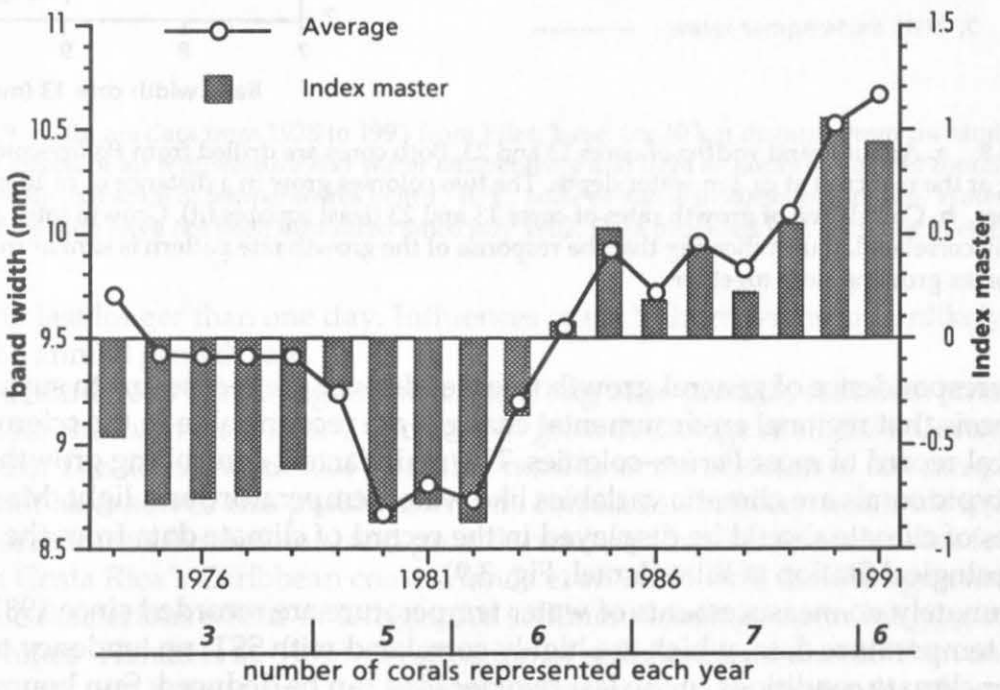

Figure 3.7 Average linear growth (mm·yr^{-1}) and annual band width chronology (index master) of 7 corals from the reef south of the Marine Science Station, Aqaba. In older portions the chronologies differ markedly because the sample size per year is low. A bias is therefore introduced in the average chronology, because not all portions of the chronology are equally weighed (Dodge and Lang 1983). The bias is greatest until 1978, when only 3 samples were measured. From 1978 on the two chronologies show similar trends.

Discussion

Change of annual growth rate

The high variability of individual growth rate patterns with occasional reverse trends (Fig. 3.5) reflects locally restricted changes of environmental conditions that affect the coral growth. Occasionally two corals, core 13 and 23 for example, do show a strong correlation in growth (Fig. 3.8). This may be a similar response to changes in their common environment.

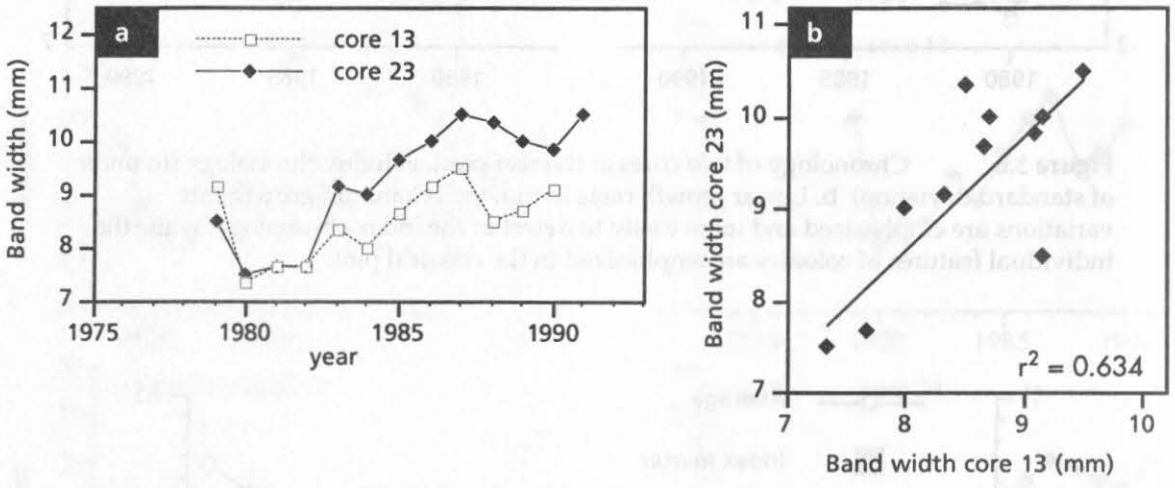

Figure 3.8 **a.** Annual band widths of cores 13 and 23. Both cores are drilled from *Porites*-colonies growing at the reef crest at ca 2 m water depth. The two colonies grow in a distance of ca 10 m from each other. **b.** Correlation of growth rates of cores 13 and 23 (least squares fit). Growth rates are positively correlated, thus indicating that the response of the growth rate pattern is similar in these two colonies growing close together.

The correspondence of general growth rate trends over the reef seems to support the hypothesis that regional environmental changes are recognizable in the sclerochronological record of most *Porites*-colonies. The main factors controlling growth of hermatypic corals are climatic variables like water temperature and light. Major changes of climate should be displayed in the record of climate data from the Meteorological Station at Eilat (Israel, Fig. 3.9).
Unfortunately no measurements of water temperature are recorded since 1982. From the air temperature data, which are highly correlated with SST, no tendency to warmer climate conditions in the last two decades can be deduced. Sun hours as a measure of light irradiance is also constant over this time range. Thus, there is no indication for climate induced variation of coral growth rates at Aqaba during the last decades. The seasonal variations of fresh water influx, which affect growth rates of corals in more humid regions like Galápagos and Tarawa (Pacific Ocean; Cole and Fairbanks 1990; Cole et al. 1993), the Philippines (Pätzold 1984; 1986), or the Gulf of Mexico (Dodge and Lang 1983) are not likely to have any consequence on corals in the Red Sea, as the annual precipitation is less than 50 mm. Even if there is a considerable discharge from wadis after the episodical rainfalls, this effect does not

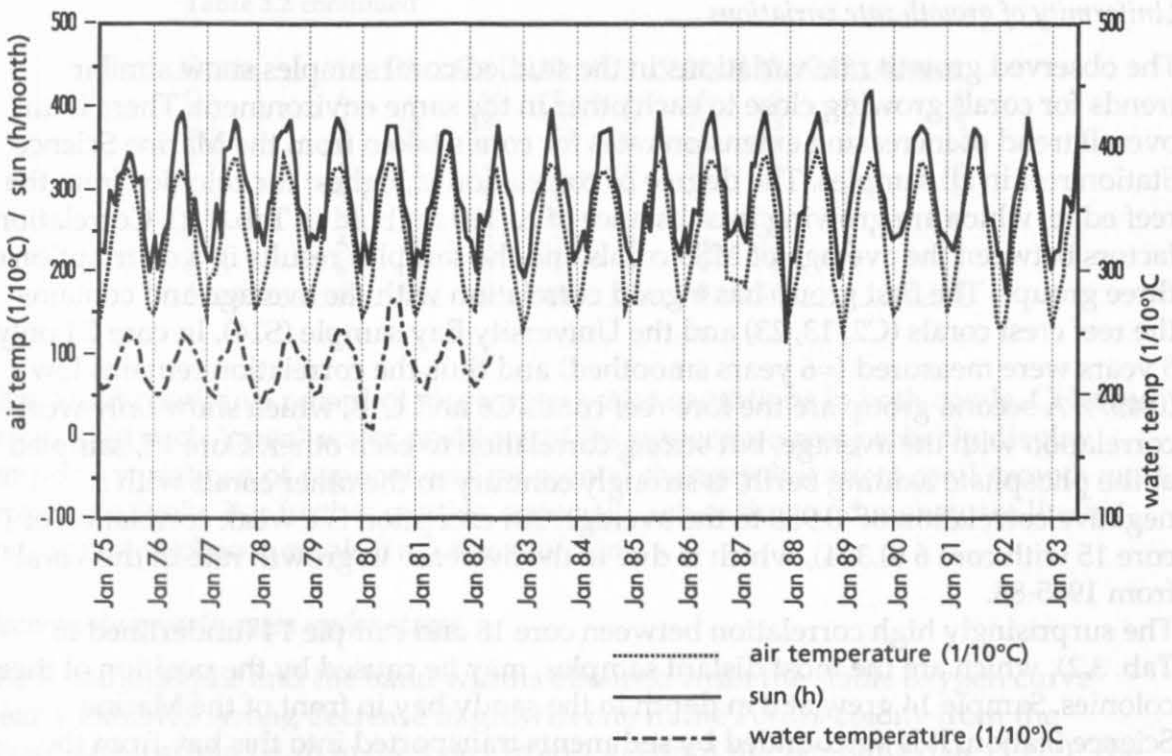

Figure 3.9 Climate data from 1975 to 1993 from Eilat, Israel (ca 10 km distance from the study area). Monthly means of air temperature and water temperature and light as hours of sun per month are plotted. Note that scale of temperatures is in 1/10°C, scale of sun is in hours per month. Water temperature data have not been measured since July 1982. Data provided by Deutscher Wetterdienst.

generally last longer than one day. Influences of such short events are unlikely to affect the annual growth rate.

From the numerous remaining factors controlling coral growth, sediment stress is in some cases the main reason for a decrease in growth (Dodge et al. 1974; Cortés and Risk 1985). The determination of insoluble residue in the skeleton of our samples would not have solved this problem, as little correlation between insoluble residue (incorporated into the skeleton) and growth band width within species was found at a reef at Costa Rica´s Caribbean coast (Hands et al. 1993). Still there is agreement about the deleterious effects of terrigenous sediment loadings upon fringing coral communities (Hands et al. 1993). A reduction of sediment load should then enhance coral growth. We believe, that this is most likely the main reason for the observed increase in extension rates. A reduction of sediment input from the hinterland could be caused by the construction of the road along the coast line and perhaps by the buildings of the Marine Science Station itself (see Chapter 2; Heiss et al. 1993). The sediment discharge is now limited to certain artificial outlets instead of the former input along the entire coast. Marked low growth rates in cores 2, 13 and 23 in 1980/81 may be a response to local building activities at the ferry harbour north of the University Bay.

Uniformity of growth rate variations

The observed growth rate variations in the studied coral samples show similar trends for corals growing close to each other in the same environment. There is an overall trend of increasing extension rates for corals taken from the Marine Science Station reef in all samples. The degree of correlation is highest for colonies from the reef edge, which are growing in a distance of ca 100 m (bold in Tab. 3.2). Correlation factors between the average of MSS corals and the samples results in a distribution of three groups. The first group has a good correlation with the average and contains the reef crest corals (C2, 13, 23) and the University Bay sample (S14). In core C1 only 8 years were measured (=6 years smoothed) and thus the correlation remains low (0.457). A second group are the fore reef corals C6 and C18, which show only weak correlation with the average, but strong correlation to each other. Core 15, sampled at the phosphate loading berth, is strongly contrary to the other corals with a negative correlation of -0.958 to the average. An exception is a weak correlation of core 15 with core 6 (0.324), which is due to the decrease in growth rate in this coral from 1985-88.

The surprisingly high correlation between core 18 and sample 14 (underlined in Tab. 3.2), which are the most distant samples, may be caused by the position of these colonies. Sample 14 grew at 8 m depth in the sandy bay in front of the Marine Science Station. It is surrounded by sediments transported into this bay from the episodical wadi outflows and probably from the reef. The "big" *Porites*-colony from which core 18 was recovered (Chapter 2; Heiss et al. 1993), stands in the upper fore-reef ca 500 m south of sample 14. The reef crest is ca 5-10 m away, the top of the colony is ca 1 m below the water surface. At first glance less similarity in coral growth patterns would be expected at these two different sites. The free-standing position of both colonies may explain the observed phenomenon. It enables a steady water exchange and reduces the very restricted changes of water temperature at the reef crest, which might influence the other corals under investigation.

Table 3.2 Correlation matrix for growth rates of coral samples (pairwise deletion). Average is computed from all corals sampled at the Marine Science Station reef, which is taken as a master chronology (for correlation coefficients it makes no difference whether raw or index values are used). Correlation coefficients are computed from the smoothed values (3 point moving average) for the period from 1972-1992 (20 years), count of years used for each correlation is plotted below. Correlation factors with high significance betweencolonies growing at the reef edge are in bold numbers, correlation between fore-reef colonies underlined (see text).

Correlations	C 1	C 2	C 6	C 13	S 14	C 18	C 23	C 15	Average
C 1	1	.647	-.868	-.445	.669	.183	-.497	-.438	.457
C 2	.647	1	.159	.570	.598	.104	.829	-.911	.881
C 6	-.868	.159	1	.296	.009	.258	.450	.346	.388
C 13	-.445	**.570**	.296	1	.237	.310	.795	-.583	.757
S 14	.669	.598	.009	.237	1	.782	.190	-.693	.850
C 18	.183	.104	.258	.310	.782	1	.481	-.853	.324
C 23	-.497	**.829**	**.450**	**.795**	.190	.481	1	-.783	.898
C 15	-.438	-.911	.346	-.583	-.693	-.853	-.783	1	-.958
Average	.457	.881	.388	.757	.850	.324	.898	-.958	1

Table 3.2 continued

Counts	C 1	C 2	C 6	C 13	S 14	C 18	C 23	C 15	Average
C 1	6	6	6	5	6	6	6	6	6
C 2	6	18	18	12	9	18	13	9	18
C 6	6	18	18	12	9	18	13	9	18
C 13	5	12	12	12	8	12	12	8	12
S 14	6	9	9	8	9	9	9	9	9
C 18	6	18	18	12	9	18	13	9	18
C 23	6	13	13	12	9	13	13	9	13
C 15	6	9	9	8	9	9	9	9	9
Average	6	18	18	12	9	18	13	9	18

This could result in a record of more open water conditions in both corals. Colonies growing in such "open" water positions of the upper fore-reef probably display temporal variations of regional environmental changes that affect coral growth most representatively. For further studies, especially when time and money are limited, we suggest to choose corals from this reef zone.

Decrease in growth rates under stress

The X-radiographs and the band widths obtained from the stable oxygen curve clearly exhibit a strong decrease in growth rate in the *Porites*-colony from the phosphate loading berth in the years from 1983 until the sampling date (1992). The comparison with growth rate data from the Marine Science Station four km south of that site shows a strong discrepancy to the accelerated growth there. Thus a local impact on the growth rate must be concluded. The first influence to look at is the effect of phosphorus in the water. Fishelson (1973) found that algal growth was stimulated by high phosphorus content at Eilat. Algae dominated the environment and coral colonies were killed. Together with the immense detrital input of apatite dust during loading these factors can override any other environmental control. It has long been acknowledged that sediment stress is able to reduce coral growth (Dodge et al. 1974; Hudson 1981; Cortés and Risk 1985). This is most probably the case in this heavily stressed environment. Additionally the reduction of light by increased turbidity will affect coral growth negatively. The great discharge of fine dust into the Gulf of Aqaba has been described already in the last two decades (Freemantle et al. 1978; Walker and Ormond 1982; Abu Hilal 1985). Nevertheless our coral sample exhibits a quite fast growth in the years 1983 to 1987, which reaches the same high rates as in a relatively undisturbed environment. The growth rate decreases steadily during the recorded time span, but falls below "normal" values not before 1987. Unfortunately no measurements of sedimentation rates were carried out in the last years. On the reasons of this sudden reduction must be speculated. An increase in sediment stress and algal growth might have happened due to an increase in phosphate export. Or a very local change of the environment occurred, so that this colony suffered from suddenly increased sediment load. It would be helpful to have exact loading rates to reveal the real reasons of the drastic decrease in growth in this coral. Analysis of trace elements and detritus incorporated in the coral skeleton might provide a pollution chronology of this area which could then be be compared to other reef areas and linked to the historical record.

CHAPTER FOUR

TWO CENTURIES CARBON AND OXYGEN ISOTOPE RECORD OF *PORITES* SP. IN THE GULF OF AQABA, RED SEA

Abstract

Growth rate variations, stable oxygen and carbon isotopic composition were investigated in two cores drilled from a large *Porites* sp. colony at Aqaba, Gulf of Aqaba. The sclerochronological record of the longest core (320 cm) reaches back to the year 1788. This core was drilled vertically. The horizontal core comprises 107 years and is drilled from the southern side into the colony. Growth rates are high with mean values of 10.72 (horizontal) and 12.52 $mm \cdot yr^{-1}$ (vertical) and seem to be enhanced by increase of water temperatures. $\delta^{18}O$ displays a decrease since 1800 by about 0.4 ‰ and indicates a warming of sea water temperature by ca 2°C. Carbon isotopes composition is mainly controlled by metabolic effects, with a higher portion of kinetic behaviour at the side of the colony. Both oxygen and carbon isotopes display responses to global variations of temperature and atmospheric CO_2. Striking similarities with coral records from other oceans are observed. Anthropogenic activities since the 1960s affected growth rates and isotopic composition drastically.

Introduction

In the Gulf of Aqaba a large *Porites* sp. colony was studied to determine the growth history of this single colony. In addition, the effect of light, temperature and the so-called vital effect were determined by isotopic analysis (Swart 1983). The combination of growth history and isotopic analysis is especially effective in scleractinian hermatypic corals. *Porites* can be used as an environmental recorders because annual growth bands (Knutson et al. 1972) allow to establish chronologies and contain valuable physical and chemical environmental information incorporated in their skeletons at the time of aragonite deposition. Combining both records supplies an accurate history of temperature variations, current histories, and upwelling intensities through time (Carriquiry et al. 1988).
Corals of the genus *Porites* are important reef builders due to their ubiquitism and their ability to secrete huge massive colonies. In contrast to most corals of branching and foliaceous growth form *Porites* colonies often persist in vivo position over the ages. This fact and the high age of individual colonies make *Porites* ideal recorders of environmental factors through time.
The studied colony of *Porites* sp. was conspicuous because of its unusual size; moreover, its surface was completely covered by living tissue which is rare in this oceanic region. On the upper fore reef where *Porites* colonies are frequent, they often represent small, relatively isolated living outcrops of large, partly eroded skeleton masses (Schuhmacher and Mergner 1985).

The aragonite skeleton of corals is precipitated in disequilibrium with surrounding seawater, but a variety of factors can affect the isotopic signal registered in the skeleton (Swart 1983; McConnaughey 1989a; 1989b). Isotopic fractionation is influenced by both so-called "kinetic" and "metabolic" effects (Swart 1983; McConnaughey 1989a; 1989b). Oxygen isotope fractionation, however, can be mainly related to kinetic effects like temperature. With increasing temperatures kinetic effects cause depletion of ^{18}O with respect to ^{16}O. Because of this relationship oxygen isotopes from corals have been used as paleothermometers for a long period (Emiliani et al. 1978; Fairbanks and Dodge 1979; Weil et al. 1981; Pätzold 1984). The $\delta^{18}O$ of calcium carbonate precipitated in equilibrium with seawater decreases by about 0.22‰ for every 1°C rise in water temperature (Epstein et al. 1953).
The kinetic effects with increasing temperatures on the carbon isotope composition is much less. This is probably the result of fractionation during hydration and hydroxylation of CO_2 (Aharon 1991). The preference of photosynthesis for the lighter ^{12}C isotope allows the use of the depletion in ^{13}C of the coral skeleton as an indicator of changes in photosynthetic performance of coral/algae symbiosis (McConnaughey 1989a).
The registration of other factors, like the effect of "bleaching", in the stable isotopic composition of *Montastrea annularis* from Florida (Leder et al. 1991) shows the difficulties in assessing these environmental factors. They are the cause of variations in the isotopic composition of a coral skeleton, but to what extent remains a point of discussion (Fitt et al. 1993).
During biological calcification CO_2 hydration and hydroxylation may result in a kinetic isotope fractionation effect causing simultaneous depletion of ^{18}O and ^{13}C (McConnaughey 1989a; 1989b; Aharon 1991). Metabolic effects like photosynthesis

also cause deviations from the equilibrium values. It preferentially uptakes the light ^{12}C isotope relatively enriching seawater in ^{13}C.
Changes of carbon isotopic composition of carbon dioxide in the atmosphere originated from the increased burning of fossil fuels since the 19th century. The decrease in the $^{14}C/^{12}C$ ratio has been called the "Suess effect" after its discoverer (Suess 1955). Another anthropogenic effect recorded in corals, the increase in ^{14}C since about 1954, is due to the release of bomb radiocarbon to the atmosphere (Druffel and Linick 1978; Druffel 1980, 1981).
Relative to atmospheric CO_2 the $^{13}C/^{12}C$ ratio is low in organic matter. Burning organic matter, fossil or recent, will thus release isotopically light CO_2 into the atmosphere disturbing the natural signal. The fast exchange of atmospheric CO_2 with surface waters of the oceans and the record of its isotopic composition in coral skeletons will register the forementioned decrease in the $^{13}C/^{12}C$-ratio in the coral skeleton. Before the beginning of fossil fuel burning the $^{13}C/^{12}C$-ratio commenced to decrease probably by increased burning of trees (Stuiver 1978). The first record of this dilution effect in corals has been described from a 200 year *Diploria labyrinthiformis* from Bermuda (Nozaki et al. 1978).
The analysis of stable isotopes is also used to reconstruct the history of El Niño-Southern Oscillation (ENSO). The resolution of these records is comparable in quality with those derived from instrumental climate data and can provide high-resolution reconstructions of ENSO behaviour that predates the historical record (Cole and Fairbanks 1990; Shen et al. 1992; Cole et al. 1993). The observed effects of ENSO on corals are mainly related to high precipitation of isotopically light rainwaters. These are strong enough to alter the $\delta^{18}O$ composition and salinity of surface waters.
The objective of this chapter is to establish a long-term record of stable isotopic variation in the northern Gulf of Aqaba. The relation to climate variations, anthropogenic influences and intra-coral effects on isotope fractionation were investigated.

Materials and methods

Drilling

In fall 1992 and spring 1993 we drilled an unusual big colony of *Porites* sp. at the fore-reef at Aqaba. The colony is situated in front of the reef edge of the fringing reef south of the Marine Science Station (see Chapter 2). The colony grows from a depth of ca 4.5 m, reaches a height of 3.5 m and a maximum diameter of approximately 5.5 m. We drilled with a hand held pneumatic drill powered by compressed air from a Scuba tank. We used a conventional 30 cm diamond-tipped drill bit and in order to obtain longer cores we constructed extensions of 100 cm each (3 in total). The extensions are made from a 17 mm diameter steel rod with a screw thread attached either to the core barrel or another extension (Fig. 4.1). Up to 320 cm long cores in 30 cm lengths with 100% recovery were obtained. The core holes were filled with cement plugs after drilling to prevent bioerosion (see Hudson 1981; Winter et al. 1991).

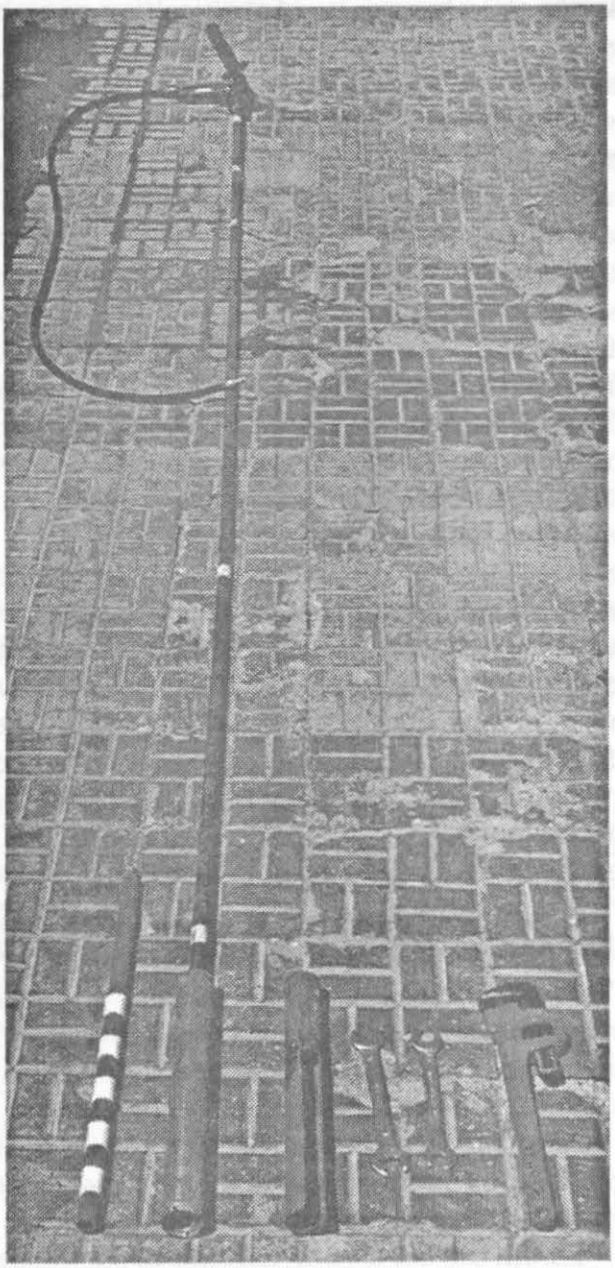

Figure 4.1 Pneumatic drill with extensions, drill bit and core catcher. Photograph: John J.G. Reijmer.

The cores were drilled parallel to the growth axis (perpendicular to the coral surface, Fig. 3.3). Five cores were extracted from the "big" *Porites* sp. at different sides of the colony. Three cores (19, 20, 21) are of 130 cm length, core 24 (lying SE-side of the colony at an angle of 45°) reached 229 cm length, and core 18 (top of the colony) recovered coral skeleton to a total length of 312 cm.
For oxygen and carbon isotope analysis core 18 (top of colony) and core 19 (horizontal core from the southern side) were selected.

Processing core samples

All cores were sawn into slices of ca 3 mm. These slabs were X-rayed using a SEIFERT-industry-X-ray-unit (Type ERESCO 120kV/5mA) at 35kV and 5mA to reveal annual density banding (Knutson et al. 1972; Hudson et al. 1976). Agfa Gevaert Structurix D4 film was used. Growth rates were measured along the major (vertical) growth axis (Buddemeier et al. 1974; Logan and Tomascik 1991) from positive prints as the distance between the top edge of low-density bands (LD) which are the most distinct boundaries in our samples. Band width measured on X-radiographs was corrected and these results were used in the assessment of growth rates (a detailed description is given in Chapter 3). Those parts of the cores not drilled parallel to the growth axis were not used in our analysis.
As Shen et al. (1992) pointed out, errors in X-radiograph mapping and physical cutting introduce small errors in absolute time assignment. In the coral skeleton no markers are imbedded that fix a calendar point to define the annual growth. It is not even known which factor actually triggers the deposition of the HD and LD bands of the coral.

X-ray-diffractometry:

In order to exclude changes of isotopic composition that occur during diagenetic conversion of aragonite to calcite X-ray analyses of 6 samples (18126=year 1868, 18145=1849, 18159=1833, 18160=1832, 18167=1825, 18187=1805) were performed with a Philips PW 1840 X-ray diffractometer (CuK_α, 35 kV, 30 mA).

Yearly average stable isotopes

Samples for isotopic analyses were treated with 35% hydrogen peroxide for 24 hours to remove oxidizable organic material. In addition they were rinsed several times in demineralized water and dried in a stove at 40°C.
Small samples to determine the average isotope composition of each year were cut with a hand held saw. They were taken along the edge of the coral slabs. The top of LD-bands was chosen as the end (respectively beginning) of an annual band. In all our samples this boundary is sharp and can be determined relatively precise. With detailed isotope analysis of *Porites* sp. (8-10 samples per year) it could be shown (own unpublished data) that LD-bands in the Gulf of Aqaba are deposited during the summer months (May-September). This agrees with the results of Klein et al. (1992). By cutting at the top boundary of the LD-band the loss of coral material is restricted to the time of declining sea water temperatures (November/December). The distance between two HD bands averaged 11-12 mm. Since the thickness of the saw is 0.2 mm, about 98 % of the aragonitic material deposited in one year was sampled. Each chip was gently powdered in an agate mortar. The samples were reacted with 100% H_3PO_4 at 75°C in an online, automated carbonate reaction device (Kiel Device) connected to a Finnigan Mat 252 mass spectrometer. Isotopic ratios were corrected for ^{17}O contribution (Craig 1957) and are reported in ‰ relative to PDB (Pedee belemnite). Average precision based on duplicate sample analysis and on multiple analysis of NBS 19 is ± 0.04‰ for $\delta^{13}C$ and ± 0.08‰ for $\delta^{18}O$.

Results

X-ray-diffractometry

Calcite was not detected in any samples. Therefore it is assumed that the isotopic composition of the samples are not affected by diagenesis which could have converted aragonite to calcite.

Growth rates

Mean annual band widths for core 18 and core 19 are shown in Table 4.1 and Figures 4.2 and 4.3. Core 18 has continuous growth, except at a relatively early stage when skeletal growth temporarily ceased but reinitiated after overgrowth by adjacent tissue. In core 18 the record with clear density banding reaches back to the year 1788. The first few cm at the bottom of this core could not be measured exactly, but contains ca 3 years of growth, calculated from the mean growth rate of the entire core. From extension rates of around 12 $mm \cdot yr^{-1}$, a peak (15-16 $mm \cdot yr^{-1}$) occurs in the 1810s, then growth decreases until 1830. High rates again occurred from 1850 to the late 1860s, when a strong decline to values below 10 $mm \cdot yr^{-1}$ was measured before 1880. From the next maximum before 1890 the growth rate falls to intermediate values between 10 and 13 $mm \cdot yr^{-1}$, which are recorded from 1890 until ca 1965 with stronger variations in the time span 1930 to 1965. From a minimum around 1968 growth accelerates to the high values above 14 $mm \cdot yr^{-1}$ since 1975.
The growth record of core 19 begins in 1886 and is quite similar in its general behaviour. The amplitude of variations between adjacent years is more accentuated than in core 18 (Fig. 4.3). Also in this core highest growth rates are measured in the last 15 years.

Table 4.1. Mean linear growth rate (± standard deviation) of cores 18 and core 19. For calculation of mean growth the corrected annual band widths were used (explanation see text). Core 18 was drilled from top of the colony (1.5 m water depth) to a length of 320 cm, and reaches an age of 207 years. 188 years were measured and corrected with the procedure described in the text. The band widths of the missing years was not calculated due to the large angle of the cutting plane. Core 19 was drilled horizontally from the southern side of the colony.

Core sample	Core position	Water depth (m)	Mean linear growth rate (mm/yr)		Number of years
18	top	1.5	12.52	(±1.79)	188
19	horizontal (south)	4.5	10.72	(±2.20)	108

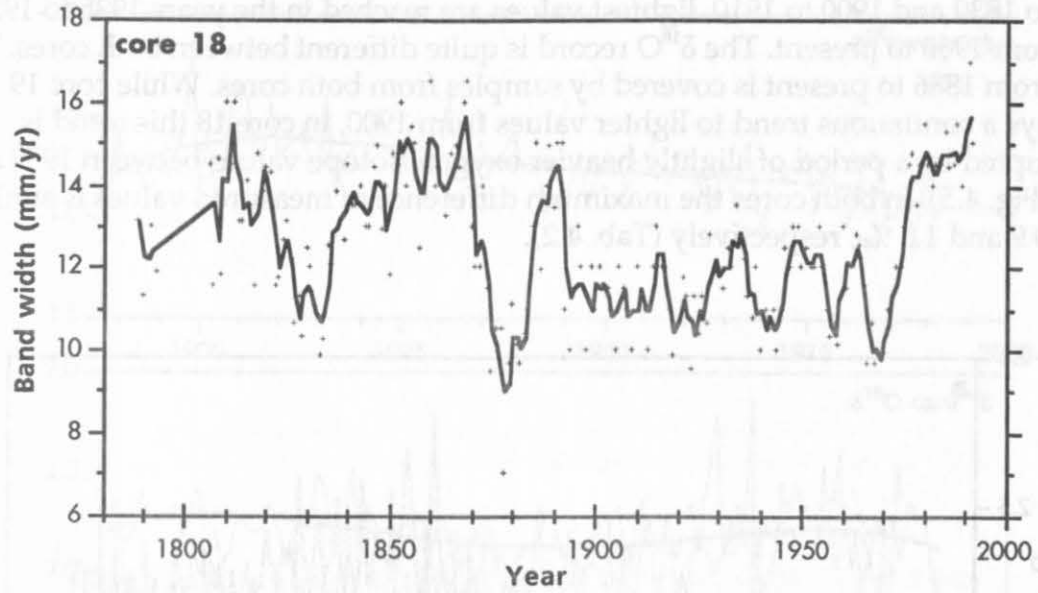

Figure 4.2 Annual band width of core 18 (drilled vertically from top of the colony). Solid line is smoothed with a 3-point moving average.

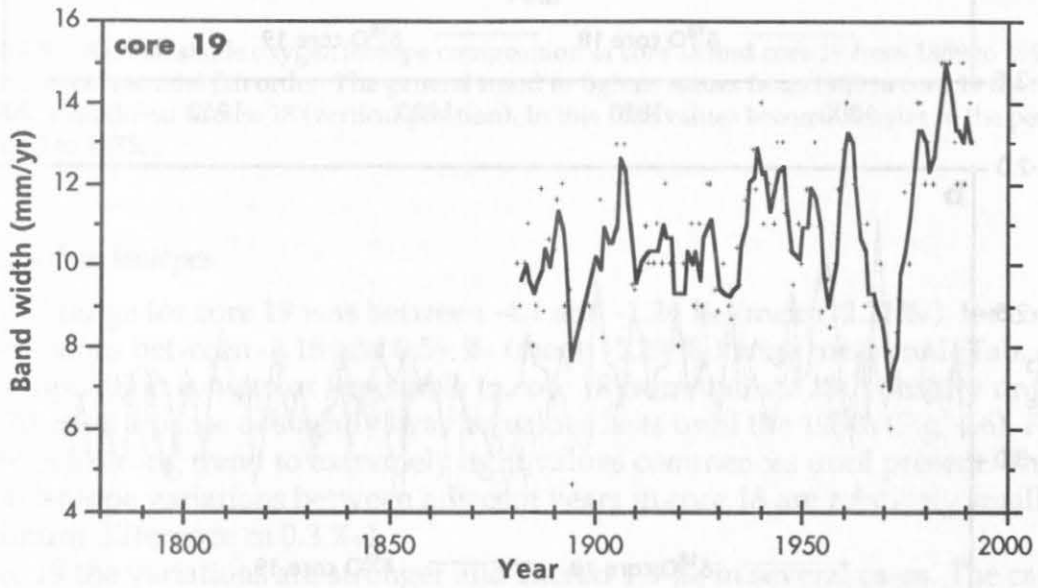

Figure 4.3 Annual band width of core 19 (drilled horizontally from southern side of the colony). Solid line is smoothed with a 3-point moving average.

Stable oxygen isotopes

Oxygen isotope composition within each core displays strong variations from year to year. The values for $\delta^{18}O$ in core 19 varied from -3.08 to -2.18 ‰. Values in core 18 varied between -3.18 and -2.14 (Tab. 4.2). Oxygen isotopes show a general trend to lighter values from 1800 to ca 1950 and from then a more or less stable level occurs with a slight trend to heavier values until 1990 (Fig. 4.4). Heaviest values date from

1820 to 1830 and 1900 to 1910, lightest values are reached in the years 1935 to 1955 and from 1960 to present. The $\delta^{18}O$ record is quite different between both cores. The time from 1886 to present is covered by samples from both cores. While core 19 displays a continuous trend to lighter values from 1900, in core 18 this trend is interrupted by a period of slightly heavier oxygen isotope values between 1950 and 1975 (Fig. 4.5). In both cores the maximum difference of measured values is similar with 0.9 and 1.0 ‰, respectively (Tab. 4.2).

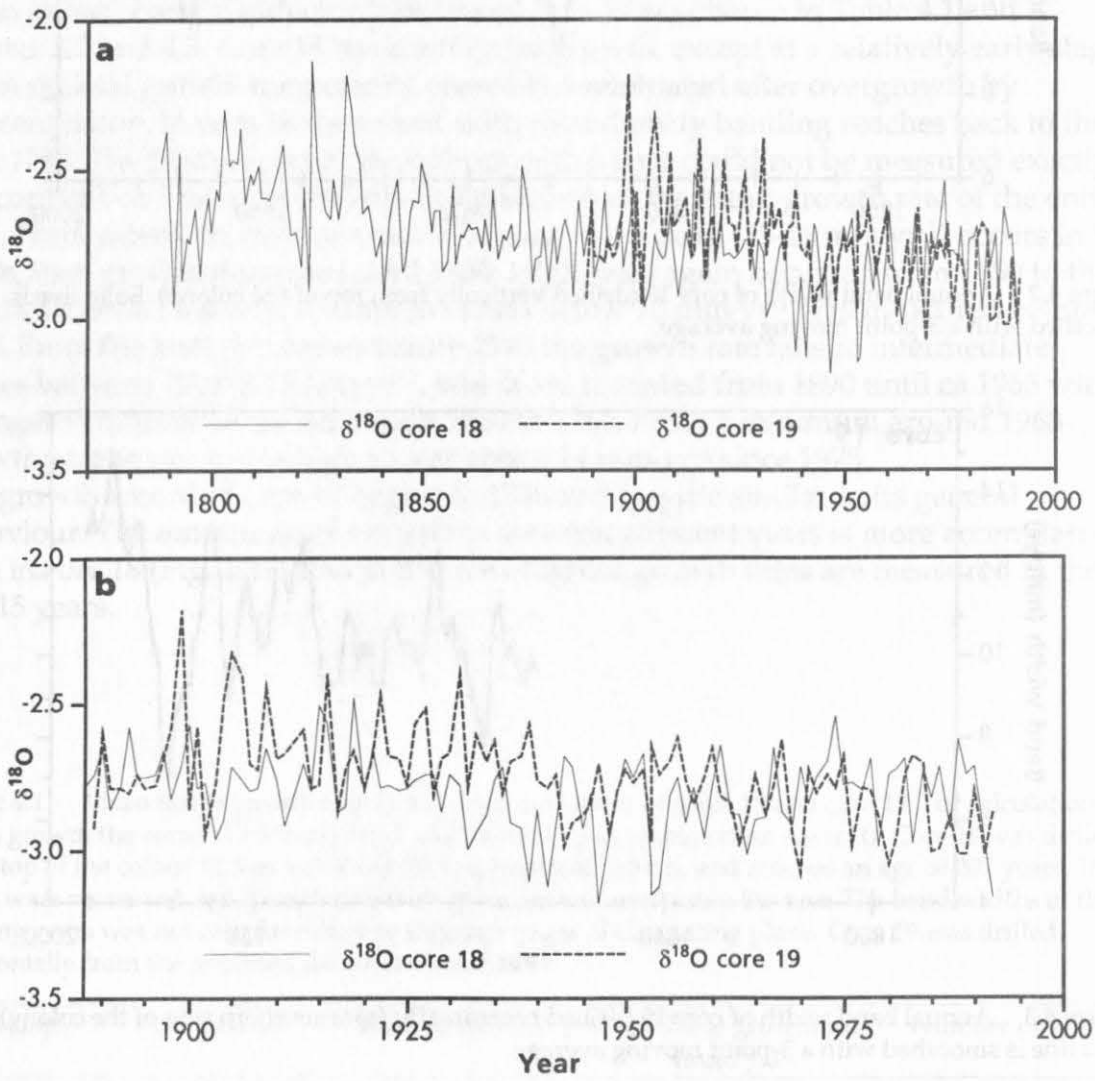

Figure 4.4 Annual stable oxygen isotope composition of core 18 and core 19. **a.** Complete dataset **b.** Enlarged plot of dataset for both cores from 1880 to present.

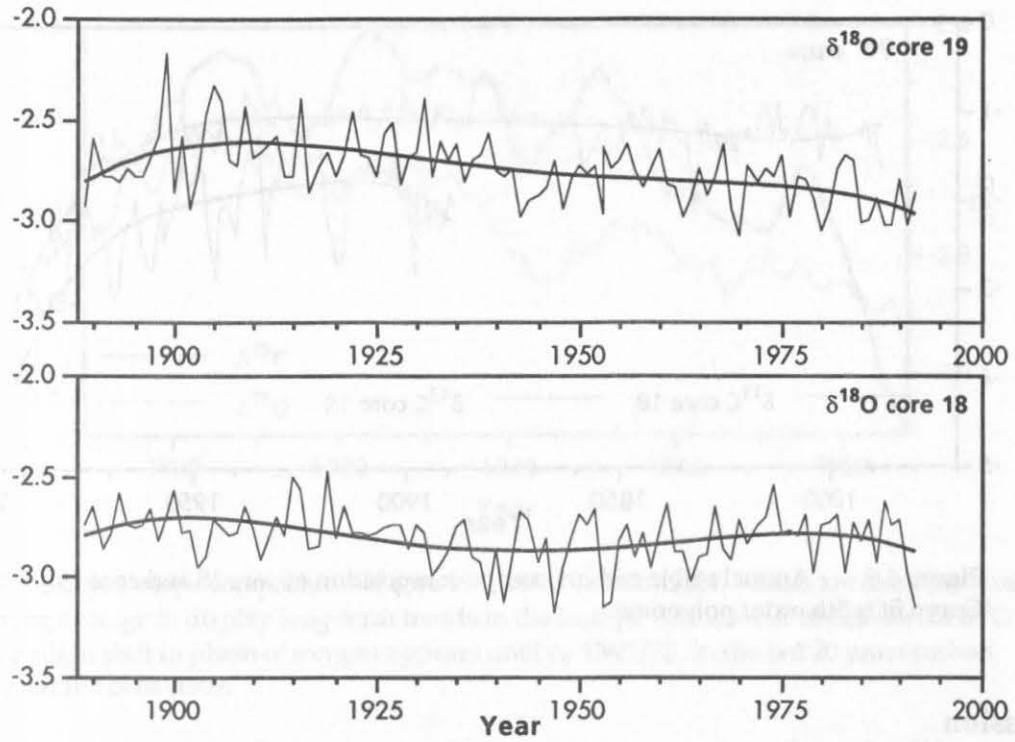

Figure 4.5 Annual stable oxygen isotope composition of core 18 and core 19 from 1889 to 1992. Curve fit is polynomial 5th order. The general trend to lighter values from 1900 in core 19 (horizontal position) is modified in core 18 (vertical position). In this core values become heavier in the period from 1950 to 1975.

Stable carbon isotopes

The $\delta^{13}C$ range for core 19 was between -4.1 and -1.26 ‰ (mean -2.21‰), for core 18 lighter values between -3.18 and 0.59 ‰ (mean -1.29 ‰) were measured (Tab. 4.2). The composition is more or less stable in core 18 from the late 18th century until ca 1860-70, then a phase of slightly heavier values lasts until the 1950s (Fig. 4.6). From the 1960s a strong trend to extremely light values commences until present. The carbon isotope variations between adjacent years in core 18 are relatively small (maximum difference ca 0.3 ‰).
In core 19 the variations are stronger and exceed 1.3 ‰ in several cases. The carbon isotope composition of this core is generally lighter than in core 18 (Fig. 4.6).

Table 4.2 Summary statistics for stable isotope determination in core 18 and 19 (in ‰)

	Mean	SD	Min	Max	n
core 19 $\delta^{13}C$	-2.21	0.65	-4.1	-1.26	107
core 19 $\delta^{18}O$	-2.75	0.16	-3.08	-2.18	107
core 18 $\delta^{13}C$	-1.29	0.43	-3.18	-0.59	206
core 18 $\delta^{18}O$	-2.73	0.17	-3.18	-2.14	206

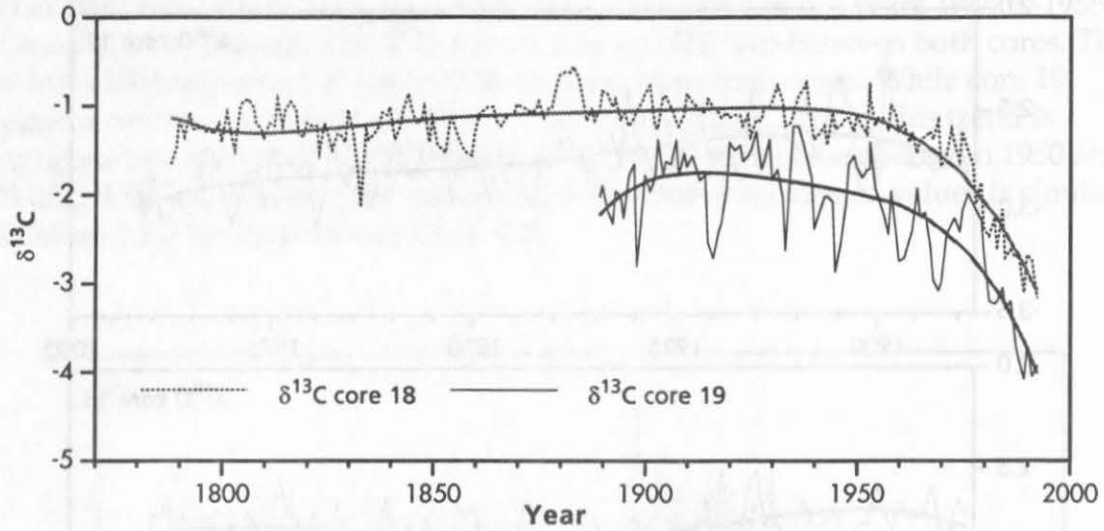

Figure 4.6 Annual stable carbon isotope composition of core 18 and core 19. Curve fit is 5th order polynome.

Discussion

A visual comparison of isotope data and growth rates from the Aqaba coral is given in the following discussion. This is compared with some long-term coral records published from Bermuda, the Caribbean, and the Pacific. Further statistical analysis was performed with simple linear regression analysis. The stable isotope record is then compared with the global climate signal represented by southern hemisphere sea surface temperature data. Spectral analysis was performed to reveal inter-annual cyclic patterns of stable isotope composition and growth rate.

Stable oxygen isotopes

Klein et al. (1992) investigated seasonal isotope variation on a *Porites* specimen from Eilat (water depth 3 m) with a sampling resolution of six to nine subsamples per year. In this study recorded sea surface temperature (SST) was compared to the isotope record. The difference of maximum and minimum $\delta^{18}O$ values could explain only ca 70 % of the expected difference from the equilibrium equation of Epstein et al. (1953). Whether insufficient sampling resolution or physiological effects are the reason for this deficiency could not be explained.
The $\delta^{18}O$ variation of the core samples, which represent approximately one year each, is similar to the seasonal $\delta^{18}O$ difference in the coral from Eilat studied by Klein et al. (1992; Tab. 4.2, Fig. 4.4). This indicates that the variations in the yearly mean SST in the last 200 years is of a similar range like the present seasonal temperature variations. A part of this high range may be due to the sampling procedure. It can not be excluded, that some samples extend over more than 12 months and thus adjacent samples include for example two winters, while the next sample consists of skeleton deposited in spring and summer. By smoothing the raw data this sampling effect can be reduced. However, even the smoothed data display a decrease of ca 0.4 ‰ in the long-term record (Fig. 4.7, 4.8).

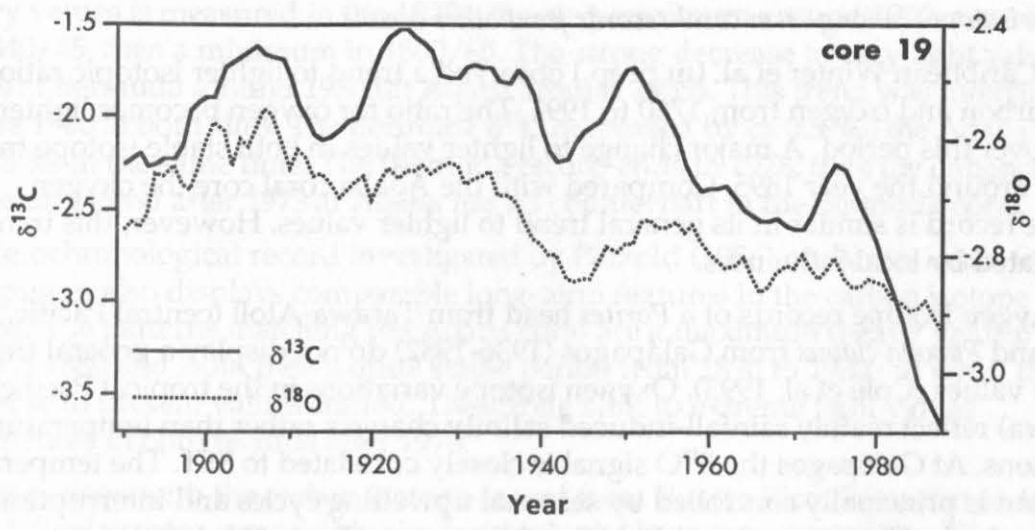

Figure 4.7 Stable isotope composition of core 19 (drilled horizonally). Values are smoothed using a 9 point moving average to display long-term trends in the isotope variation. A correlation of $\delta^{18}O$ and $\delta^{13}C$ with a slight shift in phase of oxygen appears until ca 1965/70. In the last 20 years carbon showed an erratic behaviour.

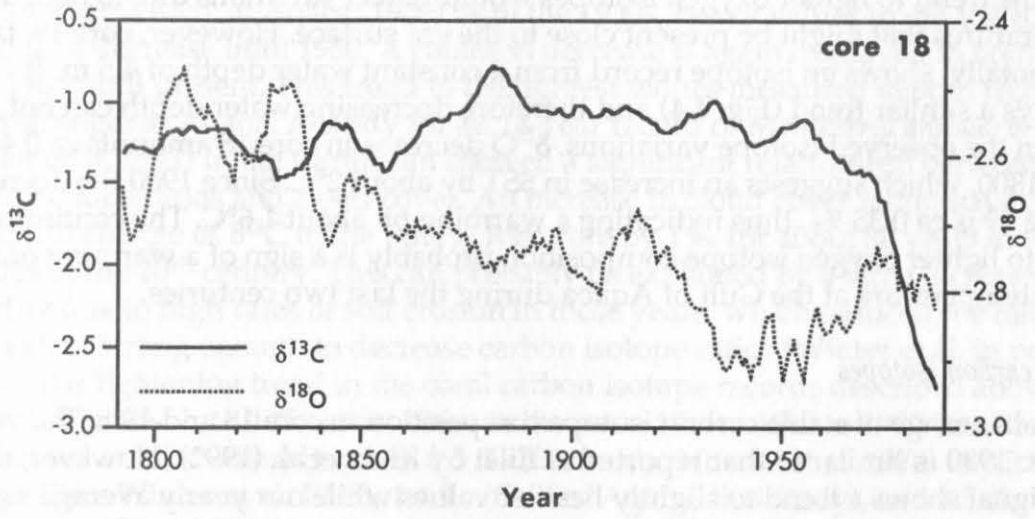

Figure 4.8 Stable isotope composition of core 18 (drilled vertically). Values are smoothed using a 9 point moving average to display long-term trends in the isotope variation.

Influence of salinity on oxygen isotope signal

The salinity of surface waters in the Gulf of Aqaba shows only minor variations throughout the year (Paldor and Anati 1979). The measured difference in salinity of ca 0.17 ‰ has a negligible effect on the isotope composition of seawater (0.17 ‰ salinity ≈ 0.05 ‰ $\delta^{18}O$, Craig 1966; Klein et al. 1992).

Another cause for isotopic variation in surface waters could be freshwater input by precipitation or river runoff. In the Gulf of Aqaba rainfall is too low (ca 20 mm/yr) to change the salinity and isotopic composition of seawater.

Oxygen isotopes in long-term coral records from other oceans

In the Caribbean Winter et al. (in prep.) observed a trend to lighter isotopic ratios for both carbon and oxygen from 1760 to 1991. The ratio for oxygen becomes lighter by 0.3‰ over this period. A major change to lighter values in both stable isotope trends occurs around the year 1895. Compared with the Aqaba coral core the oxygen isotope record is similar in its general trend to lighter values. However, this trend is modulated by local influences.

The oxygen isotope records of a *Porites* head from Tarawa-Atoll (central Pacific, 1884-1990) and *Pavona clavus* from Galápagos (1936-1982) do not display a general trend to lighter values (Cole et al. 1993). Oxygen isotope variations in the tropical Pacific (Tarawa) reflect mainly rainfall-induced salinity changes rather than temperature variations. At Galápagos the $\delta^{18}O$ signal is closely correlated to SST. The temperature variation is principally controlled by seasonal upwelling cycles and interruptions of these cycles by El Niño and anti-El Niño phenomena (Shen et al. 1992). A comparison of oxygen isotope data of the Aqaba coral with the Pacific corals does not display obvious similarities.

One might assume that the growth of the top of this colony towards shallower water depths has influenced the oxygen isotopic response recorded in the Aqaba coral. Then the trend to lighter oxygen isotopes would reflect variations due to higher temperatures that might be present close to the sea surface. However, core 19, taken horizontally, shows an isotope record from a constant water depth of 4.5 m. It displays a similar trend (Fig. 4.4) and therefore decreasing water depth can not explain the observed isotope variations. $\delta^{18}O$ decrease in core 18 amounts ca 0.4 ‰ since 1800, which suggests an increase in SST by about 2°C. Since 1900 the decrease in core 19 is ca 0.35 ‰, thus indicating a warming by about 1.6°C. The continuous trend to lighter oxygen isotope composition probably is a sign of a warming of sea water temperature at the Gulf of Aqaba during the last two centuries.

Stable carbon isotopes

The value range of stable carbon isotope composition in core 18 and 19 in the years 1976 to 1980 is similar to that reported at Eilat by Klein et al. (1992). However, this $\delta^{13}C$ signal shows a trend to slightly heavier values while our yearly average signal becomes lighter from 1976 to 1980.

Carbon isotopes in long-term coral records from other oceans

The comparison of the stable carbon isotope variations in the cores from Aqaba with other long-term records of scleractinian corals may help to reveal the influence of global atmospheric stable isotope composition on the observed patterns. It must be noted, that the direct comparison suffers from the still existing possibility of errors when counting the sclerochronological record. A shift of 1-3 years seems to be possible when counting the HD/LD band couplets in scleractinian corals (see Chapter 3).

The first long-term record of corals was published by Nozaki et al. (1978) from a *Diploria labyrinthiformis* from Bermuda. Remarkably strong similarities appear by comparing this data with the Aqaba coral record. At both sites a first maximum with

heavy values is measured in the 1820s, the next minimum around 1930, a maximum in 1840/45, then a minimum in 1860/65. The strong decrease to very light values starts at Bermuda around 1930 (at Aqaba around 1935). This trend was interrupted before 1960 at both sites. The Bermuda $\delta^{13}C$ decreased by ca 0.5 ‰, the Aqaba values by 0.8 ‰ in the same time. The Bermuda record ends in 1978, thus the enhanced lightening trend after 1973 at Aqaba has no counterpart in the Bermuda coral.

A sclerochronological record investigated by Pätzold (1986) on *Porites lobata* from the Philippines also displays comparable long-term features in the carbon isotope record. The patterns matching the Aqaba coral are a maximum (heavy values) around 1880 and from then a quite stable period from 1890 to 1930/40 when the decrease to present values started. The strong shift to extreme light values commences in both records after 1970.

A comparison with the carbon isotope record from Puerto Rico (Winter et al. in prep.) displays also remarkable similarities in the long-term variability. There $\delta^{13}C$ becomes lighter from 1760 to 1991 by approximately 1.5 ‰. The following trends are analogous in both records: increase from 1790 to 1805, decrease until 1830, increase from 1830 to 1845, a period of light values in the 1850s, from then an increase with fluctuations until the 1880/90s. In the 20th century the similarity becomes even stronger, even though the absolute difference varies. There is a decrease in $\delta^{13}C$ from 1895 (at Puerto Rico; at Aqaba: 1900) until the 1930s, heavy values in the 1940s, followed by a decrease until 1950. A common decrease is again displayed in both corals from 1965 until present. This trend to the lightest values measured in both records is much stronger at Aqaba. A study for an 18-year record of *Montastrea annularis* (Winter et al. 1991) in the Caribbean showed a significant relationship between carbon isotope ratios and cloud cover. An increase in cloud cover might have caused the abrupt change of $\delta^{13}C$ in the Puerto Rico core by 1‰ for about 30 years in the first decades of the 20th century. This can probably be explained by a large increase in turbidity due to high rates of soil erosion in these years, which reduced the radiation to an extent strong enough to decrease carbon isotope ratios (Winter et al. in prep.). The secular lightening trend in the coral carbon isotope records described above is obvious. The absolute difference varies in the period from 1880 to 1980 (the time represented in all studies) between 0.5 ‰ (Bermuda, Nozaki et al. 1978) to 0.8 ‰ (Puerto Rico, Winter et al. 1993), 1.4 ‰ (Gulf of Aqaba, this study), and 1.5 ‰ (Philippines, Pätzold 1986) if the smoothed values are considered. The difference of raw data is even higher (up to 3 ‰ at the Philippines and the Gulf of Aqaba). Even though the individual behaviour is highly variable, the similarities between these patterns are too distinct to be accidental. There is indication that the global $\delta^{13}C$ composition of atmospheric CO_2 is reflected in the skeletal isotope values of scleractinian corals, despite the strong modulations by individual variations of the regional environment (natural or anthropogenic) and the metabolic activities of the algal symbionts in the coral, as Aharon (1991) pointed out. The carbon isotope record of coral samples from one area should be treated with care as far as conclusions regarding the global carbon patterns are concerned. Nevertheless, the combined $\delta^{13}C$ record of scleractinian corals seems to be suited to provide information on long-term worldwide changes in atmospheric CO_2 when more long coral records will be available.

Growth rate vs. stable isotopes

Growth rate vs. $\delta^{18}O$ signal

In Figure 4.9 growth rate is plotted with stable isotope composition for core 19. Similarities in the minima and maxima of the curves are obvious. For $\delta^{18}O$ a positive visual correlation in the long-term trends appear in the record until ca 1965. Growth rate of *Montastrea annularis* (Winter et al. in prep.) in the Caribbean was not correlated either with carbon or oxygen isotopes. What is responsible for the similarity in the long-term variations of isotopes and growth rate at Aqaba?

Strong kinetic disequilibria are often associated with rapid growth. In several cases faster growing portions of photosynthetic corals are depleted in $\delta^{18}O$ and $\delta^{13}C$ (for example Weil et al. 1981; Pätzold 1986; McConnaughey 1989a). Pätzold (1986) found a linear correlation (r=-0.7) between growth rate and $\delta^{18}O$ in *Porites lobata* from the Philipinnes. The specimen displayed its excursions in the fastest growing parts. From the data presented by McConnaughey (1989a) it seems, that the depletion is constant above a certain growth rate. In *Pavona clavus* from Galápagos extension rates lie between 1 and 14 mm·yr^{-1} (McConnaughey 1989a). The lateral surfaces with growth rates below 2 mm·yr^{-1} are less depleted in $\delta^{18}O$ and $\delta^{13}C$ than the fast growing upper portions of the same corals. From the plotted data of Pätzold (1986) the shift to light values appears mainly to occur at growth rates higher than 15 mm·yr^{-1}, growth rates

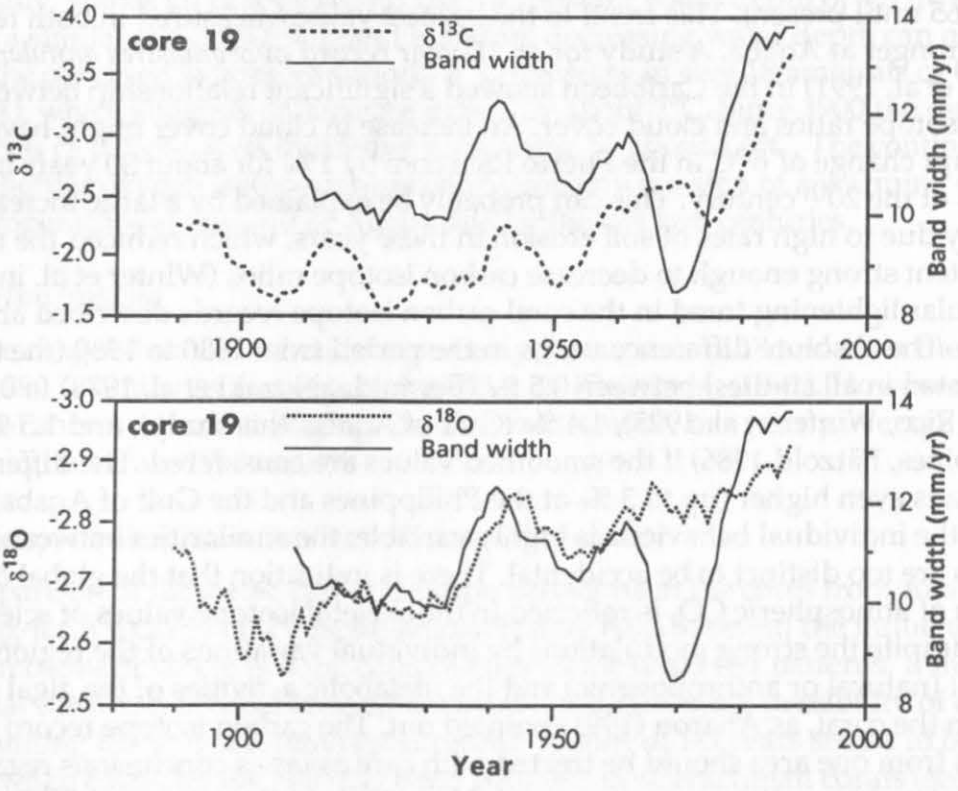

Figure 4.9 Growth rates vs. stable isotope variation in core 19 (horizontal core). Values are smoothed by 9 point moving average. A general similarity in the long-term trend between growth rate and $\delta^{13}C$ and $\delta^{18}O$ is evident. Shifts of several years in the maxima and minima occur. The strong decrease in growth rate in the 1960s is the most important discrepancy between the curves. It might be caused by sediment stress caused by building activities along the coastline.

below 9 mm·yr^{-1} were not observed. From his observations and comparisons with non-photosynthetic corals McConnaughey (1989a) concludes, that the kinetic isotopic disequilibria are consistent in fast growing parts of photosynthetic corals. As the Aqaba coral always grew with rates higher than 8 mm·yr^{-1}, it is assumed, that the isotopic variations reflect changes in environmental conditions and are not affected by growth rate variations. Of great importance for this assumption is the strong decrease of growth rates before 1970 and its recovery to extreme high values in the last years. This phenomenon could be caused by changes in the sediment load from the coast, which might have affected core 19 (horizontal, close to the bottom) stronger than core 18 (elevated position). The minimum before 1970 has no counterpart either in the oxygen or the carbon record. If kinetic effects due to extension rate were responsible for the isotope fractionation, this strong event should be seen in the isotope record. Thus, growth rate is probably not the controlling factor of the oxygen isotope ratio.

Growth rate vs. $\delta^{13}C$ signal

The comparison of growth rate with $\delta^{13}C$ of core 19 shows in the plotted curves similar behaviour from ca 1910 to 1960 with a negative correlation (Fig. 4.9). The decrease in growth rate around 1970 is not followed by the carbon isotopes. The weak negative correlation (r=-0.365 and -0.375; Tab. 4.3a, 4.4a) between $\delta^{13}C$ and growth rate in core 18 and 19 for the complete data range results probably from two simultaneous, but independent effects of anthropogenic activity on $\delta^{13}C$ and growth rate after the mid 1960s (see below).
Following the model of Erez (1978) the lighter carbon isotope composition in core 18 and 19 in the last decades results from increasing photosynthetic activity. This mechanism, the depletion of carbon isotopic composition with enhanced photosynthesis, has been contradicted by various authors (Swart 1983; Pätzold 1984; McConnaughey 1989a; Klein et al. 1992). Erez´s explanation for a negative modulation of skeletal $\delta^{13}C$ by photosynthesis did not address the separate influence of kinetic effects (McConnaughey 1989a). Apparent negative modulations of $\delta^{13}C$ by photosynthesis are explained by the association of kinetic disequilibria and photosynthesis. The metabolic $\delta^{13}C$ increase (by photosynthesis) is sometimes overpowered by the kinetic depletion of ^{13}C, causing negative correlation between photosynthesis and skeletal $\delta^{13}C$ (McConnaughey 1989a).
A negative correlation between skeletal $\delta^{13}C$ and light has been reported by McConnaughey (1989a) for a *Porites* colony at Galápagos growing in shallow water (approximately at the low tide line). It was thought to be caused by bleaching or photoinhibition during bright periods. In this colony the $\delta^{13}C$ shows a significant trend toward lower skeletal $\delta^{13}C$ between 1964 and 1982. The author attributes this to decreased photosynthesis as the coral approached the sea surface. A deeper coral didn´t show a similar trend,"presumably because the reduction in depth caused by coral growth was insignificant compared to total depth" (McConnaughey 1989a).
$\delta^{13}C$ values and thus photosynthetic activity in core 18 of the Aqaba coral has not changed remarkably until ca 1960. Core 19 showed higher variations in photosynthesis at a generally lower activity level (Fig. 4.6). However, the stable trend until 1960 and the sudden decrease until present is common in both cores. Thus, reduction

of water depth from 4 to 1 meter had obviously no influence on the $\delta^{13}C$ ratio in core 18.

Table 4.3 Correlation matrix for yearly growth rates and stable isotopes of core 18. **a.** Correlations for the complete dataset from 1788 to 1992. **b.** Correlations for the time from 1788 to 1967.

a. Core 18 (1788-1992) Correlation Matrix

	C18 growth	C18 ∂13C	C18 ∂18O
C18 growth	1	-0.365	0.122
C18 ∂13C	-0.365	1	0.066
C18 ∂18O	0.122	0.066	1

Fisher's r to z

	Correlation	P-Value
C18 growth, C18 ∂13C	-0.365	<0.0001
C18 growth, C18 ∂18O	0.122	0.0945
C18 ∂13C, C18 ∂18O	0.066	0.3682

b. Core 18 (1788-1967) Correlation Matrix

	C18 growth	C18 ∂13C	C18 ∂18O
C18 growth	1	-0.121	0.206
C18 ∂13C	-0.121	1	-0.17
C18 ∂18O	0.206	-0.17	1

Fisher's r to z

	Correlation	P-Value
C18 growth, C18 ∂13C	-0.121	0.1251
C18 growth, C18 ∂18O	0.206	0.0082
C18 ∂13C, C18 ∂18O	-0.17	0.0299

Table 4.4 Correlation matrix for yearly growth rates and stable isotopes of core 19. **a.** Correlations for the complete dataset from 1886 to 1992. **b.** Correlations for the time from 1886 to 1967.

a. Core 19 (1886-1992) Correlation Matrix

	C19 growth	C19 ∂13C	C19 ∂18O
C19 growth	1	-0.375	-0.269
C19 ∂13C	-0.375	1	0.413
C19 ∂18O	-0.269	0.413	1

Fisher's r to z

	Correlation	P-Value
C19 growth, C19 ∂13C	-0.375	<0.0001
C19 growth, C19 ∂18O	-0.269	0.0049
C19 ∂13C, C19 ∂18O	0.413	<0.0001

b. Core 19 (1886-1967) Correlation Matrix

	C19 growth	C19 ∂13C	C19 ∂18O
C19 growth	1	-0.158	-0.187
C19 ∂13C	-0.158	1	0.159
C19 ∂18O	-0.187	0.159	1

Fisher's r to z

	Correlation	P-Value
C19 growth, C19 ∂13C	-0.158	0.1571
C19 growth, C19 ∂18O	-0.187	0.0922
C19 ∂13C, C19 ∂18O	0.159	0.1545

Oxygen vs. carbon isotopes

Correlations between skeletal $\delta^{18}O$ and $\delta^{13}C$ for both cores display different patterns. In the horizontal core (C19) carbon and oxygen display a rough positive visual correlation (Fig. 4.7). This suggests that the highest photosynthetic activity occurs in years with lower sea surface temperatures (SST). The correlation seems to be significant, if the complete record is computed (1886-1992; $r=0.413$, $p<0.0001$; Tab. 4.5a). However, if the period from 1967 to present is not respected, no significant correlation is obtained ($r=0.159$, $p=0.1545$; Tab. 4.5b). The coincidence of several maxima and minima in the carbon and oxygen record of core 19 seen in the plotted

values (Fig. 4.7) is either just accidental or controlled by factors which we don't know. A strong kinetic effect, which simultaneously depletes $\delta^{13}C$ and $\delta^{18}O$ (McConnaughey 1989a) might explain this phenomenon, but the changes in growth rates, which could cause this kinetic effect, are not correlated to the isotope variations (see below).
In core 18, no correlation between $\delta^{13}C$ and $\delta^{18}O$ exists (Fig. 4.8 and 4.10, Tab. 4.5).

Comparison of the stable isotope record of core 18 and core 19

The time-dependent changes in stable isotope composition of $\delta^{18}O$ and $\delta^{13}C$ in core 18 and 19 display a different behaviour (Fig. 4.7 and 4.8). In the record of core 19 (the horizontal core) corresponding maxima of $\delta^{13}C$ occur around 1905, 1923-25, and 1950. Minima are measured before 1890 and 1920, and around 1950-55. After 1970 the

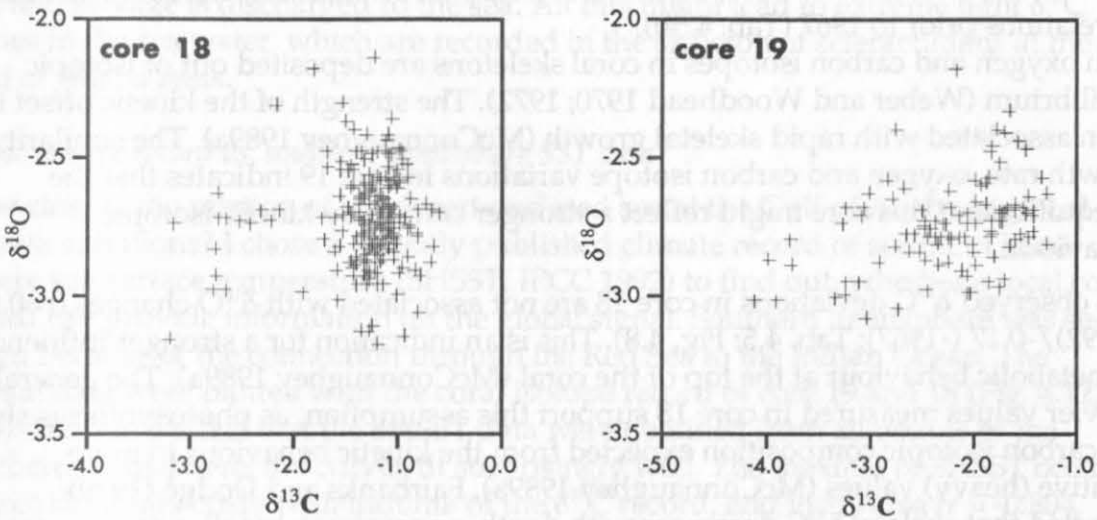

Figure 4.10 Skeletal $\delta^{18}O$ vs. $\delta^{13}C$ for core 18 and core 19

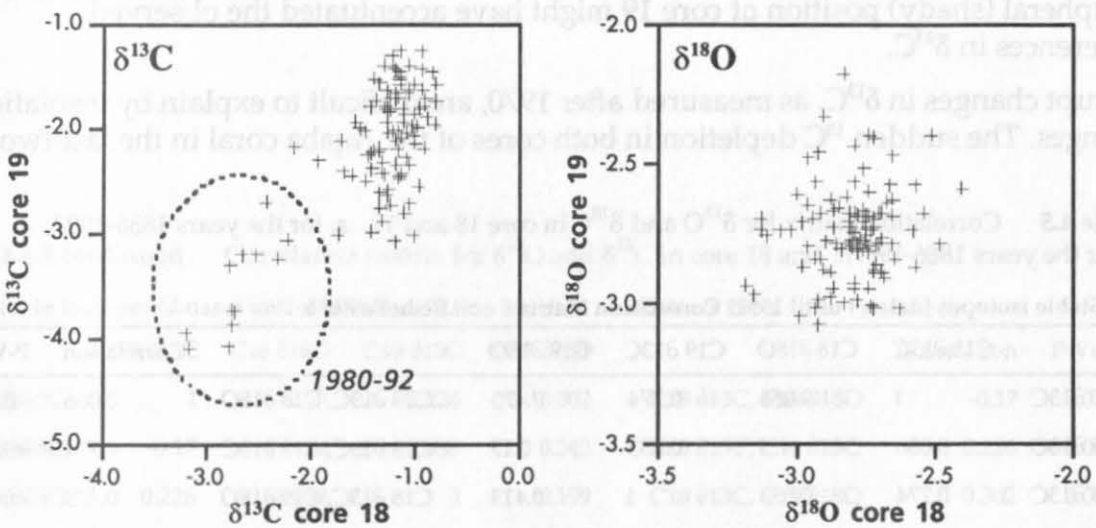

Figure 4.11 Skeletal $\delta^{18}O$ and $\delta^{13}C$ for core 18 vs. core 19. Most negative values in the $\delta^{13}C$ composition were measured in the years after ca 1960 (explanation see text).

carbon isotopes trend towards extremely light values .
$\delta^{18}O$ values between the cores do not correlate (r=0.170, p=0.0807), while $\delta^{13}C$ is closely correlated (r=0.774, p<0.0001, Tab. 4.5a, Fig. 4.11). What are the reasons for this different behaviour? $\delta^{13}C$ values remain on a relatively stable level in both cores until ca 1960 (Fig. 4.6). A sudden trend to lighter values in $\delta^{13}C$ in both cores begins after 1960 (Fig. 4.6). If a correlation matrix excluding the values of the last 25 years is computed, no significant correlation of stable isotopes remains (Tab. 4.5b, Fig. 11). Thus it seems that $\delta^{13}C$ values of the two cores were independent of each other before that time. The increase of correlation is an indication for a change in the environmental conditions that affected both parts of the coral simultaneously. This effect commenced to override the natural signals of isotope composition in the coral skeleton in the 1960s (see below).

The discussion of the natural conditions of isotope fractionation refers to data and correlations prior to 1967 (Tab. 4.5b).
Both oxygen and carbon isotopes in coral skeletons are deposited out of isotopic equilibrium (Weber and Woodhead 1970; 1972). The strength of the kinetic offset is often associated with rapid skeletal growth (McConnaughey 1989a). The similarity in growth rate, oxygen and carbon isotope variations in core 19 indicates that the disequilibria of this core might reflect a stronger control by kinetic isotopic behaviour.

The observed $\delta^{13}C$ deviations in core 18 are not associated with $\delta^{18}O$ changes (r=0.066 (-1992)/-0.17 (-1967); Tab. 4.5; Fig. 4.8). This is an indication for a stronger influence of metabolic behaviour at the top of the coral (McConnaughey 1989a). The generally heavier values measured in core 18 support this assumption, as photosynthesis shifts the carbon isotopic composition expected from the kinetic behaviour to more positive (heavy) values (McConnaughey 1989a). Fairbanks and Dodge (1979) reported that skeletal $\delta^{13}C$ decreases with depth, approximately following the curve of relative light intensity. A similar pattern was reported recently by Bosscher (1992) from Curaçao. Thus, the depth difference of 3 m between the two cores and the peripheral (shady) position of core 19 might have accentuated the observed differences in $\delta^{13}C$.

Abrupt changes in $\delta^{13}C$, as measured after 1970, are difficult to explain by insolation changes. The sudden ^{13}C depletion in both cores of the Aqaba coral in the last two

Table 4.5 Correlation matrix for $\delta^{18}O$ and $\delta^{13}C$ in core 18 and 19. **a.** for the years 1886-1992, **b.** for the years 1886-1967.

a. Stable isotopes (dataset until 1992) Correlation Matrix

	C18 ∂13C	C18 ∂18O	C19 ∂13C	C19 ∂18O
C18 ∂13C	1	0.066	0.774	0.473
C18 ∂18O	0.066	1	0.033	0.17
C19 ∂13C	0.774	0.033	1	0.413
C19 ∂18O	0.473	0.17	0.413	1

Fisher's r to z

	Correlation	P-Value
C18 ∂13C, C18 ∂18O	0.066	0.3682
C18 ∂13C, C19 ∂13C	0.774	<0.0001
C18 ∂13C, C19 ∂18O	0.473	<0.0001
C18 ∂18O, C19 ∂13C	0.033	0.7342
C18 ∂18O, C19 ∂18O	0.17	0.0807
C19 ∂13C, C19 ∂18O	0.413	<0.0001

decades suggests an influence of anthropogenic activities in the Gulf of Aqaba. From ecological studies it is known that besides the catastrophic effects of major oil spills the chronic pollution at sublethal levels can cause high mortality, decrease of coral cover and reproduction of reef corals (Fishelson 1973; Rinkevich and Loya 1977; Guzmán and Holst 1993). From 1965 the harbour at Eilat (Israel) developed remarkably and an oil terminal was constructed north of the Nature reserve at the western coast of the Gulf. This is a distance of only 7.5 km from the Marine Science Station at Aqaba. From the beginning at least 2-3 big oil spills per month were reported (Fishelson 1973). Many more minor oil spills occurred in the vicinity, which were not officially reported (Rinkevich and Loya 1977). As the stable carbon isotope composition of crude oil is extremely light, the chronic input could have diluted the natural ^{13}C content of sea water. The generally clockwise circulation transports this isotopically light water along the coast via the city and harbour of Aqaba, where even more fuel and sewage is discharged to the sea. All this might lead to extreme light $\delta^{13}C$ values in the sea water, which are recorded in the skeleton of scleractinians at the Gulf of Aqaba reefs.

Stable isotope record vs. southern hemisphere SST data

How close is the relation of the desert-enclosed sea at the Gulf of Aqaba to global climate variations? I chose a recently published climate record of southern hemisphere sea surface temperature (SHSST, IPCC 1992) to find out, whether a local coral record can provide information on the global signal. Southern hemisphere was selected because of the connection through the Red Sea to the Indian Ocean. The annual data were plotted with the coral isotope record of core 19 and 18 (Fig. 4.12, 4.13). Despite the fact that the SHSST data were obtained from all oceans of the southern hemisphere, the curves fit surprisingly well. The maxima of SHSST occur almost simultaneously with minima of the $\delta^{13}C$ record, and vice versa (r = -0.804, Tab. 4.6). The $\delta^{13}C$ excursion from the 1960s does not match the SHSST record. This is another indication for a change in environmental conditions which is not correlated with other natural effects.

Table 4.5 continued Correlation matrix for $\delta^{18}O$ and $\delta^{13}C$ in core 18 and 19.

b. Stable isotopes (dataset until 1967) Correlation Matrix

	C18 ∂13C	C18 ∂18O	C19 ∂13C	C19 ∂18O
C18 ∂13C	1	-0.17	0.226	0.302
C18 ∂18O	-0.17	1	-0.038	0.243
C19 ∂13C	0.226	-0.038	1	0.159
C19 ∂18O	0.302	0.243	0.159	1

Fisher's r to z

	Correlation	P-Value
C18 ∂13C, C18 ∂18O	-0.17	0.0299
C18 ∂13C, C19 ∂13C	0.226	0.0405
C18 ∂13C, C19 ∂18O	0.302	0.0056
C18 ∂18O, C19 ∂13C	-0.038	0.7371
C18 ∂18O, C19 ∂18O	0.243	0.0276
C19 ∂13C, C19 ∂18O	0.159	0.1545

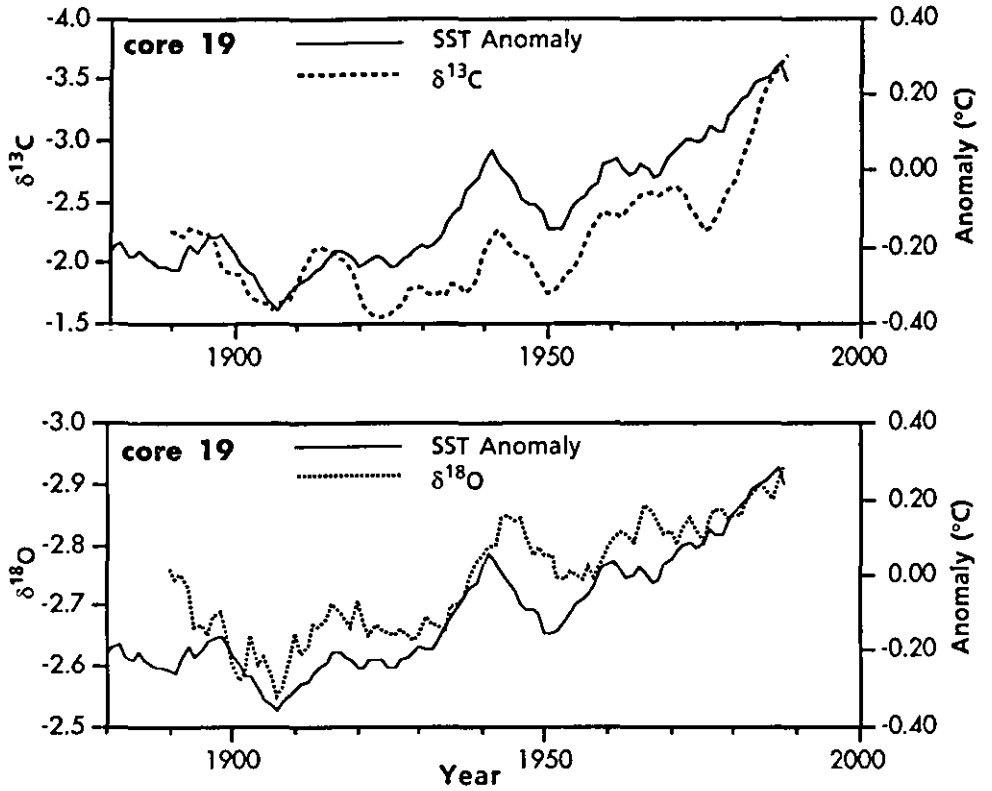

Figure 4.12 Stable isotope record of core 19 vs. SST anomaly data of the southern hemisphere. SST anomalies relative to 1951-1980 (from IPCC 1992). All data are smoothed with 9 point moving average. $\delta^{18}O$ and $\delta^{13}C$ are plotted reversed. Both carbon and oxygen isotopes from the Aqaba coral record display similar trends to the SST variations in the southern hemisphere. $\delta^{13}C$ changes of trends occur simultaneous with the SST, while $\delta^{18}O$ seems to follow the global signal with a time lag of a few years.

Table 4.6 Correlation matrix for core 19. Growth rate, stable carbon and oxygen isotopes, and southern hemisphere SST data are correlated. Data of 9 point moving averages were used for this correlation matrix. P-value is <0.0001 for all correlations.

Core 19	Growth rate	SHSST	$\delta^{18}O$	$\delta^{13}C$
Growth rate	-	0.593	-0.509	-0.555
SHSST	0.593	-	**-0.907**	**-0.840**
$\delta^{18}O$	-0.509	**-0.907**	-	0.786
$\delta^{13}C$	-0.555	**-0.840**	0.786	-

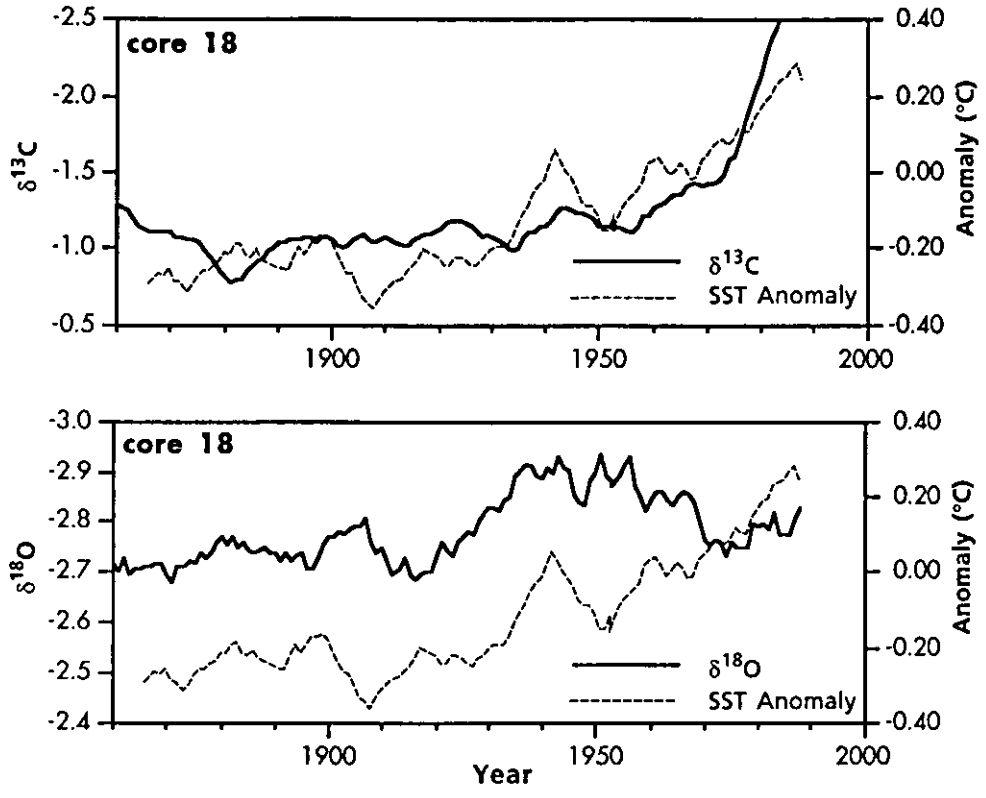

Figure 4.13 Stable isotope record of core 18 vs. SST anomaly data of the southern hemisphere. SST anomalies relative to 1951-1980 (from IPCC 1992). All data are smoothed with 9 point moving average. $\delta^{18}O$ and $\delta^{13}C$ are plotted reversed. Both carbon and oxygen isotopes display only low similarities to the SST variations in the southern hemisphere, in contrast to core 19 (Fig. 4.12). Early stable oxygen record seems to correlate well with SHSST, until ca 1900. The global variation in temperature from 1920 to 1960 is reflected as well in the Aqaba record, however the warming from 1955 to 1990 is not present in the isotope record of core 18.

Table 4.7 Correlation matrix for core 18. Growth rate, stable carbon and oxygen isotopes, and southern hemisphere SST data are correlated. Data of 9 point moving averages were used for this correlation matrix. P-value is <0.0001 for correlations without special note.

Core 18	Growth rate	SHSST	$\delta^{18}O$	$\delta^{13}C$
Growth rate	-	0.318 (P=0.0003)	0.359	-0.494
SHSST	0.318 (P=0.0003)	-	-0.416	-0.839
$\delta^{18}O$	0.359	-0.416	-	0.012 (P=0.869)
$\delta^{13}C$	-0.494	-0.839	0.012 (P=0.869)	-

Scleractinian corals promise to provide valuable information on world-wide changes of CO_2. In the interpretation of $\delta^{13}C$ records of corals, conditions of the local environment and the individual metabolic behaviour of the colonies must be respected. The information can only be trustworthy in the context with records from other sites in the region and other oceans in the world. It seems that sites with low variations in the carbon reservoir by upwelling, nutrient input, or environmental pollution by hydrocarbons are best suited for studies of carbon isotopic variations. The amount of precipitation has probably a negligible effect on the long-term record of stable carbon isotopes.
The connection between $\delta^{18}O$ and the SHSST is also obvious and a strong negative correlation in core 19 is evident (r = -0.907, Tab. 4.6, Fig. 4.12). The correlation in core 18 is lower (r = -0.416, Tab. 4.7). Trends of water temperature are followed with a time lag of ca 3-5 years by the oxygen isotope record from Aqaba. This shift varies, possibly caused by variations in the assignment of growth bands to certain years. The long-term temperature differences are accentuated at Aqaba. If a decrease of 0.22 ‰ in ^{18}O for an increase of water temperature by 1°C (Epstein et al. 1953) is assumed, the warming of Aqaba sea water from ca 1905 to present equals ca 1.7°C, while the warming of the southern hemisphere is ca 0.6°C.

Cycles

In order to reveal eventual long-term cycles recorded in the growth and stable isotope record of the cores, we performed spectral analysis on our data. Spectral analysis in corals has been applied to show variability in the El Niño-Southern Oscillation (ENSO) in the present century (Shen et al. 1992; Cole et al. 1993). Spectral analysis was also carried out by Winter et al. (1993) on a 270 year record of *Montastrea annularis* in the eastern Caribbean. This analysis for both carbon and oxygen, showed very little power. Periods of 6.6 years (significant, although weak power) for carbon and between 10 and 12 years (>sunspot cycle) for oxygen were found in this coral record.
Our spectral analysis showed distinct peaks in the $\delta^{18}O$ record of core 18 at periods of ~27, 22, 15.6, 12.5, 9.2, 8.6, 7.7, 6.9, 6.3, 5.6, and 5.3 years (Fig. 4.14). Of these periods the 27, 8.6, 6.9, and 5.6 year periods are present as well in the $\delta^{18}O$ of core 19. Compared with the spectra of the southern hemisphere SST record (~23, 14.7, 9.4, 6.2, and 5.2 years) there is no indication for a common control on the cycle length in $\delta^{18}O$ at Aqaba and SST in the southern hemisphere.
The cycle lengths of $\delta^{13}C$ of core 18 are ~23, 10.9, 9.4, 7.7, 6.3, and 5.3 years. Compared with core 19 (23.8, 14.3, 9.6, 7.4, 5.9 years) the cycle of ~23, ~9.5, and 7.4-7.7 years are common. Growth rates of core 19 (core 18 was not examined due to missing growth data in some parts of the core) exhibits cycles of ~28, 12.2, 7.6, 6.6, and 5.7 years.
A comparison with published cycle lengths of various environmental parameters, listed in Table 4.8, shows only a few similarities for the patterns observed in our samples. The sunspot cycle (11 years), which was expected to be present in the coral record, has probably no influence on the Aqaba coral, in contrast to the results of Winter et al. (in prep.) and Linsley et al. (1993;see Tab. 4.8). The luni-solar constituent, which is found in numerous climate records (O`Brien and Currie 1993), might be responsible for the 18.5 year period in $\delta^{18}O$. High frequency cycles between 5 and 7

years might be linked to ENSO related cycles in the global circulation. Strong ENSO teleconnections occur in east African rainfall records see (Chave et al. 1972; Adey 1978; Cole et al. 1993), thus a connection to climate in the Gulf of Aqaba seems not to be impossible.
The high variability of cycles influencing the climate (see Lassen and Friis-Christensen 1992; Shen et al. 1992) and locally restricted environmental changes (natural and anthropogenic) might mask the climate signals. Furthermore, endogenic physiological processes in the coral might have their own, yet unknown, cyclicity and could complicate the pattern. Additional sites, preferably in environments distant from anthropogenic influences, and a high resolution sampling of long coral cores are needed to decipher the natural signals of cyclicity locked in the coral skeleton.

Table 4.8 Observed variability in some environmental parameters showing cycle lengths between 3 and 100 years.

parameter	cycle length (yrs)	found in	source
solar activity	80-90 (Gleissberg-period)	northern hemisphere land air temperature	Friis-Christensen and Lassen (1991)
luni-solar constituent tide	18.6	various climate data, tree rings, oceanic circulation system	review in O`Brien and Currie (1993)
sunspot	11 (7-17)	northern hemisphere land air temperature	Friis-Christensen and Lassen (1991)
ENSO (El Niño-Southern Oscillation)	3.8 (~2 and ~4-5)	coral $\delta^{18}O$	Shen et al. (1992)
ENSO	5.6; 3.6; 3.0; 1.9 to 2.4	coral (central Pacific)	Cole et al. (1993)
$\delta^{13}C$	6.6	coral (Caribbean)	Winter et al. (in prep.)
$\delta^{13}C$	~23; 9.5; 7.4-7.7	coral (Red Sea)	this study
$\delta^{18}O$	10-12	coral (Caribbean)	Winter et al. (in prep.)
$\delta^{18}O$	27; 18.5; 11; 9; 7.5; 6; 3	coral (eastern Pacific)	Linsley et al. (1993)
$\delta^{18}O$	27; 8.6; 6.9; 5.6	coral (Red Sea)	this study
coral growth rate	28; 12; 7.6; 6.6; 5.7	coral (Red Sea)	this study

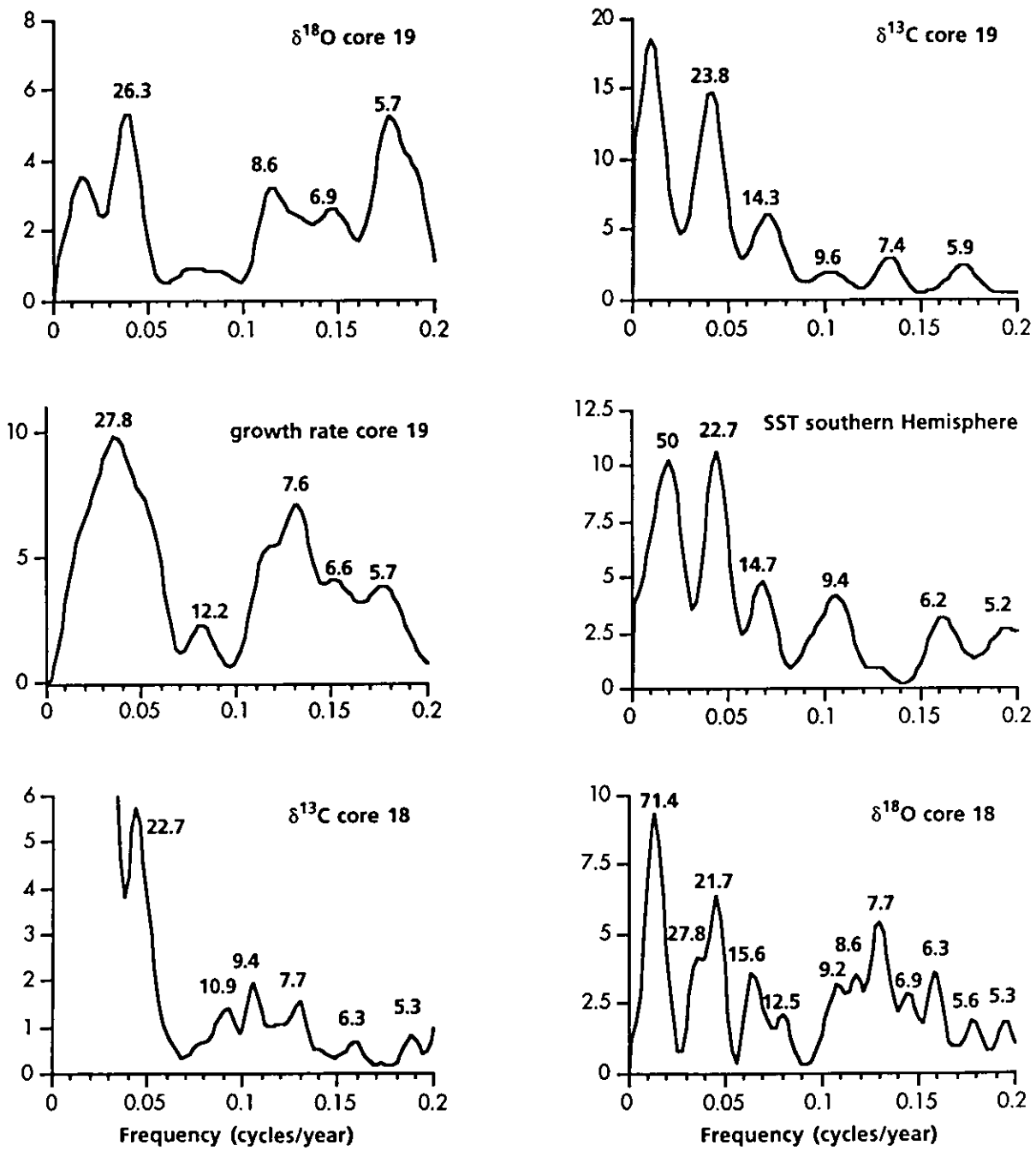

Figure 4.14 Spectral analysis of stable carbon and oxygen isotopes of core 18 (204 yrs) and 19 (107 yrs), southern hemisphere SST (130 yrs), and growth rate of core 19 (107 yrs). Numbers at the peaks are cycle periods in years.

CHAPTER FIVE

RED SEA CORAL GROWTH RATES: RELATION WITH DEPTH AND LATITUDE

Abstract

Annual growth rates of the scleractinian coral genus *Porites* were investigated in Red Sea fringing reefs. Locations extend from Aqaba, Gulf of Aqaba, in the North over the northern and southern Egyptian coast and islands to the Gulf of Tadjoura in the Gulf of Aden (Djibouti). The upper limit of growth potential decreases with depth with the decrease of light availability. The variation of growth rates is very high in shallow depth, indicating that other environmental factors than light are able to depress coral growth markedly. This zone reaches at Aqaba (29°27´N) to a depth of ca. 10 m. At the southern Egyptian reefs (24°30´N) this zone extends to ca. 15 m water depth. This effect is probably a result of the stronger reduction of winter light levels and water temperature to the northern regions. Mean growth rates in the shallow water zone increase with decreasing latitude and are highest at the southernmost studied reefs in the Gulf of Tadjoura. However, the observed latitudinal growth reduction is restricted to the upper ca. 15 m of the water column. Compared to other oceans the decrease of growth with increasing latitude of Red Sea *Porites* corals is far less, and growth rates at Aqaba are the highest observed at these latitudes.

Introduction

Environmental factors which could influence coral growth are almost unlimited in number (Buddemeier and Kinzie 1976). Water depth and geographical location are the factors most easy to determine. The relation of the growth of scleractinian corals to water depth has long been recognized (Vaughan 1919). Depth is a mixed environmental variable, including mainly the effects of light, water movement, and resuspension of sediment. A thorough review of the extensive studies on environmental relations to coral growth is given in Buddemeier and Kinzie (1976).
Light is assumed to be the primary environmental factor controlling growth of hermatypic corals, and light-enhanced calcification is responsible for most of the skeletal growth of reef-building corals (Goreau 1959; Chalker et al. 1988; Bosscher 1992).
In laboratory experiments the dependency of coral growth on both temperature and insolation was observed for corals of the genera *Porites, Pocillopora, Montipora, Cyphastrea* and *Pavona* (Houck et al. 1977). Some species had sharp growth optima at characteristic temperatures *(Porites, Pocillopora)*, while *Montipora* had a poorly defined maximum. Response to decreasing insolation is also different. *Porites* and *Pocillopora* growth decreased with decreasing light intensity, while *Montipora* growth was enhanced (Houck et al. 1977).
A decrease in growth rates with increasing water depth is generally caused by the decrease of illumination and was reported for the Caribbean corals *Montastrea annularis*, (Baker and Weber 1975; Dustan 1975; Hubbard and Scaturo 1985; Huston 1985), *Porites astreoides* and *Diploria labyrinthiformis* (Logan and Tomascik 1991). A similar pattern is reported for indopacific species like *Porites lutea , Favia pallida*, and *Goniastrea retiformis* (Buddemeier et al. 1974; Highsmith 1979). Bosscher (1992) could show that the growth rate of *Montastrea annularis* decreases exponentially with depth following a photosynthetic hyperbolic tangent function.

Growth rate relation with latitude

Growth rates of scleractinian corals decrease generally with increasing latitude in the Atlantic, Pacific and Indian Oceans (Grigg 1982; Crossland et al. 1991; Logan and Tomascik 1991). Although the coral *Montastrea annularis* in the Caribbean is extensively studied, the relation for this species is ambiguous (review by Logan and Tomascik 1991). Nevertheless the general trend remains a credible theory. The Red Sea with its extension over almost 20° of latitude and living coral reefs growing along the greatest part of its coastline presents an unique area of study for latitudinal effects on coral growth. The Red Sea is an ocean which is today enclosed by deserts. This fact is important if we consider that the growth patterns of corals are influenced by precipitation, cloud cover, and freshwater discharge with its effects on salinity and turbidity. In the Red Sea at least these environmental factors remain unchanged over its whole extension. However, in the Gulf of Aqaba clouds and episodical rainfalls as well as groundwater discharge occur occassionally winter.

The main objective of this part of the study was to compare coral growth patterns of the genus *Porites* in relation to latitude and water depth in the Red Sea-Gulf of Aden reef province. Our study area extends from Aqaba, at the northern end of the Gulf of Aqaba, through the reefs of the northern Red Sea off Hurghada and off the southern Egyptian coast to the reefs in the western Gulf of Aden (Fig. 5.1). *Porites* was chosen because corals of this genus are probably the most important reef builders due to their ubiquitism and their ability to secrete huge massive colonies. *Porites* skeletons display in most cases a clear defined density banding, which enables the measurement of annual linear extension rates. Studies on coral growth are rare for the Red Sea, but a few data are published from the reefs at Eilat, Gulf of Aqaba (Klein and Loya 1991; Klein et al. 1993).

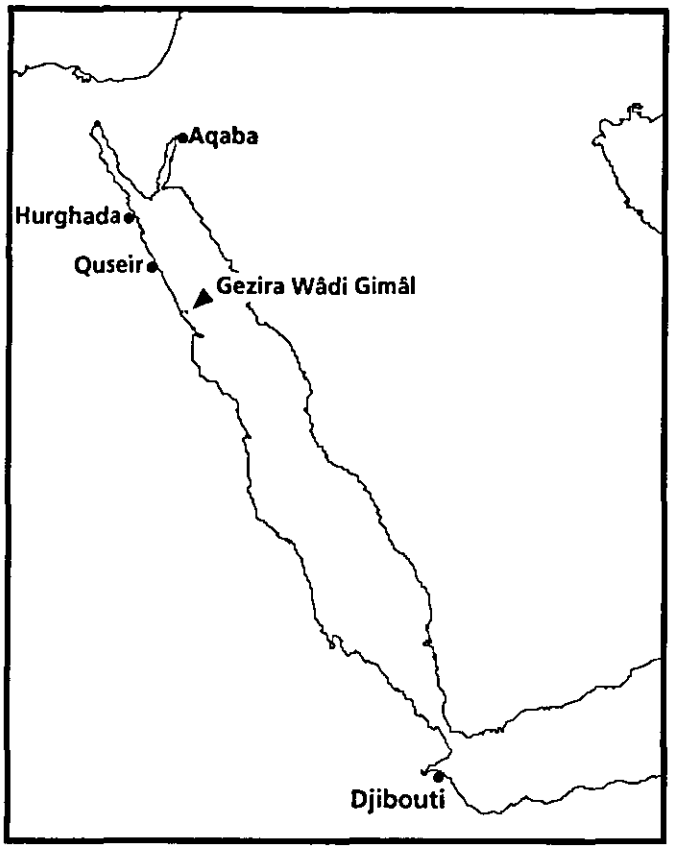

Figure 5.1
Collection sites in the Red Sea and Gulf of Aden

Extensive studies on coral reefs exist from the Gulf of Aqaba (e.g. Mergner and Schuhmacher 1974, 1981; Mergner 1979; Bouchon et al. 1981; Schuhmacher and Mergner 1985; Klein and Loya 1991; Klein et al. 1993). Even though not a part of the proper Red Sea, the reefs in the Gulf of Tadjoura belong biogeographically to the Red Sea coral reef province. The Gulf of Tadjoura is almost unknown in the coral literature. There has been no work on corals in this region published since Gravier (1911).

Materials and Methods

In total 100 complete coral colonies and 6 core samples of the genus *Porites* were sampled by Scuba-diving in 5 field periods in the fringing reefs of Aqaba, Jordan (29°27'N), along the Red Sea coast of Egypt, and in the fringing reefs of Djibouti in 1991 and 1992 (Fig. 5.1). Twenty samples from Aqaba were taken at the fringing reef off the Marine Science Station at water depths from 1 to 50 m. At a fore-reef slope close to the Jordan-Saudi Arabian border eighteen samples were collected from depths between 2 and 45 m (Fig. 5.2), and one sample at a depth of 3 m halfway between the Marine Science Station and the Saudi border site. In order to increase the sample size, growth rate data from six cores (Chapter 2) from the Marine Science Station reef are included in the calculations. Growth rate data of nine samples from a *Porites* pinnacle (Chapter 7) in the fore-reef of the Marine Science Station are displayed for comparison in Fig. 5.6. However, these samples are not included in the calculations shown in Tables 5.1 and 5.2 because this pinnacle provides particular conditions different from the reef bottom (see Chapter 7).

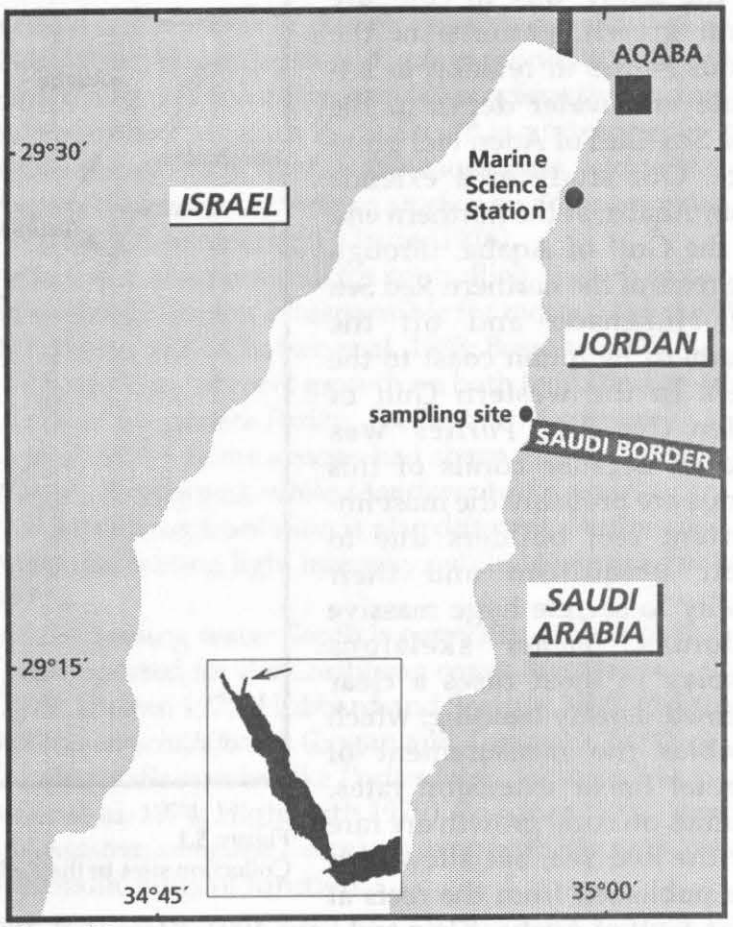

Figure 5.2
Sampling sites at the Jordanian coast , northern Gulf of Aqaba.

Samples from the northern part of the Egyptian coast (14 specimen) derive from the islands of Gûbal, Tawîla, Giftûn el Kabîr, Giftûn el Saghîr, and Abu Rimâthi, a fringing reef off Hurghada, and a fringing reef north of Quseir (Fig. 5.3). The colonies were sampled in depths between 1 and 15 m from lagoonal to fore-reef environments.

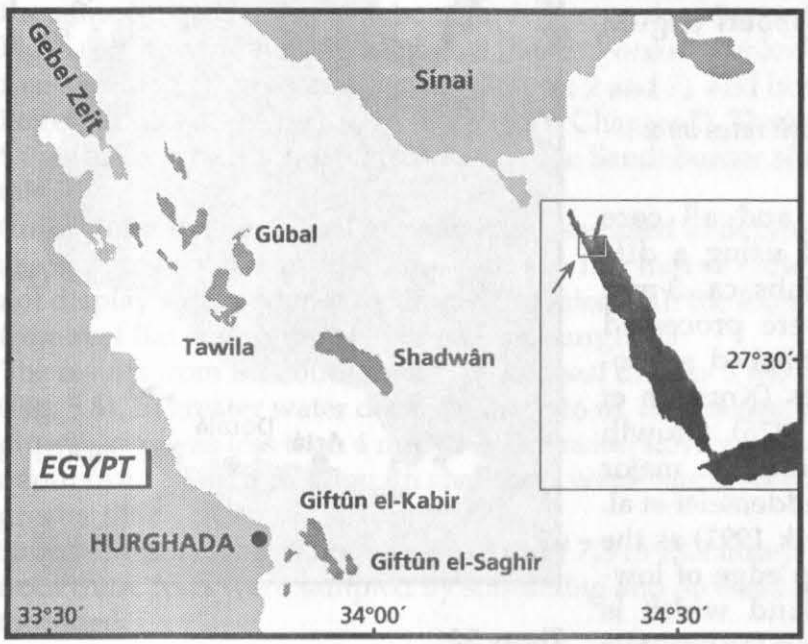

Figure 5.3
Sampling sites at the reefs off the northern Egyptian coast and the islands

Twenty-two samples were collected in the reefs of the islands Gezira Showârît and Gezira Wadî Gîmal and the coastal fringing reef at Ras Abu Ghusum. Another ten specimen were sampled from 2.4 m to 42 m water depth at the slope of a fringing reef off the Southern Egyptian coast at Gezira Showârît (Fig. 5.4).

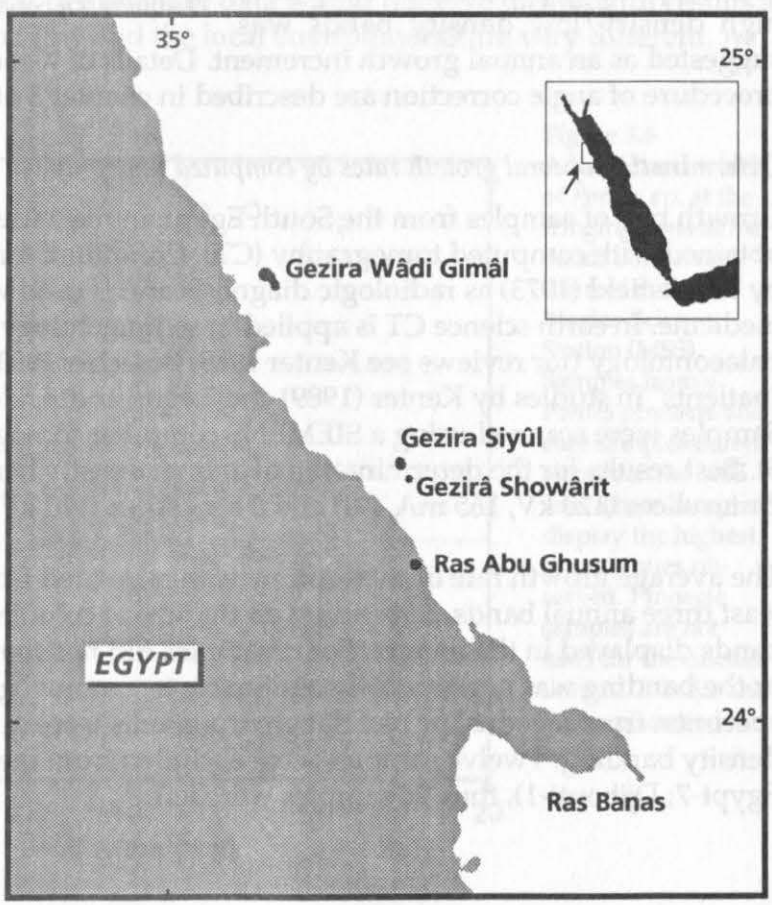

Figure 5.4
Sampling sites at the reefs off the southern Egyptian coast

In August 1992 five samples were collected at the reef crest of two fringing reefs (Arta Plage and Doralé, water depth 4 to 6 m) at the southern coast of the Gulf of Tadjoura, Djibouti (Figure 5.5).

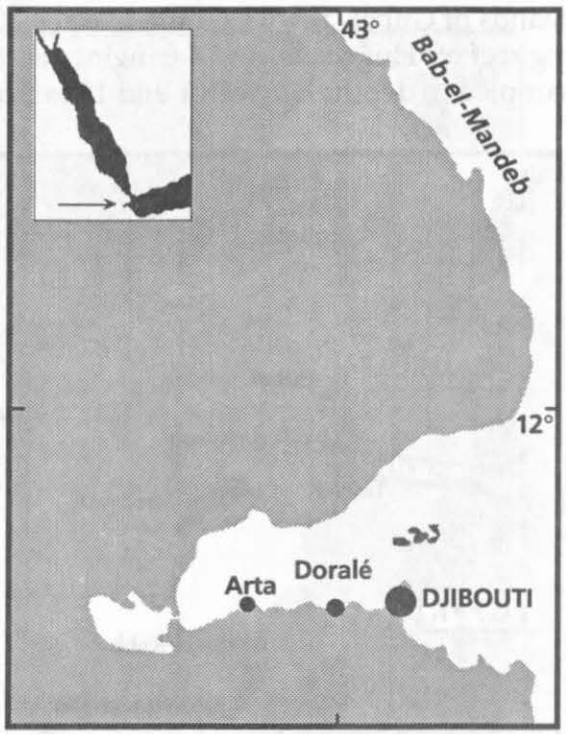

Figure 5.5
Sampling sites at the fringing reefs in the Gulf of Tadjoura, Djibouti

Determination of coral growth rates by x-radiography

Most of the specimen and all core samples were sectioned using a diamond rock saw into slabs ca. 3 mm thick. X-radiographs were processed following the well established sclerochronological procedures (Knutson et al. 1972; Hudson et al. 1976). Growth rates were measured along the major (vertical) growth axis (Buddemeier et al. 1974; Logan and Tomascik 1991) as the distance between the top edge of low-density bands (LD). Band width is measured either directly on the negative or from positive prints. Each couplet of high density/low density bands was suggested as an annual growth increment. Details of X-radiographic method and the procedure of angle correction are described in chapter 3 of this thesis.

Determination of coral growth rates by computed tomography

Growth rate of samples from the South Egyptian reefs was determined from images obtained with computed tomography (CT). Computed tomography was introduced by Hounsfield (1973) as radiologic diagnosis and is used with great success in medicine. In earth science CT is applied in sedimentology, reservoir geology and palaeontology (for reviews see Kenter 1989; Bosscher 1993). Corals first appeared as "patients" in studies by Kenter (1989) and Logan and Anderson (1991) Samples were scanned using a SIEMENS computer tomograph (Type Somatom Plus-S). Best results for the determination of annual density bands were obtained with 2 mm slices (120 kV, 165 mA, 2 s) and 3 mm slices (120 kV, 125 mA, 2x2 s).

The average growth rate of each colony was calculated from the measurement of at least three annual bands, depending on the size of colonies and quality of growth bands displayed in the images. Some samples did not show distinct annual banding or the banding was not definitely assignable to a annual growth pattern. Especially specimen from lagoonal or reef flat environments were questionable regarding their density banding. Twelve samples were excluded from the calculations (Aqaba-4; Egypt-7; Djibouti-1), thus 94 samples were left.

Results

At Aqaba growth rates of single *Porites* specimen ranged from 4 to ca. 10 mm·yr^{-1} in shallow water and decreased to 1.25 mm·yr^{-1} in a depth of 50 m (Fig. 5.6). Values from the sampling sites at the Marine Science Station and at the Saudi Border are in the same range and thus can be regarded as parts ot the same population (Tab. 5.1, Fig. 5.6). Growth rates higher than 8 mm·yr^{-1} occur in colonies which derive from a free-standing *Porites* pinnacle (see Chapter 2 and 7), and in core samples drilled from large colonies at the reef edge (Fig. 5.6, cf. Chapter 2). These samples were derived from the Marine Science Station reef, at the Saudi border site no core samples were taken.

Corals from the northern Egyptian coast, sampled in depths between 1 and 15 m, show a range of linear extension from 4 to 12.9 mm·yr^{-1} (Fig. 5.7). Growth rate does not display a dependence on depth. Colonies with the lowest growth rates derive from reef flat environments at a reef off Hurghada.

The results from the southern Egyptian coast display a more detailed picture (Fig. 5.8). In greater water depths (below 16 m, the deepest colony at 38.6 m) the growth rate was less than 4 mm·yr^{-1}. Extension slowly increases with decreasing depth from 40 m to ca. 15 m. In shallower water high growth rates with values greater than 7 mm·yr^{-1} are frequent.

Samples from Djibouti grew with a rate of 7.3 to 13.3 mm·yr^{-1} (Fig. 5.9). All samples from these reefs were sampled by snorkeling and no exact water depth could be determined.

From the raw data we calculated mean growth rates for different depth zones (Tab. 5.2). A further statistical treatment of data would not give meaningful results as the number of samples is too low and the local environments are very different. At

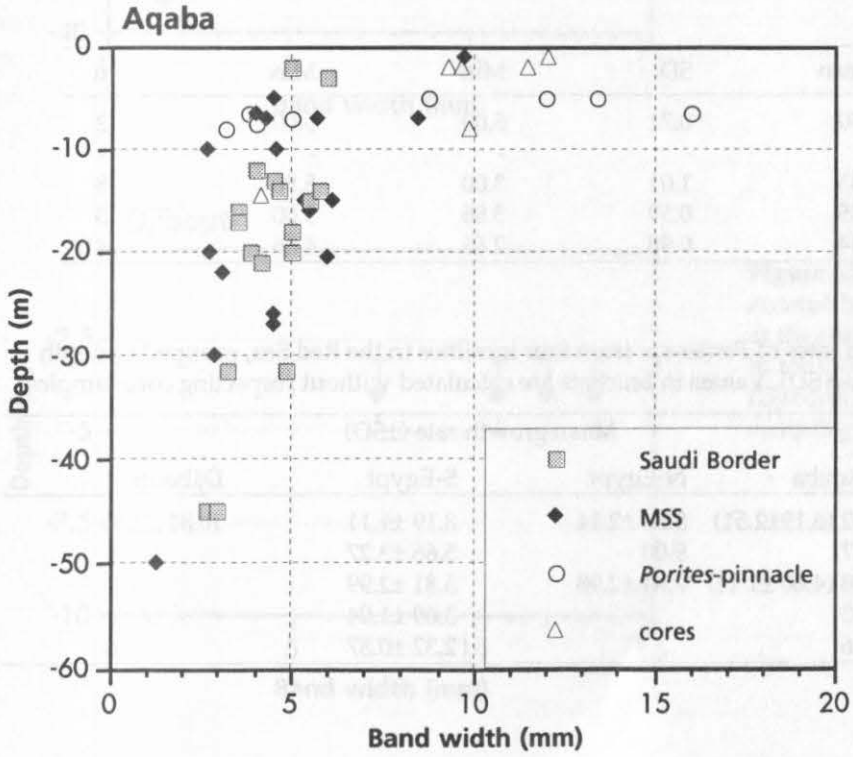

Figure 5.6
Annual band width of *Porites* sp. at the fringing reefs at the Saudi Border and the reef at the Marine Science Station (MSS). Samples from a *Porites* pinnacle and core samples derive also from the MSS reef. These samples display the highest growth rates observed. Pinnacle samples are not used for the calculations of Tab. 5.1 and 5.2 (explanation see text).

all sites the growth rates in shallow depths are of a much wider range than in depths below ca. 10-15 m (Fig. 5.6, 5.7, 5.8 and Tab. 5.2).
The sample size allows a comparison between the data obtained at Aqaba and the southern Egyptian reefs. Mean growth rates in the different depth zones are remarkably similar (Tab. 5.2, Fig. 5.10). A decrease of growth with increasing depth is evident in both regions (Fig. 5.10). The greater part of this decrease occurs in shallow water above ca. 15 m depth (Fig. 5.6, 5.8, and 5.10). The variation within each depth zone, shown by standard deviation, is highest in shallow depth. The samples display more consistency in deeper parts of the reefs (Tab. 5.2). At Aqaba growth rate distribution is relatively consistent from 10 m downwards, while at South Egypt the variation is still high and stabilizes below 20 m. The samples from Djibouti fall in the fast growing group of studied corals and display the highest mean value (10.81 mm·yr^{-1}) for the upper 5 m (Tab. 5.2 and Fig. 5.9). Below this depth no samples from the Gulf of Tadjoura are available, thus a relation to depth could not be examined.

Table 5.1 a, b Summary statistics for annual mean growth rates (mm·yr^{-1}), standard deviation (SD), minimum value (Min), maximum value (Max), and number of colonies sampled (n) at each depth zone at the Marine Science Station reef (MSS) and the reef slope at the Saudi border. Core samples are included in the calculation.

a

MSS	Mean	SD	Min	Max	n
0-5 m	10.46	1.24	9.33	12.08	5
5-10 m	6.16	2.47	4.00	9.90	6
10-20 m	4.76	1.23	2.70	6.17	6
20-30 m	4.19	1.29	2.78	6.00	5
30-50 m	2.07	1.17	1.25	2.90	2

b

Saudi Border	Mean	SD	Min	Max	n
0-5 m	5.50	0.71	5.00	6.00	2
5-10 m	-	-	-	-	-
10-20 m	4.43	1.01	3.00	5.80	8
20-30 m	4.35	0.59	3.86	5.00	3
30-50 m	3.44	0.98	2.66	4.86	4

Table 5.2 Mean growth rates of *Porites* sp. from four localities in the Red Sea, grouped in depth zones (± standard deviation SD). Values in brackets are calculated without respecting core samples.

Depth zone	Mean growth rate (±SD)			
	Aqaba	N-Egypt	S-Egypt	Djibouti
0-5 m	8.41 ±3.02 (6.19±2.51)	5.83 ±2.14	8.19 ±1.11	10.81 ±2.55
5-10 m	6.16 ±2.47	9.00	5.66 ±3.27	
10-20 m	4.57 ±1.08 (4.60 ±1.11)	7.84 ±2.98	5.81 ±2.99	
20-30 m	4.25 ±1.03		3.69 ±1.04	
30-50 m	2.98 ±1.16		2.32 ±0.87	

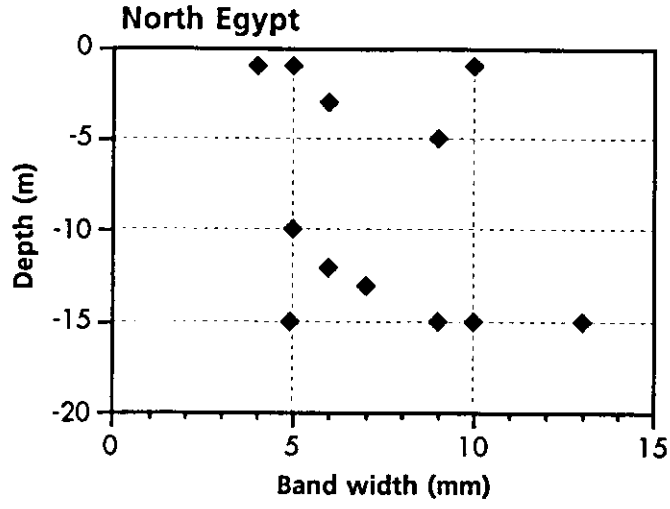

Figure 5.7
Annual band width of *Porites* sp. at the reefs at the northern part of the Egyptian coast (see Fig. 5.3).

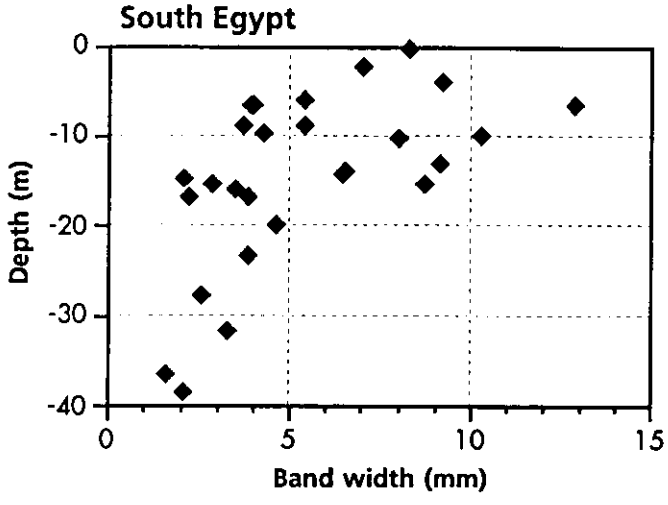

Figure 5.8
Annual band width of *Porites* sp. at the reefs at the southern part of the Egyptian coast (see Fig. 5.4).

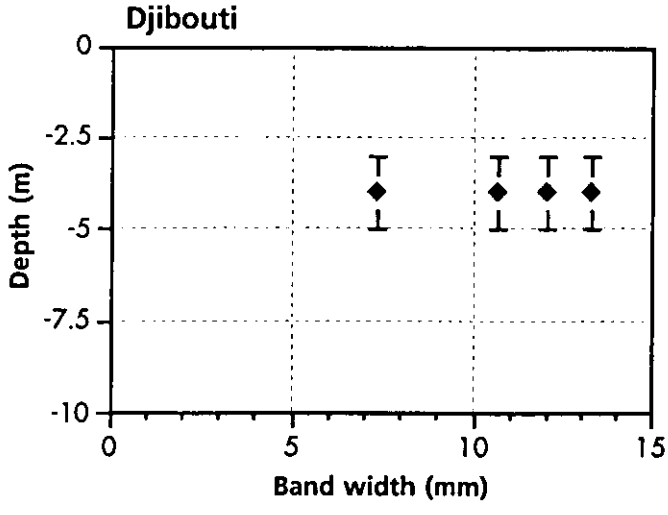

Figure 5.9
Annual band width of *Porites* sp. at the reefs of the southern coast in the Gulf of Tadjoura (Djibouti). Exact water depth of sampling locations is not known.

Discussion

Growth rate vs. depth

In the discussion on the growth rate-depth relationship we refer mainly to the results obtained at Aqaba and South Egypt. At the other sites the sample distribution does not reach depths below 15 m (northern Egypt) and from Djibouti only five samples were available, which were taken at aproximately the same depth of ca. 4 m.
We observe some interesting patterns in the variation of growth rates within different depth zones. The greatest variation is measured in the samples from a depth zone shallower than 10 m at Aqaba (Fig. 5.6) and 15 m at South Egypt (Fig. 5.8). In studies on coral growth from the Caribbean a similar pattern is observed (Hubbard and Scaturo 1985; Bosscher 1992). At Jamaica Huston (1985) studied the growth of several scleractinian species in relation to depth. Data for *Porites astreoides* display a similar trend like the samples from the Red Sea and the Gulf of Aqaba. At Aqaba two groups seem to be present. One group displays an almost linear increase of growth rate from 1-2 mm·yr^{-1} at the outer fore-reef at 50 m depth to ca. 6 mm·yr^{-1} in the shallow upper fore-reef. The second group is characterised by annual extension rates higher than 8 mm. All corals which were sampled by drilling fall in this group. This is probably an effect of the selection of samples. When we collected entire specimen, we took relatively small colonies maximal as big as a fist. For drilling, colonies of at least 0.5 m diameter were chosen. Thus the cores represent growth patterns of quite large colonies. These are growing particularly at the reef crest. Colonies in the fore-reef rarely reach this size.

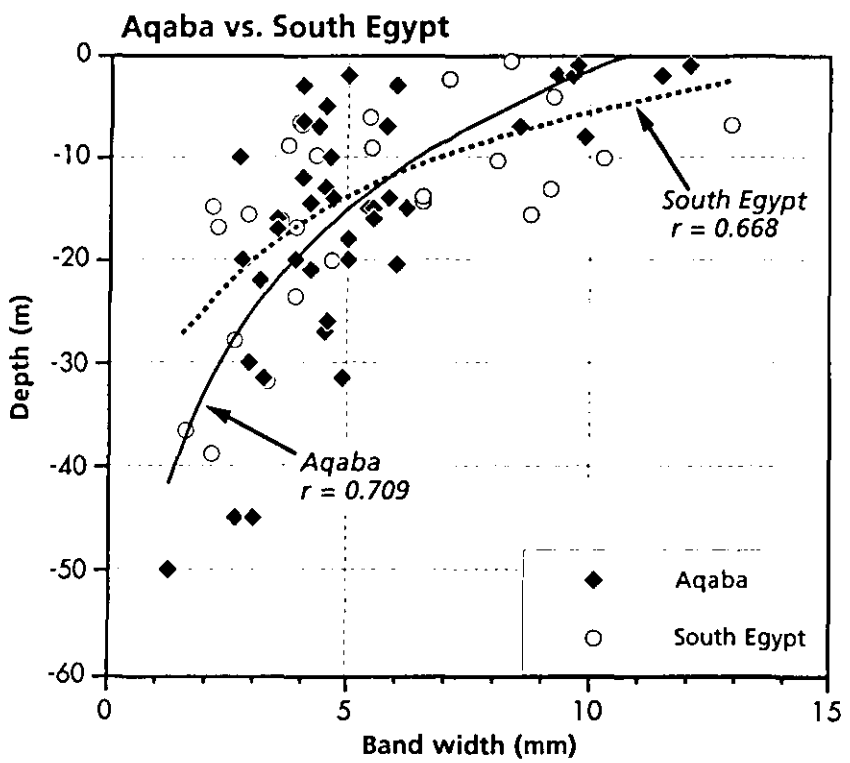

Figure 5.10
Annual band width of *Porites* sp. at Aqaba (including MSS samples, cores, and Saudi border samples) and South Egypt. Curve fit is logarhythmic. The decrease of growth rate with depth is evident. In the southern Egyptian reefs the growth reaches high values down to a depth of ca. 16 m, while at the Gulf of Aqaba fast growth is restricted to the upper 10 m.

The colonies which derive from a *Porites* pinnacle in the fore-reef contribute the other part of the fast-growing group. These colonies grew at the top of a 5 m high pinnacle under favoured conditions with very low sediment stress (see Chapter 2). Samples from Egypt were all entire specimen taken from the reef ground and thus do not represent particular environmental or size conditions.
Temperature effects are most probably not the reason for the decrease of growth rates with depth. Red Sea and Gulf of Aqaba are isothermal over the studied depth range. Only at the reef flat extreme temperatures in summer and winter may occur. Sedimentation and resuspension can also not induce a decrease of growth, as both are highest in the shallow parts of the reef. Thus, light seems to be the primary controlling factor of coral growth rates in the Red Sea, as it is in the other oceans. From the Caribbean a critical depth of 15 to 18 m for coral growth, which divides shallow from deep populations, is reported (Dustan 1975; Hubbard and Scaturo 1985; Bosscher 1992). Bosscher (1992) suggests that this sharp decrease reflects the lower limit of light saturation. Our observations do not contradict this assumption. However, a relation to a photosynthetic hyperbolic tangent function, as described by Bosscher, is not evident. To support this hypothesis with data from the Red Sea, continuous light measurements over a longer period should be carried out.
The growth potential of *Porites* seems to be controlled mainly by light availability. If the light saturation limit is exceeded, the genetical potential can lead to high growth rates in shallow depths, unless no suppressing factors like sedimentation, salinity and temperature changes, etc. occur.

Growth rate vs. latitude

A sudden increase of growth rates occurs at Aqaba above ca. 10 m depth, while values above 8 mm·yr^{-1} are reached at Egypt already at 15 m depth (Fig. 5.6, 5.8, 5.10). Furthermore, most of the samples in shallow depths grew with relatively high rates compared to Aqaba. The mean growth rate at Aqaba computed only for whole specimen samples for the 0-10 m depth zone is 6.17 mm·yr^{-1}, thus similar to the results from northern Egypt and slightly lower than at southern Egypt with 6.42 mm·yr^{-1}. If core samples are included (Tab. 5.2), corals from Aqaba show the highest values, which is also an effect of sample selection (see above). Differences between 10 m and 20 m depth with lowest values at Aqaba are prominent. The growth of shallow samples from Djibouti lies in the upper range of the values recorded from the Red Sea and suggests generally high growth rates in the Gulf of Tadjoura. However, due the small sample size this remains to be proven.
Grigg (1982) found at the Hawaiian Archipelago an inverse relationship between latitude and coral growth. Growth rates declined from 13 mm·yr^{-1} at the southeastern end of the chain to 3 mm·yr^{-1} in the northwest, within ca. 9° of latitude. A comparison between growth rates for *Diploria labyrinthiformis* and *Porites astreoides* at the high-latitude reefs of Bermuda with those of low latitude West Indian localities revealed also an inverse relationship of growth rates with latitude (Logan and Tomascik 1991). These differences are controlled by reduction of winter water temperatures and light levels with increasing latitude (Logan and Tomascik 1991).
The growth rate of *Porites* in the Red Sea seems to decrease as well to higher latitudes. However, the dimension of this decrease over an even higher latitude range of 17° between Aqaba and Djibouti is far less than that observed in the Pacific by Grigg.

The main cause for the low rate of decrease are the high growth rates in the Gulf of Aqaba up to 29°30'N. The high species diversity suggests (Schuhmacher and Mergner 1985) that the reefs at Aqaba do not mark the northernmost ecophysiological outpost of the Indian Ocean. Reefs would occur at even higher latitudes, if the Gulf extended farther north. This conclusion is supported by the results of growth rate investigations presented in this study.
What does enable the unexpected high growth rates in the northern part of the Red Sea and the Gulf of Aqaba?
The Red Sea has very particular oceanic parameters. As a semi-enclosed basin with restricted water exchange with the Indian Ocean and no connection to the north, it provides generally better conditions for coral growth than most other areas at the same latitudes. Water is of exceptional transparency in the Red Sea and Gulf of Aqaba, which permits coral growth to extreme depth (Fricke and Knauer 1986).
The inverse relationship between latitude and growth rates in the Atlantic and Caribbean was explained by Logan and Tomascik (1991) to result from reduction of winter water temperatures and illumination. Probably the same effects can be attributed to the observed pattern in the Red Sea. The temperature difference between northern and southern Red Sea is ca. 5-6°C in winter and summer (see Chapter 1). Difference from the Gulf of Aqaba to the northern Red Sea off southern Egypt is ca. 3°C. We assume the higher yearly growth rates to the South to be enabled by higher temperatures and light levels in winter. The suppression of growth is probably not as strong as in the Gulf of Aqaba, where light availability is reduced by cloud cover and the shorter period of daylight. Water temperature falls below 20°C in several years, thus approaching the lower limit of coral growth (Buddemeier and Kinzie 1976). In summer the environmental conditions enables high extension rates at the Gulf of Aqaba, while in the central and southern Red Sea temperature exceeds 30°C, which is much higher than the field of growth optimum (≈ 27°C, Buddemeier and Kinzie 1976). Additionally the higher oceanic productivity levels in the southern Red Sea might have negative influences on coral growth. At the northern end coral growth is suppressed by low temperatures and light levels in winter (≈December and January), while in the southern areas high temperatures and productivity levels probably reduce growth rates in summer (≈July and August). Latitudinal differences in annual growth rates are therefore more ambigous and sensitive to local influences as in other parts of the world. The detailed study of seasonal growth rate patterns of corals from the central and southern Red Sea will clarify these hypothesis.

An indication for higher growth rates to the South of the Red Sea is detectable from our results. However, varying number and depth distribution of samples, and the differences of local environmental influences, which could not be investigated in detail make us cautious in conclusions on latitudinal control of coral growth. Further and more detailed studies are necessary. Mainly the selection of study areas should receive special attention. Islands in some distance from coastal sedimentary influx promise to provide the most illustrative results.

CHAPTER SIX

STABLE ISOTOPE RECORD FROM RECENT AND FOSSIL *PORITES* SP. IN THE NORTHERN RED SEA

Abstract

The stable isotopic composition of scleractinian corals (Porites sp.), two recent and one fossil, from the Egyptian Red Sea coast was studied. The oxygen isotope record proves the assumption that recent sea surface temperatures are comparable to the time of last sea level highstand in Eemian (stage 5e, 125,000 yBP). Deposition of high-density and low-density bands in respect to season shows the same patterns as today with high-density band deposition in winter (low water temperatures) and low-density band deposition in summer (high water temperatures). $\delta^{18}O$ is negatively correlated with $\delta^{13}C$ with a shift in phase of 1 to 2 months. Thus a coupling of carbon isotopes to light intensity and oxygen isotopes to water temperature is suggested. To get an overview on seasonal patterns of stable isotope composition a sampling technique with a resolution of four samples per year is of sufficient precision.

Introduction

Uplifted pleistocene coral reefs occur widespread along the coasts of the Red Sea. Age and diagenesis of these reefs were discussed by several authors in the last decades (Gvirtzman and Friedman 1977; Dullo 1984, 1986, 1990; Al-Rifaiy and Cherif 1988; Andres and Radtke 1988; Klein et al. 1990; Strasser et al. 1992 among others). The objective of this part of the study is to focus on patterns in seasonal growth band deposition and stable isotopic composition of scleractinian coral skeleton deposited in Pleistocene and recent fringing reefs in the Red Sea. The efficacy of two different drilling tools and different sampling resolution in order to reveal seasonality in the stable isotope composition of fossil corals was tested. From the density band formation and the stable isotope composition the time of high and low density band deposition of corals in the northern Red Sea was examined. Further, depth related differences in isotope composition of recent corals was studied exemplarily.
For recent corals in the northern Gulf of Aqaba, a clear seasonal depositional pattern of annual growth bands was found, based on X-radiographic and stable oxygen isotope measurements (Klein and Loya 1991; Klein et al. 1992). High-density (HD) bands occur during winter (December to May), low-density (LD) bands are formed during summer (June to November). Klein et al. (1990) could show that corals from late Quaternary reefs in the southern Sinai exhibit distinct flourescent bands in the low-density portion of the skeleton, which indicates a wet climate with a summer rainfall regime for the Sinai peninsula. In living corals flourescent bands are absent, due to the present extreme desert conditions (Klein et al. 1990). Recently stable isotope studies on a pliocene coral *(Solenastrea bournoni)* from Florida demonstrated a clear seasonal signal of both carbon and oxygen isotopes with a shift between both curves (Roulier 1993) The objective of this part of the study was to examine similarities and differences between fossil and recent scleractinian corals from the Red Sea.

Material

A fossil scleractinian coral of the genus *Porites* (sample E2) was sampled during a field trip in June 1991 at Gebel Zeit (33°32´E) at the Egyptian Red Sea coast 50 km north of Hurghada (Fig. 6.1). Gebel Zeit is an isolated uplift of precambrian granitic basement rocks of ca 30 km length. At least three fossil beach levels of Pleistocene age are present at a maximum elevation of +65 m, +50 m, +15 m, and a Holocene reef at +2 m, respectively. At the 15 m level we found an excellently preserved raised fossil reef with the reef flat presently lying at about 10-15 m above sea level. This reef grew during the maximum of the last interglacial period (stage 5e, Eemian, 125,000 yBP), based on absolute dating with U/Th- and ESR-dating (Andres and Radtke 1988). Considering the higher sea level (+5 m) during the last interglacial maximum the present level of the Eemian reef implies a tectonic uplift of 5 to 10 m in the last 125,000 years.
Two samples of recent *Porites* sp. were sampled at the reef fringing the southern coast of the island Giftun Kebir off Hurghada in July 1991 (Fig. 6.1). The corals were taken at depths of 5 m (sample E16) and 10 m (sample E15).

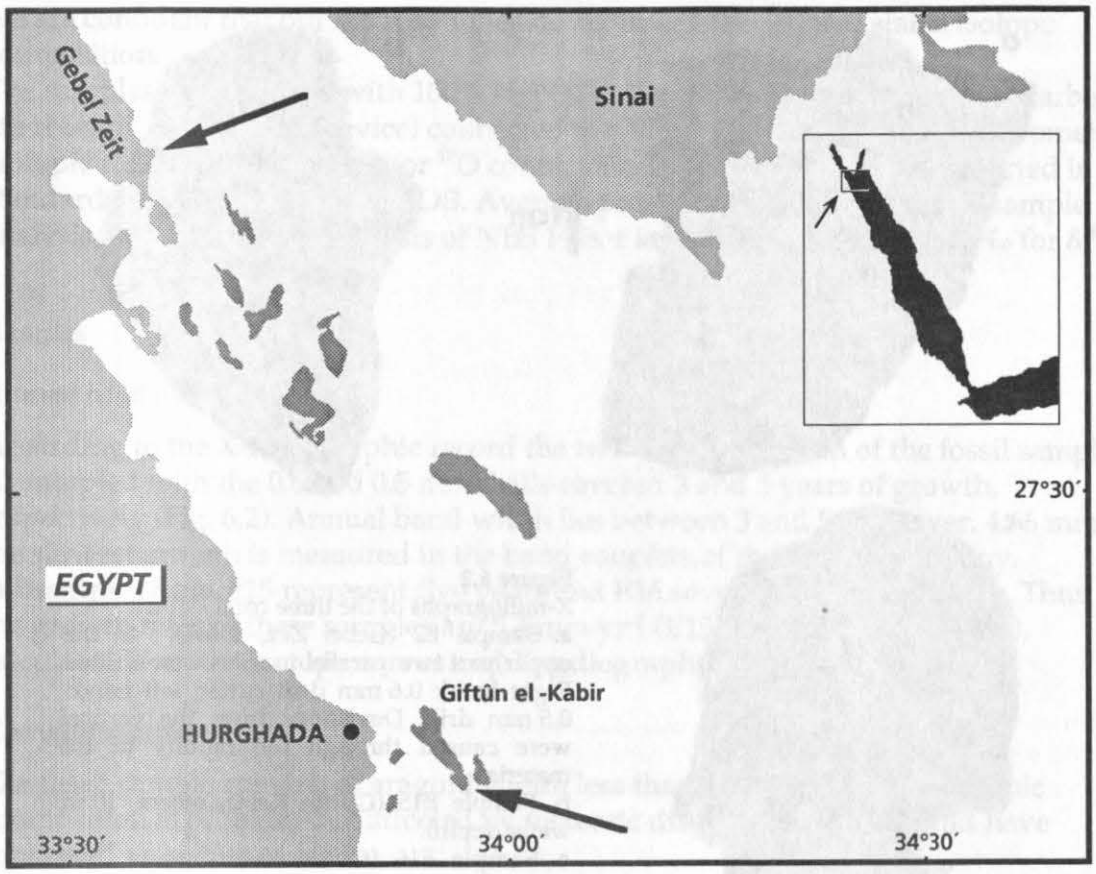

Figure 6.1 Map showing locations of sampling sites in the northern Red Sea

Methods

Annual band width

Coral samples were sectioned with a diamond rock saw to a thickness of ca 5 mm. The slabs were x-rayed using a SEIFERT-Industry-X-ray-unit (Type ERESCO 120kV/5ma) at 35kV and 5mA to reveal annual density banding (Knutson et al. 1972; Hudson et al. 1976). Agfa Gevaert Structurix D4 film was used. Annual band width was measured along the vertical growth axis (Buddemeier et al. 1974) as the distance between top of LD-bands.

X-ray-diffractrometry

X-ray analyses of the fossil sample was performed with a Philips PW 1710 X-ray diffractometer (CuK_α, 45 kV, 35 mA), angle from 5-70 (°2θ), step width: 0.02, time per step: 0.5 s. One sample of several grams was taken from the region where isotope samples were drilled later.

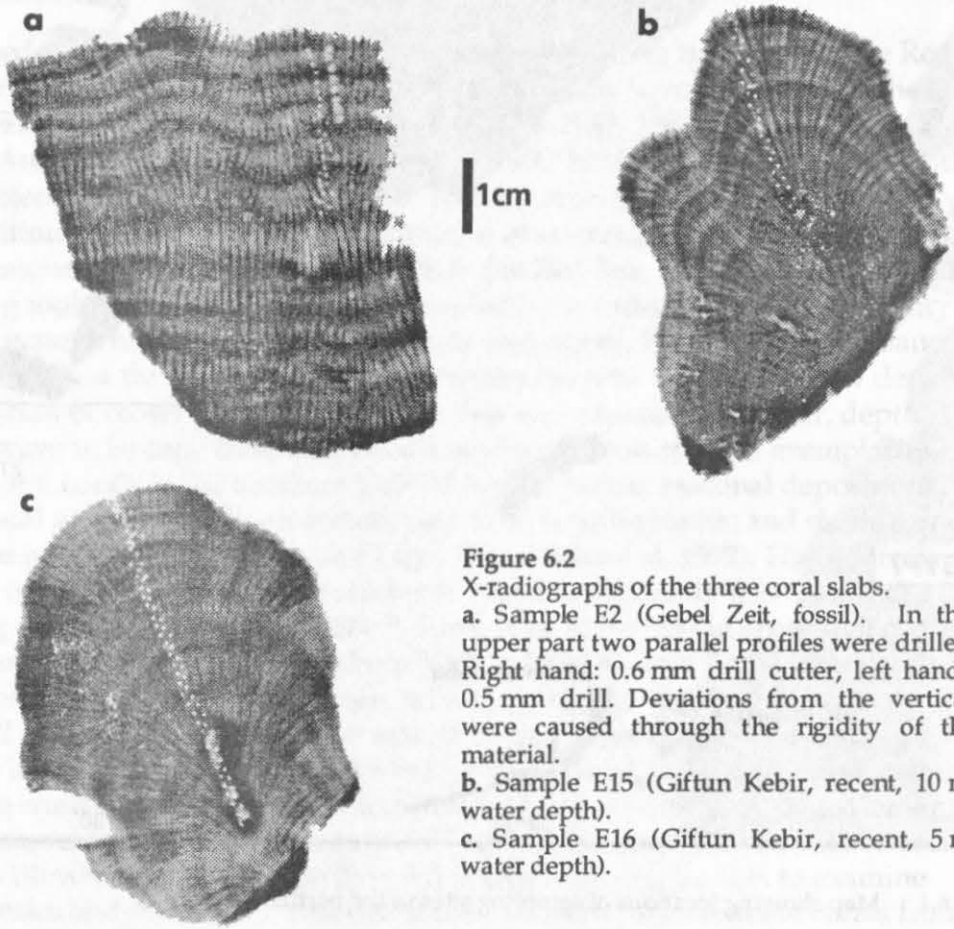

Figure 6.2
X-radiographs of the three coral slabs.
a. Sample E2 (Gebel Zeit, fossil). In the upper part two parallel profiles were drilled. Right hand: 0.6 mm drill cutter, left hand: 0.5 mm drill. Deviations from the vertical were caused through the rigidity of the material.
b. Sample E15 (Giftun Kebir, recent, 10 m water depth).
c. Sample E16 (Giftun Kebir, recent, 5 m water depth).

Stable isotope composition

The stable isotope composition was measured along profiles parallel to the growth direction. Microsamples of E15 and E16 were collected using a 0.5 mm dental drill. Two parallel lines of the fossil sample (E2) were sampled using different drill tools. One profile was obtained with a 0.5 mm drill (sample 310-319), the other using a 0.6 mm milling device (drill cutter, sample 320-327, Fig. 6.2). Drilling procedure with the 0.6 mm drill cutter could be better controlled and deviation from the initial position was low. Both sampling devices were run at lowest speed to avoid heat alteration of the material. The first profile was later extended further into the coral (samples 351-370). Care was taken to remove loose material completely between drilling. Samples were cleaned with a brush and compressed air. Aharon (1991) concluded from his experiments, comparing "dry drilling" and "wet coring" of *Tridacna* shells, that dry drilling of isotope samples caused isotope fractionation. However, Leder et al. (1991) and Bosscher (1992) found no deviation of different sampling techniques. Fractionation effects might be caused by high pressures and/or dull drill bits (Leder et al. 1991). The drilling of *Porites* samples is more a "breaking off" of small skeleton elements than a hard drilling. Since the aragonite-calcite conversion causes mainly problems when drilling solid substrates with high speed,

we are confident that our microsamples do represent the original stable isotope composition.
The samples were reacted with 100% H_3PO_4 at 75°C in an online, automated carbonate reaction device (Kiel Device) connected to a Finnigan Mat 252 mass spectrometer. Isotopic ratios were corrected for ^{17}O contribution (Craig 1957) and are reported in standard δ notation relative to PDB. Average precision based on duplicate sample analysis and on multiple analysis of NBS 19 is ± 0.04‰ for $\delta^{13}C$ and ± 0.08‰ for $\delta^{18}O$.

Results

Annual band width

According to the X-radiographic record the two parallel profiles of the fossil sample E2 sampled with the 0.6 and 0.5 mm drills covered 3 and 5 years of growth, respectively (Fig. 6.2). Annual band width lies between 3 and 5 mm (aver. 4.66 mm), the slowest growth is measured in the band couplets at the top of the colony. Subsamples from E15 represent five years and E16 seven years, respectively. Thus the growth rates of these samples are 5.4 mm·yr^{-1} (E15) and 7.8 mm·yr^{-1} (E16), calculated from the isotope curves and X-radiographs.

X-ray-diffractometry

The fossil sample consists of aragonite with less than 0.5 % calcite. The isotopic composition is probably not affected by meteoric diagenesis which would have converted aragonite to calcite.

Flourescence

Fluorescence under ultraviolet light could not be observed in our samples, neither in fossil nor recent samples. The presence of flourescence would indicate incorporation of terrestrial humic acids into the skeleton, transported by runoff.

Stable oxygen isotopes

In sample E2 the 0.5 mm drill yielded a resolution of between four and eight samples per year, compared to the 0.6 mm drill with three samples per year (Fig. 6.2). Between 6 and 11 samples per year were obtained from samples E15 and E16 (Fig. 6.2).
Oxygen isotope values in all samples show a clear seasonal variation which is coupled to the deposition of HD and LD bands (Fig. 6.3, 6.4). For sample E15 $\delta^{18}O$ is between -2.39 and -3.82 ‰ (mean -3.82 ‰), for sample E16 $\delta^{18}O$ is slightly lighter with a range between -2.78 and -4.03 ‰ (mean -3.48 ‰, Tab. 6.1). The fossil sample has a greater variation with a maximum of -2.58 ‰ and a minimum of -4.76 ‰ (mean -3.47 ‰). The parallel profile drilled with a 0.6 mm bit displays comparable values (Fig. 6.5). The intra-annual oxygen isotope variation is between 0.54 ‰ and 1.19 ‰ for sample E15 (average 0.85 ‰), 0.85 to 1.14 ‰ for sample E16 (avg. 1.05 ‰), and from 0.82 to 2.1 ‰ (avg. 1.5 ‰) for the fossil sample E2 (Tab. 6.1).

Light oxygen isotope composition is associated with the LD bands of all samples, and heavy values were found in the HD bands. The deposition of HD bands commences when $\delta^{18}O$ increases. The onset of the LD band occurs in most cases exactly at the time of heaviest $\delta^{18}O$ values (coldest water temperatures). This indicates that the density band formation is not strictly dependent on water temperatures.

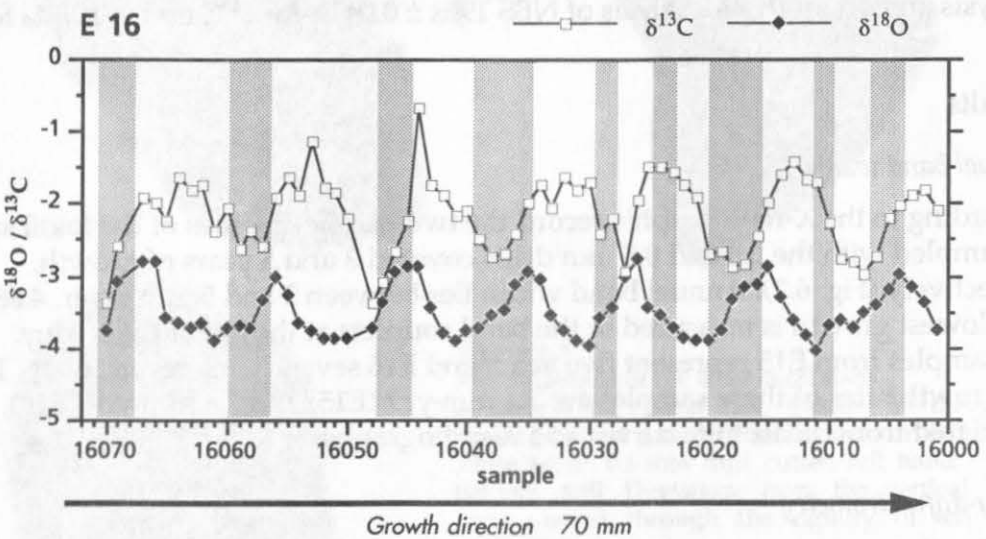

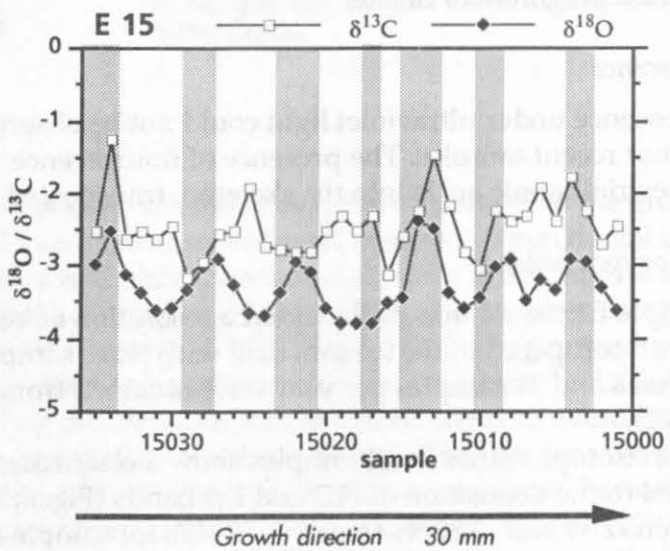

Figure 6.3
Stable carbon and oxygen isotope composition of recent samples E16 (above) and E15 (right). Growth rate of sample E16 is 7.8 mm/yr, E15 is 5.4 mm/yr. Shaded areas mark position of HD bands.

Table 6.1 Summary statistics for stable oxygen isotope determination in samples E2, E15, E16.

$\delta^{18}O$	Mean	SD	Min	Max	n
E 2	-3.47	0.58	-4.76	-2.58	37
E 15	-3.28	0.37	-3.82	-2.39	35
E 16	-3.48	0.35	-4.03	-2.78	68

Stable carbon isotopes

Stable carbon isotopes also display a seasonal variation. Light values are reached in most cases at the onset or within HD bands. This pattern occurs in all samples, however it is not as clearly defined as the oxygen isotope composition. For the recent sample E15 (10 m depth) $\delta^{13}C$ varies between -1.28 and -3.18 ‰ (mean -2.46 ‰), in sample E16 (5 m depth) values from -0.68 to -3.38 ‰ were measured (Tab. 6.2). Remarkably heavy skeletal $\delta^{13}C$ is deposited in the fossil sample E2 (Tab. 6.2). $\delta^{13}C$varies between -0.02 and -3.12 ‰ (mean -1.13 ‰), while the amplitude is generally lower than in the recent corals (Fig. 6.4). An abrupt change to lighter values occurs in the second band below the surface.

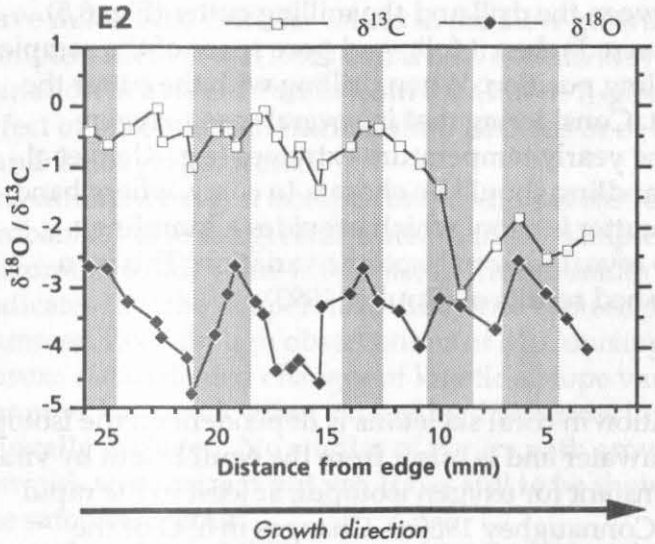

Figure 6.4
Stable oxygen and carbon isotope compositon of the fossil sample E2. X-axis is the distance from the edge of the sample. Shaded areas mark the position of HD bands. Oxygen isotopes display a clear seasonal variation. The carbon isotope record is ambigous in its correlation with oxygen.

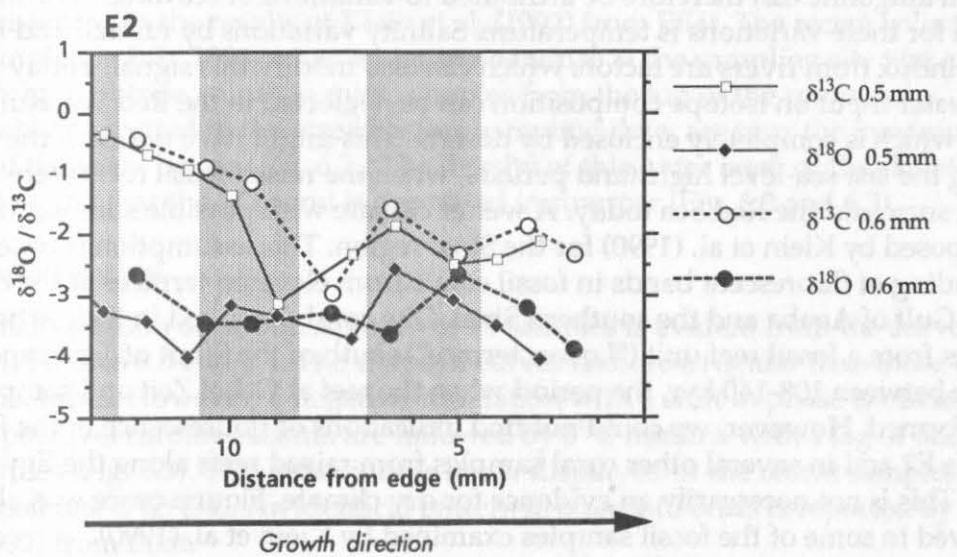

Figure 6.5 Stable carbon and isotope composition of fossil sample E2. Two parallel profiles were drilled with 0.5 and 0.6 mm drill bits. Seasonal variation is visible in both profiles.

Table 6.2 Summary statistics for stable carbon isotope determination in samples E2, E15, E16.

$\delta^{13}C$	Mean	SD	Min	Max	n
E 2	-1.13	0.87	-3.12	-0.02	37
E 15	-2.46	0.42	-3.18	-1.28	35
E 16	-2.15	0.52	-3.38	-0.68	68

Discussion

Sampling procedure

The analysis of samples obtained with two different drill tools in the fossil sample E2 displayed no major differences between the drill and the milling cutter (Fig. 6.5). Problems with the 0.5 mm drill occurred when it followed pore space of the sample and deviated from the original drilling position. When drilling with the cutter the drill position could be kept straight. Considering that in several cases oxygen isotopic analyses does not match the yearly temperature extremes (e.g. Klein et al. 1992), the device with the easiest handling should be chosen. In corals where band width is at least 4 mm, the milling cutter is a tool which provides a sampling resolution which is high enough to reveal seasonal isotopic variation. This is in accordance with the recently published results of (Roulier 1993).

Stable oxygen isotopes

The stable oxygen isotope composition in coral skeletons is dependent on the isotope composition of the surrounding seawater and is offset from the equilibrium by vital effects of the coral. This offset is constant for oxygen isotopes, at least in the rapid growing part of their skeleton (McConnaughey 1989a). Changes in $\delta^{18}O$ of the skeletal aragonite can therefore be attributed to variations of seawater. The main reason for these variations is temperature. Salinity variations by rainfall and freshwater influx from rivers are factors which can also modify this signal. Today the freshwater input on isotope composition can be neglected in the Red Sea as it is an ocean which is completely enclosed by deserts. This might have not been the case during the last sea-level highstand periods, when the raised fossil reefs were formed, which surround the Red Sea today. A wetter climate with possible summer rainfalls is proposed by Klein et al. (1990) for the Sinai region. This assumption is based on the finding of fluorescent bands in fossil corals from elevated terraces at the coastline of the Gulf of Aqaba and the southern Sinai. One coral described in their article derives from a fossil reef unit ("Lower terrace") south of the Strait of Tiran and is of an age between 108-140 kyr, the period when the reef at Gebel Zeit and sample E2 were formed. However, we could not find indications of flourescence in the fossil sample E2 and in several other coral samples from raised reefs along the Egyptian coast. This is not necessarily an evidence for dry climate. Flourescence was also not observed in some of the fossil samples examined by Klein et al. (1990).
The main difference in the $\delta^{18}O$ patterns of fossil and recent samples is the greater intra-annual range in the fossil one. The heavy (cold season) values (ca -2.5 to -2.8 ‰) are similar to present conditions, but the fossil light (warm season) values (from -3.7 to -4.8 ‰, Fig. 6.4) exceed the recent values (-3.5 to -3.8‰, Fig. 6.3). From Epstein´s

paleotemperature equation a temperature increase of 1°C is equivalent to a oxygen isotope decrease of ca 0.22 ‰ (Epstein et al. 1953). Thus temperature difference between summer and winter of recent samples represent 5.6 to 6.5°C and of the fossil sample ca 10°C. Seasonal water temperature difference at the Egyptian coast is today around ca 10°C (pers. observation). Variations by meteoric diagenesis are not likely, as the fossil sample still consists of pure aragonite.

Four explanations are possible for the observed differences between fossil and recent samples. (1) The seasonal temperature difference was greater in Eemian than it is today or (2) freshwater discharge caused by summer rainfall resulted in lighter $\delta^{18}O$ values in the northern Red Sea waters or (3) our sample grew under special conditions (e.g. in a shallow lagoon or at the reef crest), where higher summer temperatures occur than at the sites of coral E15 and E16. (4) Our sampling might have missed the extreme values in the slow growing (winter) part of the recent samples. Klein et al. (1992) could also explain only ca 70 % of the expected isotope variation in a recent *Porites* from the Gulf of Aqaba. The question whether this is an effect of physiological fractionation patterns or of low sampling efficiency in the HD band is not yet answered.
The different oxygen isotope composition of the recent samples from Giftun is probably due to the greater water depth of sample E15 (10 m). The difference in the maximum (cold) value is 0.39 ‰, in the minimum (warm) value 0.19 ‰. This indicates that the temperature difference is more pronounced in winter than in summer. Even though observations of McConnaughey (1989a) from Galápagos on *Pavona clavus* denied changes of kinetic isotope variation above a growth rate of 2 mm·yr^{-1}, a kinetic effect caused by differences in growth rate can not be categorically excluded. No studies of *Porites* with growth rates comparable to our samples were carried out yet. It has still to be shown whether *Porites* corals display the same behaviour.
The light values of $\delta^{18}O$ measured in the LD bands and heavy oxygen in HD bands are consistent with the results of Klein et al. (1992) from Eilat. The recent colonies were sampled in July 1991, when water temperature at the sampling site was ca 24°C. Oxygen isotope values in microsamples from the top of the colonies, presumably deposited in the weeks before sampling date, are near the maximum values of the years before (Fig. 6.3). The density of this outer layer of the skeleton is low, indicating that the LD band is deposited in summer (Fig. 6.2 and 6.3).

Stable carbon isotopes

A seasonal variation of carbon isotopes of all samples is evident from the curves shown in Figures 6.3 and 6.4. The shape of curves is more irregular than those of oxygen isotopes. However, a negative correlation with a shift in phase is obvious. Heavy (positive) carbon maxima are followed by $\delta^{13}C$ minima with a lag of one to two samples (Fig. 6.3). This behaviour is better displayed in the recent samples than in the fossil one (Fig. 6.4). An identical pattern in a recent *Porites* is reported by Klein et al. (1992) from Eilat.
The abrupt shift of $\delta^{13}C$ in the last two years of the isotope record in the fossil coral is conspicious (Fig. 6.4). This shift might be caused by an undetected diagenetic freshwater influx at the surface of the colony. However, the $\delta^{18}O$ record does not display a similar abrupt disturbance, but a trend to heavier values. More likely, the

photosynthetic activity decreased drastically prior to the death of this coral. Combined with the trend to heavier $\delta^{18}O$ values an event can be speculated to have influenced the coral negatively and started a few years before the coral's death. This could be a cooling of seawater, leading to more positive $\delta^{18}O$ and lower photosynthetic acticity (=more negative $\delta^{13}C$). Other influences, like high sedimentation, might have the same effects on stable isotope composition, by reducing the growth rate (see Fig. 6.2) and thus reducing the kinetic effect on the $\delta^{18}O$ signal. From this effect the trend to heavier $\delta^{18}O$ can be explained without a cooling of seawater. The growth of the coral decreased already a few years prior to the death of the reef, probably caused by sedimentation and possibly lower water temperatures.

The discussion in the literature on the controlling factors of carbon isotope composition suggests a very complex system. At present the model of Weber and Woodhead (1970), that light enhances photosynthesis, and fractionation during photosynthesis shifts the carbon to more positive values is widely accepted (reviews in Swart 1983; McConnaughey 1989a, 1989b; Aharon 1991). The results of Klein et al. (1992) showed that the photosynthetic activity and the carbon isotope composition is coupled directly to sun irradiance, while the oxygen isotopes are controlled by SST, which follows the phases of light intensity with a lag of time. We analysed climate data from Eilat with spectral analysis (unpublished) and found a shift of light intensity to air temperature of ca one month and between air temperature and water temperature of another month. Unfortunately no climate data for the Egyptian coast are available. From our experience during field trips the maximum water temperature is reached in the late August, approximately the same time as in the Gulf of Aqaba. Roughly estimated, this is a comparable shift between sun irradiance and SST.
The difference in carbon isotopes between the two recent samples can be attributed to the difference in water depth and enhanced photosynthetic activity and not to kinetic fractionation effects. Sample E16 grew at a depth of 5 m with a rate of ca 9 $mm \cdot yr^{-1}$, coral E15 at 10 m depth with a rate of ca 5 $mm \cdot yr^{-1}$. In the shallow sample heavier stable carbon isotope composition is measured, that is probably caused by higher metabolic activity (Tab 6.2). A kinetic effect of rapid growth should in contrast result in lighter $\delta^{13}C$ (McConnaughey 1989a). This indicates a higher photosynthetic activity, combined with a higher growth rate in the sample from 5 m depth compared with the 10 m sample.

CHAPTER SEVEN

CORAL GROWTH RATES RELATED TO LIGHT

Abstract

Porites sub-colonies from a 6 m high pinnacle in the middle fore-reef at Aqaba, which are assumed to be genetically identical, show a wide range of skeletal extension rates from ca 3 to 17 $mm \cdot yr^{-1}$. The decrease of growth rates of these sub-colonies can be attributed almost exclusively to decreasing light intensity due to increasing water depth from ca 5 to 10 m and the peripheral position of the colonies at the sides of this pillar. Colonies sampled at the top of the pillar show high growth rates which can be attributed to the ideal conditions for coral growth due to rapid water exchange and optimal light exposure. The absence of resuspension of bottom sediments in the pinnacle-environment may enable the high growth rates of these colonies. Sediment stress through resuspension might depress growth rates of colonies from the fore-reef at similar depths.

Introduction

Light has been acknowledged as an important environmental factor controlling vertical distribution of corals, rates of reef building, the form of reefs and atolls, and the shapes of individual colonies (Muscatine 1973). The importance of light is deduced from changes of water depth (e.g. Baker and Weber 1975; Huston 1985) or cloud cover (e.g. Highsmith 1979; Lough and Barnes 1990). Few studies attempted to examine the individual effects of light and temperature on coral growth. Houck et al. (1977) found in aquaria experiments for *Porites lobata* a sharp temperature optimum between 26 and 27°C. The decrease of insolation lead to a decrease of coral growth rates. A decrease of light intensity by 65% reduced the growth rate by 27%. In this part of our study the objective was to determine the effect of light intensity on growth rate in a natural environment. Intraspecific variations often obscure results of investigations of environmental influences on corals and other organisms. Generally researchers try to extract these effects statistically by increasing the number of specimen studied. The occurence of a *Porites*-colony in the fore-reef at Aqaba, Gulf of Aqaba, which is split into numerous sub-colonies gave the opportunity to estimate almost exclusively the light effects on growth rates.
The samples allowed further a comparison between growth rates of corals on this pinnacle to growth rates of *Porites*-colonies from the fore-reef area.

Materials

Test subject was a large *Porites* sp.-pinnacle growing in the fringing reef south of the Marine Science Station at Aqaba, Jordan (29°27´N, Fig. 7.1). This colony forms a pillar in the fore-reef of ca 6 m height and 4 m diameter, growing from the sea bottom in 10.5 m depth, so that the upper part lies at a depth of 4.5 m below water surface (Fig. 7.3).
The tide range in the northern Gulf of Aqaba is about 0.4-0.7 m (Mergner 1979) and changes in water depth are not strong enough to affect coral growth below the low tide line significantly. This pillar consists of hundreds of sub-colonies independently growing with diameters of 5 to 20 cm and individual heights of up to 0.5 m. Only the upper parts of these

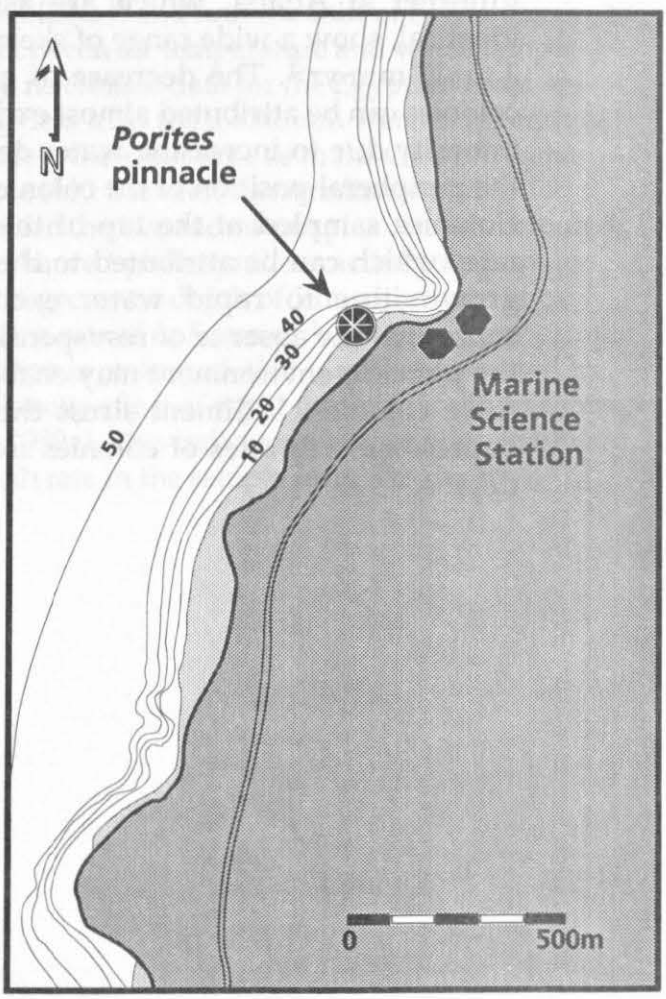

Figure 7.1
Location of *Porites*-pinnacle in the middle fore-reef of the fringing reef at the MSS at Aqaba, Gulf of Aqaba.

small pillars are coated with living coral tissue (Fig. 7.2.). In the history of growth the "mother"-colony has separated into different "daughter"-colonies which lost connection of living tissue with increasing height. Space between sub-pillars serves as ideal hiding place for fish, sea-urchins, and other animals. Lower parts of sub-pillars are in several cases overgrown by coralline algae and incrusting scleractinian corals (e.g. *Pavona, Montipora*). From growth habit and uniform composition of species we believe, that all parts of this pillar derive from the same individual which began its growth several hundred years ago.

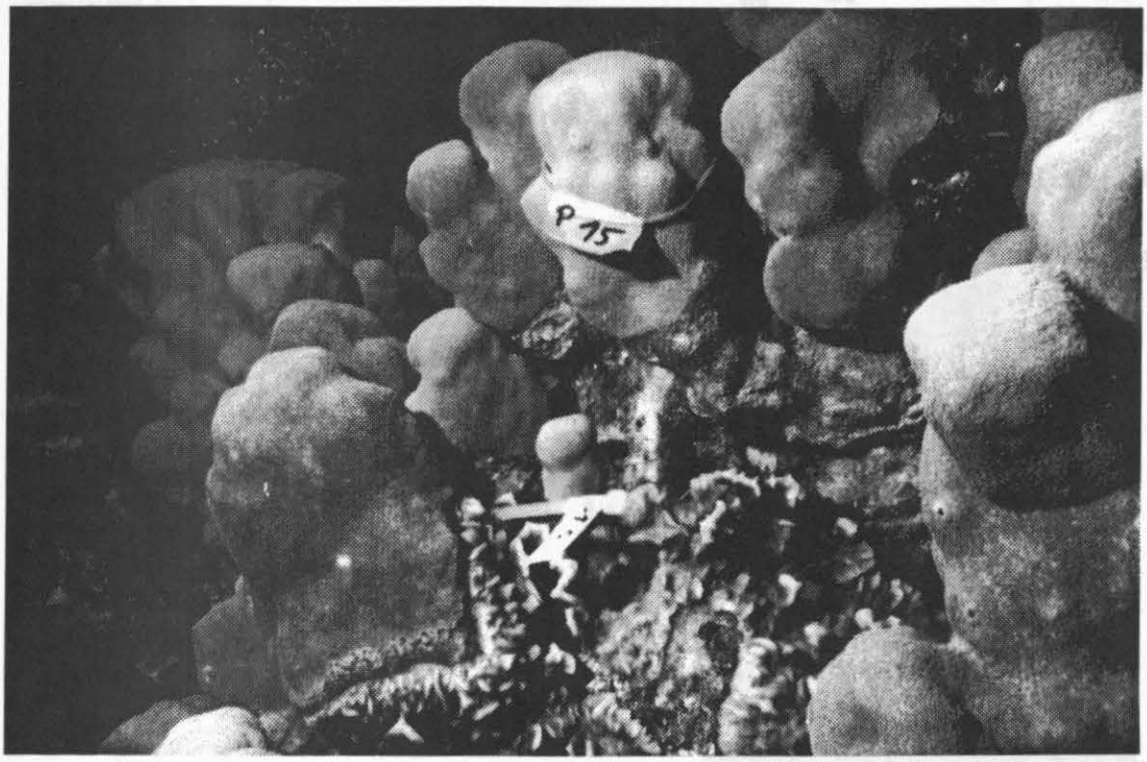

photograph: Elja de Vries

Figure 7.2 Sub-colonies growing at the top of the *Porites*-pinnacle in the fore-reef at the MSS Aqaba. Water depth ca 5 m, colony height (label P15) is 17 cm.

This leads us to the assumption that all parts are genetically identical (if we exclude spontaneous mutations from this hypothesis). Therefore we are able to exclude intraspecific variations of growth rate and attribute differences exclusively to environmental factors. The position of this solitary pillar in the outer fore-reef makes us sure that other exogenic factors than light, like water temperature, nutrients, currents, and sediment input, remain more constant than close to the shore and are relatively unchanged on different sides ofthe pinnacle.

The pillar has in its upper part a greater diameter than at its foot and forms an overhang to the SW-side. This morphology already indicates favoured growth conditions to the light exposed side. Living corals cover the surface of the pillar above a quite discrete boundary. The limit of this boundary lies on the northern side at a depth of 7.5 m, in the East and West at about 5 m and descends to SW to a depth of 9 m where living corals are growing close to the pillar´s foot. Below this limit soft corals, coralline and green algae are growing on dead coral surface.

Sampling

In November 1991 and November 1992 we sampled 20 subcolonies (no. 91-100; 101-110) from this reef pinnacle in the fore-reef from a depth of 10 m to a height of 6 m. The samples were taken along two parallel transect lines of 10 m length in a distance of approx. one meter. Transect lines were laid over the pillar in NE-SW orientation (Fig. 7.3).

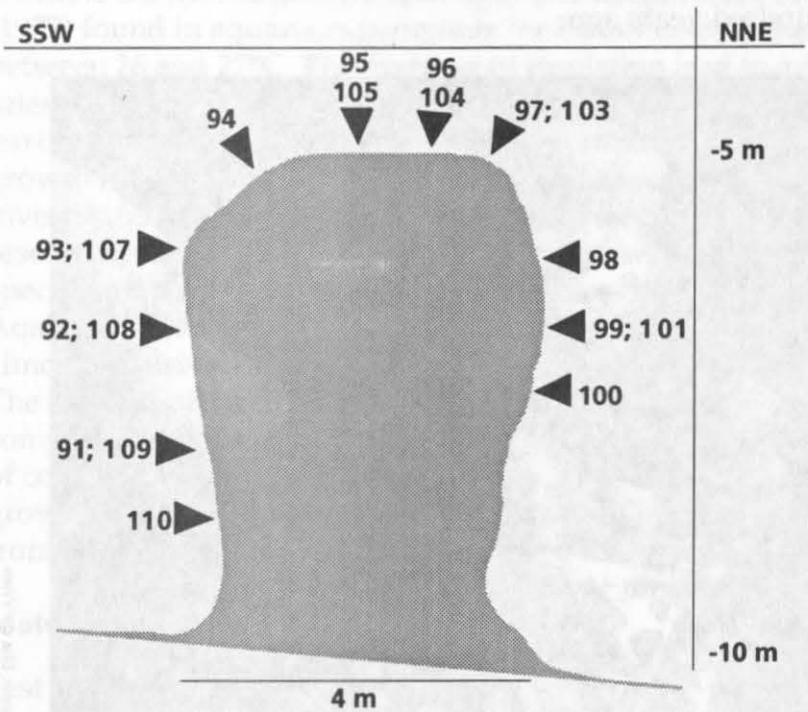

Figure 7.3
Location of samples from the *Porites*-pillar.

Methods

Light measurements

A LI-COR Quantum Radio-/Photometer Type LI-185B in an underwater-case with a sensor (PAR) LI-COR, Type LI-192 SB was used for measurements of light intensity. Results are given in $\mu E\ m^{-2}s^{-1}$, 1 $\mu E\ m^{-2}s^{-1}$ is ca 0.435 W m^{-2}. Two light profiles from the surface to a depth of 10 m were carried out in the open water at November 25, 1991 in a distance of some meters from the colony. The radiation levels at air and directly below the water surface were recorded before and after the measurements at the *Porites*-pillar. Exactly at the coral sample position of samples 91-100 light energy was measured three times before removal (Nov 25th, 28th and 30th, 1991). We recorded light values in horizontal and vertical direction and in direction of maximum light intensity. No clouds were present at the days we performed the measurements.

X-radiography

Samples 91 to 100 were sectioned using a diamond rock saw to a thickness of ca 3 mm. Coral slabs were x-rayed using a SEIFERT-Industry-X-ray-unit (Type ERESCO 120kV/5ma) at 35kV and 5mA to reveal annual density banding (Knutson et al. 1972; Hudson et al. 1976). Agfa Gevaert Structurix D4 film was used.

Computer-tomography

Samples 101 to 110 were scanned using a SIEMENS computer tomograph (Type Somatom Plus-S). Best results were obtained with 2 mm slices (120 kV, 165 mA, 2 s) and 3 mm slices (2x2 s) (Fig. 7.4.). A detailed description of this method is given in Chapter 5 of this thesis.

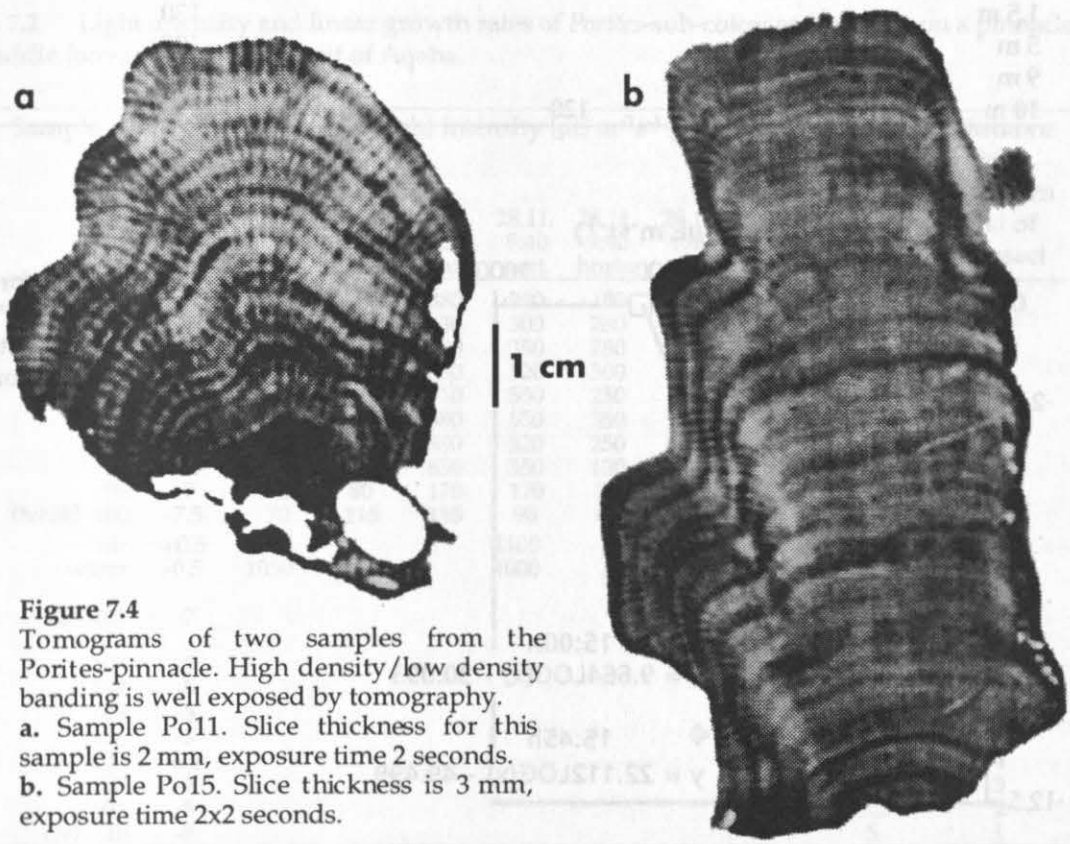

Figure 7.4
Tomograms of two samples from the Porites-pinnacle. High density/low density banding is well exposed by tomography.
a. Sample Po11. Slice thickness for this sample is 2 mm, exposure time 2 seconds.
b. Sample Po15. Slice thickness is 3 mm, exposure time 2x2 seconds.

Growth rates were measured along the major growth axis (Buddemeier et al. 1974; Logan and Tomascik 1991) from positive prints as the distance between the top edge of low-density bands (LD) which are the most distinct boundaries in our samples. Average growth rate was computed from at least three HD/LD couplets, each representing one year of coral growth. Two samples did not show unambiguous annual banding and were therefore not respected in the further examination.

Results

Light measurements

The light profiles show a decrease of light intensity from the surface to a depth of 10 m (Tab. 7.1). Light extinction with depth follows an exponential function and produces a straight line when plotted on a semi-log scale (Fig. 7.5).

Table 7.1 Light profiles in the open water column in the fore-reef at the Marine Science Station at Aqaba, close to the *Porites*-pinnacle.

depth	light intensity 15:00h ($\mu E\ m^{-2}s^{-1}$)	light intensity 15:45h ($\mu E\ m^{-2}s^{-1}$)
air	1500	690
water surface	1300	190
1.5 m		130
5 m		100
9 m		75
10 m	120	

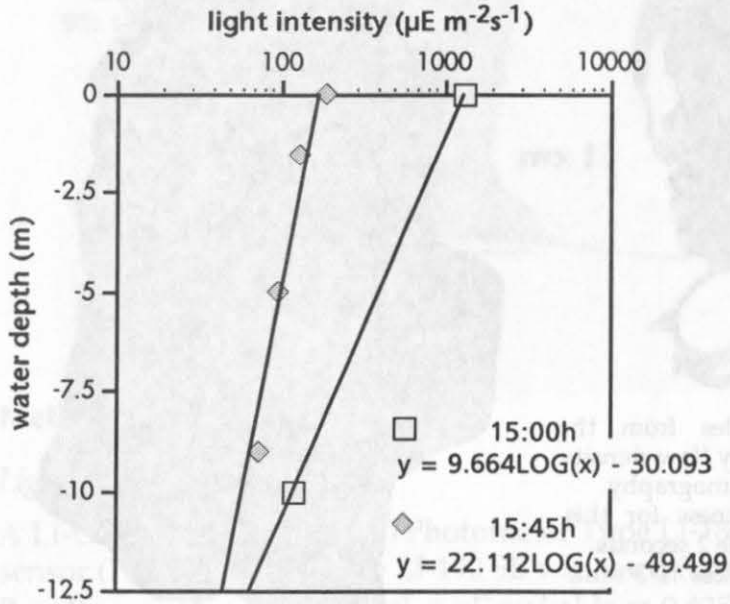

Figure 7.5
Light extinction profiles for open water column close to the *Porites*-pillar (Marine Science Station, Aqaba, fore-reef position) on 25th November 1991.

Radiation directly below water surface was in the range of 1000 to 1300 $\mu E\ m^{-2}s^{-1}$ during the week of our measurements. Maximum light intensity at the top of the pinnacle is reduced to 55-65% of the intensity at the water surface (measurements at 09:30h and 09:40h), colonies at the sides get 10-20% of the surface values. In the afternoon (15:00h) only 15% of the light reaches the pinnacle.
Light intensity at the lower limit of coral growth was between 30 and 90 $\mu E\ m^{-2}s^{-1}$ in the afternoon. This limit lies in the northern part of the pinnacle at a depth of 6-7 m and descends to the south to a depth of ca 9 m. The complete data set of light measurements is listed in Table 7.2.

Annual band width

The growth rates vary in a wide range from 2.1 to 17.3 mm·yr^{-1}. The average band width of samples is listed in Table 7.2.
Corals growing at the ends of transects (i.e. the sides of the pinnacle) have growth rates between 2.1 and 5 mm·yr^{-1}. Samples taken at the top of the pillar grow with 12 to 17 mm·yr^{-1} and thus reach values, which are among the highest observed in the Gulf of Aqaba (cf. Chapter 5 of this thesis). Linear extension rates are highly variable even for subcolonies growing in a distance of only 1 m.
The relation between light intensity and growth rate is probably not linear. As the example in Figure 7.6 suggests, a certain light intensity divides the slow and the fast growing group. Below this value growth rates do not exceed 5 mm·yr^{-1}, above this limit fast growth occurs, with strongly varying rates.

Table 7.2 Light intensity and linear growth rates of *Porites*-sub-colonies, growing on a pinnacle in the middle fore-reef at Aqaba, Gulf of Aqaba.

Sample		Depth (m)	Light intensity (µE m^{-2}s^{-1})							Growth rate (mm/yr)	Distance from northern end of transect
			30.11. 9:30 vert.	30.11. 9:30 horiz.	30.11. 9:30 max.	28.11. 9:40 vert.	28.11. 9:40 horiz.	28.11. 9:40 max.	25.11. 15:00 max.		
(SSW)	91	-8	350	280	380	220	180	250	100	3.2	8.6
	92	-7	390	310	430	300	280	320	150	5	7.9
	93	-6.5	500	310	580	350	250	430	150	3.8	7
	94	-5.5	580	400	680	520	300	600	175	-	6
	95	-5	640	420	710	550	250	650	170	12	5.4
	96	-5	680		680	550	350	650	190	13.38	4.7
	97	-5	520	150	650	520	250	660	175	8.75	3
	98	-6.5	500	60	550	550	130	550	150	16	2
	99	-7	150	80	170	170	70	240	43	4	1
(NNE)	100	-7.5	70	115	135	90	65	120	29	4	0.3
	air	+0.5	1200			1100			1500		
	water	-0.5	1050			1000			1300		
(S)	101	-7								2.1	10
	102									-	9
	103	-5								12.79	8
	104	-5								14.1	7
	105	-5								16.6	6
	106	-5								17.3	5
	107	-6.5								13.38	4
	108	-7								8.9	3
	109	-8								3.2	2
(N)	110	-9								5	1

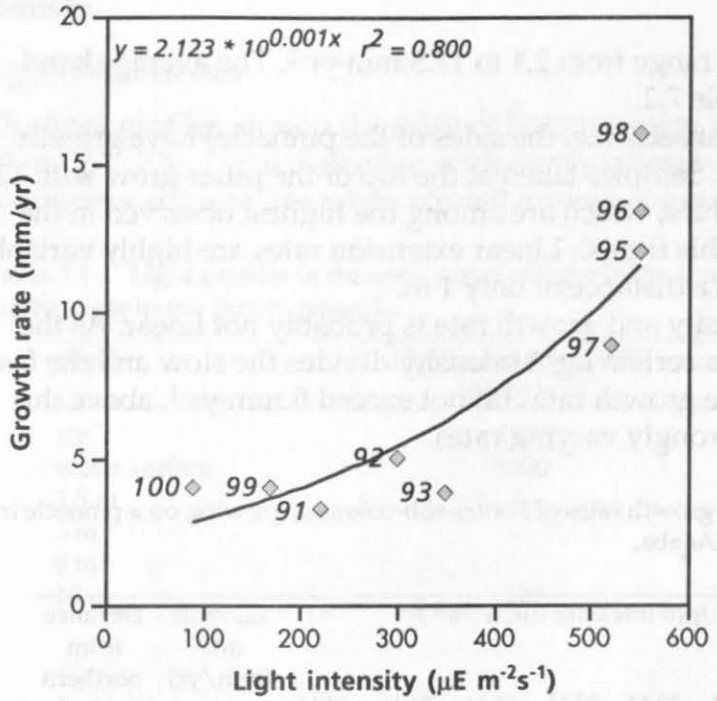

Figure 7.6
Growth rate of *Porites*-colonies from a coral-pillar in the fore-reef at Aqaba, Marine Science Station. Light intensity values measured at Nov 28th, 09:40h plotted as an example. Growth rates are obviously not correlated linear with light intensity. A limiting light intensity divides two groups. A light intensity below a certain value (here between 400 and 500 µE $m^{-2}s^{-1}$ at 09:40h) results in an upper growth limit of ca 5 mm·yr^{-1}, while above this limit growth rates range in a wide spectrum. Curve fit is exponential.

Discussion

In the following discussion we refer to the growth rates of series 91-100. Correlation coefficients for growth rates and light measurements are displayed in Table 7.3. Positive correlation between depth and light intensity is highest for vertical and maximum light values. Horizontal measurements do not show strong relation to depth. Correlation between growth rate and depth is high, and correlation between radiation and growth is high for vertical and maximum values. The strikingly good correlation of depth to growth ($r=0.93$, $P<0.0001$) shows the strong influence of depth on coral growth. However, depth itself is a mixed environmental variable. *Porites*-colonies sampled in the same depth range (4 to 10 m) in the fore-reef of Aqaba do not exhibit a depth related reduction of extension rates down to a depth of ca 10 m (see Chapter 5). The decrease of radiation at the sides of the pinnacle suppresses the growth of shallow water corals to levels normally reached in depths of more than 30 m.

The range of growth rate in the studied samples reflects remarkably well the total range of growth rate of *Porites* in the Gulf of Aqaba down to a depth of 50 m, as described in Chapter 5 of this thesis. The observed decrease in growth rates is closely related to depth. This is not surprising, as light intensity decreases exponentially with depth. But the high rate at which this occurs can not only be explained by the effect of increasing depth. The decreasing growth rate coincides with decreasing light levels at the sides of the coral-pillar, which are lower than in the open water. At the northern side this decrease is stronger than at the southern side of the pinnacle. Extension rate decreases continuously until a certain value is reached, where *Porites*

growth ends. The fact that this limit lies in the northern, shady side of the pinnacle several meters higher than at the southern, light exposed side, implies a dependency to the total amount of light received by the corals throughout the day. We conclude that the growth of the peripheral sub-colonies is depressed mainly by the reduced light availability.

The study of growth rates of colonies in the fore-reef at Aqaba´s Marine Science Station, which are generally sampled from the flat bottom, showed a much smaller range of growth rates in water depths between 5 and 10 m (2.7-8.5 mm·yr^{-1}, mean 6.16±2.47, see Chapter 5). The main difference in the growth rate patterns between the fore-reef and the pinnacle are the extremely high values which are observed in the sub-colonies on the top of the pinnacle. Extension rates of this range (>10 mm·yr^{-1}) have been measured only at two sites in the reef under investigation: from a colony growing at 1 to 2 m depth at the reef crest (11.5 mm·yr^{-1}) and from a unique "giant colony" in the upper fore-reef (Chapter 5 of this thesis, Heiss et al. 1993) at the same depth. What are the reasons for the rapid growth of the colonies at the top of the pinnacle? Light is commonly regarded as the primary environmental factor influencing coral growth (e.g. Bosscher 1992). If we compare the colonies on the top of the pinnacle with those growing in the same depth in the fore-reef, we see that the pillar-colonies are growing much faster. From our observations in several long field campaigns there is no remarkable difference in water transparency between the reef and the pinnacle. Generally the light level in five meters depth is high enough to enable a maximum coral growth. A significant decrease in coral growth rates is observed in the Gulf of Aqaba as well as in other oceans below 10 - 15 m (see Chapter 5; Huston 1985; Bosscher 1992).

Temperatures

Water temperature might influence the rates of coral growth by extreme fluctuations in the vicinity of the lagoon. In summer water temperatures can reach extremely high values and might inhibit coral growth (e.g. Hudson 1981). Under these conditions the fore-reef pinnacle would provide a more advantageous environment for coral growth what might explain the high growth rates at the top of the pinnacle.

Table 7.3 Correlation coefficient matrix for growth rates and light measurements at the *Porites*-pinnacle in the fore-reef (if r ≥ 0.7, *P* is at least ≤ 0.05).

Correlation	Depth	28.11. 9:40 vert.	28.11. 9:40 horiz.	28.11. 9:40 max.	30.11. 9:30 vert.	30.11. 9:30 horiz.	30.11. 9:30 max.	25.11. 15:00 max.	Growth rate 11-110	Growth rate 91-100
Depth	1	.858	.658	.927	.797	.345	.825	.768	.676	.930
28.11. 9:40 vert.	.858	1	.669	.981	.932	.331	.939	.911	.866	.839
28.11. 9:40 horiz.	.658	.669	1	.697	.845	.802	.826	.887	.312	.848
28.11. 9:40 max.	.927	.981	.697	1	.927	.357	.945	.900	.792	.888
30.11. 9:30 vert.	.797	.932	.845	.927	1	.610	.983	.966	.691	.872
30.11. 9:30 horiz.	.345	.331	.802	.357	.610	1	.587	.561	-.120	.591
30.11. 9:30 max.	.825	.939	.826	.945	.983	.587	1	.968	.661	.887
25.11. 15:00 max.	.768	.911	.887	.900	.966	.561	.968	1	.627	.868
Growth rate 11-110	.676	.866	.312	.792	.691	-.120	.661	.627	1	.622
Growth rate 91-100	.930	.839	.848	.888	.872	.591	.887	.868	.622	1

Currents and sedimentation

Different patterns of sediment load are the most probable reasons for the high growth rates on the fore-reef pinnacle. This pinnacle is free-standing in a distance of ca 100 m from the shore-line and 50 m from the reef-crest. The negative effects of water movement, namely resuspension of sediments, has been shown to reduce growth rates of corals (Dodge et al. 1974; Hudson 1981; Cortés and Risk 1985). Turbidity inhibits coral growth not only by reducing light levels, but also by depositing sediment on the tissues of corals. This sediment must be removed and this effort needs energy which otherwise would be directed toward feeding and growth (Dodge et al. 1974). Turbidity levels at Aqaba are sometimes quite high, reducing the visibility from 50 to less than 10 m. This murky conditions occur episodically in the northern Gulf of Aqaba and their reason is not yet clear. However, the effect is similar for corals in the fore-reef and the reef crest. The greater distance to the shore-line might favour the fore-reef pillar to the reef crest environment in times of sediment input through the episodical rainfalls. But the distance is so short and the events so rare that it seems not to be a decisive factor for the observed differences.

What actually distinguishes the environments is the resuspension of bottom sediment. This does not occur on the top of the pinnacle. Cortés and Risk (1985) found in sediment traps 75 cm above substrate only ca 50 % of the amount of resuspended sediment as in 25 cm height above the substrate. The samples from the pinnacle at Aqaba grew at least one meter above the substrate, resuspended sediment load is therefore probably very low. Additionally, the rough and disintegrated surface does not enable any sediment accumulation on the top of the pinnacle (6 m above substrate). Resuspension thus cannot occur, providing the corals growing on the top with clear, steadily changing water and high light levels throughout the year. In contrast, sediment is accumulated in the lagoonal, reef-crest, and the upper fore-reef environments and can be re-agitated by waves and currents.

CHAPTER EIGHT

CARBONATE PRODUCTION BY SCLERACTINIAN CORALS AT AQABA, GULF OF AQABA, RED SEA

Abstract

In a fringing reef at Aqaba at the northern end of the Gulf of Aqaba (29°27´N) growth rates, density and calcification rate of *Porites* was investigated in order to establish calculations of gross carbonate production for the reefs in this area. Colony accretion of *Porites* decreases linearly with depth as a function of decreasing growth rates and increasing skeletal density. Calcification rate of *Porites* is highest in shallow water (0-5 m depth) with 0.94 $g \cdot cm^{-2} \cdot yr^{-1}$ and decreases to 0.49 $g \cdot cm^{-2} \cdot yr^{-1}$ below 30 m. Scleractinian coral gross production is calculated from potential productivity and coral coverage and is mainly dependent on living coral cover and to a lesser extent on potential productivity. Maximum gross carbonate production by corals at Aqaba occurs at the reef crest (0.29 $g \cdot cm^{-2} \cdot yr^{-1}$) and in the middle fore reef from 10 to 15 m water depth (0.21 to 0.27 $g \cdot cm^{-2} \cdot yr^{-1}$). Production is low in sandy reef parts. Below 30 m depth values are still at 0.14 $g \cdot cm^{-2} \cdot yr^{-1}$. Mean potential production of colonies and gross carbonate production of the whole reef community at Aqaba is lower than in tropical reefs. However, carbonate production is higher than in reef areas at the same latitude in the Pacific, thus indicating a northward shift of reef production in the Red Sea.

Introduction

In this chapter a calculation of gross carbonate productivity of the coral reef off Aqaba's Marine Science Station is given. The objective is to quantify carbonate production for a later calculation of a carbonate budget for this reef.
Several studies on carbonate production have been carried out in the Caribbean and the Pacific Ocean in the last two decades. Budgets of carbonate mounds (Bosence et al. 1985; Bosence 1988), bank lagoons (Neumann and Land 1975) and coral reefs were established, the different environments of coral reefs were studied (e.g. Smith and Harrison 1977; Charpy-Roubaud 1988; Furnas et al. 1990; Le Campion-Alsumard et al. 1993) and the individual contribution of some carbonate producing biota to the total production were examined in detail (e.g. Ghiold and Enos 1982; Payri 1988; Edmunds and Davies 1989; Guillaume 1990; Guillaume and Montaggioni 1992). The most intensive investigations on carbonate production were carried out in the Caribbean. A detailed carbonate budget was established at Barbados (Stearn et al. 1977; Scoffin et al. 1980). In a series of studies on coral growth, carbonate production, sediment transport and Holocene accumulation at St. Croix, U.S. Virgin Islands, the patterns and quantities of carbonate accumulation were investigated (Sadd 1980, 1984; Hubbard et al. 1981, 1986, 1990; Dodge and Brass 1984; Hubbard and Scaturo 1985; Hubbard 1986).
In the Indian Ocean and the Red Sea no studies on reef carbonate production exist yet. Carbonate production in reefs was described by Chave et al. (1972) as potential, gross and net carbonate production. Potential production refers to the calcification rate of an individual or a colony, gross production is the carbonate produced by the entire community, and net production is carbonate permanently retained in the reef. A carbonate budget has to take into account the production of the material, the rate and quantity of this material which is converted from framework to sediment, and the amount of sediment which is transported out of the system. The remaining part of this sediment is incorporated in the reef and contributes to the net production. This is summarized by the equation (Land 1979):

$$P_G - P_N = P_S = T_S$$

where:

P_G = gross carbonate productivity (standing crop x production rate).
P_N = Net productivity (carbonate ultimately incorporated in the reef).
P_S = Sediment produced by the destruction of a portion of the original reefal material (P_G).
T_S = Sediment transported out of the system.

This equation should be modified, as not the entire sediment produced is exported, but stays within the reef framework and contributes to net production.

$$T_S = P_S - P_I$$

P_I = Sediment which remains in the reef system.

So that: $$P_G - P_N = P_I + T_S = P_S$$

As the first part of an extended study this paper tries to examine the gross production, based on standing crop and growth rates of the individual organisms of the reef in the northern Gulf of Aqaba. An outlook to production potentials of reefs in the northern and central Red Sea is given and the use of density evaluation by computed tomography is described.

The density of coral skeletons is, beside the growth rate, the other important factor for the assessment of carbonate production rates by corals. The relation between density of coral skeletons and water depth has been studied by various authors with remarkably different results (see chapter 8). Recently computed tomography has been introduced as a new method for the evaluation of skeletal density. In this chapter a brief outline of the methodology and the results of the density measurements used for production calculations in chapter 8 is given.
Various techniques for the evaluation of density have been applied in the last decades: Photodensitometry of X-radiographs (Buddemeier et al. 1974; Baker and Weber 1975; Chalker et al. 1985; Pätzold 1986), displacement in water (Hughes 1987), mercury displacement (Dustan 1975), and gamma densitometry (Chalker and Barnes 1990). Bosscher (1992; 1993) performed systematic density measurements by computed tomography (CT) in a depth range from 0 to 30 m at Curaçao, Caribbean. The use of CT has been shown to be a relatively quick, exact and non-destructive method for density evaluation (Bosscher 1993). We evaluated structure and density of Red Sea corals in order to define optimal parameters and to evaluate the image quality of state of the art CT-equipment and its use in band width assessment.

Marine Science Station Aqaba

The fringing reef south of the Marine Science Station at Aqaba extends over a length of ca. 1 km (Fig. 8.1). The lagoon is max. 200 m wide, the reef crest reaches a height between 1 and 5 m above the mostly sandy upper fore-reef. The fore-reef can be divided in upper, middle and lower fore-reef zone (Mergner and Schuhmacher 1974) and slopes seawards with angles increasing from 5 to 15°.

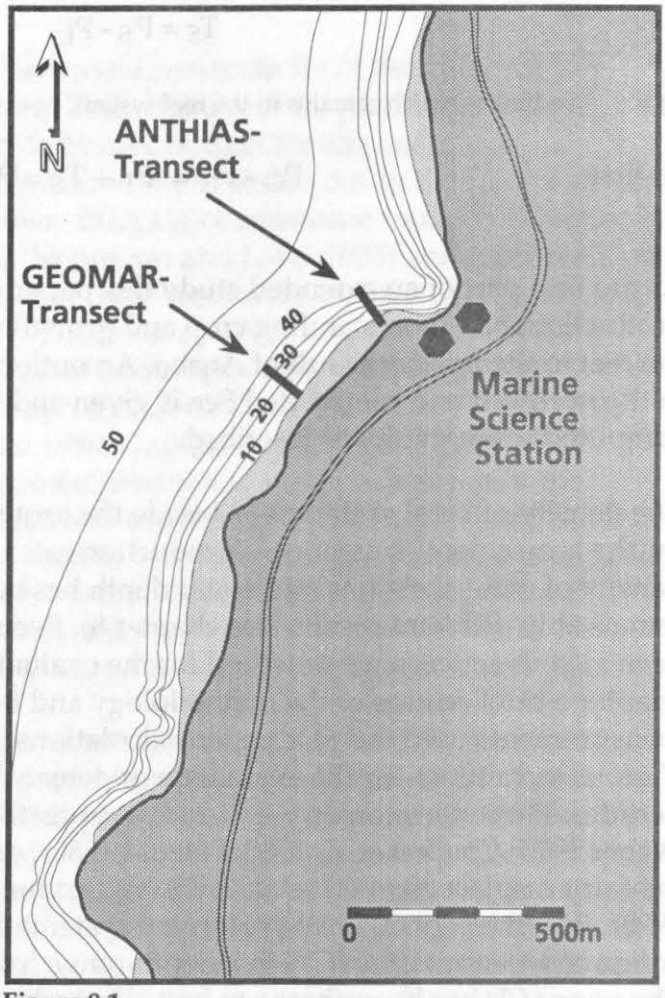

Figure 8.1
Location of transect lines in the Marine Science Station reef. ANTHIAS-Transect is located at the lower end of transect I as mapped in Mergner and Schuhmacher (1974; 1981) and was placed for studies on population structure of Anthiine fish (Krupp 1989; Schuhmacher et al. 1989) . GEOMAR-Transect was put in place for this study in 1991.

Scleractinia in the coral reef community

From their extensive long-term observations of coral communities in Aqaba Mergner and Schuhmacher (1974; 1981; 1985) conclude that "these reefs mark the northernmost outpost of the Indian Ocean only geographically but not ecophysiologically; they would occur at even higher latitudes, if the Gulf of Aqaba extended farther north". Species diversity is comparable to that of the central Red Sea (e.g. Sanganeb Atoll) with 48 genera of hermatypic scleractinia at Aqaba and 51 at Sanganeb, respectively (Schuhmacher and Mergner 1985). Using the quadrat method with test areas of 25 m^2 Schuhmacher and Mergner (1985) found that uninhabited parts (i.e. dead coral rock and sediments) amount 56 % of a fore-reef test area in ca. 10 m depth at Aqaba. Hermatypic scleractinia inhabit 21.6 % of the test area. The contribution of incrusting forms is 6 %, of massive colonies 10 %, and of ramose species 5.25 % of the total area.

The carbonate which is produced by corals and coralline algae and fixed in the frame of the reef becomes eroded by mechanical destruction and erosion through the activity of organisms (bioerosion). The main agent of mechanical erosion is the energy of waves, particularly in storms, which reduce the limestone through rubble to sand to suspended finer particles. Members of the "destroyer guild" (Fagerstrom 1987) like grazing parrotfish and sea urchins remove large quantities of dead and living corals and algae and excrete it in fine particles over the reef. Endolithic eroders like sponges, bivalves, fungi and barnacles also destroy great amounts of reef

framework. In the reefs of the northern Gulf of Aqaba mechanical erosion can only be a subordinate agent because wave energy is generally low due to the mostly northerly winds. Wind-driven waves coming from N-NNW have only 10 km run up distance. These waves reach generally only 0.3 - 0.5 m height. Severe storms are not reported for this region (Mergner 1981). A swell does develop, however during periods of continuous southern winds blowing the length of the Gulf, usually during winter. The swell does not persist more than 24 to 48 hours (Hulings 1989).

Materials and methods

The calculations of carbonate production rates presented here are exclusively for scleractinian corals. *Millepora* (Hydrozoan) and crustose coralline algae are not taken into consideration. At present no reliable data on growth rates for these groups are available, which are measured with a comparable accuracy like those for scleractinians. Furthermore, no studies of relation between depth and growth rates of coralline algae and *Millepora* are published. Although Hubbard et al. (1981) included these organisms in their calculation of production rates at St. Croix, they already pointed out the lack of information on these groups. An average accretion rate of 6.51 $kg \cdot m^{-2} \cdot yr^{-1}$ reported by Adey and Vasser (1975) was used for all depth zones. Being aware of the inaccuracy two values for total carbonate production are calculated in the report of Hubbard et al. (1981). One was determined without coralline algae and *Millepora*, another including these groups with an assumed maximum production of 6.51 $kg \cdot m^{-2} \cdot yr^{-1}$, thus a range of carbonate productivity was obtained.

In our study we did not follow this method. The inherent inaccuracy seems not to improve the determination of total carbonate accretion. It is thus important to notice, that the production rates given in this study represent minimum values. The true carbonate production will certainly be higher than our values and might be corrected, as soon as reliable data on growth rates of crustose coralline algae and *Millepora* and other carbonate producing organisms in the Red Sea are available. The greatest part of carbonate is produced by scleractinian corals. In a Caribbean reef about 93 % of the total carbonate production is contributed by the calcification of corals (Hubbard et al. 1990). The contribution of coralline algae and *Millepora* to the carbonate budget of the reef under investigation is not yet known. Mergner and Schuhmacher (1981) reported that coralline algae inhabit only 0.2 % and *Millepora* 0.09 % of the area in the fore-reef of the Marine Science Station. A different pattern was reported by Gabrié and Montaggioni (1982) when they investigated several reefs of the Jordanian Red Sea coast. They found the contribution of coralline algae to the sediment of the reef flat zone and of the upper parts of the fore reef zone (0-20 m) to be more than 20 %. This figure seems more reliable since coralline algae grow abundantly in hidden places, e.g. below scleractinians and therefore not occur in transect census techniques in plan view. This ambiguity between different sites and methods demonstrates the difficulty to evaluate the contribution of coralline algae to the carbonate budget. Therefore we did not take coralline algae into account.

Coral coverage

The percentage of different reef units with their carbonate production potential was determined along a 200 m transect line, the GEOMAR-transect, installed perpendicular to the shoreline (Fig. 8.2). This transect runs from the reef crest (ca. 1 m depth) down to the outer fore-reef to a depth of 35 m (Fig. 8.2). We photographed the transect in portions of 2 m length in 1991 and 1992 and measured the substrate lying under the line to the nearest 10 cm on paper prints. Surface coverage was classified in five categories: Branching corals, massive corals (including encrusting species), soft corals, dead coral surface, and sediment.

The species composition within these "morphological" groups in different depth zones was obtained from detailed line transect measurements. Transects of 10 m length were installed at depths of 10, 15, 20, and 30 m depth at two sites of the fore-reef (perpendicular to the GEOMAR-transect and ANTHIAS-transect, Fig. 8.1). ANTHIAS-transect served as a reference for the positions of the 10 m-transects and was not measured in respect to coral coverage. Transect data from 20 m and 30 m depth at the ANTHIAS-transect were kindly provided by G. Reinicke (University of Essen). The coverage below these transect lines was censused by Scuba-diving to the nearest centimeter (Loya 1972). For calculation of production on the reef flat we used the coverage data published by Mergner (1979, Tab. 8.1). Scleractinia cover only ca. 3 % of reef flat surface, the greatest area is covered by dead coral rock, loose sediment, and benthic macroalgae.

In 1980 a quantitative study of coral communities of Jordanian coral reefs was carried out by Bouchon (1980) about 2 km south of the Marine nature reserve. The coral coverage recorded using the transect method (i.e. linear percentage of species under the line) of Loya (1972) is given in Tab. 8.2, the dominant species for the different reef units are listed in Table 8.3. Coral coverage is lowest in the boat channel, on the reef

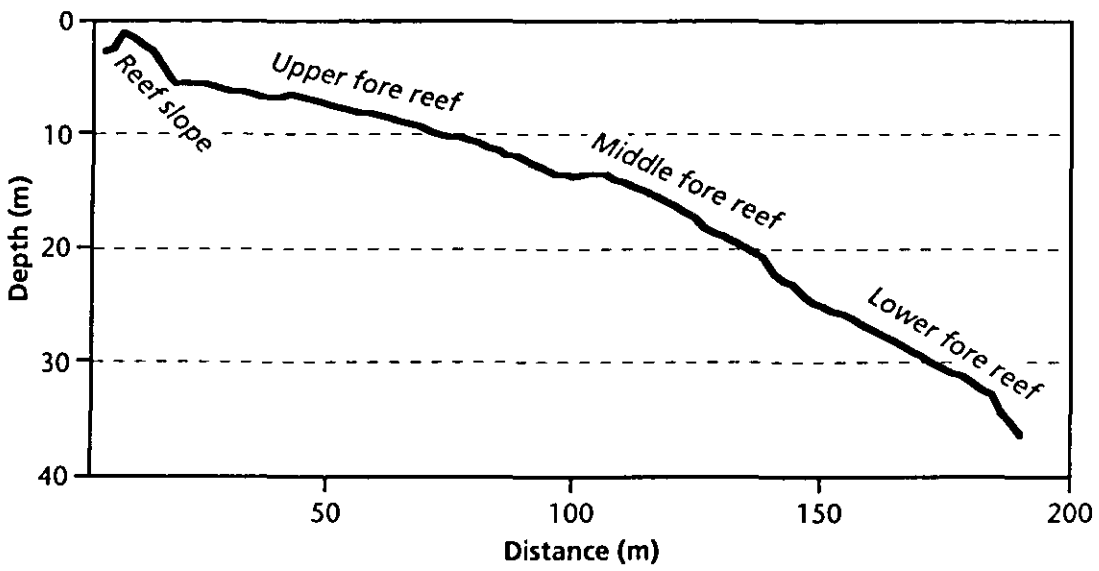

Figure 8.2 Depth profile of transect-line at a reef south of the Marine Science Station ("GEOMAR-transect"). Length of transect line is 191 m.

flat ca. one third of the area is covered by corals. Highest coral coverage occurs in depths below 10 m (50-70 %). The composition of the coral community changes in different parts of the reef in response to water energy, light levels and depth.

Reef surface area data are gathered from aerial photographs computed by computer processing of digitalized colour slides (Tab. 8.4, Maniere and Jaubert 1984).
The total area of the reef from the shoreline to the foot of the drop off in ca. 50 m water depth is about 31974 m^2. About 50 % of this area can be regarded as "carbonate factory" with considerable growth of scleractinian corals (Tab. 8.4)

Comparison between the coverage data obtained at our transect by linear percentage sampling and the data obtained from a 25 m^2 quadrat in the fore-reef published by Mergner and Schuhmacher (1981) show strong differences in the coverage data (Tab. 8.5). These differences are based on the use of different methods, lateral changes of coral coverage, and temporal changes of reef community composition. Linear percentage sampling technique reveals the major-reef building species in large reefs, while other sampling techniques (like line transects with 1x1 m grids) provide better tools for characterizing reef communities (Chiappone and Sullivan 1991).

Species	Abundance in % of total area
Cyphastrea microphtalmata	0.57
Favia pallida	0.37
Favites melicerum	0.30
Goniastrea retiformis	0.93
Montipora tuberculosa	0.16
Pavona decussata	0.01
Stylophora pistillata	0.60
Scleractinia total	2.94

Table 8.1
Scleractinia population and surface area data for a 25 m^2 quadrat (L1) in the lagoon of a fringing reef, about one km south of the MSS. The quadrat is situated ca. 60 m seaward of the mean high water level. Data from Mergner (1979).

Station	Coral coverage (%)
Boat channel	1
Inner reef flat	25
outer reef flat	33
5m	50
10m	70
20m	60
30m	50
40m	65

Table 8.2
Variations of the scleractinian corals coverage rate on a fringing reef at the Jordanian Red Sea coast (5 km south of the Marine Science Station, data from Bouchon 1980)

Table 8.3 Dominant scleractinian coral species for a fringing reef at the Jordanian Red Sea coast (5 km south of the Marine Science Station, data from Bouchon 1980).

Station	Dominant species
boat channel	*Stylophora pistillata, S. prostrata, Seriatopora hystrix, Platygyra lamellina*
reef flat	*Stylophora pistillata, Seriatopora hystrix, Acropora cf. humilis, Fungia scutaria, Pavona (pseudocolumnastrea) pollicata, Platygyra lamellina, Echinopora gemmacea, Acanthrastrea echinata*
Outer slope, upper part (0-20 m)	*Stylophora, Seriatopora, Acropora, Echinopora, Porites Lobophyllia, Mycedium*
Outer slope, middle zone (20-50 m)	*Montipora, Astreopora, Porites, Faviidae*
Outer slope, lower part (deeper than 60 m)	*Pachyseris, Leptoseris*

Table 8.4 Surface area of units in the reef south of the Marine Science Station, automatically computed from a classified image taken from aerial colour diapositive (from Maniere and Jaubert 1984).

Unit no.	Unit name	Unit area (m^2)	Percentage
1.	Coral built outer slope	15292	47.8
2.	Coral sand (sandy spreads)	3746	11.7
3.	Outer reef flat	1948	6.0
4.	*Turbinaria* and *Sargassum* belt	359	1.1
5.	Compact inner reef flat	2061	6.5
6.	Sandy coral flagstone	1817	5.6
7.	Reef flat with pebbles, dead corals and scattered coral growth	1818	5.6
8.	Zone of micro-atolls and sandy pockets	1671	5.3
9.	Dense seagrass beds	1841	5.8
10.	Scattered seagrass beds and green algae	1163	3.8
11.	Beach rock	258	0.8
	Total surface	31974	

Table 8.5 Population and surface area data for a 25 m^2 quadrat (U 7) and a 10 m transect in the middle fore-reef of a fringing reef at the Marine Science Station (10 m depth). U 7 Data from Mergner and Schuhmacher (1981).

Group	Abundance in % of total area	
	U 7	Transect 1
branching corals (*Pocillopora, Seriatopora, Stylophora, Acropora)*	5.25	15.80
encrusting corals (mainly *Montipora, Psammocora, Pavona, Echinophyllia, Mycedium, Turbinaria)*	6.00	10.00
massive growing forms *(Poritidae, Faviina, Astreopora, Gardinoseris, Leptoseris, Pachyseris)*	10.02	8.90
solitary forms *(Cycloseris, Fungia)*	0.16	-
calcareous algae	0.20	not considered
total scleractinia	21.49	34.70

Table 8.6 Scleractinian linear extension and calcification rates. Data for Indo-Pacific corals present in the Red Sea or similar species.

Species	Depth range (m)	Growth rate (mm yr^{-1})	Density ($g \cdot cm^{-3}$)	Calcification rate ($g \cdot cm^{-2} \cdot yr^{-1}$)	Locality	Source
Acropora sp.		100-200			Indo-Pacific	Maragos (1972)
Astreopora myriophtalmata	7 18	7.5-13 5-5.5			Enewetok (11°N,162°E)	Buddemeier et al. (1974)
Hydnophora microconus	5	11.5			Enewetok	Buddemeier et al. (1974)
Porites lutea	0-30	7.6(3.5-11.8)	1.41 (1.26-1.50)	1.07 (0.49-1.66)	Enewetak	Highsmith (1979)
Favia pallida	2-30	5.7 (4.1-7.1)	1.43	0.82 (0.59-1.32)	Enewetak	Highsmith (1979)
Goniastrea retiformis	5-17	6.8 (4.9-8.5)	1.70	1.16 (0.83-1.45)	Enewetak	Highsmith (1979)
Goniastrea retiformis	4-5	7.8-13			Enewetok	Buddemeier et al. (1974)
Goniastrea retiformis	10		1.92-2.06		Aqaba	Ramm (1993)
Montipora verrucosa	10 15		1.51 (±0.14) 1.28 (±0.04)		Aqaba	Ramm (1993)
Pavona clavus	5-7		1.86		Gulf of Chiriqui	Wellington and Glynn (1983)
Pavona clavus	5-7		1.44		Gulf of Chiriqui	Wellington and Glynn (1983)
Favia speciosa	3-19	4.6-8.5			Enewetok	Buddemeier et al. (1974)
Favia pallida	10		1.40 (±0.05)		Aqaba	Ramm (1993)
Favia pallida	27		1.43 (±0.12)		Aqaba	Ramm (1993)
Platygyra sp.		5-12			Indo-Pacific	Land (1979)
Platygyra lamellina	7	6.7, 7.5, 8			Enewetok	Buddemeier et al. (1974)
Platygyra lamellina	few m	7.9			Hurghada	Cember (1988)
Pocillopora damicornis	3	30.8	≈1	0.96	Gulf of Panama, 8°40'N, 79°W	Glynn (1977)
Pocillopora damicornis	3-5	38.6	≈1	0.96	Gulf of Chiriquí, 8°N,82°W	Glynn (1977)

Coral growth rates

Because we could not measure growth rates for all coral genera in our study area, we used growth rates reported in other studies for the Pacific - Indian Ocean - Red Sea reef province for the calculations of carbonate production. For the Red Sea proper only few data on growth rates of corals are reported (Tab. 8.6). Interesting remarks are made by Buddemeier and Kinzie (1976) on the growth rates of branching coral colonies. Referring to the studies of Maragos (1972), the increase in mean solid radius of five colonial Hawaiian corals (*Porites compressa, P. lobata, Pocillopora damicornis, P. meandrina, Montipora verrucosa*) is 5 to 15 mm·yr^{-1}. Even though the growth forms are substantially different, these values are strikingly close to extension rates of hemispherical massive colonies. These observation indicate "much more consistency in inherent calcification capability than linear growth rates and growth form comparisons would suggest" (Buddemeier and Kinzie 1976). Linear extension rates for *Porites lobata* from Hawaii vary between 10 to 15 mm·yr^{-1} (Grigg 1982). It seems reasonable that the mean solid radius increase is actually comparable to the values measured as linear extension, as suggested by Buddemeier and Kinzie (1976).

Density

Bulk density of coral skeletons can be determined by various techniques. Measuring the weight of a cube or a tube of known volume of the coral sample, displacement in water or mercury, gamma- and photodensitometry, and computed tomography have been applied.
For density evaluation 12 samples of *Porites* sp. from the reefs at the Marine Science Station (MSS) and 10 samples from the reef close to the Saudi border were selected (Fig. 5.2). These samples cover a depth range from 1 to 26 m water depth at the Marine Science Station and 2 to 45 m at Saudi Border, resp. (Tab. 8.7). One sample was taken half-way between these two sites ("Gorgon 2").

Bulk density measurements by computed tomography

Computed tomography (CT) produces images of patients or objects in the transversal plane by rotating an X-ray source and detectors around the object and measuring the absorption of the X-ray beams. From numerous projections (usually 360 - 720) pictures are calculated through complex data processing, displayed on monitors and printed with Laser-cameras on photographic film in a resolution of 512 * 512, interpolated to 1024 * 1024 picture elements (pixel). In interpreting the pictures, care has to be taken since the displayed pixel represent volume elements (voxel) of various size depending on the chosen slice thickness, which can be varied between 1 and 10 mm. In this study a Siemens Somatom Plus S Computed Tomography Scanner was used.
A fundamental factor in density measurements in corals is the thickness of the slices. The first aim is to measure a maximum volume of the sample. The largest area and thickness give the best average value of density. From the images in Figure 8.3a the consistency of the mean density in three ROIs (region of interest) is demonstrated. even though the standard deviation within each ROI are high, mean density differs only by ±10 %. In contrast, parts of the sample in Figure 8.3b display strongly different densities, despite the low variation within each ROI. In our measurements,

a slice thickness of 2 mm displayed growth bands in *Porites* samples most clearly, 5 mm were chosen for the density measurements. In the first case, thinner slices resulted in coarse pictures due to a low signal to noise ratio; broader slices gave an insufficient spatial resolution. In the latter case, the standard deviation around the mean density measurement was too high in thinner slices while slices bigger than 5 mm resulted in an increased risk of "partial volume" effects. If the slices are too thick, empty space in boreholes might not be detected in the CT image, and therefore, will reduce the density value. A comparison between slices of 2 and 5 mm is shown in Figure 8.3. In the 2 mm slice the thickness of slice and calice diameter are in the same range. The skeleton looks like a meshwork and the resulting density values are highly variable (seen from the standard deviation). The 5 mm slice covers a greater part of the coral and the density values within each ROI show less variability.

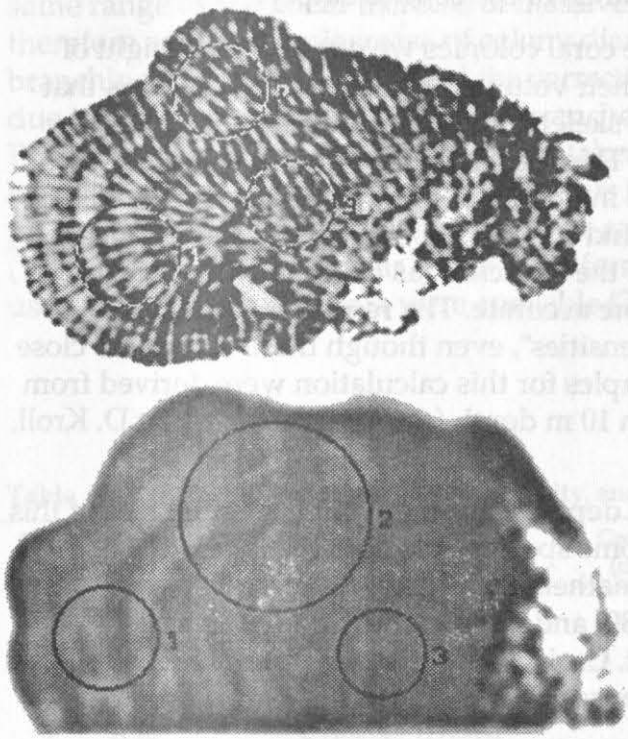

Figure 8.3

a. CT image of *Cyphastrea* sp. from the Red Sea coast of Egypt. Slice thickness 2 mm. Mean density (ME) varies between 1609 HU (ROI 1), 1756 HU (ROI 2) and 1711 HU (ROI 3), standard deviation (SD) within each ROI is very high (315-426). Image width: 7 cm.

b. CT image of *Porites* sp. from Aqaba. Slice thickness 5 mm. Mean density (ME) varies between 1296 HU (ROI 1), 1463 HU (ROI 2) and 1562 HU (ROI 3), standard deviation (SD) is relatively low (100-119). Image width: 6 cm.

For density measurements a slice thickness of 5 mm was chosen. For each sample the density of circular ROIs of the maximum possible size was determined, whereby bioeroded parts of the coral were excluded. Another potential source of error are artefacts in the vicinity of strong density differences at the boundaries of the sample or holes within the skeleton. ROIs must therefore be positioned in a certain distance from the edge of the sample and boreholes.

Density values from CT are given in Hounsfield-units (HU), where -1000 HU is the density of air and 0 HU the density of water. CT density was calibrated to density in $g \cdot cm^{-3}$ with a calcite crystal, several rectangular samples of coral material (*Porites*) and cubes of *Goniastrea retiformis* and *Hydnophora* sp. These were measured with a precision caliper and weighed to a precision of ±0.01 g. The sample size of *Porites* skeleton was approximately 8 x 8 x 1.7 cm and its weight between 110 and 130 g. Cubes were of a volume of 25 - 48 cm^3 (Ramm 1993). Possible errors in the evaluation

of density lie mainly in the change of density in different parts of the skeleton and in an undetected bioerosion. Therefore, we scanned the calibration samples in slices of 2 mm thickness before we measured the density. All samples were scanned when submerged in water to avoid the occurrence of negative values. For the standard measurements of coral samples we did not follow the detailed procedure of measuring thin and thick slices subsequently. Only if the difference in density between the different ROIs (three per sample) was conspiciously high we checked the sample for holes by scanning a series of 2 mm slices.

For calculations of carbonate production the increase in carbonate is related to the surface area covered by the organism. Therefore the density of the skeleton must be combined with the empty space between skeleton elements. Mainly for branching scleractinian corals this reduces the productive part drastically, as ca. 75 to >90% of the volume enclosed by the mean solid radius of the coral is empty.

To get a value for the density of complete coral colonies we divided the weight of measured colonies of several species by their volume. It is important to notice, that this does not give the density of the coral skeletal aragonite, but the density of the colony volume as if it would be massive. This means that the empty space between the branches of ramose corals is included in the calculation. Thus a correction factor for branching corals is already included and has not to be calculated from a visual observation of space filling percentage of the branches (as applied by Hubbard et al. (1981). We consider our method to be more accurate. The resulting values are "colony densities" rather than "skeletal densities", even though these values are close together for massive growing corals. Samples for this calculation were derived from the U7 quadrat at the Anthias-Transect in 10 m depth (samples provided by D. Kroll, University of Essen).

A decrease in carbonate production with depth is common, but the actual rate of this decrease has been determined only for some species. It is possible to relate the changes in production rates with depth mathematically to a "standard species". Such a procedure was performed by Sadd (1980) and used in the carbonate budget calculations of Hubbard et al. (1981) at St. Croix, Caribbean. The premise of the reliability of this method is that the response of different corals to changing environmental factors should be similar.
For each species we calculated its carbonate production potential for each depth zone and multiplied this value with the portion of bottom surface covered by this species. Thus we got the amount of carbonate contribution per area. The sum of these values gives the total carbonate production of each depth zone in $g \cdot cm^{-2} \cdot yr^{-1}$.

Carbonate productivity

Carbonate production of massive growing coral colonies is commonly expressed in $g \cdot cm^{-2} \cdot yr^{-1}$ or $kg \cdot m^{-2} \cdot yr^{-1}$ and computed as linear extension ($mm \cdot yr^{-1}$) multiplied with bulk density ($g \cdot cm^{-3}$). If we regard branching colonies as hemispheres with much empty space between skeletal elements, we can apply this calculation to all main reef building corals.

Correction of production rates

Calcium carbonate production rates were calculated for *Porites* spanning a depth range from 0 to 50 m.
The production rate was correlated with production rates for *Porites* from Eniwetok, calculated from the data of Highsmith (1979, Fig. 8.4). The production rates are lower at Aqaba, the equation of the decrease of production with depth was applied to the genera *Favia* and *Goniastrea*. Correction factor for branching genera (*Acropora, Stylophora, Pocillopora*) was calculated by dividing colony density by the density of *Porites* in the depth range 7-14 m (see above). The linear extension rates in the literature are of no use for our method, as the increase in diameter of the colony is far less than the linear growth of the branches. As Buddemeier and Kinzie (1976) describe, the increase in mean colony radius is for the most branching corals in the same range as the linear increase of massive hemispherical colonies (see above). We therefore assumed an increase of colony diameter comparable to *Porites* for the branching forms and introduced the correction factor for the lower density, which is due to the empty space between the branches.
Production rates for other species were taken from the literature (Tab. 8.6). We calculated correction factors for each genus for each depth step of 5 m, as far as production rates are available or could be calculated from our own samples (Tab. 8.8). Groups of similar corals were formed and corresponding correction factors used when no specific data were available (Tab. 8.8).

Table 8.7 *Porites* growth rates, skeletal density, and production rates from computed tomography.

Depth (m)	Sample id.	Site	Growth rate ($mm \cdot yr^{-1}$)	CT density (HU)	Density (g/cm^3)	Production ($g \cdot cm^{-2} \cdot yr^{-1}$)
-1	A 49	MSS Reef crest	9.75	951.0	1.00	0.98
-2	A 10	Saudi border	5.00	1711.7	1.69	0.84
-3	A 29	Saudi border	6.00	1721.2	1.70	1.02
-5	A 48	MSS Reef crest	4.50	1596.3	1.58	0.71
-7	A 39	MSS Anthias-Transect	5.75	1752.8	1.73	0.99
-7	A 40	MSS Anthias-Transect	4.33	1633.8	1.62	0.70
-7	A 47	MSS Geomar-Transect	8.50	1271.9	1.29	1.10
-10	A 37	MSS Anthias-Transect	4.60	1697.6	1.68	0.77
-13	A 26	Saudi border	4.50	1848.0	1.81	0.82
-14	A 5	Saudi border	4.67	1638.9	1.62	0.76
-15	A 44	MSS Geomar-Transect	5.38	1738.0	1.71	0.92
-16	A 22	Saudi border	3.50	1606.1	1.59	0.56
-20	A 1	Saudi border	5.00	1726.8	1.70	0.85
-20	A 2	Saudi border	3.86	1458.5	1.46	0.56
-20	A 34	MSS Anthias-Transect	2.78	1889.6	1.85	0.51
-22	A 32	MSS Anthias-Transect	3.10	1749.2	1.72	0.53
-26	A 30	MSS Anthias-Transect	4.55	1624.8	1.61	0.73
-31.5	A 12	Saudi border	3.24	1711.7	1.69	0.55
-45	A 14	Saudi border		1893.5	1.85	
-45	A 15	Saudi border	3.00	1582.4	1.57	0.47
-45	A 16	Saudi border	2.66	1735.1	1.71	0.45
-3	A 12-7	Gorgon 2	4.00	1231.7	1.26	0.50
-2	core 2	MSS Reef crest	11.49	1483.8	1.48	1.70
-1.5	core 23	MSS Reef crest	9.33	944.2	1.00	0.93

Reference	similar	Correction factor
Acropora	*Pocillopora,*	0.4
Stylophora	*Pavona, Echinopora, Echinophyllia, Psammocora, Mycedium*	0.35
Favia	*Favites, Platygyra*	0.72-0.6
Goniastrea		0.93-0.48
Porites	all other corals	1

Table 8.8
Groups of corals assigned similar production rates

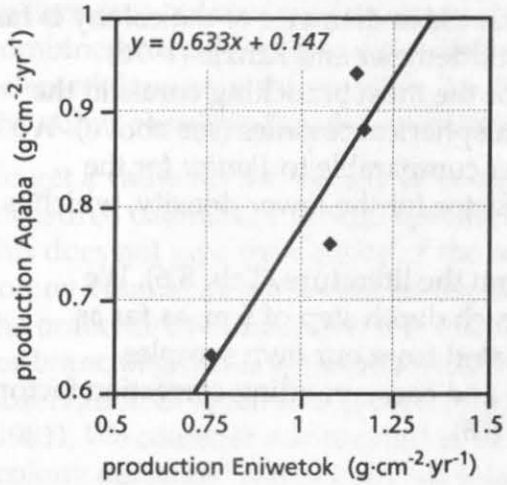

Figure 8.4
Comparison between production rates of *Porites* at Eniwetok (Highsmith 1979) and Aqaba. The equation derived from the linear regression is used to calculate the depth dependent decrease of the genera *Favia* and *Goniastrea* (Tab. 8.8).

Results

Growth rates, density and production potential

Growth rates for scleractinian corals of the genus *Porites* used in this study decrease strongly with depth. The greatest part of this decrease occurs at ca. 10 m water depth, where an upper limit of extension rate of ca. 7 mm·yr^{-1} exists (Fig. 8.5). Mean growth rate decreases from 8.41 mm·yr^{-1} in the shallow water (0-5 m) to 2.99 mm·yr^{-1} in a depth greater than 30 m (see Chapter 5 for details).
Results of density measurements are listed in Table 8.7. Density of *Porites* at the reefs of Aqaba varies between 1.00 and 1.85 g/cm^3, with lowest density restricted to the shallow water. An increase of density with increasing depth has been observed (Fig. 8.6). From Figure 8.6 we see, that in a depth range between sea surface and 10 m depth the variability in density is high with very low density values in some samples. In shallow water (0-5 m) mean density is 1.35 g/cm^3 (±0.4), in 5 to 10 m depth 1.56 g/cm^3 (±0.19). The most densely deposited skeleton is restricted to depths below 10 m (Tab. 8.9). The increase in density does not occur continuously with increasing depth. The greatest part of the increase at the northern Gulf of Aqaba happens at ca. 10 m depth (Fig. 8.6).

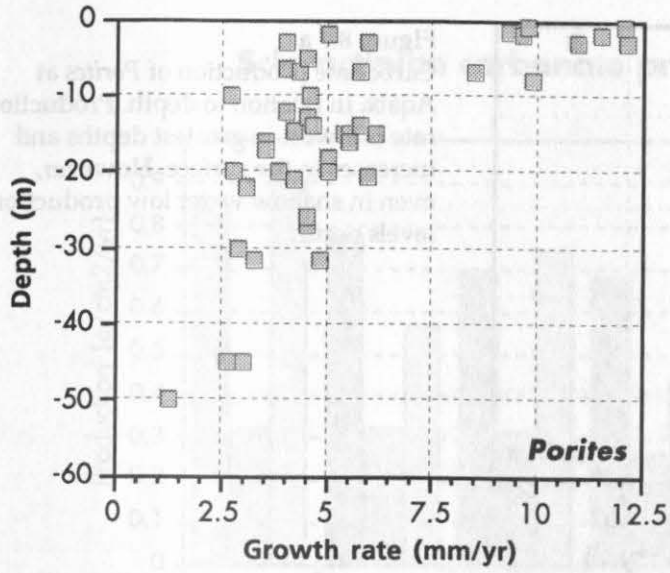

Figure 8.5
Growth rate of *Porites* samples plotted versus depth. Growth rates cdecrease with increasing depth, while highest growth rates and greatest variation is present between 0 and 10 m depth.

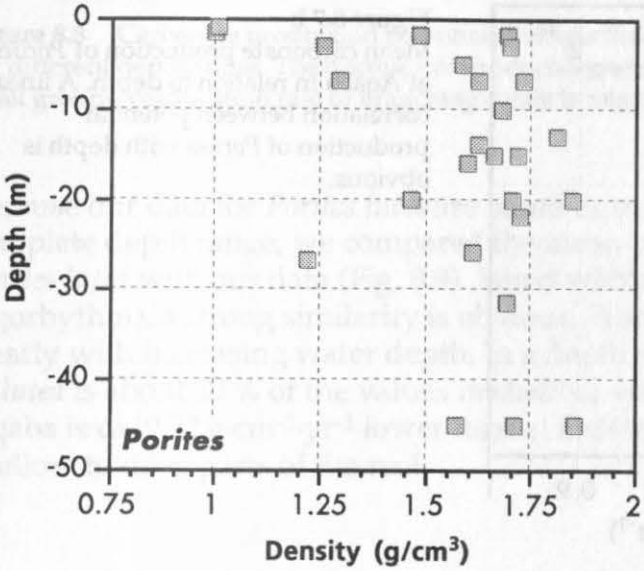

Figure 8.6
Density of *Porites* samples plotted versus depth. Lowest density values occur in shallow water depths, below 8-10 m depth skeletal density is generally higher than 1.6 $g \cdot cm^{-2} \cdot yr^{-1}$.

Depth	Mean density (g/cm^3)	SD
0-5m	1.35	0.40
5-10m	1.56	0.19
10-20m	1.68	0.08
20-30m	1.59	0.22
30-50m	1.71	0.11

Table 8.9
Mean density of *Porites* samples in different depth zones at Aqaba with standard deviation (SD).

Mean production rate for *Porites* is 0.94 $g \cdot cm^{-2} \cdot yr^{-1}$ in 0-5 m depth and decreases to 0.49 $g \cdot cm^{-2} \cdot yr^{-1}$ below 30 m (Fig. 8.7). Extreme high values can be reached in fast growing colonies at the reef crest (1.7 $g \cdot cm^{-2} \cdot yr^{-1}$).

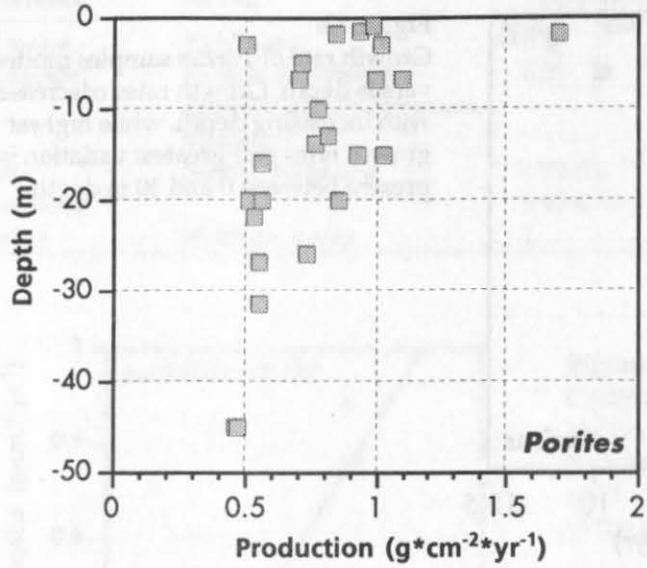

Figure 8.7 a
Carbonate production of *Porites* at Aqaba in relation to depth. Production rate is lowest in greatest depths and increases to the surface. However, even in shallow water low production levels occur.

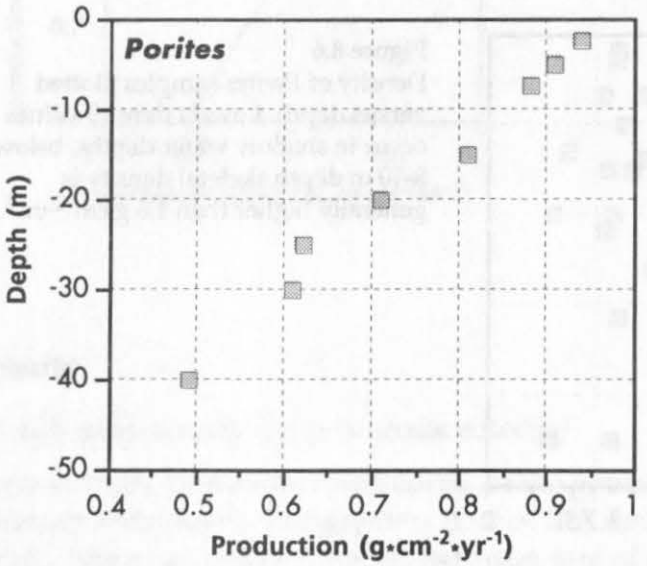

Figure 8.7 b
Mean carbonate production of *Porites* at Aqaba in relation to depth. A linear correlation between potential production of *Porites* with depth is obvious.

The production potential of all corals is highest in the shallow part of the reef (Fig. 8.8). Massive corals have a maximum of 0.87 $g \cdot cm^{-2} \cdot yr^{-1}$ (100%) at 2 m depth, and production decreases to 0.6 $g \cdot cm^{-2} \cdot yr^{-1}$ (70%) at 30 m. Branching corals can produce 0.33 $g \cdot cm^{-2} \cdot yr^{-1}$ (100%) in depths down to 15 m and still 72% (0.23 $g \cdot cm^{-2} \cdot yr^{-1}$) at 30 m. The group of encrusting corals has a potential of 0.91 $g \cdot cm^{-2} \cdot yr^{-1}$ (100%) in the shallow water with a strong decrease to 41% (Fig. 8.8). The high value for encrusting corals is due to the production of *Montipora*, which we assumed to have at least the same production potential as *Porites*. This assumption is supported by the data of Houck et al. (1977) who found higher production rates for *Montipora* than for *Porites* in laboratory experiments and indications for similar extension rates observed in X-radiographs (own unpublished data).

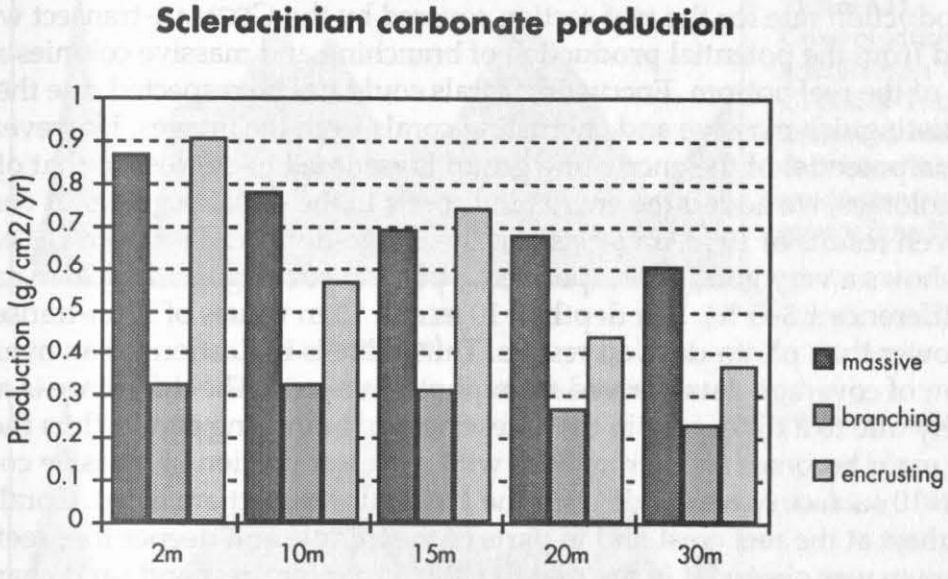

Figure 8.8 Carbonate production potential of scleractinian corals at Aqaba, in morphological groups for different depth zones. The decrease of production rate (given in $g \cdot cm^{-2} \cdot yr^{-1}$) with depth is present in all groups, calcification rate of branching corals is relatively low.

Because our data for *Porites lutea* are based on a great number of samples over the complete depth range, we compared the mean production rates from Eniwetok for *Porites lutea* with our data (Fig. 8.9). Fitted with a linear regression line (least squares algorhythm), a strong similarity is obvious. Production rates at both sites decrease clearly with increasing water depth. In a depth of 30 m the carbonate production of *P. lutea* is about 50 % of the values in shallow water (≈ 1-5 m). The production at Aqaba is ca. 0.22 $g \cdot cm^{-2} \cdot yr^{-1}$ lower than at Eniwetok. This value is constant from shallow to deep parts of the reef.

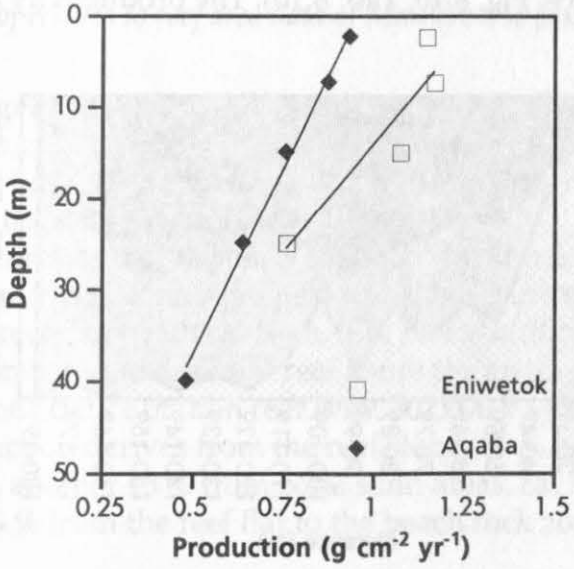

Figure 8.9
Carbonate production rates for *Porites lutea* at Eniwetok (data from Highsmith (1979) and Aqaba. Solid line is linear regression (Eniwetok: $r^2=0.846$; Aqaba: $r^2=0.992$).

Coral coverage

Gross production rate for the reef section covered by the GEOMAR-transect was computed from the potential production of branching and massive colonies and their coverage of the reef bottom. Encrusting corals could not be respected due the difficulty to distinguish massive and encrusting corals from the images. However, as the production potential of the encrusting group is assumed to be close to that of the massive colonies, we added the encrusting corals to the massive group. A comparison between results of 10 m-transects and the image-derived data from GEOMAR-transect shows a very good coorespondence of coral coverage data at 20 m and 30 m depth (difference ± 3–5 %). In a depth of 10 m and 15 m values of 10 m-transects are ca. 25% lower than photo-derived results. Thus there is indication for an overestimation of coverage data derived from photo-transects. The difference is almost exclusively due to a difference in the assessment of branching corals, thus the potential error becomes smaller in areas with a greater portion of massive corals.
In Table 8.10 surface coverage data for the GEOMAR-transect are listed. Coral coverage is highest at the reef crest and in parts of the middle and deeper fore reef. Very low coverage was observed in the reef flat, the upper fore-reef and sand channel (Fig. 8.10). Branching corals cover 20 % of the reef area, massive and encrusting forms ca. 14.5 %. Total scleractinian area is ca. 35 % of the reef area from the reef crest to a depth of 36 m, with a maximum of ca. 50 % in the middle fore-reef. In front of the reef crest a sand flat is developed with only scattered coral growth. Soft corals, which generally do not contribute to the carbonate production, cover ca. 10 % of the reef surface (up to 20 % in the deeper fore reef). Dead coral rock shares great percentage of area at the reef crest and in the middle and deeper fore-reef (>50 %). In general, the portion of living and carbonate producing corals is relatively high at the reef crest, low at the reef flat and in the upper fore-reef and increases to the middle fore-reef (Fig. 8.10).

Gross production at the GEOMAR-transect is highest at depths of ca. 2-3 m at the reef crest, due to high growth rates, and in a depth of ca. 10-15 m as a result of high coral coverage of the reef bottom (Fig. 8.11). A deeper maximum is reached at a depth of 23-26 m, where massive corals reach their highest productivity level, again due to the high coverage (34% of reef surface, Fig. 8.10, Tab. 8.10). The productivity of

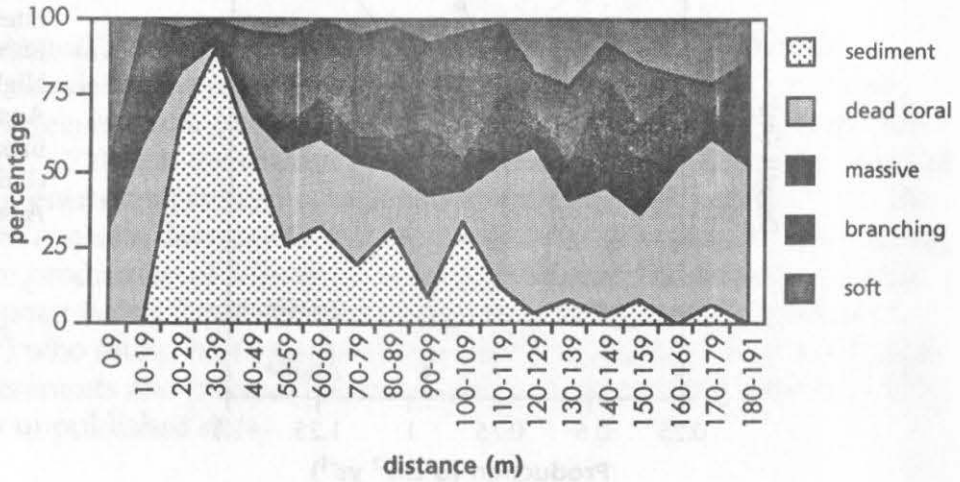

Figure 8.10 Surface area coverage obtained from photo-transects at the GEOMAR-transect at the Marine Science Station reef.

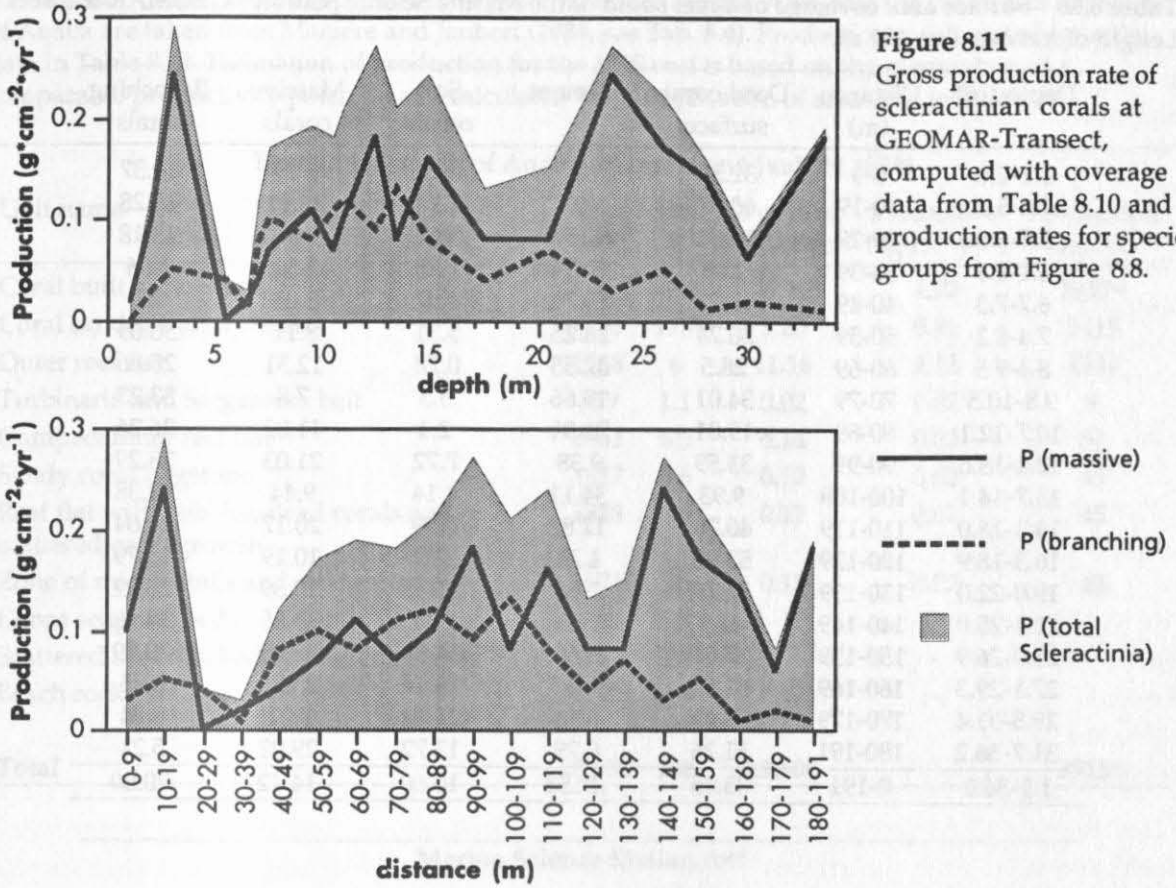

Figure 8.11
Gross production rate of scleractinian corals at GEOMAR-Transect, computed with coverage data from Table 8.10 and production rates for species groups from Figure 8.8.

branching corals is highest in the upper fore-reef from 7 to 15 m, and decreases then continuously with depth (Fig. 8.11, Tab. 8.11). In contrast, massive and encrusting corals have a productivity maximum at the reef crest and in the depth from 20-25 m (Fig. 8.11) which is caused by the increase in coverage to a third of the reef area (Fig. 8.10).

Application of results to reef area data of Maniére and Jaubert (1984) and Marine Science Station reef

In order to get an estimate of the total gross carbonate production of the entire Marine Science Station reef we calculated the gross production for reef zones comparable to those mapped by Maniere and Jaubert (1984, see Tab. 8.4) with the reef area of the Marine Science Station reef.

The surface area of the reef part computed by Maniere is 32,000 m^2. The reef part where our investigations were performed has a greater area of ca. 260,000 m^2 (length ca. 1000 m, reef flat width ca. 60 m, fore reef width ca. 200 m). Calculated with the production rate of the different reef zones the gross production of scleractinian corals at the Marine Science Station reef is ca. 302,000 $kg \cdot yr^{-1}$ (Tab. 8.12). The greatest part of gross production derives from the reef slope (86 % of carbonate production on 48 % of the area), another 13 % from coral sand areas, ca. 1 % from the outer reef flat and less than 0.5 % from the reef flat to the beach rock zone.

Table 8.10 Surface area coverage of a reef south of the Marine Science Station ("GEOMAR-transect"). Length of transect line 191 m.

Depth (m)	Distance (m)	Dead coral surface	Sediment	Soft corals	Massive corals	Branching corals
1.1-2.0	0-9	32.35	0	47.99	9.29	10.37
1.4-5.4	10-19	60.57	0	1.24	22.91	15.28
5.5-6.0	20-29	16.64	66.57	3.61	0	13.18
6.1-6.6	30-39	2.03	90.31	1.25	2.34	4.06
6.7-7.3	40-49	12.21	55.71	4.07	5.01	23
7.4-8.2	50-59	30.24	26.25	5.31	8.11	30.09
8.4-9.5	60-69	28.5	32.55	0.78	12.31	25.86
9.8-10.5	70-79	34.01	19.66	5.3	7.8	33.23
10.7-12.1	80-89	19.01	31.31	2.4	11.02	36.26
12.4-13.6	90-99	33.59	9.38	7.72	21.03	28.29
13.7-14.1	100-109	9.93	34.11	4.14	9.44	42.38
14.3-16.0	110-119	40.78	12.82	1.59	20.17	24.64
16.3-18.9	120-129	53.92	4.23	17.87	10.19	13.79
19.0-22.0	130-139	32.79	7.94	22.35	10.59	26.32
22.1-25.0	140-149	42.9	2.65	8.11	33.85	12.48
25.0-26.9	150-159	27.61	8.66	14.71	28.43	20.59
27.1-29.3	160-169	52.56	0	18.14	23.26	6.05
29.5-31.4	170-179	54.69	6.14	21.12	9.21	8.84
31.7-36.2	180-191	51.26	0.79	13.72	29.02	5.21
1.1-36.2	0-191	33.45	21.53	10.60	14.42	20.00

		Production $g \cdot cm^{-2} \cdot yr^{-1}$		
depth	distance (transect)	massive	branching and encrusting	total scleractinia
reef flat (Mergner 1979)		0.02	0.00	0.02
1-3 m	0-9	0.10	0.03	0.13
1-5 m	10-19	0.24	0.05	0.29
5-6 m	20-29	0.00	0.04	0.04
6-7 m	30-39	0.02	0.01	0.03
7 m	40-49	0.04	0.08	0.12
7-8 m	50-59	0.07	0.10	0.17
9-10 m	60-69	0.11	0.08	0.19
10-11 m	70-79	0.07	0.11	0.18
10-12 m	80-89	0.10	0.12	0.21
12-13 m	90-99	0.18	0.09	0.27
13-14 m	100-109	0.08	0.13	0.21
14-16 m	110-119	0.16	0.08	0.24
16-19 m	120-129	0.08	0.04	0.13
19-22 m	130-139	0.08	0.07	0.15
22-25 m	140-149	0.24	0.03	0.27
25-27 m	150-159	0.17	0.05	0.22
27-29 m	160-169	0.14	0.01	0.16
29-31 m	170-179	0.06	0.02	0.08
31-36 m	180-191	0.18	0.01	0.19

Table 8.11
Summary of coral gross production rates for GEOMAR-transect at the reef at the Marine Science Station Aqaba.

Table 8.12 Gross carbonate production by scleractinia at Aqaba. Area data for the reef 12 km south of Aqaba are taken from Maniére and Jaubert (1984, see Tab. 8.4). Production is calculated from the data in Table 8.11. Estimation of production for the MSS reef is based on the assumption of a comparable productivity potential and calculated by multiplication of area data (see text).

Reef 12 km south of Aqaba (Maniére and Jaubert 1984)					
Unit name	Area (m^2)	Area %	% of total production	Production ($kg \cdot m^{-2} \cdot yr^{-1}$)	Production (kg/yr)
Coral built outer slope	15292	47.8	79.12	1.92	29379
Coral sand (sandy spreads)	3746	11.7	9.20	0.91	3415
Outer reef flat	1948	6	11.16	2.13	4144
Turbinaria and Sargassum belt	359	1.1	0.02	0.02	9
Compact inner reef flat	2061	6.5	0.14	0.02	51
Sandy coral flagstone	1817	5.6	0.12	0.02	45
Reef flat with pebbles, dead corals and scattered coral growth	1818	5.6	0.12	0.02	45
Zone of micro-atolls and sandy pockets	1671	5.3	0.11	0.02	42
Dense seagrass beds	1841	5.8		-	
Scattered seagrass beds and green algae	1163	3.8		-	
Beach rock	258	0.8		-	
Total	**31974**	**100**	**100.00**		**37130**

Marine Science Station reef					
Reef unit	Area (m^2)	Area %	% of total production	Production ($kg \cdot m^{-2} \cdot yr^{-1}$)	Production (kg/yr)
Reef slope (fore-reef)	124280	47.8	79.12	1.92	238617
Coral sand (upper fore-reef)	30420	11.7	9.20	0.91	27682
Outer reef flat	15600	6	11.16	2.13	33228
Inner reef flat	62660	24.1	0.51	0.02	1253
Total	**232960**	**89.6**	**99.99**		**300780**

Discussion

The decrease of extension rates with depth is shown at our reference genus *Porites* . The same relation is valid for most of the reef-building scleractinia (Highsmith 1979; Hubbard and Scaturo 1985; Huston 1985). The degree of this decrease is different between species (Buddemeier and Kinzie 1976), and some specially adapted species have their growth maximum at deeper reef areas (e.g. *Leptoseris*). However, the relationship between different corals and depth is known for some genera and can be used to estimate the decrease of other scleractinians. Even though the actual growth rate in relation to depth has been determined in our study only for *Porites* we assume that the degree of calcification decrease can be applied to other hermatypic corals with the above mentioned correction. These corrections may be subject to changes in the future, as soon as more data on other reef-building corals are determined.

The major benefits of CT-examination are twofold; firstly, the optimum "cut" for evaluating the width of the growth-bands can easily be defined since multiple slices are taken. Secondly, besides low- and high-density growth-bands, the overall density along the growth direction is appreciably lower than in adjacent areas; therefore, the "blind" cutting of cubes from a coral might give misleading results that can be avoided by visual control of the volume in which the density is measured.
CT greatly simplifies the measurements of age, thickness of growth-bands and density of corals without a need to destroy the specimen. The visual control of the sampled volumes helps to reduce sampling errors. Despite the fact that CT has a lower spatial resolution than a conventional X-ray image taken from a coral physically cut in slices, the resulting image is of more than sufficient quality.

The relation between depth and density in scleractinian corals is ambiguous. The increase in density with increasing depth found in *Porites* at Aqaba is consistent with the results of Bosscher (1992) in *Montastrea annularis* from the Caribbean, but in contrast to the observations of Guillaume and Carrio-Schaffhauser (1985), who found no significant relation between depth and density (1.17 $g \cdot cm^{-3}$ ±0.17) over a depth range from 0.6 to 40 m for *Porites lutea* from Réunion Island. Buddemeier et al. (1974) found no systematic change of density with depth for several coral species at Eniwetok. Hughes (1987) reported from Jamaica an increase in density for *Agaricia agaricites* and *M. annularis* but no significant changes for *Porites astreoides, Leptoseris cucullata* and *Agaricia* spp.

The productivity of a coral can be related to the area by multiplicating its linear extension rate with the skeleton density. The result is the potential production (or calcification rate) of this coral. Mean potential production of *Porites* in shallow water at Aqaba (0.94 $g \cdot cm^{-2} \cdot yr^{-1}$) is comparable with production rates reported by Grigg (1982) from reefs at a latitude of 25-26°N. The northernmost reefs of the Hawaiian chain at 29°N had potential production of 0.5 $g \cdot cm^{-2} \cdot yr^{-1}$. This shift of carbonate production potential to the North in the Red Sea is in agreement with the finding of Mergner and Schuhmacher (1985), derived from analysis of species composition, that the reefs of Aqaba are not at the northern limit of reef development.
To evaluate the potential production of the reef at Aqaba in different depth zones, we computed mean values (Fig. 8.8). These were later used in combination with coverage data from the GEOMAR-Transect to determine gross production. Production potential data are most reliable for massive growing corals, because they are relatively close in their variations to the reference genus *Porites* (Tab. 8.6). From the above mentioned close relations between colony radius increase in branching corals and the growth of massive hemispherical corals (Buddemeier and Kinzie 1976), we are confident that the values for branching corals are in the range of the actual production rates. Most vulnerable are the calculations for the encrusting species. As no rates on the actual growth rates of most of these species are known, we assumed similar values to morphological similar groups (e.g. *Pavona - Stylophora*). However, the coverage of these corals at the shallow part of the reef is lower than at the deeper parts (ca. one third of the scleractinian coverage at 10 m). At a depth of 20 m encrusting corals occupy ca. two thirds of the total scleractinia coverage (22% of the reef area). This leads to an increase of the potential error with depth.

The decrease in carbonate production rate with depth has been shown at Eniwetok (Highsmith 1979). There three scleractinian species (*Porites lutea, Goniastrea retiformis,* and *Favia pallida*) were studied over a depth range from 0 to 30 m. The decrease in production is different for the three species studied, and is almost linear for each species (Fig. 8.12). *P. l utea* and *G. retiformis* show production rate of ca. 1.2g·cm^{-2}·yr^{-1}, in shallow depth and a strong decrease to ca. 0.8 g·cm^{-2}·yr^{-1} below 20m. *F. pallida* has a production rate of 0.9 g·cm^{-2}·yr^{-1} in 2 m depth and decreases to 0.75 g·cm^{-2}·yr^{-1} at 25 m depth. It is important to note, that the production rates for Eniwetok were calculated with a constant density for each species. The data provided by Highsmith (1979) did not differentiate changing density in deeper water.
The study of growth rates and calcification of *Montastrea annularis* at Curaçao showed a non-linear (hyperbolic tangent) relation between depth and calcification (Bosscher 1992). This is in contrast to our results which indicate a linear relationship of calcification with depth (Fig. 8.7). Bosscher relates the non-linear decrease of growth and calcification to the depth of light saturation (ca. 15 m in the Caribbean). The difference to more gradual growth rate changes with depth of *Porites lutea* from Eniwetok (Buddemeier et al. 1974; Highsmith 1979) was explained by the greater transparency of seawater at Eniwetok. This explanation can only partly help to understand the pattern at Aqaba. The decrease of growth rate is rather exponential (Fig. 8.5) than gradual (Eniwetok) or hyperbolic (Curaçao). The transparency of Red Sea water is generally very high (Reiss and Hottinger 1984), resulting in the occurrence of corals to a depth of 130 m (Fricke and Schuhmacher 1983). However, the abundant coral growth in the Gulf of Aqaba occurs in the upper 30 m of the water column and the growth in depths below 10 m is lower than at Eniwetok. The strong seasonality at Aqaba might be the reason for the exponential decrease of growth. The effect of temperature is similar in all depth, but the amount of light

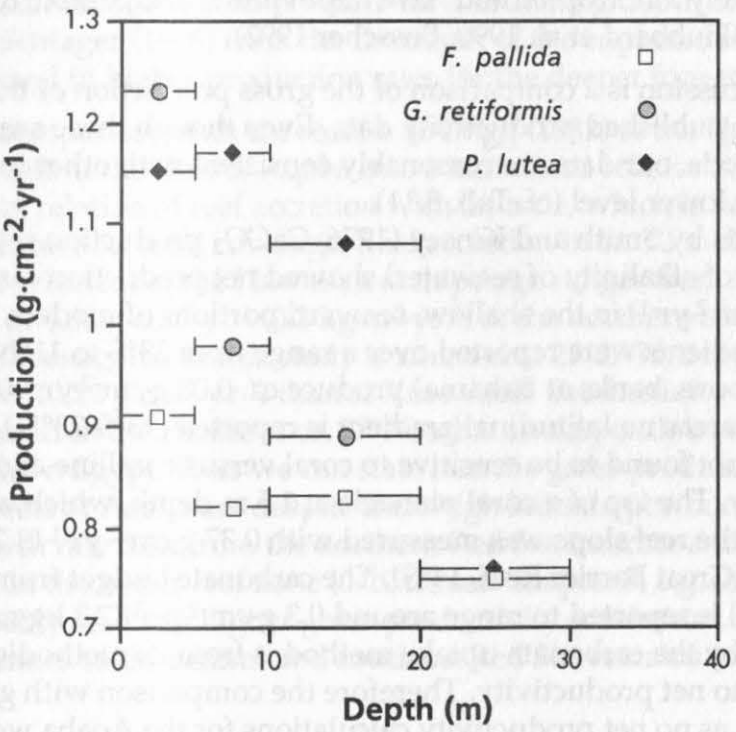

Figure 8.12
Carbonate production rates from Eniwetok for three scleractinian species. Production rates are calculated from linear extension rate (taken from Fig.2, Highsmith 1979) multiplied by mean density for all samples.

penetrating the water surface is dependent on the angle of incidence. This angle is lower in winter and time of sun high stand is reduced, as well as the total radiation during the day. Hence, the amount of light reaching corals in intermediate depth is more reduced in winter and the light saturation zone is smaller. This seasonal shift of the light saturation zone might be responsible for the non-existence of a discrete boundary of light-saturated coral growth as observed in the Caribbean. A similar pattern is present in the results of Logan and Tomascik (1991, Fig. 2; *Porites astreoides*). At Bermuda their plot indicates an exponential decrease of growth with depth (r^2=0.60), while the plot of growth rates at Jamaica indicates a decrease similar to the pattern described by Bosscher (1992) at Curaçao. Logan and Tomascik (1991) did not point out this pattern and computed an exponential correlation resulting in a lower correlation (r^2=0.48).
Calcification rates of *Porites lobata* at the Tiahura barrier reef flat at Moorea, French Polynesia are reported with 0.8 $g \cdot cm^{-2} \cdot yr^{-1}$ (8 $kg \cdot m^{-2} \cdot yr^{-1}$), measured with the carbonate uptake method (Le Campion-Alsumard et al. 1993), and 1.3 $g \cdot cm^{-2} \cdot yr^{-1}$ (13 $kg \cdot m^{-2} \cdot yr^{-1}$; Guillaume 1990), very close to our results for shallow water *Porites* (0.94 $g \cdot cm^{-2} \cdot yr^{-1}$). Compared with calcification of *Porites lobata* at the Hawaiian chain from 1.8 $g \cdot cm^{-2} \cdot yr^{-1}$ (18 $kg \cdot m^{-2} \cdot yr^{-1}$) to 0.5 $g \cdot cm^{-2} \cdot yr^{-1}$ (5 $kg \cdot m^{-2} \cdot yr^{-1}$, potential production at Aqaba lies between the extremes.

The potential production of *Porites* was taken as the standard for the changes in carbonate production with depth at Aqaba. Colonies of this genus appear over the complete depth range from the reef-flat to the lower fore-reef down to 50 m and deeper. They grow in almost all habitats of the coral reef and growth rates can be determined relatively easy. The assumption that other scleractinian species and photosynthetic carbonate producers (like *Halimeda*) react similarly to changing environmental conditions may lead to errors. However, as long as the data base for these organisms is in its beginning, this method seems to provide reasonable results, as coralline algae are completely autotrophic and have depth limits comparable to those of reef-building corals (Hubbard et al. 1990; Bosscher 1992).

The following part of the discussion is a comparison of the gross production of the reef under investigation with published productivity data. Even though these are obtained with different methods, our data are reasonably consistent with other reef areas, however at a generally lower level (cf. Tab. 8.11).
Production rate measurements by Smith and Kinsey (1976; $CaCO_3$ production rate determined by the reduction of alkalinity of seawater) showed net production rates of about 0.4 $g \cdot cm^{-2} \cdot yr^{-1}$ (4 $kg \cdot m^{-2} \cdot yr^{-1}$) in the shallow, seaward portions of modern coral reefs. No latitudinal gradients were reported over a range from 23°S to 11°N. Protected environments (lagoons, banks at Bahama) produce ca. 0.08 $g \cdot cm^{-2} \cdot yr^{-1}$ (0.8 $kg \cdot m^{-2} \cdot yr^{-1}$). As well in these areas no latitudinal gradient is reported (23°S-25°N). The $CaCO_3$ production was not found to be sensitive to coral versus coralline algal dominance of the community. The top of a coral pinnacle at 1.5 m depth, which was assumed to be equivalent to the reef slope was measured with 0.37 $g \cdot cm^{-2} \cdot yr^{-1}$ (3.7 $kg \cdot m^{-2} \cdot yr^{-1}$) at Lizard Island (Great Barrier Reef, 14°S). The carbonate budget from Tiahura barrier reef (Moorea) is reported to range around 0.3 $g \cdot cm^{-2} \cdot yr^{-1}$ (2-3 $kg \cdot m^{-2} \cdot yr^{-1}$). The budget evaluation by the carbonate uptake method is from its methodic approach an approximation to net productivity. Therefore the comparison with gross productivity data is difficult, as no net productivity calculations for the Aqaba were

carried out yet. However, the fact that gross production at Aqaba is similar in a comparable depth (ca. 0.29 $g \cdot cm^{-2} \cdot yr^{-1}$, Tab.8.11), and bioerosion will reduce this value, leads to the conclusion that the reef at Aqaba has probably a production rate clearly below the above mentioned values.

Most studies measured productivity in shallow water, therefore our data for reef crest (0.29 $g \cdot cm^{-2} \cdot yr^{-1}$) and the upper and middle fore-reef are relevant for comparison. However, even at the lower fore-reef (below 14 m depth) mean gross production by corals at Aqaba has still a remarkably high value (0.18 $g \cdot cm^{-2} \cdot yr^{-1}$).
Carbonate production by organisms in the Caribbean at Cane Bay, St. Croix, was determined with similar methods and reported as 0.121 $g \cdot cm^{-2} \cdot yr^{-1}$ (1.21 $kg \cdot m^{2} \cdot yr^{-1}$). The greatest part (95 % = 0.115 $g \cdot cm^{-2} \cdot yr^{-1}$) was produced by corals (Hubbard et al. 1990). These data were obtained over the same depth range as in our study. For the entire reef we calculated mean coral gross production with 0.165 $g \cdot cm^{-2} \cdot yr^{-1}$ (1.65 $kg \cdot m^{-2} \cdot yr^{-1}$). The different morphology at Cane Bay, where a broad nearshore zone with high sediment coverage exists, might cause the lower total reef production at St. Croix.
Detailed productivity rates of reef areas at Cane Bay were calculated by Sadd (1984) and are in good accordance with the data from Aqaba. The data of the comparison are given in $g \cdot cm^{-2} \cdot yr^{-1}$. Hardground (-2 to -6 m): 0.12, Aqaba 0.14. Shallow reef (-5 to -8 m): 0.31, Aqaba 0.09. Coral gardens (-6 to -20 m): 0.5, sand flat and slope (-6 to -20 m): 0.085, what gives an average for the depth zone 6-20 m of 0.29. At Aqaba this depth range has a production of 0.17 $g \cdot cm^{-2} \cdot yr^{-1}$. In the deep reef (-20 to -32 m) the production at Aqaba is higher (0.18 compared to 0.10 $g \cdot cm^{-2} \cdot yr^{-1}$). The main differences are the higher rates in the intermediate depth zone at St. Croix, in the shallow zone production is similar and at greater depth the productivity at Aqaba is much higher (0.18 $g \cdot cm^{-2} \cdot yr^{-1}$).This is probably an effect of the different reef morphology and the deep euphotic zone in the Gulf of Aqaba. The high transparency of water in the Gulf of Aqaba is responsible for a drowning depth of ~50 m, assumed by Hallock and Schlager (1986) from the the depth of the euphotic zone. This seems to be reflected in higher production rates for the deeper fore-reef found in this study.

The comparison with the results of Grigg (1982) at the Hawaiian chain shall integrate the reefs at the Gulf of Aqaba into a latitudinal relation. Grigg´s studies revealed a strong relation of reef accretion with latitude, which is dependent both on colony accretion and coral coverage. Reef accretion in ca. 10 m depth (where Grigg´s stations were selected) at the Hawaiian archipelago ranges from 1.5 $g \cdot cm^{-2} \cdot yr^{-1}$ (15 $kg \cdot m^{2} \cdot yr^{-1}$) to 0.03 $g \cdot cm^{-2} \cdot yr^{-1}$ (0.3 $kg \cdot m^{2} \cdot yr^{-1}$) at the northern end at Kure Atoll (29°N). The reef investigated in this study is situated at 29°27´N, but productivity is strikingly higher (0.22 $g \cdot cm^{-2} \cdot yr^{-1}$) than at Kure Atoll. Productivity of this range would be expected in the Pacific at ca. 27°N, what corresponds in the Red Sea to latitudes of southern Egypt. Thus we can state that the gross productivity values indicate that the reefs at Aqaba are despite their high latitude position not at the limit of existence. Growth rate data from the northern Red Sea indicate a higher potential production at least in the upper reef zone (0-10 m; see Chapter 5, e.g. Fig. 5.10). This might probably lead to a higher gross productivity southward. Whether this trend continues to the central and southern Red Sea remains to be studied.

The gross production by corals seems to be a good estimate for the net accretion of reefs (Grigg 1982). The growth rate of massive head corals like *Porites* and *Montastrea* agrees well with Holocene reef accretion rates (maximum ca. 12 mm·yr^{-1}, for an overview see Bosscher 1992). The mean growth rate of *Porites* at Aqaba can therefore be assumed as the maximum growth potential for the reefs in the Gulf of Aqaba. The average sea level rise during the Holocene transgression between 15,000 and 6,000 yBP was about 14 mm·yr^{-1} (Chappell 1974; Adey 1978). However, this rise was far from being constant. Meltwater pulses and/or redistribution of water masses due to spatial changes in the Earth's geoid (Eisenhauer et al. 1993) resulted in rapid changes of sea level, which probably could not be tracked by coral reefs. In the central Red Sea reef growth started 6,000 years ago (Braithwaite 1982), when the rise of sea level moderated considerably. Estimates for the Pacific give an average value of 0.33 mm·yr^{-1} (Chappell 1974; Adey 1978). Eisenhauer et al. (1993) report a moderate sea level rise by 3.2 mm·yr^{-1} at the Houtman Abrolhos Islands (western continental margin of Australia) from 8,200 yBP to 6,300 yBP, when sea level reached a highstand above its present height in the southern oceans. As the present mean coral growth rate for the upper 5 m is 8.4 mm·yr^{-1} at Aqaba, this is more than enough. Even if we consider a sea level highstand in the Red Sea ca 3,000 years ago (0.5 m above present sea level), the required accretion rate of 2 mm·yr^{-1} for a keep-up reef is present.

The challenge of establishing an estimation of gross productivity for the complex system of a coral reef suffers from many possibilities for inaccuracy. These are for example: the assessment of growth rates: Sampling cannot be really random. Collected corals are taken were they grow, greater corals on the surface of the reef are preferentially sampled. Assessment of the coverage of the reef by the various carbonate producers is influenced by the method which is used. Further questions arise regarding the calculations of production rates: Is *Porites* productivity representative for all corals, and how strong does the obviously different growth pattern of depth-adapted corals like *Leptoseris* and *Madracis* (Fricke and Hottinger 1983; Fricke and Knauer 1986; Schlichter et al. 1986) contribute to the budget? Is the contribution of coralline algae, Octocorallia and other carbonate producing organisms like *Sinularia* (alcyonaria, soft coral), echinoderms etc. really negligible? Despite these and other problems the results of this study are reasonably well consistent with the results from other reef areas. However, when looking at the presented data, the reader should ever keep in mind the high variability in the reef ecosystem and the fact that all quantitative approaches to a reef can only provide rough estimates of the actual condition.

For further studies the improvement of the methods is suggested. Growth rate and density relationship with depth for other major reef-building corals and the assessment of bottom coverage of the reef are the most crucial factors in production evaluation. For reasons of comparison between reefs over the world methods should be standardized in a way that the production of reefs can be estimated in short time and without highly developed technologies. We believe that our approach to the problem can provide the base of such a method.

CONCLUSIONS

Coral growth and carbonate production

Coral growth is influenced by numerous environmental variables, whereby the importance of each factor is changing in space and time (Chapter 2 and 3). Thus carbonate production is far from a constant level over the centuries. A very important variable affecting gross carbonate production of a reef is the coverage with carbonate producing organisms. Long-term studies on coral communities have shown high dynamic in the bottom coverage (e.g. Mergner 1979; Schuhmacher et al. 1993). Thus, the estimation of gross carbonate production can only provide a snap shot of geologically relevant patterns. This is illustrated by the fact that the greatest part of coral growth data in this study are obtained from samples with growth bands deposited in the last two decades. In that time, however, exceptionally high growth rates occured, as we see from the long-term record of the "giant" *Porites* -colony (Chapter 3 and 4). This might lead to an overestimation of coral carbonate production. Without this long growth record the present favourable conditions for coral growth would have been assumed to be normal. Or, even more critical, considering the modern anthropogenically induced environmental changes (see Chapter 4) we would have assumed that we observed a relatively detrimental stage of reef development. A negative effect of environmental changes seems not to be present for the reef at the Marine Science Station, however short disturbances occurred in the last decades (Chapter 2 and 3). So, more long-term records are needed to evaluate the present-day carbonate production.

Climate influence on coral growth and carbonate production

Sea surface temperature in the northern Gulf of Aqaba seems to have varied strongly during the last two centuries (Chapter 4). A regional warming of surface seawater might have been as high as ca 2°C. This seems to have influenced coral growth positively. A further warming, which is expected from the greenhouse effect, would probably not lead to deleterious effects on coral growth in the Gulf of Aqaba. The present temperature range of 18°C to 28°C is in the lower range of optimal coral growth. Decrease of coral growth occurs in most species beyond 30°C, hence a further increase of water temperatures would rather enhance coral growth and carbonate production, by shortening the period of slow coral growth in winter. The increase of coral growth towards the central Red Sea can be attributed to such conditions (Chapter 5). Of course, other effects of climate change, like cloudiness, precipitation, storms, or changes in the ocean current system, also might modify the temperature effect.

Holocene accretion rate

If we compare the results of our study with the excellent study of Hubbard et al. (1990), we find a higher total carbonate production at Aqaba than at St. Croix in the Caribbean, despite the higher latitude and the lower potential production and lower gross production in most depth zones. This difference results mainly from the different morphology of the shelf edge. Low-productive sediment-covered areas have a higher share of reef area at Cane Bay, St. Croix, while the relatively high-productive zone at Aqaba occupies a great area of the reef. From the gross carbonate production of 1.21 $kg \cdot m^{-2} \cdot yr^{-1}$ about 75 % is permanently retained in the reef at Cane Bay and contributes to net production and reef accretion. Rate of reef accretion rate over the past 3,000-5,000 years at St. Croix was estimated by Hubbard et al. (1990) from core data as 0.73 m/ky. Applying these results to the reefs at Aqaba, assuming a comparable percentage of export carbonate, a similar ratio between net production and reef accretion rate, and constant productivity, a net production of ca. 1.24 $kg \cdot m^{-2} \cdot yr^{-1}$ and a reef accretion rate of 0.99 m/ky at Aqaba over the last 6000 years is estimated. Investigating the reef at the Marine Science Station, which serves as a good example for the reefs in the northern Gulf of Aqaba, we observed a maximum height of the reef wall of 5 to 6 m. This fits remarkably well to the forementioned accretion rate and indicates that our estimations of productivity are fairly reasonable.

Application to fossil reefs

With the investigation of fossil reef corals the reconstruction of fossil climate (see Chapter 6) is possible. Temperature and precipitation can be reconstructed, and the effect on growth rate and carbonate production determined. The chance of an application of productivity calculations combined with quantitative analysis of ancient reefs (Weidlich et al. 1993) might improve comparative reef research. The assessment of the production potential of fossil reef builders and the implications for reef accretion might help to reveal the reasons for the drowning of reefs.

ACKNOWLEDGEMENTS

MAIN ADVISOR	Prof. Dr. Wolf-Christian Dullo
SECOND ADVISOR	Prof. Dr. Priska Schäfer

There are a large number of friends and colleagues who I thank for their help in field work, analysis of samples, and critical reading of the manuscripts. I would especially like to thank Chris Dullo, John J.G. Reijmer, Michael Joachimski, and Bill Kiene. However, without the help of the people and institutions mentioned below, the completion of this dissertation would not have been possible.

I wish especially to thank: Moshira Hassan, Corinna Hoffmann, Daniela Gerstner, Andrea Perl, Elja de Vries, Peter Emmermann, Marcus Ramm, Ralf Tiedemann, Chris Wold, and Rainer Zahn at GEOMAR.

Wilma Rehder and Wolfgang Reimers (Geologisch-Paläontologisches Institut an der Universität Kiel), Andreas Fink (Institut für Radiologische Diagnostik an der Universität Kiel) and Richard Cember (Northeast Regional Climate Center, Cornell University) assisted with sample preparation, X-radiography, and CT.

I thank Helmut Schuhmacher, Dieter Kroll, and Goetz-Bodo Reinicke (Institut für Ökologie, Universität Essen) for their help. Climate data were provided by the Deutscher Wetterdienst Hamburg. Marco Taviani (Istituto di Geologia Marina, Bologna), Lucien Montaggioni (C.N.R.S. Université de Provence, Marseille), Sabine Böhler (Geologisch-Paläontologisches Institut an der Universität Kiel), and the crew of the "Ernesto Leoni", Renato Marchesan, Christina Pulliero and Ilaria, made fieldwork at Egypt a pleasure.

Field work at Aqaba was made possible by the Universities of Jordan (Amman) and Yarmouk. The staff of the Marine Science Station, Nigem Yussuf, Anne-Marie and Jan-Erik Buer, Kirk J. Green, and the other Hush-people took care of logistical and social support.

I wish to thank the GEOMAR for the use of its facilities and the DFG (Deutsche Forschungsgemeinschaft) for financing the research activities. Field work was partly supported by the EC programme RED SED. This thesis is part of the DFG-Projekt Du 129/4 "Biogene und abiogene Steuerungsprozesse der holozänen Karbonatproduktion im Roten Meer" in the DFG-Schwerpunktprogramm "Globale und regionale Steuerungsprozesse biogener Sedimentation".

REFERENCES

Abu Hilal, A.H. (1985): Phosphate pollution in the Jordan Gulf of Aqaba.- Marine Pollution Bulletin, **16/7:** 281-285.

Adey, W. (1978): Coral reef morphogenesis: A multidimensional model.- Science, **202:** 831-837.

Adey, W. and Vasser, J.M. (1975): Succession and accretion rates in Caribbean crustose corallines.- Phycologia, **14:** 55-70.

Aharon, P. (1991): Recorders of reef environment histories: stable isotopes in corals, giant clams, and calcareous algae.- Coral reefs, **10/2:** 71-90.

Al-Rifaiy, I.A. and Cherif, O.H. (1988): The fossil coral reefs of Al-Aqaba, Jordan.- Facies, **18:** 219-230.

Andres, W. and Radtke, U. (1988): Quartäre Strandterrassen an der Küste des Gebel Zeit (Golf von Suez/ Ägypten).- Erdkunde, **42:** 7-16.

Baker, P.A. and Weber, J.N. (1975): Coral growth rate: variation with depth.- Earth and Planetary Science Letters, **27:** 57-61.

Barnes, D.J. and Lough, J.M. (1989): The nature of skeletal density banding in scleractinian corals: fine banding and seasonal patterns.- Journal of Experimental Marine Biology and Ecology, **126:** 119-134.

Bosence, D.W. (1988): Carbonate budgets for carbonate mounds, Florida, USA.- 6th International Coral Reef Symposium Australia, **2:** 529-534.

Bosence, D.W.J., Rowlands, R.J. and Quine, M.L. (1985): Sedimentology and budget of a recent carbonate mound, Florida Keys.- Sedimentology, **32:** 317-343.

Bosscher, H. (1992): Growth potential of coral reefs and carbonate platforms.- PhD thesis, Vrije Universiteit Amsterdam.

Bosscher, H. (1993): Computerized tomography and skeletal density of coral skeletons.- Coral Reefs, **12/2:** 97-103.

Bosscher, H. and Schlager, W. (1992): Computer simulation of reef growth.- Sedimentology, **39:** 503-512.

Bouchon, C. (1980): Quantitative study of the scleractinian coral communities of the Jordanian coast (Gulf of Aqaba, Red Sea): preliminary results.- Tethys, **9/3:** 243-246.

Bouchon, C., Jaubert, J., Montaggioni, L. and Pichon, M. (1981): Morphology and evolution of the coral reefs of the Jordanian coast of the Gulf of Aqaba (Red Sea).- Proceedings of the Fourth International Coral Reef Symposium Manila, **1:** 559-565.

Braithwaite, C.J.R. (1982): Patterns of accretion of reefs in the Sudanese Red Sea.- Marine Geology, **45:** 297-325.

Brown, B., Le Tissier, M., Howard, L.S., Charuchinda, M. and Jackson, J.A. (1986): Asynchronous deposition of dense skeletal bands in *Porites lutea*.- Marine Biology, **93:** 83-89.

Buddemeier, R.W. and Kinzie, R.A. (1976): Coral growth.- Oceanogr. Mar. Biol. Ann. Rev., **14:** 183-225.

Buddemeier, R.W., Maragos, J.E. and Knutson, D.W. (1974): Radiographic studies of reef coral exoskeletons: rates and patterns of coral growth.- Journal of Experimental Marine Biology and Ecology, **14:** 179-200.

Burke, R.B., Adey, W.H. and Macintyre, I.G. (?): Overview of the holocene history, architecture, and structural components of Tague Reef and Lagoon.- In: Hubbard, D.K. (ed.): Terrestrial and Marine Geology of St. Croix, U.S. Virgin Islands. Special Pub., **8:** 105-109; Teague Bay, St. Croix, U.S.V.I. (West Indies Laboratory).

Carriquiry, J.D., Risk, M.J. and Schwarcz, H.P. (1988): Timing and temperature record from stable isotopes of the 1982-1983 El Niño warming event in Eastern Pacific corals.- Palaios, **3:** 359-364.

Cember, R.P. (1988): On the sources, formation, and circulation of Red Sea deep water.- Journal of Geophysical Research, **93/C7:** 8175-8191.

Chalker, B., Barnes, D. and Isdale, P. (1985): Calibration of x-ray densitometry for the measurement of coral skeletal density.- Coral Reefs, **4/2:** 95-100.

Chalker, B.E. and Barnes, D.J. (1990): Gamma densitometry for the measurement of skeletal density.- Coral Reefs, **9/1:** 11-23.

Chalker, B.E., Barnes, D.J., Dunlap, W.C. and Jokiel, P.L. (1988): Light and reef-building corals.- Interdisciplinary Science Reviews, **13:** 222-237.

Chappell, J. (1974): Relationship between sea levels, ^{18}O variations and orbital perturbations during the last 250,000 years.- Nature, **252:** 199-202.

Charpy-Roubaud, C.J. (1988): Production primaire des fonds meubles du lagon de Tikehau (atoll des Tuamotu, Polynésie française).- Oceanologica Acta, **11/3:** 241-248.

Chave, K., Smith, S. and Roy, K. (1972): Carbonate production by coral reefs.- Marine Geology, **12:** 123-140.

Chiappone, M. and Sullivan, K.M. (1991): A comparison of line transect versus linear percentage sampling for evaluating stony coral (*Scleractinia* and *Milleporina*) community similarity and area coverage on reefs of the central Bahamas.- Coral Reefs, **10/3:** 139-154.

Cole, J.E. and Fairbanks, R.G. (1990): The Southern Oscillation recorded in the $\delta^{18}O$ of corals from Tarawa Atoll.- Paleoceanography, **5:** 669-683.

Cole, J.E., Fairbanks, R.G. and Shen, G.T. (1993): Recent variability in the southern oscillation: isotopic results from a Tarawa atoll coral.- Science, **260:** 1790-1793.

Cortés, J. and Risk, M.J. (1985): A reef under siltation stress: Cahuita, Costa Rica.- Bulletin of Marine Science, **36/2:** 339-356.

Craig, H. (1957): Isotopic standards for carbon and oxygen and correction factors for mass spectrometric analysis of carbon dioxide.- Geochimica et Cosmochimica Acta, **12:** 133-140.

Craig, H. (1966): Isotopic composition and origin of the Red Sea and Salton Sea Geothermal Brines.- Science, **154:** 1544-1548.

Crossland, C.J., Hatcher, B.G. and Smith, S.V. (1991): Role of coral reefs in global ocean production.- Coral Reefs, **10/2:** 55-64.

Davies, P.J. and Stewart, D.B. (1976): Scuba operated coring device.- Bureau of Mineral Resources Journal, Australia - Geology and Geophysics, **1:** 246-247.

Dodge, R.E. and Brass, G.W. (1984): Skeletal extension, density and calcification of the reef coral, *Montastrea annularis*: St. Croix, U.S. Virgin Islands.- Bulletin of Marine Science, **34/2:** 288-307.

Dodge, R.E. and Lang, J.C. (1983): Environmental correlates of hermatypic coral (*Montastrea annularis*) growth on the East Flower Gardens Bank, northwest Gulf of Mexico.- Limnol. Oceanogr., **28/2:** 228-240.

Dodge, R.E. and Vaisnys, J.R. (1975): Hermatypic coral growth banding as environmental recorder.- Nature, **258:** 706-708.

Dodge, R.E., Aller, R.C. and Thomson, J. (1974): Coral growth related to resuspension of bottom sediments.- Nature, **247:** 574-576.

Druffel, E.M. (1980): Radiocarbon in annual coral rings of Belize and Florida.- Radiocarbon, **22/2:** 363-371.

Druffel, E.M. (1981): Radiocarbon in annual coral rings from the Eastern Tropical Pacific Ocean.- Geophysical Research Letters, **8/1:** 59-62.

Druffel, E.M. (1982): Banded corals: Changes in oceanic carbon-14 during the Little Ice Age.- Science, **218:** 13-19.

Druffel, E.M. and Linick, T.W. (1978): Radiocarbon in annual coral rings of Florida.- Geophysical Research Letters, **5/11:** 913-916.

Dullo, W.-C. (1984): Progressive diagenetic sequence of aragonite structures: Pleistocene coral reefs and their modern counterparts on the eastern Red Sea coast, Saudi Arabia.- Palaeontographica Americana, **54:** 254-260.

Dullo, W.-C. (1986): Variation in Diagenetic Sequences: An example from pleistocene coral reefs, Red Sea, Saudi-Arabia.- In: Schroeder, J.H. and Purser, B.H. (ed.): Reef Diagenesis: 77-90; Heidelberg (Springer).

Dullo, W.-C. (1990): Facies, fossil record, and age of Pleistocene reefs from the Red Sea (Saudi Arabia).- Facies, **22:** 1-46.

Dullo, W.-C., Heiss, G.A. and de Vries, E. (1993): A 200 year sclerochronological record from the Red Sea: Growth rates, stable isotopes and environmental stress.- Proceedings of Conference on "Global Aspects of Coral reefs" Miami, University of Miami, Rosenstiel School of Marine and Atmospheric Science: (submitted).

Dunbar, R.B. and Wellington, G.M. (1981): Stable isotopes in a branching coral monitor seasonal temperature variation.- Nature, **293:** 453-455.

Dustan, P. (1975): Growth and form in the reef-building coral *Montastrea annularis*.- Marine Geology, **33:** 101-107.

Edmunds, P.J. and Davies, P.S. (1989): An energy budget for *Porites porites* (Scleractinia), growing in a stressed environment.- Coral Reefs, **8/1:** 37-43.

Eisenhauer, A., Wasserburg, G.J., Chen, J.H., Bonani, G., Collins, L.B. et al. (1993): Holocene sea-level determination relative to the Australian continent: U/Th (TIMS) and ^{14}C (AMS) dating of coral cores from the Abrolhos Islands.- Earth and Planetary Science Letters, **114:** 529-547.

Emiliani, C., Hudson, J.H., Shinn, e.A. and George, R.Y. (1978): Oxygen and carbon isotopic record in a reef coral from the Florida keys and a deep-sea coral from Blake Plateau.- Science, **202:** 627-629.

Epstein, S., Buchsbaum, R., Lowenstam, H.A. and Urey, H.C. (1953): Revised carbonate-water isotopic temperature scale.- Bulletin of the Geological Society of America, **64:** 1315-1326.

Erez, J. (1978): Vital effect on stable-isotope composition seen in foraminifera and coral skeletons.- Nature, **273:** 199-202.

Fagerstrom, J.A. (1987): The evolution of reef communities.- New York (Wiley): 600 pp.

Fairbanks, R.G. and Dodge, R.E. (1979): Annual periodicity of the $^{18}O/^{16}O$ and $^{13}C/^{12}C$-ratios in the coral *Montastrea annularis*.- Geochimica et Cosmochimica Acta, **43**: 1009-1020.

Fishelson, L. (1973): Ecology of coral reefs in the Gulf of Aqaba (Red Sea) influenced by pollution.- Oecologia, **12**: 55-67.

Fishelson, L. (1980): Marine reserves along the Sinai peninsula (northern red Sea).- Helgoländer wissenschaftliche Meeresuntersuchungen, **33**: 624-640.

Fitt, W.K., Spero, H.J., Halas, J., White, M.W. and Porter, J.W. (1993): Recovery of the coral *Montastrea annularis* in the Florida Keys after the 1987 Caribbean "bleaching event".- Coral Reefs, **12/2**: 57-64.

Freemantle, M.H., Hulings, N., Mulqi, M. and Watton, E.C. (1978): Calcium and phosphate in the Jordan Gulf of Aqaba.- Marine Pollution Bulletin, **9**: 79-80.

Fricke, H.W. and Hottinger, L. (1983): Coral bioherms below the euphotic zone in the Red Sea.- Marine Ecology-Progress Series, **11**: 113-117.

Fricke, H.W. and Knauer, B. (1986): Diversity and spatial pattern of coral communities in the Red Sea upper twilight zone.- Oecologia, **71**: 29-37.

Fricke, H.W. and Schuhmacher, H. (1983): The depth limits of Red Sea stony corals: an ecophysiological problem.- Mar. Ecol., **4**: 163-194.

Friis-Christensen, E. and Lassen, K. (1991): Length of the solar cycle: an indicator of solar activity closely associated with climate.- Science, **254**: 698-700.

Furnas, M.J., Mitchell, A.W., Gilmartin, M. and Revelante, N. (1990): Phytoplankton biomass and primary production in semi-enclosed reef lagoons of the central Great Barrier Reef, Australia.- Coral Reefs, **9/1**: 1-10.

Gabrié, C. and Montaggioni, L. (1982): Sedimentary facies from the modern coral reefs, Jordan Gulf of Aqaba, Red Sea.- Coral Reefs, **1**: 115-124.

Ghiold, J. and Enos, P. (1982): Carbonate production of the coral *Diploria Labyrinthiformis* in south Florida patch reefs.- Marine Geology, **45**: 281-296.

Glynn, P.W. (1977): Coral growth in upwelling and nonupwelling areas off the Pacific coast of Panama.- Journal of Marine Research, **35/3**: 567-585.

Goreau, T.J. (1959): The physiology of skeleton formation in corals. I. A method for measuring the rate of calcium deposition by corals under different conditions.- Biological Bulletin, **116**: 59-75.

Goreau, T.J. (1977): Carbon metabolism in calcifying and photosynthetic organism: Theoretical models based on stable isotope data.- Proceedings, Third International Coral Reef Symposium Miami, University of Miami.

Gravier, C. (1911): Les recifs de coreaux et les madreporairres de la Baie de Tadjourah: Gulf of Aden.- Annales de l'Institut Océanograhique, **2**: 99.

Grigg, R.W. (1982): Darwin point: A threshold for atoll formation.- Coral Reefs, **1**: 29-34.

Grigg, R.W. (1992): Coral reef environmental science: truth versus the Cassandra syndrome.- Coral Reefs, **11/4**: 183-186.

Guillaume, M. (1988): La croissance du squelette de *Porites lutea*, scléractinaire hermatypique, sur la recif frangeant de La Saline, Ile de la Réunion, Océan Indien.- PhD thesis, Université d'Aix-Marseille II.

Guillaume, M. (1990): Growth and calcium carbonate production of massive *Porites* (barrier reef flat of French Polynesia).- Proceedings ISRS Congress Nouméa: 87-90.

Guillaume, M. and Carrio-Schaffhauser, E. (1985): Non-influence of depth on porosity of *Porites lutea* in Réunion Island (West Indian Ocean).- Fifth International Coral Reef Congress Tahiti: 193-197.

Guillaume, M.M. and Montaggioni, L.F. (1992): Growth and calcium carbonate production of *Acropora* sp. on a barrier reef flat of French Polynesia.- 7th International Coral Reef Symposium, Abstracts Guam: 39.

Guzmán, H.M. and Holst, I. (1993): Effects of chronic oil-sediment pollution on the reproduction of the Caribbean reef coral *Siderastrea siderea*.- Marine Pollution Bulletin, **26/5**: 276-282.

Guzmán, H.M. and Jiménez, C.E. (1992): Contamination of coral reefs by heavy metals along the Caribbean coast of Central America (Costa Rica and Panama).- Marine Pollution Bulletin, **24/11**: 554-561.

Guzmán, H.M., Jackson, J.B.C. and Weil, E. (1991): Short-term ecological consequences of a major oil spill on Panamanian subtidal reef corals.- Coral Reefs, **10/1**: 1-12.

Gvirtzman, G. and Friedman, G.M. (1977): Sequence of progressive diagenesis in coral reefs.- In: Frost et al., S.H. (ed.): Reefs and related carbonates - Ecology and sedimentation.- Studies in Geology, **4**: 357-380 (American Association of Petroleum Geologists).

Hallock, P. and Schlager, W. (1986): Nutrient excess and the demise of coral reefs and carbonate platforms.- Palaios, **1**: 389-398.

Hands, M.R., French, J.R. and O'Neill, A. (1993): Reef stress at Cahuita Point, Costa Rica: anthropogenically enhanced sediment influx or natural geomorphic change?- Journal of Coastal Research, **9/1**: 11-25.

Heiss, G.A., Dullo, W.-C. and Reijmer, J.J.G. (1993): Short- and long-term growth history of massive *Porites* sp. from Aqaba (Red Sea).- Senckenbergiana maritima, **23/4/6:** 135-141.

Highsmith, R.C. (1979): Coral growth rates and environmental control of density banding.- Journal of Experimental Marine Biology and Ecology, **37:** 105-125.

Houck, J.E., Buddemeier, R.W., Smith, S.V. and Jokiel, P.L. (1977): The response of coral growth rate and skeletal strontium content to light intensity and water temperature.- Proceedings of the 3rd International Coral Reef Symposium Miami, **2:** 425-431.

Hubbard, D.K. (1986): Sedimentation as a control of reef development: St. Croix, U.S.V.I.- Coral Reefs, **5/3:** 117-125.

Hubbard, D.K. and Scaturo, D. (1985): Growth rates of seven species of scleractinean corals from Cane Bay and Salt River, St. Croix, USVI.- Bulletin of Marine Science, **36/2:** 325-338.

Hubbard, D.K., Burke, R.B. and Gill, I.P. (1986): Styles of reef accretion along a steep, shelf-edge reef, St. Croix, U.S. Virgin Islands.- Journal of Sedimentary Petrology, **56/6:** 848-861.

Hubbard, D.K., Miller, A.I. and Scaturo, D. (1990): Production and cycling of calcium carbonate in a shelf-edge reef system (St. Croix, U.S. Virgin Islands): applications to the nature of reef systems in the fossil record.- Journal of Sedimentary Petrology, **60/3:** 335-360.

Hubbard, D.K., Sadd, J.L., Miller, A.I., Gill, I.P. and Dill, R.F. (1981): The production, transportation and deposition of carbonate sediments on the insular shelf of St. Croix, U.S.Virgin Islands.- Technical Report, /MG-1: 1-145; St. Croix, U.S.V.I. (West Indies Laboratory).

Hudson, J.H. (1977): Long-term bioerosion rates on a Florida reef: a new method.- Proceedings of the 3rd International Coral Reef Symposium Miami, University of Miami, **2:** 491-497.

Hudson, J.H. (1981): Growth rates in *Montastrea annularis*: a record of environmental change in Key Largo Reef Marine Sanctuary, Florida.- Bulletin of Marine Science, **31/2:** 444-459.

Hudson, J.H., Shinn, E.A., Halley, R.B. and Lidz, B. (1976): Sclerochronology: A tool for interpreting past environments.- Geology, **4:** 361-364.

Hughes, T.P. (1987): Skeletal density and growth form of corals.- Marine Ecology - Progress Series, **35:** 259-266.

Hulings, N.C. (1979): Currents in the Jordan Gulf of Aqaba.- Dirasat, **6:** 21-33.

Hulings, N.C. (1989): A review of marine science research in the Gulf of Aqaba.- Publications of the Marine Science Station Aqaba, Jordan.- Amman (The University of Jordan Press), **6:** 267.

Hulings, N.C. and Abu-Hilal, A. (1983): The temporal distribution of nutrients in the surface waters of the Jordan Gulf of Aqaba.- Dirasat, **10/2:** 91-105.

Huston, M. (1985): Variation in coral growth rates with depth at Discovery Bay, Jamaica.- Coral Reefs, **4:** 19-25.

IPCC (1992): Climate Change 1992. The supplementary report to the IPCC scientific assessment.- Houghton, J.T., Callander, B.A. and Varney, S.K. (ed.); Cambridge (University press).

Isdale, P. (1977): Variation in growth rate of hermatypic corals in a uniform environment.- Proceedings of the 3rd International Coral Reef Symposium Miami, School of Marine and Atmospheric Sciences, **1:** 403-408.

Isdale, P. (1984): Flourescent bands in massive corals record centuries of coastal rainfall.- Nature, **310:** 578-579.

Klein, R. and Loya, Y. (1991): Skeletal growth and density patterns of two *Porites* corals from the Gulf of Eilat, Red Sea.- Marine Ecology Progress Series, **77:** 253-259.

Klein, R., Loya, Y., Gvirtzman, G., Isdale, P.J. and Susic, M. (1990): Seasonal rainfall in the Sinai Desert during the late Quaternary inferred from flourescent bands in fossil corals.- Nature, **345/6271:** 145-147.

Klein, R., Pätzold, J., Wefer, G. and Loya, Y. (1992): Seasonal variations in the stable isotopic composition and the skeletal density pattern of the coral *Porites lobata* (Gulf of Eilat, Red Sea).- Marine Biology, **112:** 259-263.

Klein, R., Pätzold, J., Wefer, G. and Loya, Y. (1993): Depth-related timing of density band formation in *Porites* spp. corals from the red Sea inferred from X-ray chronology and stable isotope composition.- Marine Ecology - Progress Series, **97:** 99-104.

Knutson, D.W., Buddemeier, R.W. and Smith, S.V. (1972): Coral chronometers: seasonal growth bands in reef corals.- Science, **177:** 270-272.

Krupp, F. (1989): Beobachtungen an Fahnenbarschen.- Natur und Museum, **119:** 262-266.

Land, L.S. (1979): The fate of reef-derived sediment on the north Jamaican island slope.- Marine Geology, **29:** 55.

Land, L.S., Lang, J.C. and Barnes, D.J. (1975): Extension rate: a primary control on the isotopic composition of West Indian (Jamaican) scleractinian reef coral skeletons.- Marine Biology, **33:** 221-233.

Lassen, K. and Friis-Christensen, E. (1992): Solar activity parameters used in geophysical studies at DMI.: 1-11; Copenhagen (Danish Meteorological Institute).

Le Campion-Alsumard, T., Romano, J.-C., Peyrot-Clausade, M., Campion, J.L. and Paul, R. (1993): Influence of some coral reef communities on the calcium carbonate budget of Tiahura reef (Moorea, French Polynesia).- Marine Biology, **115/4**: 685-693.

Leder, J.J., Szmant, A.M. and Swart, P.K. (1991): The effect of prolonged "bleaching" on skeletal banding and stable isotopic composition in *Montastrea annularis*.- Coral Reefs, **10/1**: 19-27.

Linsley, B.K., Dunbar, R.B. and Wellington, G.M. (1993): A coral based reconstruction of intertropical covergence zone variability over Central America since 1707 A.D.- Geological Society of America Annual Meeting Boston, **Abstracts**: A-387.

Locke, S. and Thunell, R.C. (1988): Paleoceanographic record of the last glacial/interglacial cycle in the Red Sea and Gulf of Aden.- Palaeogeography, Palaeoclimatology, Palaeoecology, **64**: 163-187.

Logan, A. and Anderson, I.H. (1991): Skeletal extension growth rate assessment in corals, using CT scan imagery.- Bulletin of Marine Science, **49/3**: 847-850.

Logan, A. and Tomascik, T. (1991): Extension growth rates in two coral species from high-latitude reefs of Bermuda.- Coral Reefs, **10/3**: 155-160.

Lough, J.M. and Barnes, D.J. (1990): Possible relationships between environmental vriables and skeletal density in a coral colony from the central Great Barrier Reef.- Journal of Experimental Marine Biology and Ecology, **134**: 221-241.

Lough, J.M. and Barnes, D.J. (1992): Comparisons of skeletal density variations in *Porites* from the central Great Barrier Reef.- Journal of Experimental Marine Biology and Ecology, **155**: 1-25.

Loya, Y. (1972): Community structure and species diversity of hermatypic corals at Eilat, Red Sea.- Marine Biology, **13**: 100-123.

Macintyre, I.G. (1975): A diver-operated hydraulic drill for coring submerged substrates.- Atoll Research Bulletin, **185**: 21-26.

Macintyre, I.G. (1978): A hand-operated submersible drill for coring reef substrata.- In: Stoddard, D.R. and Johannes, R.E. (ed.): Coral Reefs: Research Methods.- Monographs on Oceanographic Methodology, **5**: 75-80; Paris (UNESCO).

Macintyre, I.G., Burke, R.B. and Stuckenrath, R. (1981): Core holes in the outer fore reef off Carrie Bow Cay, Belize: a key to the Holocene history of the Belizean barrier reef complex.- Proceedings of the 4th International Coral Reef Symposium Manila, **1**: 567-574.

Maniere, R. and Jaubert, J. (1984): Coral reef mapping in the Gulf of Aqaba (Red Sea) using computer image processing techniques for coral reefs survey.- Proc. Symp. Coral Reef Environ. Red Sea Jeddah: 614-623.

Maragos, J.E. (1972): PhD thesis, University of Hawaii, Honolulu.

McConnaughey, T. (1989): ^{13}C and ^{18}O isotopic disequilibrium in biological carbonates: I. patterns.- Geochimica et Cosmochimica Acta, **53**: 151-162.

McConnaughey, T. (1989b): ^{13}C and ^{18}O isotopic disequilibrium in biological carbonates: II. in vitro simulation of kinetic isotope effects.- Geochimica et Cosmochimica Acta, **53**: 163-171.

Mergner, H. (1979): Quantitative ökologische Analyse eines Rifflagunenareals bei Aqaba (Golf von Aqaba, Rotes Meer).- Helgoländer wissenschaftliche Meeresuntersuchungen, **32**: 476-507.

Mergner, H. (1981): Man-made influences on and natural changes in the settlement of the Aqaba reefs (Red Sea).- Proceedings of the 4th International Coral Reef Symposium Manila, **1**: 193-207.

Mergner, H. and Schuhmacher, H. (1974): Morphologie, Ökologie und Zonierung von Korallenriffen bei Aqaba, (Golf von Aqaba, Rotes Meer).- Helgoländer wissenschaftliche Meeresuntersuchungen, **26**: 238-358.

Mergner, H. and Schuhmacher, H. (1981): Quantitative Analyse der Korallenbesiedlung eines Vorriffareals bei Aqaba (Rotes Meer).- Helgoländer Meeresuntersuchungen, **34**: 337-354.

Mergner, H. and Schuhmacher, H. (1985): Quantitative Analyse von Korallengemeinschaften des Sanganeb-Atolls (mittleres Rotes Meer). I. Die Besiedlungsstruktur hydrodynamisch unterschiedlich exponierter Außen- und Innenriffe.- Helgoländer Meeresuntersuchungen, **39**: 375-417.

Muscatine, L. (1973): Nutrition of corals.- In: Jones, O.A. and Endean, R. (ed.): Biology and geology of coral reefs, Vol. 1. Geology: 77; New York (Academic Press).

Neumann, A.C. and Land, L.S. (1975): Lime mud deposition nad calcareous algae in the bight of Abaco, Bahamas: a budget.- Journal of Sedimentary Petrology, **45**: 763-786.

NOAA (1993): Coral records of ocean-atmosphere variability: report from the workshop on coral paleoclimate reconstruction.- (NOAA Climate and Global Change Program).

Nozaki, Y., Rye, D.M., Turekian, K.K. and Dodge, R.E. (1978): A 200 year record of Carbon-13 and Carbon-14 variations in a Bermuda coral.- Geophysical Research Letters, **5/10**: 825-827.

O'Brien, D. and Currie, R. (1993): Observations of the 18.6- year cycle of air pressure and a theoretical model to explain certain aspects of this signal.- Climate Dynamics, **8**: 287-298.

Paldor, N. and Anati, D.A. (1979): Seasonal variations of temperature and salinity in the Gulf of Elat (Aqaba).- Deep-Sea Research, **26/6a:** 661-672.

Pätzold, J. (1984): Growth rhythms recorded in stable isotopes, and density bands in the reef coral *Porites lobata* (Cebu, Philippines).- Coral Reefs, **3:** 87-89.

Pätzold, J. (1986): Temperatur- und CO_2-Änderungen im tropischen Oberflächenwasser der Philippinnen während der letzten 120 Jahre: Speicherung in stabilen Isotopen hermatyper Korallen.- PhD thesis, Universität Kiel.

Pätzold, J. and Wefer, G. (1992): Bermuda coral reef record of the last 1000 years.- Fourth International Conference on Paleoceanography, Abstracts Kiel: 224-225.

Payri, C.E. (1988): *Halimeda* contribution to organic and inorganic production in a Tahitian reef system.- Coral Reefs, **6/3/4:** 251-262.

Potts, D.C., Done, T.J., Isdale, P.J. and Fisk, D.A. (1985): Dominance of a coral community by the genus *Porites* (Scleractinia).- Marine Ecology - Progress Series, **23:** 79-84.

Ramm, M. (1993): Bioerosion durch Makroendolithen im Vorriff bei Aqaba, Jordanien (Rotes Meer).- Master thesis, University of Kiel.

Reid, G.C. (1991): Solar total irradiance variations and the global sea surface temperature record.- Journal of Geophysical Research, **96/D2:** 2835-2844.

Reiss, Z. and Hottinger, L.S. (1984): The Gulf of Aqaba: Ecological Micropaleontology.- Ecological Studies.- Berlin (Springer), **50:** 1-354.

Rinkevich, B. and Loya, Y. (1977): Harmful effects of chronic oil pollution on a Red Sea scleractinian coral population.- Proceedings of the 3rd International Coral Reef Symposium Miami, **2:** 585-591.

Roulier, L.M. (1993): Reconstructing seasonal variations during the mid-Pliocene using the carbon and oxygen isotope geochemistry of *Solenastrea bournoni*.- Geological Society of America Annual Meeting, Abstracts Boston: A-329.

Sadd, J.L. (1980): Sediment transport in a fringing reef, Cane Bay, St. Croix, U.S.V.I.- M.Sc. thesis, Dept. of Geology, University of Texas, Austin.

Sadd, J.L. (1984): Sediment transport and $CaCO_3$ budget on a fringing reef, Cane Bay, St. Croix, U.S. Virgin Islands.- Bulletin of Marine Science, **35/2:** 221-238.

Schlichter, D., Fricke, H.W. and Weber, W. (1986): Light harvesting by wavelength transformation in a symbiotic coral of the Red Sea twilight zone.- Marine Biology, **91:** 403-407.

Schneider, R.C. and Smith, S.V. (1982): Skeletal Sr content and density in *Porites* spp. in relation to environmental factors.- Marine Biology, **66:** 121-131.

Schuhmacher, H. and Mergner, H. (1985): Quantitative Analyse von Korallengemeinschaften des Sanganeb-Atolls (mittleres Rotes Meer). II. Vergleich mit einem Riffareal bei Aqaba (nördliches Rotes Meer) am Nordrande des indopazifischen Riffgürtels.- Helgoländer Meeresuntersuchungen, **39:** 419-440.

Schuhmacher, H., Kroll, D.K. and Reinicke, G.B. (1993): Long-term fluctuations of coral communities at Aqaba and on Sanganeb-Atoll (northern and central Red Sea) over a decadal period.- ISRS First European Regional Meeting, Abstracts, Vienna.

Schuhmacher, H., Krupp, F. and Randall, J.E. (1989): *Pseudoanthias hemstrai*, a new species of Anthiine fish (Parciformis, Serranidae) from the Gulf of Aqaba, Red Sea.- Fauna of Saudi Arabia, **10:** 338-346.

Scoffin, T.P., Stearn, C.W., Boucher, D., Frydl, P., Hawkins, C.M. et al. (1980): Calcium carbonate budget of a fringing reef on the west coast of Barbados, Part II - erosion, sediments and internal structure.- Bulletin of Marine Science, **30/2:** 475-508.

Scoffin, T.P., Tudhope, A.W., Brown, B.E., Chansang, H. and Cheeney, R.F. (1992): Patterns and possible environmental controls of skeletogenesis of *Porites lutea*, South Thailand.- Coral Reefs, **11:** 1-11.

Shen, G.T. and Boyle, E.A. (1987): Lead in corals: reconstruction of historical industrial fluxes to the surface ocean.- Earth and Planetary Science Letters, **82:** 289-304.

Shen, G.T. and Boyle, E.A. (1988): Determination of lead, cadmium and other trace metals in annually-banded corals.- Chemical Geology, **67:** 47-62.

Shen, G.T., Cole, J.E., Lea, D.W., Linn, L.J., McConnaughey, T.A. et al. (1992): Surface ocean variability at Galápagos from 1936-1982: Calibration of geochemical tracers in corals.- Paleoceanography, **7/5:** 563-588.

Sheppard, C.R.C. and Sheppard, A.L.S. (1991): Corals and coral communities of Arabia.- Fauna of Saudi Arabia, **12:** 1-170.

Smith, S.V. and Harrison, J.T. (1977): Calcium carbonate production of the *Mare Incognitum*, the upper windward reef slope, at Enewetak Atoll.- Science, **197:** 556-558.

Smith, S.V. and Kinsey, D.W. (1976): Calcium carbonate production, coral reef growth, and sea level change.- Science, **194:** 937-939.

Stearn, C.W. and Colassin, C. (1983): A simple underwater pneumatic hand drill.- Journal of Paleontology, **53:** 1257-1259.

Stearn, C.W., Scoffin, T.P. and Martindale, W. (1977): Calcium carbonate budget of a fringing reef on the west coast of Barbados. Part I-zonation and productivity.- Bulletin of Marine Science, **27/3:** 479-510.

Strasser, A., Strohmenger, C., Davaud, E. and Bach, A. (1992): Sequential evolution and diagenesis of Pleistocene coral reefs (South Sinai, Egypt).- Sedimentary Geology, **78:** 59-79.

Stuiver, M. (1978): Atmospheric carbon dioxide and carbon reservoir changes.- Science, **199:** 253-258.

Suess, H. (1955): Radiocarbon concentration in modern wood.- Science, **122:** 414-417.

Swart, P.K. (1983): Carbon and oxygen isotope fractionation in scleractinian corals: a review.- Earth Science Reviews, **19:** 51-80.

Te, F.T. (1992): Response to higher sediment loads by *Pocillopora damicornis* planulae.- Coral Reefs, **11/3:** 131-134.

Tomascik, T. and Logan, A. (1990): A comparison of peripheral growth rates in the recent solitary coral *Scolymia Cubensis* (Milne-Edwards and Haime) from Barbados and Bermuda.- Bulletin of Marine Science, **46/3:** 799-806.

Vaughan, T.W. (1919): Corals and the formation of coral reefs.- Smithsonian Institution Annual Review: 189-238.

Wahbeh, M.I. (1993): An agenda for scientific research in the Gulf of Aqaba.- In: Sandler, D., Adly, E. and Al-Khosman, M.A. (ed.): Protecting the Gulf of Aqaba. A regional environmental challenge: 25-39; Washington, D.C. (Environmental Law Institute).

Walker, D.I. and Ormond, R.F.G. (1982): Coral death from sewage and phosphate pollution at Aqaba, Red Sea.- Marine Pollution Bulletin, **13/1:** 21-25.

Walther, J. (1888): Die Korallenriffe der Sinai Halbinsel. Geologische und biologische Betrachtungen.- Abh. Math.-Naturwiss. Kl. Königl. Sächs. Gesellsch. Wissensch., **14:** 439-506.

Weber, J.N. and Woodhead, P.M.J. (1970): Carbon and oxygen isotope fractionation in the skeletal carbonate of reef-building corals.- Chemical Geology, **6:** 93-117.

Weber, J.N. and Woodhead, P.M.J. (1972): Temperature dependence of oxygen-18 concentration in reef coral carbonates.- Journal of Geophysical Research, **77:** 463-473.

Weidlich, O., Bernecker, M. and Flügel, E. (1993): Combined quantitative analysis and microfacies studies of ancient reefs: an integrated approach to Upper Permian and Upper Triassic reef carbonates (Sultanate of Oman).- Facies, **28:** 115-144.

Weil, S.M., Buddemeier, R.W., Smith, S.V. and Kroopnick, P.M. (1981): The stable isotopic composition of coral skeletons: control by environmental variables.- Geochimica et Cosmochimica Acta, **45:** 1147-1153.

Wellington, G.M. and Glynn, P.W. (1983): Environmental influences on skeletal banding in eastern Pacific (Panama) corals.- Coral Reefs, **1/4:** 215-222.

Winter, A., Goenaga, C. and Maul, G.A. (1991): Carbon and oxygen isotope time series from an 18-year Caribbean reef coral.- Journal of Geophysical Research, **96/C9:** 16673-16678.

Winter, A., Erlenkeuser, H., Zahn, R., Goenaga, C. and Maul, G. (in prep.): A 270 year annual stable isotope record from the eastern Caribbean.- .

Wittenberg, M. and Hunte, W. (1992): Effects of eutrophication and sedimentation on juvenile corals I. Abundance, mortality and community structure.- Marine Biology, **112:** 131-138.

APPENDIX

Appendix Coral and core samples stable isotope data

Coral E15

sample	$\delta^{13}C$	std.dev.	$\delta^{18}O$	std.dev.
15001	-2.46	0.11	-3.63	0.09
15002	-2.70	0.01	-3.31	0.05
15003	-2.26	0.03	-2.95	0.04
15004	-1.79	0.02	-2.94	0.03
15005	-2.40	0.03	-3.34	0.04
15006	-1.94	0.03	-3.21	0.06
15007	-2.31	0.04	-3.47	0.06
15008	-2.39	0.01	-2.93	0.04
15009	-2.24	0.02	-3.03	0.03
15010	-3.08	0.02	-3.44	0.06
15011	-2.81	0.02	-3.58	0.02
15012	-2.17	0.02	-3.39	0.03
15013	-1.48	0.02	-2.50	0.03
15014	-2.25	0.02	-2.39	0.02
15015	-2.62	0.04	-3.45	0.04
15016	-3.13	0.03	-3.53	0.02
15017	-2.31	0.06	-3.82	0.03
15018	-2.53	0.02	-3.82	0.03
15019	-2.34	0.02	-3.82	0.02
15020	-2.54	0.02	-3.60	0.02
15021	-2.80	0.02	-3.09	0.03
15022	-2.83	0.02	-2.96	0.03
15023	-2.78	0.02	-3.37	0.03
15024	-2.73	0.03	-3.69	0.03
15025	-1.95	0.03	-3.65	0.03
15026	-2.55	0.02	-3.27	0.05
15027	-2.57	0.02	-2.91	0.02
15028	-2.96	0.02	-3.02	0.04
15029	-3.18	0.02	-3.34	0.03
15030	-2.48	0.02	-3.59	0.04
15031	-2.65	0.01	-3.62	0.01
15032	-2.53	0.02	-3.39	0.04
15033	-2.64	0.02	-3.15	0.02
15034	-1.28	0.01	-2.53	0.03
15035	-2.53	0.02	-2.99	0.04

E2 (fossil)

sample	$\delta^{13}C$	std.dev.	$\delta^{18}O$	std.dev.
310	-2.13	0.05	-4.06	0.07
311	-2.42	0.05	-3.53	0.05
312	-2.51	0.04	-3.10	0.06
313	-1.58	0.03	-2.58	0.04
314	-2.33	0.05	-3.73	0.03
315	-3.12	0.05	-3.32	0.03
316	-1.37	0.03	-3.19	0.04
317	-0.94	0.04	-4.01	0.04
318	-0.66	0.04	-3.42	0.06
319	-0.35	0.04	-3.24	0.06
320	-2.31	0.05	-3.88	0.05
321	-1.88	0.07	-3.21	0.03
322	-2.31	0.05	-2.67	0.05
323	-1.57	0.05	-3.65	0.05
324	-2.98	0.04	-3.28	0.06
325	-1.15	0.06	-3.48	0.02
326	-0.89	0.06	-3.48	0.04
327	-0.42	0.05	-2.66	0.08

Coral E16

sample	$\delta^{13}C$	std.dev.	$\delta^{18}O$	std.dev.
16001	-2.09	0.02	-3.74	0.04
16002	-1.80	0.03	-3.38	0.02
16003	-1.87	0.03	-3.15	0.04
16004	-2.03	0.01	-2.97	0.04
16005	-2.20	0.02	-3.18	0.02
16006	-2.72	0.02	-3.41	0.03
16007	-2.98	0.02	-3.51	0.02
16008	-2.79	0.02	-3.73	0.02
16009	-2.76	0.02	-3.63	0.06
16010	-2.27	0.04	-3.68	0.06
16011	-1.72	0.03	-4.03	0.04
16012	-1.67	0.02	-3.84	0.03
16013	-1.42	0.02	-3.61	0.04
16014	-1.59	0.02	-3.29	0.02
16015	-2.01	0.01	-2.89	0.02
16016	-2.45	0.02	-3.12	0.02
16017	-2.85	0.02	-3.14	0.03
16018	-2.86	0.03	-3.34	0.05
16019	-2.67	0.03	-3.77	0.04
16020	-2.71	0.01	-3.89	0.02
16021	-1.93	0.02	-3.89	0.04
16022	-1.73	0.02	-3.85	0.03
16023	-1.57	0.02	-3.71	0.03
16024	-1.50	0.03	-3.56	0.02
16025	-1.49	0.02	-3.44	0.03
16026	-1.95	0.01	-2.78	0.05
16027	-2.96	0.02	-3.01	0.02
16028	-2.21	0.02	-3.44	0.03
16029	-2.42	0.03	-3.57	0.02
16030	-1.72	0.02	-3.96	0.04
16031	-1.80	0.02	-3.90	0.05
16032	-1.65	0.02	-3.74	0.04
16033	-2.06	0.02	-3.54	0.02
16034	-1.75	0.01	-3.05	0.03
16035	-1.99	0.02	-2.93	0.01
16036	-2.41	0.04	-3.13	0.04
16037	-2.69	0.02	-3.46	0.03
16038	-2.74	0.02	-3.56	0.02
16039	-2.50	0.01	-3.71	0.03
16040	-2.09	0.02	-3.76	0.03
16041	-2.18	0.01	-3.90	0.03
16042	-1.88	0.02	-3.78	0.02
16043	-1.74	0.02	-3.45	0.02
16044	-0.68	0.01	-2.86	0.01
16045	-2.24	0.02	-2.89	0.02
16046	-2.68	0.02	-2.96	0.03
16047	-3.10	0.02	-3.38	0.03
16048	-3.37	0.02	-3.71	0.02
16050	-2.21	0.02	-3.85	0.03
16051	-1.84	0.01	-3.87	0.02
16052	-1.78	0.01	-3.88	0.04
16053	-1.13	0.02	-3.75	0.02
16054	-1.88	0.02	-3.64	0.01
16055	-1.65	0.02	-3.26	0.02
16056	-1.94	0.02	-3.03	0.02
16057	-2.61	0.01	-3.34	0.02
16058	-2.37	0.01	-3.72	0.02
16059	-2.64	0.02	-3.68	0.01
16060	-2.06	0.03	-3.71	0.04
16061	-2.38	0.02	-3.91	0.04
16062	-1.76	0.03	-3.65	0.04
16063	-1.82	0.01	-3.71	0.02
16064	-1.65	0.03	-3.66	0.04
16065	-2.25	0.02	-3.58	0.03
16066	-1.99	0.01	-2.80	0.01
16067	-1.92	0.02	-2.82	0.04
16069	-2.58	0.01	-3.08	0.03
16070	-3.38	0.02	-3.77	0.03

	Core 18					Core 19				
year	sample	$\delta^{13}C$	std.dev.	$\delta^{18}O$	std.dev.	sample	$\delta^{13}C$	std.dev.	$\delta^{18}O$	std.dev.
1992	18001	-3.18	0.02	-3.16	0.05	19001	-3.96	0.02	-2.87	0.04
1991	18002	-2.77	0.02	-2.98	0.03	19002	-4.08	0.03	-3.02	0.05
1990	18003	-2.70	0.01	-2.72	0.02	19003	-3.75	0.02	-2.80	0.03
1989	18004	-3.14	0.01	-2.74	0.03	19004	-4.10	0.02	-3.02	0.04
1988	18005	-2.72	0.02	-2.63	0.02	19005	-3.88	0.04	-3.02	0.07
1987	18006	-2.73	0.01	-2.93	0.05	19006	-3.74	0.02	-2.89	0.04
1986	18007	-2.64	0.02	-2.72	0.03	19007	-3.22	0.05	-3.00	0.07
1985	18008	-2.75	0.01	-2.83	0.03	19008	-3.31	0.04	-3.01	0.05
1984	18009	-2.20	0.02	-2.73	0.03	19009	-3.07	0.02	-2.71	0.03
1983	18010	-2.64	0.02	-2.98	0.03	19010	-3.21	0.03	-2.68	0.02
1982	18011	-2.29	0.02	-2.69	0.02	19011	-3.25	0.03	-2.74	0.03
1981	18012	-2.50	0.02	-2.73	0.04	19012	-3.21	0.01	-2.95	0.04
1980	18013	-2.40	0.01	-2.74	0.02	19013	-2.71	0.02	-3.05	0.05
1979	18014	-1.90	0.02	-2.99	0.05	19014	-2.32	0.03	-2.89	0.01
1978	18015	-2.13	0.02	-2.69	0.03	19015	-2.19	0.03	-2.80	0.04
1977	18016	-1.69	0.01	-2.80	0.03	19016	-2.12	0.03	-2.79	0.05
1976	18017	-1.51	0.01	-2.77	0.02	19017	-2.01	0.01	-2.99	0.03
1975	18018	-1.32	0.01	-2.78	0.02	19018	-2.20	0.03	-2.68	0.03
1974	18019	-1.66	0.01	-2.54	0.02	19019	-2.42	0.03	-2.79	0.03
1973	18020	-1.43	0.02	-2.70	0.02	19020	-2.27	0.03	-2.74	0.03
1972	18021	-1.29	0.01	-2.75	0.03	19021	-2.33	0.02	-2.81	0.03
1971	18022	-1.59	0.02	-2.84	0.03	19022	-2.46	0.01	-2.73	0.03
1970	18023	-1.71	0.02	-2.72	0.03	19023	-3.02	0.02	-3.08	0.03
1969	18024	-1.18	0.01	-2.92	0.02	19024	-3.09	0.01	-2.95	0.02
1968	18025	-1.39	0.01	-2.87	0.02	19025	-2.99	0.03	-2.63	0.03
1967	18026	-1.31	0.01	-2.65	0.04	19026	-2.63	0.02	-2.78	0.01
1966	18027	-1.38	0.02	-2.89	0.03	19027	-2.23	0.03	-2.88	0.04
1965	18028	-1.41	0.01	-2.90	0.02	19028	-2.25	0.04	-2.74	0.03
1964	18029	-1.55	0.01	-3.02	0.02	19029	-1.95	0.02	-2.89	0.03
1963	18030	-1.30	0.02	-2.88	0.03	19030	-2.43	0.02	-2.98	0.03
1962	18031	-1.44	0.02	-2.88	0.02	19031	-2.51	0.01	-2.84	0.03
1961	18032	-1.21	0.02	-2.64	0.02	19032	-2.74	0.02	-2.82	0.05
1960	18033	-1.31	0.01	-2.78	0.02	19033	-2.77	0.03	-2.65	0.03
1959	18034	-1.12	0.01	-2.96	0.01	19034	-2.46	0.02	-2.75	0.03
1958	18035	-1.01	0.01	-2.79	0.03	19035	-1.98	0.03	-2.84	0.02
1957	18036	-1.27	0.01	-2.91	0.03	19036	-2.45	0.02	-2.76	0.01
1956	18037	-1.15	0.02	-2.75	0.02	19037	-2.21	0.02	-2.62	0.05
1955	18038	-1.15	0.01	-2.82	0.03	19038	-2.03	0.03	-2.70	0.03
1954	18039	-1.25	0.01	-3.13	0.01	19039	-1.95	0.03	-2.74	0.05
1953	18040	-0.78	0.02	-3.06	0.01					
1953	18041	-0.92	0.01	-3.15	0.03	19040	-1.74	0.02	-2.97	0.03
1952	18042	-1.35	0.02	-2.67	0.03	19041	-1.44	0.01	-2.64	0.02
1951	18043	-1.24	0.01	-2.75	0.01	19042	-1.74	0.02	-2.73	0.02
1950	18044	-1.13	0.02	-2.69	0.04	19043	-1.82	0.02	-2.77	0.02
1949	18045	-1.32	0.02	-2.81	0.01	19044	-1.71	0.01	-2.73	0.02
1948	18046	-1.16	0.02	-2.96	0.03	19045	-1.57	0.02	-2.80	0.01
1947	18047	-1.16	0.02	-3.18	0.04	19046	-1.68	0.01	-2.94	0.02
1946	18048	-1.24	0.02	-2.81	0.03	19047	-2.12	0.02	-2.71	0.02
1945	18049	-1.29	0.02	-2.93	0.02	19048	-2.60	0.02	-2.84	0.02
1944	18050	-1.11	0.01	-2.72	0.01	19049	-2.89	0.03	-2.88	0.02
1943	18051	-1.46	0.02	-2.68	0.02	19050	-2.10	0.02	-2.91	0.04
1942	18052	-1.24	0.01	-2.92	0.01	19051	-2.03	0.01	-2.99	0.02
1941	18053	-1.33	0.01	-3.13	0.02	19052	-2.05	0.02	-2.74	0.02
1940	18054	-1.39	0.01	-2.86	0.03	19053	-2.23	0.02	-2.79	0.02
1939	18055	-1.22	0.01	-3.11	0.01	19054	-2.39	0.02	-2.76	0.06
1938	18056	-0.77	0.01	-2.93	0.02	19055	-1.83	0.02	-2.57	0.02
1937	18057	-0.82	0.03	-2.91	0.01	19056	-1.58	0.01	-2.68	0.04
1936	18058	-0.92	0.01	-2.72	0.01	19057	-1.47	0.02	-2.70	0.02
1935	18059	-1.12	0.01	-2.76	0.01	19058	-1.26	0.02	-2.81	0.04
1934	18060	-1.21	0.01	-2.88	0.03	19059	-1.26	0.02	-2.63	0.03
1933	18061	-1.25	0.02	-2.94	0.02	19060	-1.71	0.02	-2.70	0.05
1932	18062	-0.99	0.02	-3.00	0.02	19061	-2.65	0.02	-2.61	0.03
1931	18063	-0.79	0.02	-2.78	0.04	19062	-2.07	0.01	-2.79	0.03
1930	18064	-0.98	0.02	-2.74	0.02	19063	-1.75	0.02	-2.40	0.03
1929	18065	-1.03	0.01	-2.87	0.02	19064	-1.87	0.01	-2.67	0.02
1928	18066	-1.04	0.02	-2.74	0.02	19065	-1.41	0.02	-2.69	0.02
1927	18067	-1.18	0.02	-2.74	0.02	19066	-1.64	0.03	-2.82	0.04
1926	18068	-1.20	0.01	-2.76	0.04	19067	-1.73	0.01	-2.52	0.02
1925	18069	-1.37	0.02	-2.79	0.03	19068	-1.31	0.03	-2.57	0.03
1924	18070	-1.12	0.02	-2.80	0.04	19069	-1.53	0.02	-2.78	0.02
1923	18071	-1.25	0.02	-2.78	0.05	19070	-1.58	0.01	-2.69	0.04
1922	18072	-1.13	0.01	-2.79	0.02	19071	-1.65	0.01	-2.68	0.03
1921	18073	-1.12	0.01	-2.65	0.02	19072	-1.47	0.01	-2.47	0.03
1920	18074	-1.17	0.01	-2.81	0.03	19073	-1.51	0.01	-2.68	0.02
1919	18075	-1.10	0.01	-2.48	0.02	19074	-1.44	0.02	-2.79	0.02
1918	18076	-1.16	0.02	-2.85	0.03	19075	-1.95	0.02	-2.66	0.02
1917	18077	-1.11	0.02	-2.87	0.03	19076	-2.35	0.02	-2.73	0.03

	Core 18 (continued)					Core 19 (continued)				
year	sample	$\delta^{13}C$	std.dev.	$\delta^{18}O$	std.dev.	sample	$\delta^{13}C$	std.dev.	$\delta^{18}O$	std.dev.
1916	18078	-1.03	0.02	-2.57	0.03	19077	-2.44	0.03	-2.87	0.03
1915	18079	-0.94	0.02	-2.51	0.05	19078	-2.73	0.01	-2.40	0.02
1914	18080	-1.10	0.01	-2.80	0.05	19079	-2.56	0.02	-2.78	0.02
1913	18081	-1.08	0.01	-2.71	0.04	19080	-1.81	0.02	-2.79	0.03
1912	18081a	-0.99		-2.55		19081	-1.87	0.02	-2.59	0.02
1911	18082	-0.98	0.02	-2.92	0.02	19082	-1.80	0.03	-2.46	0.02
1910	18083	-0.88	0.02	-2.76	0.02	19083	-1.59	0.03	-2.67	0.02
1909	18084	-1.12	0.01	-2.65	0.03	19084	-1.72	0.01	-2.69	0.04
1908	18085	-1.25	0.03	-2.79	0.03	19085	-1.54	0.02	-2.44	0.02
1907	18086	-1.20	0.02	-2.80	0.04	19086	-1.81	0.02	-2.73	0.02
1906	18087	-1.04	0.02	-2.76	0.02	19087	-1.41	0.02	-2.71	0.04
1905	18088	-0.91	0.01	-2.72	0.03	19088	-1.67	0.01	-2.41	0.03
1904	18089	-0.93	0.01	-2.90	0.03	19089	-1.64	0.01	-2.33	0.03
1903	18090	-1.27	0.01	-2.96	0.04	19090	-1.81	0.01	-2.48	0.02
1902	18091	-1.24	0.02	-2.77	0.02	19091	-1.40	0.01	-2.77	0.03
1901	18092	-0.79	0.03	-2.79	0.02	19092	-1.84	0.01	-2.95	0.02
1900	18093	-0.89	0.02	-2.57	0.04	19093	-1.97	0.02	-2.58	0.02
1899	18094	-0.98	0.01	-2.71	0.02	19094	-1.79	0.01	-2.86	0.03
1898	18095	-1.08	0.01	-2.83	0.02	19095	-2.15	0.01	-2.18	0.02
1897	18096	-1.16	0.01	-2.66	0.03	19096	-2.82	0.01	-2.58	0.02
1896	18097	-1.26	0.02	-2.74	0.02	19097	-1.68	0.02	-2.69	0.03
1895	18098& 18099	-1.07		-2.755		19098	-1.80	0.01	-2.78	0.01
1894	18100	-1.19	0.02	-2.75	0.04	19099	-2.29	0.01	-2.79	0.03
1893	18101	-0.96	0.01	-2.58	0.02	19100	-3.04	0.02	-2.68	0.04
1892	18102	-1.03	0.03	-2.78	0.04	19101	-2.48	0.01	-2.69	0.02
1891	18103	-0.89	0.01	-2.86	0.03	19102	-2.03	0.02	-2.74	0.02
1890	18104	-0.86	0.02	-2.65	0.02	19103	-1.99	0.01	-2.81	0.04
1889	18105	-1.06	0.02	-2.74	0.03	19104	-2.35	0.01	-2.79	0.02
1888	18106	-1.20	0.01	-2.79	0.03	19105	-2.20	0.01	-2.79	0.03
1887	18107	-1.06	0.02	-2.60	0.03	19106	-1.91	0.03	-2.60	0.01
1886	18108	-1.19	0.01	-2.92	0.03	19107	-2.05	0.01	-2.93	0.02
1885	18109	-0.87	0.02	-2.75	0.04					
1884	18110	-0.71	0.02	-2.67	0.01					
1883	18111	-0.59	0.01	-2.70	0.02					
1882	18112	-0.64	0.01	-2.82	0.03					
1881	18113	-0.65	0.02	-2.69	0.02					
1880	18114	-0.67	0.03	-2.88	0.02					
1879	18115	-0.78	0.02	-2.69	0.05					
1878	18116	-1.05	0.02	-2.79	0.03					
1877	18117	-1.03	0.02	-2.80	0.01					
1876	18118	-1.15	0.01	-2.88	0.04					
1875	18119	-0.99	0.01	-2.61	0.04					
1874	18120	-1.08	0.02	-2.49	0.02					
1873	18121	-1.10	0.01	-2.74	0.02					
1872	18122	-1.08	0.01	-2.77	0.03					
1871	18123	-1.03	0.02	-2.68	0.02					
1870	18124	-1.01	0.02	-2.74	0.03					
1869	18125	-1.11	0.02	-2.72	0.03					
1868	18126	-1.13	0.01	-2.80	0.03					
1867	18127	-1.16	0.02	-2.57	0.02					
1866	18128	-1.26	0.01	-2.77	0.02					
1865	18129	-1.20	0.01	-2.67	0.02					
1864	18130	-1.05	0.01	-2.76	0.02					
1863	18131	-1.05	0.01	-2.69	0.03					
1862	18132	-1.08	0.02	-2.70						
1861	18133	-1.11	0.01	-2.68	0.02					
1860	18134	-1.33	0.04	-2.73	0.05					
1859	18135	-1.58	0.01	-2.72	0.02					
1858	18136	-1.54	0.03	-2.82	0.02					
1857	18137	-1.52	0.01	-2.55	0.02					
1856	18138	-1.40	0.01	-2.81	0.01					
1855	18139	-1.21	0.01	-2.84	0.02					
1854	18140	-1.14	0.02	-2.64	0.04					
1853	18141	-1.54	0.02	-2.64	0.05					
1852	18142	-1.51	0.02	-2.71	0.03					
1851	18143	-1.45	0.01	-2.55	0.01					
1850	18144	-1.17	0.02	-2.48	0.02					
1849	18145	-1.42	0.01	-2.61	0.03					
1848	18146	-1.04	0.01	-2.60	0.02					
1847	18147	-1.19	0.01	-2.64	0.03					
1846	18148	-1.22	0.02	-2.82	0.02					
1845	18149	-1.03	0.02	-2.84	0.04					
1844	18149b	-0.90		-2.53						
1843	18150	-1.08	0.02	-2.61	0.03					
1842	18151	-1.24	0.01	-2.67	0.03					
1841	18152a	-1.41		-2.93						

	Core 18 (continued)				
year	sample	$\delta^{13}C$	std.dev.	$\delta^{18}O$	std.dev.
1840	18152b	-1.04		-2.72	
1839	18153a	-1.12		-2.79	
1838	18154	-1.10	0.02	-2.67	0.03
1837	18155	-1.24	0.01	-2.62	0.02
1836	18156	-1.33	0.01	-2.65	0.02
1835	18157	-1.39	0.02	-2.48	0.02
1834	18158	-1.28	0.01	-2.42	0.03
1833	18159	-2.15	0.01	-2.31	0.04
1832	18160	-1.79	0.02	-2.18	0.04
1831	18161	-1.31	0.01	-2.60	0.03
1830	18162	-1.06	0.01	-2.67	0.03
1829	18163	-1.42	0.01	-2.53	0.02
1828	18164	-1.35	0.01	-2.67	0.01
1827	18165	-1.34	0.01	-2.64	0.02
1826	18166	-1.53	0.02	-2.52	0.03
1825	18167	-1.32	0.02	-2.48	0.03
1824	18168	-1.21	0.01	-2.14	0.02
1823	18169	-1.56	0.01	-2.91	0.03
1822	18170	-1.26	0.01	-2.56	0.02
1821	18171	-1.24	0.01	-2.83	0.03
1820	18172	-1.22	0.02	-2.71	0.03
1819	18173	-1.36	0.01	-2.72	0.06
1818	18174	-1.34	0.02	-2.64	0.02
1817	18175	-1.08	0.02	-2.42	0.03
1816	18176	-0.98	0.01	-2.47	0.03
1815	18177	-1.08	0.01	-2.54	0.03
1814	18178	-1.24	0.02	-2.60	0.02
1813	18179	-0.96	0.03	-2.59	0.02
1812	18180	-1.24	0.02	-2.59	0.02
1811	18181	-1.23	0.02	-2.49	0.02
1810	18182	-1.41	0.02	-2.55	0.02
1809	18183	-1.29	0.02	-2.51	0.03
1808	18184	-1.23	0.02	-2.61	0.02
1807	18185	-1.04	0.04	-2.36	0.02
1806	18186	-0.95	0.02	-2.48	0.01
1805	18187	-0.98	0.02	-2.47	0.01
1804	18188	-1.05	0.01	-2.49	0.02
1803	18189	-1.51	0.02	-2.30	0.04
1802	18190	-1.41	0.01	-2.60	0.03
1801	18191	-1.10	0.02	-2.57	0.02
1800	18192	-1.44	0.01	-2.71	0.03
1799	18193	-1.23	0.01	-2.59	0.03
1798	18194	-1.35	0.01	-2.70	0.02
1797	18195	-1.30	0.02	-2.85	0.06
1796	18196	-1.30	0.02	-2.63	0.02
1795	18197	-1.26	0.02	-2.75	0.02
1794	18198	-1.29	0.01	-2.73	0.02
1793	18199	-1.28	0.02	-2.87	0.03
1792	18200	-1.09	0.02	-2.44	0.02
1791	18201	-1.37	0.03	-2.96	0.02
1790	18202	-1.15	0.02	-2.58	0.02
1789	18203	-1.48	0.02	-2.37	0.04
1788	18204	-1.67	0.02	-2.48	0.01